Environmental
Studies
Revolving
Funds

014 Underwater Iceberg Geometry

Canada

September 1985

The Environmental Studies Revolving Funds are financed from special levies on the oil and gas industry and administered by the Canada Oil and Gas Lands Administration for the Minister of Energy, Mines and Resources, and by the Northern Affairs Program for the Minister of Indian Affairs and Northern Development.

ENVIRONMENTAL STUDIES REVOLVING FUNDS

REPORT NO. 014

SEPTEMBER, 1985

UNDERWATER ICEBERG GEOMETRY

Terry Buckley
Byron Dawe
Adam Zielinski
Surendra Parashar
Derek MacDonald
Herbert Gaskill
Duncan Finlayson
Wayne Crocker

NORDCO Limited
P.O. Box 8833
St. John's, Newfoundland
A1B 3T2

Scientific Advisor: Dr. Philip Staal

The correct citation for this report is:

Buckley, T., B. Dawe, A. Zielinski, S. Parashar, D. MacDonald, H. Gaskill, D. Finlayson and W. Crocker. 1985. Underwater Iceberg Geometry. Environmental Studies Revolving Fund Report No. 014. Ottawa. XiX + 225p.

Published under the auspices of
the Environmental Studies
Revolving Funds
ISBN 0-920783-13-9

TABLE OF CONTENTS

TABLE OF CONTENTS (CONTINUED)

TABLE OF CONTENTS (CONTINUED)

LIST OF FIGURES

LIST OF FIGURES (CONTINUED)

LIST OF FIGURES (CONTINUED)

LIST OF TABLES

SUMMARY

The lack of accurate underwater dimensional information has lead to considerable uncertainty in engineering planning and calculations. The Environmental Studies Revolving Fund (ESRF) Committee determined that a study was needed to assess the current state of knowledge of underwater iceberg geometry and to investigate and evaluate alternative methods for mapping the underwater portion of icebergs.

This report identifies and reviews all previous recorded measurements of the underwater portion of icebergs. Analysis of previous keel measurements show that, at best, only a general three-dimensional impression of the underwater shape can be obtained. Analysis of the data base also indicates that there is not a good functional relationship between the draft and the above-water parameters of icebergs and thus above-water dimensions form a poor basis for estimating iceberg draft. Factors affecting performance of an acoustic iceberg mapping system including frequency versus range and resolution, angle of incidence and beam bendering are investigated. The use of alternative sensors for iceberg mapping, primarily underwater low-light TV, lidars, and impulse radars, and it is concluded that because of the significant research and development required and the short operational ranges achievable that optical/electro-optical devices are not at present feasible sensors for underwater iceberg shape determination. Impulse radar deployed from a helicopter has potential as an iceberg draft measurement device.

Original conceptual designs are presented for two iceberg imaging systems both of which use the combined effect of the directionalities of the transmitter and receiver to generate a series of searchlight-type beams on a narrow area of the iceberg representing its vertical profile.

In the TIMS1 (Towed Iceberg Mapping System 1) design, one transducer projects in the horizontal direction a narrow fan-shaped beam which can be steered in the vertical direction by mechanical rotation of the transducer. The second transducer (the receiver) is fixed to receive acoustic returns from a narrow fan-shaped window oriented in the vertical direction. The combination of these beam patterns creates the effects of narrow, searchlight-type beam scanning. The time delay, before the return of the acoustic signal from the iceberg is received, is sufficient for the projector beam to scan the iceberg into vertical direction by constantly changing its angular position and transmitting short pulses at the selected positions.

In the TIMS2 design, the projector is oriented to produce the fan-shaped beam in the vertical direction. The receiver consists of a multi-element linear array. Using beam-fanning techniques, with proper time delays and summation of the signals from each individual sensor in the array, it is possible to simultaneously synthesize a series of narrow beams. In this case, the intersection of a single probing beam with a series of multi-beams formed synthetically represents a series of small resolution cells along the vertical profile of the face of the iceberg.

LIST OF SYMBOLS

$a(x)$	spectral absorption coefficient
A_c	effective area of collector optics
A_T	area of target within field of view
B	projector frequency range (band-width)
$b(\theta,\phi)$	beam pattern or pattern function
c	speed of light in water
c'	sound velocity propagation (m/s)
C_l	sound velocity in the liquid
C_{p2}	compressional wave velocity in the solid
C_{s2}	share wave velocity in the solid
C_o	sound velocity at the sonar depth
D_i	directivity index
DI	directivity index expressed in dB
DI_T	transmitting directivity of a projector
D	line diameter
ε_o	permittivity of free space
ε_v	dielectric constant of the medium (water)
$E_{o\tau}$	illuminence (in lumen/m^2) at object
$E_{I\lambda}$	illuminence (in lumen/m^2) at image place
f	focal length
f_o	reference projector frequency (central frequency)
f_r	pulse repetition frequency
g	velocity gradient (i.e.,g = dc/dz)
g	maximum rate of increase of g

h	Planar constant (6.626×10^{-34} J-s)
I	wave intensity (i.e. p^2/z)
I_o	reference intensity for logarithmic scaling
$I_2(0)$	incident radiation at a distance 0
$I_2(x)$	incident radiation at a distance x
j	value of j in $\sqrt{-1} = i$
$L_{e\tau}$	spectral radiance of object
n	complex index of separation (refraction)
ML	number of scan lines comprising an image on the photocathode
M_i	imaginary part of complex n above where; $n = n_r + i\ n_i$
M_r	real part of complex n above
n^2	total noise power admitted to the system by the hydrophone array with beam pattern $b(\theta, \phi)$
n_r^2	total reverberation power
N_L	total number of scan lines perpendicular to the height
NL	ambient noise level at the central frequency f_o
NR	in-band noise level admitted to the system and expressed in dB
N	selective apertise of the lens
$N(\theta, \phi, f)$	noise power per unit solid angle Ω in the 1 Hz band-width at frequency f in the angular polar direction (θ, ϕ) with respect to the receiving hydrophone array
p	sound presure (w/m^2)

P_o	reference pressure for logarithmic scaling (i.e., $I_\mu Pa$)
P_r	received radiant power (watts)
P_t	transmitted power (watts)
P_T	spectral radiant power
Q	Q-factor of a transducer (i.e., f_o/b)
R	distance to the object (range)
R_o	radius of circular arc along which an acoustic ray will propagate for a linear variation of sound velocity
r_p	straight line short range
R'	cross-sectional radius of projector beam at the target
Γ	distance between a projector and a target
R(0,0)	normalizing factor for $R(\theta,\phi)$ because the direction (θ=0, ϕ=0) yields maximum response from $R(\theta,\phi)$
$R(\tau)$	extinction or attenuation coefficient
$R(\theta,\phi)$	actual pressure generated by an acoustic projector (transmitter) in the polar direction (θ,ϕ) (i.e., radiation pattern)
R_{12}	reflection coefficient for water-ice interface and normal incidence

$$R_{12} = \frac{A-B}{A+B}$$

where:

$$A = 4\ \gamma_2\ \delta_2\ \alpha^2 + (\delta_2{}^2 - \alpha^2)^2$$

$$B = (\rho_1/\rho_2)\ (\gamma_2/\gamma_1)\ c_{s2}{}^{-4}$$

$$\alpha = \sin\ \theta_1/c_1$$

$$\gamma_1 = \cos\ \theta_1/c_1$$

$$\gamma_2 = \frac{1}{C_{p2}} \left[1 - \frac{C_{p2}}{C_1} \sin \theta_1)^2\right]^{1/2}$$

$$\delta_2 = \frac{1}{C_{s2}} \left[1 - \frac{C_{s2}}{C_1} \sin \theta_1)^2\right]^{1/2}$$

S	salinity in parts per thousand
S_a	sound travel path arc
SL	source level, the pressure level (in dB re I_μPa)/m away from the transducer
SNR	signal-to-noise ratio (in dB)
t	observation time
Δt	elapsed time (change in time)
T	temperature of water in °C
$T_o(\lambda)$	transmittivity of optics over, λ
TL	transmission loss of the beam
TS	target strength of the beam
$T_w(\tau)$	transmittivity of intervening water over the wave length of interest, τ
$T(\tau)$	transmittance at length, τ
μ	particle velocity (m/s)
$V(\theta, \phi)$	normalized radiation pattern
X_c	height of the photocathode
X_T	height of the target
y	quantum efficiency of detector
z	specific acoustic impedance (rayls)
Z_a	actual depth at which the target is intercepted by the bent ray
Z_c	depth of water (in m) used for finding C

Z_p	depth at which a straight-line ray projected at angle α_p by the transmitter intercepts the target line
α	absorption coefficient (in dB/m)
α_a	angle at which $a = R_o \sin \alpha_p - r$ can be reached by a straight-line ray in the direction described by α_a
Δ_p	error due to position
Δ_α	angular error associated with the position error
α_p	angular direction toward a linear target located at a distance r from the sonar
ρ_1	density of the liquid
α'	attenuation coefficient
ρ_2	density of the solid
ρ_n	required minimum number of signal photoelectrons
ρ	reflectivity of the object
ρ'	water density
Ψ	projector beam-width
α_t	target scattering cross-sectional area
σ'	conductivity of water
δ	sonar radial resolution
γ	frequency of the radiation
ν	optical frequency, c/λ
ω	angular frequency
τ	wavelength of the radiation
τ	duration time of a sinusoidal pulse
Ω	solid angle

Θ_1	angle between incident ray and normal to interface
Δ_c	error in velocity c
Δ_r	range error
Δ_z	error in depth ($\Delta_z = z_a - z_o$) where, $z_o = C_o / g$

RÉSUMÉ

Le manque d'exactitude dans les renseignements obtenus sur les dimensions des icebergs est à l'origine de certains problèmes de planification et de calculs pour les ingénieurs. Le comité du Fonds renouvelable pour l'étude de l'environnement (FRÉE) a décidé qu'il était nécessaire de faire une étude afin d'évaluer le niveau actuel des connaissances en géométrie sous-marine des icebergs et de rechercher des méthodes alternatives pour tracer la carte de la partie sous-marine des icebergs.

Dans ce rapport, nous identifions et nous révisons toutes les mesures déjà relevées de la portion sous-marine des icebergs. L'analyse des mesures de la quille montre qu'on ne peut obtenir, dans le meilleur des cas, qu'une impression générale à trois dimensions de sa forme. Si on analyse les données, on voit aussi qu'il n'existe pas de relation fonctionnelle entre les paramètres des portions d'icebergs au-dessus et au-dessous de l'eau, ce qui veut dire que la partie supérieure de l'iceberg ne peut pas être utile à l'évaluation de son tirant d'eau. On tient compte des facteurs qui affectent la performance d'un système accoustique de traceur de cartes d'icebergs, y compris la fréquence par rapport à la portée et la résolution, l'angle d'incidence et la courbe du rayon. On envisage aussi l'utilisation de détecteurs alternatifs pour relever le contour des icebergs: télévision sous-marine à faible éclairage, lidars et radars à impulsions. On conclut que, puisqu'il est nécessaire de faire de la recherche et du développement pour des opérations à faible portée, l'utilisation d'engins optiques/électro-optiques comme détecteurs n'est pas actuellement faisable pour déterminer la forme sous-marine des icebergs. Un radar à impulsions placé à bord d'un hélicoptère est un instrument possible de mesure du tirant d'eau d'un iceberg.

Des conceptions originales de système de relevé d'image sont présentées pour deux icebergs et les deux utilisent les effets combinés des orientations possibles du transmetteur et du receveur pour générer une série de rayons du type projecteur sur une section étroite de l'iceberg, formant ainsi son profil vertical.

Dans la conception du système TIMS1 (Towed Iceberg Mapping System 1), un transducteur projette en direction horizontale un rayon étroit en éventail que l'on peut mettre dans la direction verticale à l'aide d'une rotation mécanique du transducteur. Le deuxième transducteur (receveur) garde une position fixe de manière à pouvoir recevoir des signaux accoustiques provenant d'une étroite ouverture en éventail orientée à la verticale. La combinaison

de ces deux rayons crée un effet de balayage étroit semblable à celui d'un faisceau lumineux de lampe de poche. Le délai de retour du signal accoustique provenant de l'iceberg est suffisant pour laisser le temps au rayon au projecteur de balayer l'iceberg à la verticale en changeant constamment sa position angulaire et en transmettant de courtes pulsions à certains endroits déterminés.

Dans le système TIMS2, l'orientation du projecteur permet de produire un rayon en éventail à la verticale. Le receveur est formé d'un dispositif linéaire à éléments multiples. En utilisant les techniques de rayon en éventail et en tenant compte des retards exacts ainsi que des rappels de signal pour chaque détecteur individuel du groupe, il est possible de synthétiser simultanément une série de rayons étroits. Dans ce cas l'intersection d'un unique rayon chercheur avec une série de rayons multiples synthétiquement formés représente une série de cellules de haute résolution le long du profil vertical de la paroi de l'iceberg.

ACKNOWLEDGEMENTS

This study was financed by the Environmental Studies Revolving Fund (EMR), administered by the Canada Oil and Gas Lands Administration, Ottawa, Canada. The Scientific Adviser was Dr. Philip Staal.

INTRODUCTION

Icebergs transported by the Labrador Current from the northern Baffin Sea pose a serious environmental hazard for offshore hydrocarbon exploration and development in the Grand Banks area. An iceberg's keel could damage bottom or subsea structures and there is always potential for collision between an iceberg and a floating platform.

To manage icebergs effectively during oil and gas operations, information is needed urgently regarding draft in real-time to determine whether an iceberg could threaten a bottom or subsea installation, thereby determining the course of evasive action. Such data are also needed for input to the scientific study of iceberg draft. Knowledge of their three-dimensional shape could input into drift prediction models and stability analyses. Designers of platforms also require the shape of the collision surface or face (indentor) for determining potential impact forces.

No operational techniques have yet been developed to determine the actual underwater shape of an iceberg. In the spring of 1984, a scientific field program was conducted to map the underwater shape of icebergs. Using techniques described in the section on "System Designs."

A large data base exists for iceberg draft, however, the standard technique (vertically deployed side scan sonar) for obtaining the data has been found to have potentially large errors (NORDCO 1980), which leads to the data base being suspect. Some attempts have been made to extrapolate underwater shape using this technique but, at best, only a general three-dimensional impression of the underwater shape can be obtained.

The lack of accurate underwater dimensional information has led to considerable uncertainty in engineering planning and calculations. The Environmental Studies Revolving Fund (ESRF) Committee determined that a study was needed to assess the current state of knowledge of underwater iceberg geometry and to investigate and evaluate alternative methods for obtaining the required information.

To achieve that objective, a study approach was developed:

- to identify, collect, and review all previous measurements of the underwater portion of icebergs;

- to analyse previous keel measurements to determine the feasibility of constructing three-dimensional shapes from this data base;

- to investigate the factors affecting performance of an acoustic iceberg mapping system (including frequency versus range and resolution, angle of incidence, and beam bending);

- to investigate the use of alternative sensors for iceberg mapping, primarily underwater low-light TV, Lidars, and Impulse radars;

- to develop design and operational criteria for the mapping system based on discussion with, and survey of, the offshore industry, governments, and scientific institutes; and

- to optimize conceptual design (or designs) for underwater iceberg mapping system (or systems).

This document comprises the results of the study. It provides a detailed evaluation of the current database, examines a variety of sensing devices for their potential use in this application, addresses the sensor platform stability and positioning problem, investigates potential methods of sensor deployment, examines the signal processing requirements, and provides conceptual designs for potential systems. All the aspects of the problem are addressed in terms of the operational requirements and constraints to which any system must adhere.

In each section detailed summary of the work undertaken provides focus to the report, outlines the various points to be discussed, and summarizes all relevant information presented therein.

Original conceptual designs are presented for two iceberg imaging systems both of which use the combined effect of the directionalities of the transmitter and receiver to generate a series of searchlight-type beams on a narrow area of the iceberg representing its vertical profile.

TOWED ICEBERG MAPPING SYSTEM 1

The towed acoustic sensor is equipped with two transducers. One transducer projects in the horizontal direction a narrow fan-shaped beam which can be steered in the vertical direction

by mechanical rotation of the transducer. The second transducer (the receiver) is fixed to receive acoustic returns from a narrow fan-shaped window oriented in the vertical direction. The combination of these transducer beams creates the effects of a narrow, searchlight-type beam scanning. The transducers themselves are typical of those found in conventional side-scan sonar systems.

The range to the iceberg is estimated to be between 75 to 150 m with a corresponding delay time before the return of the acoustic signal of 200 to 400 millisecond (ms). This time is sufficient for the projector beam to scan the iceberg in the vertical direction by constantly changing its angular position and transmitting short pulses at the selected positions. The last pulse will be transmitted before the first echo is received. The received echos form a series of small resolution cells along the vertical profile of the face of the iceberg. The returns from different resolution cells are distinguished by their order of arrivals. Although the problem of ambiguity in interpreting the different resolution cells still exists, with proper timing of the transmitted pulses, surveying the majority of the icebergs should not present any significant problem.

TOWED ICEBERG MAPPING SYSTEM 2

The general scanning scenario and tow fish is similar to the system described previously. In this system, however, the projector is oriented to produce the fan-shaped beam in the vertical direction. The receiver consists of a multi-element linear array. Using beam-forming techniques, with proper time delays and summation of the signals from each individual sensor in the array, it is possible simultaneously to synthesize a series of narrow beams. In this case, the intersection of a single probing beam with a series of multibeams formed synthetically represents a series of small resolution cells along the vertical profile of the face of the iceberg.

The system incorporates no moving parts. However, it does involve relatively complex data acquisition and processing of signals from each sensor of the receiving array. The individual components of the system are now available. The system design involves what may be regarded as state-of-the-art packaging of proven technology. The problems associated with ambiguity in interpreting the different resolution cells are for all practical purposes eliminated.

BACKGROUND

One objective of this study was to review the state-of-the-art of techniques for measurement of the underwater dimensions of icebergs and to evaluate their potential use in an underwater iceberg mapping system.

An extensive literature review regarding all the techniques that have been used for measuring the thickness, draft, and underwater shape or topography of icebergs and sea ice was undertaken. This literature review shows that a variety of techniques have been used, primarily relying on acoustic sensors. Operationally, all efforts have concentrated on the determination of iceberg draft. The operational technique currently employed by most east coast operators involves vertical deployment of a rotating side-scan sonar transducer from an operational support vessel. The only non-acoustic technique employed to measure draft has been radio echo-sounding, which has been used successfully in a limited number of experimental tests. A major drawback with all the techniques has been the lack of verification data obtained through independent measurements. For the only documented project, verification of side-scan sonar measurements using a remote-controlled submersible to measure the draft within a confidence limit of 2 percent showed that the side-scan sonar technique can give large errors (NORDCO 1980).

An evaluation of the current data base on iceberg underwater shape and draft showed that some attempts have been made to derive underwater shape using the side-scan technique, but the lack of information regarding the transducer attitude and position and the horizontal beam-width characteristic of the radiation pattern results in this derivation being fraught with errors.

Draft has been the only parameter for which a significant amount of data exists. The lack of information regarding quality control, the inability to get access to the raw data records, and the potential system errors, makes this data base virtually useless for extrapolation to underwater shape. Indirect methods using regression analysis to relate above-water parameters to the draft have shown no consistency among independent investigators. One possible explanation is the large errors present in the draft data base which was compiled using, for the most part, the spinning side-scan sonar technique.

LITERATURE REVIEW

General Iceberg Information

To appreciate better some of the concepts put forward in this report, some background information on general icebergs information is useful. However, so that the flow of this report is expedited, the bulk of this information has been separated into Appendix 1. Among the topics covered are iceberg drift, deterioration, distribution, and summary of size and shape classifications.

Acoustic Measurement Techniques

Many acoustic techniques have been used to measure sea ice and iceberg draft, including a spinning, vertically deployed, side-scan sonar; a scanning sonar; an omni-directional transducer array; and an inverted echo-sounder. They have been tried from various platforms, including the sea floor, submarines, unmanned submersibles, and surface vessels. Complete details of the historical development of these methods are contained in Appendix 2.

Electromagnetic Measurement Techniques

The only electromagnetic technique that has been employed for iceberg draft measurement is the method of radio echo-sounding, which was first used in the measurement of glacier thickness. Since then it has been used fairly routinely for a wide range of purposes including sounding peat bogs, measuring permafrost depths, and surveying sea ice thickness. Appendix 3 contains an historical review of underwater dimensional measurements of icebergs using this technique.

Draft Estimation Techniques

The draft of all icebergs in the vicinity of an exploration well site are estimated from data on the above-water portion of an iceberg as a standard practice in determining the threat to the blow-out-preventor (BOP) should the drilling vessel be forced to move to avoid collision with an iceberg. This section addresses the accuracy of these draft estimation techniques to determine if these methods are a good tool for predicting iceberg draft.

Studies of the above-water dimension to estimate draft fall into two categories:

- the estimation of actual iceberg draft for use in iceberg drift prediction, deterioration studies, and towing techniques; and

- the estimation of maximum possible draft to assess the risk to sea-floor installations.

A complete review of the literature, together with relevant tables, is presented in Appendix 4.

Based on the information contained in Appendix 4, there does not appear to be a good functional relationship between the draft and the above-water parameters of icebergs. It may be possible to improve the estimates with the use of other relationships or a larger, more reliable data base, however, the data indicate that above-water dimensions form poor bases for estimating iceberg draft. This conclusion is supported by a lack of agreement between the various researchers in attempts to obtain functional relationships (Figure 1).

REVIEW AND EVALUATION OF DATA BASE

The available underwater measurement data are comprised almost entirely of side-scan sonar records, gathered mainly in operational support of various exploratory drilling programs on the Labrador Shelf and Grand Banks, although some were collected by purely scientific expeditions.

Responses received to requests for data from the offshore oil industry indicated that most data sets are proprietary and are of questionable quality.

Limited data are available in a report to the Bedford Institute of Oceanography (BIO) (Ice Engineering Ltd., 1983), collected during a cruise in the Strait of Belle Isle. A side-scan sonar, in conventional iceberg profiling mode, was used for measurement of draft and underwater shape, whereas photographic and sextant techniques were used to record above-water parameters. A typical product resulting from this work is presented in Figure 2.

Information on underwater iceberg profiles is summarized and presented graphically in Figure 3. The curves shown represent a range of submerged profiles of icebergs observed on the east coast. The profiles A and B are relatively rare whereas the shapes indicated by curves C and D are the most

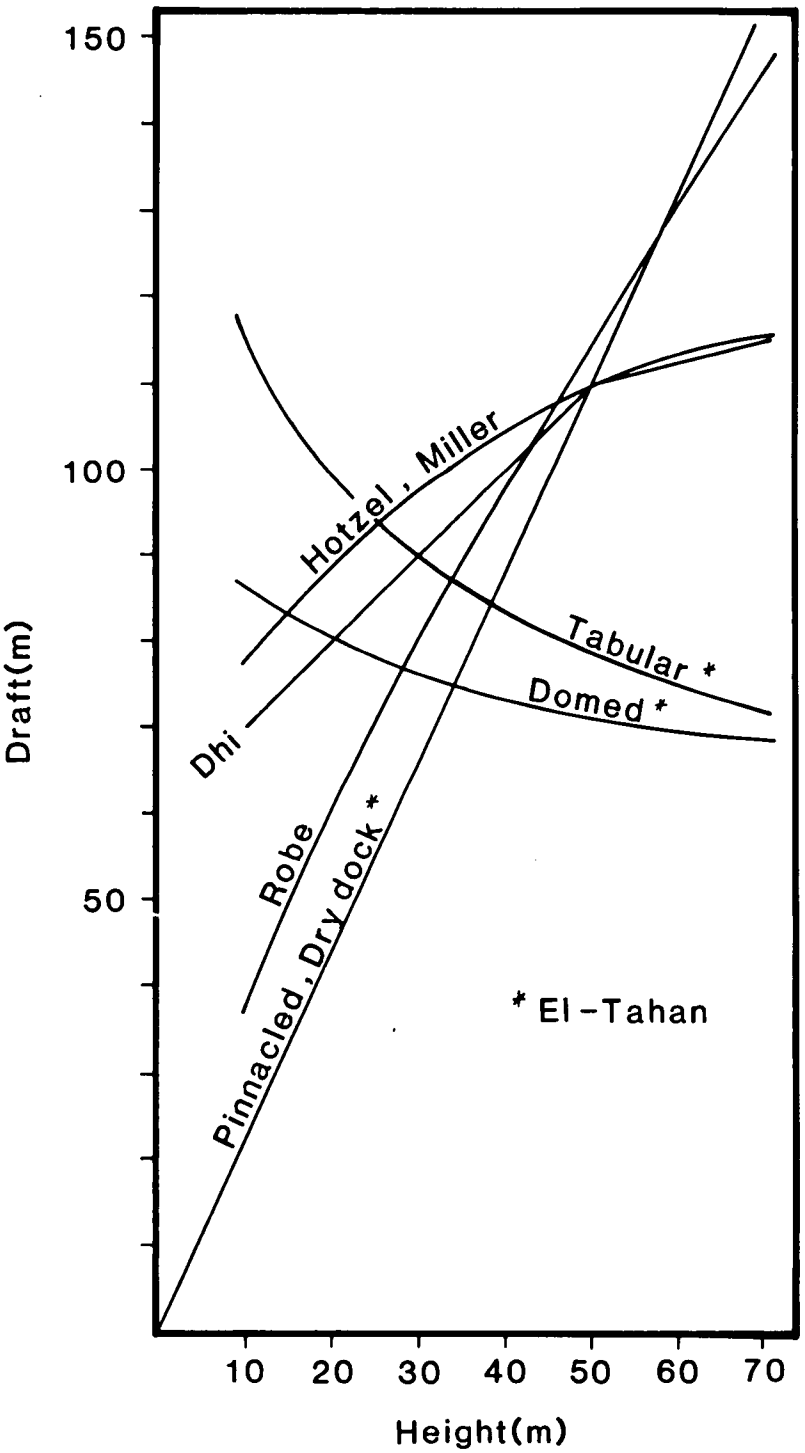

Fig. 1. Comparison of the various techniques for the estimation of iceberg draft.

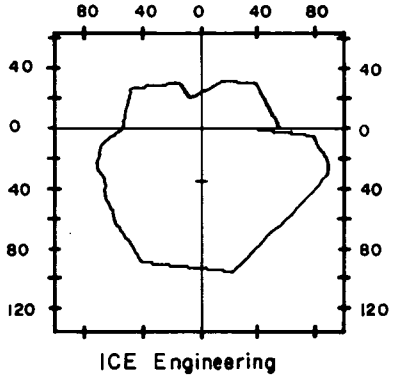

BIO 2A

South Face

Cross-Sectional Areas:

Above Water = 2,740 sq. m.
Below Water = 11,600 sq. m.
Total = 14,340 sq. m.

Berg No: BIO 2A

Date: 25 June, 1983 Survey Started: 0820
Status: Floating Shape: Drydock

H	32 m
L	117 m
W	95 m
D	96 m
Vabove	112,000 cu. m.
M	800,000 tonnes

East Profile

Depth (m)		Range (m)
5	31.0	232.5
13	30.7	230.3
20	29.8	223.5
30	29.7	222.8
33	30.0	225.0

West Profile:

Depth (m)		Range (m)
10	23.8	178.5
19	23.4	175.5
27	23.3	174.8
35	24.0	180.0
43	23.9	179.3
49	24.3	182.3
57	24.9	186.8
63	25.0	187.5
68	25.7	192.8
75	26.4	198.0
82	26.7	200.3
89	27.3	204.8

Fig. 2. Typical format for data presentation (courtesy Bedford Institute of Oceanography).

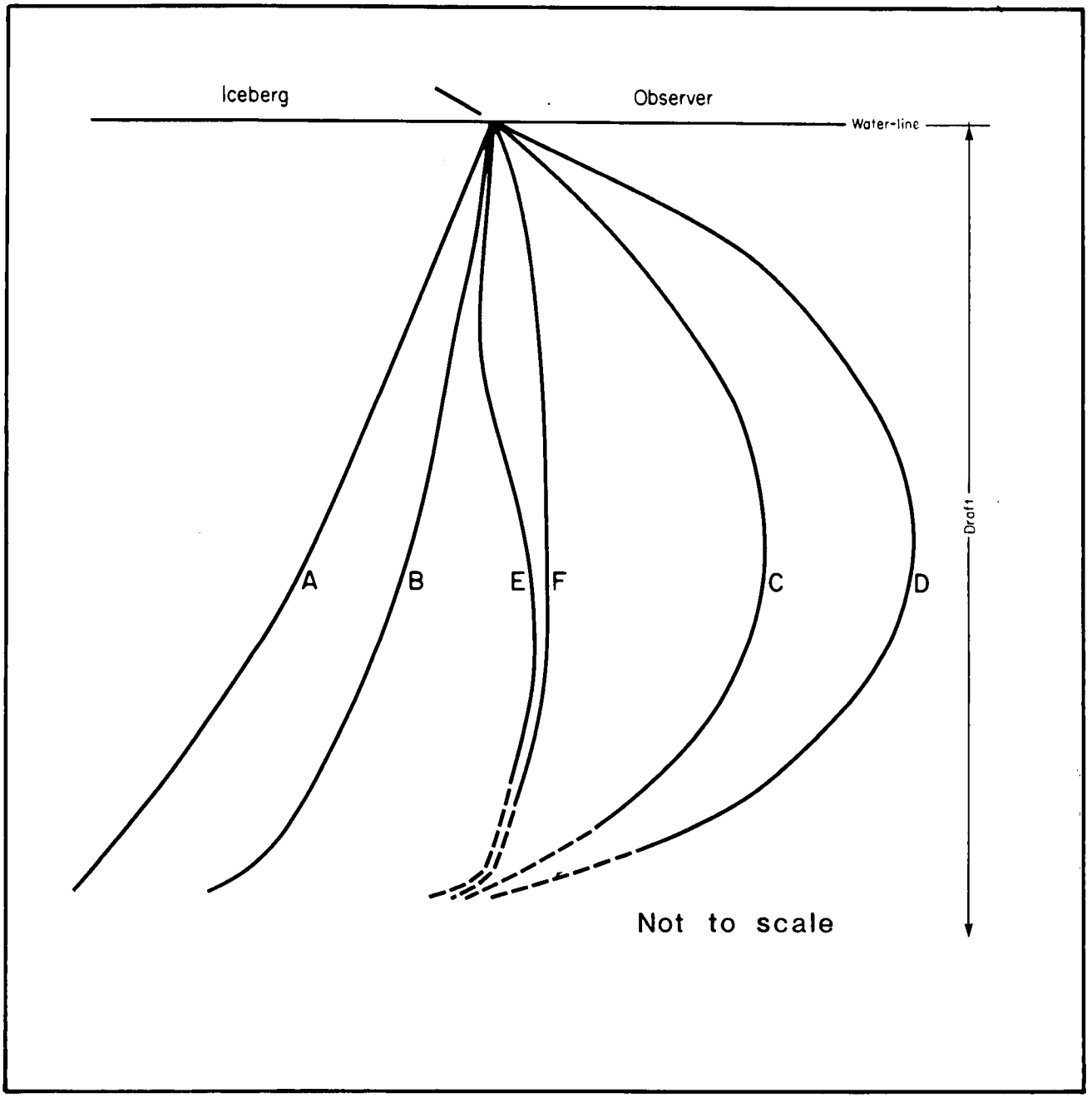

Fig. 3. Typical underwater profiles of icebergs.

commonly occurring for Arctic icebergs. Shapes E and F are more common than A and B, but are less common than C and D. The continuation of the profiles towards maximum draft are shown as extrapolated dashed lines in the figure, reflecting the fact that the intensity of side-scan sonar returns falls off rapidly as maximum draft is reached.

The assessment that current data are of limited value is supported by the results of a study using a remote-controlled vehicle (RCV) and side-scan sonar in conventional iceberg profiling mode (NORDCO, 1980). The results of measurements made on 14 icebergs with both systems revealed significant discrepancies between the two (Table 1) and an average error of 11.4 percent. Typical data output from this work is shown in Figure 4.

The report identified five areas of error in the side-scan measurements:

- sea-bed echoes resulting from towfish inclination, which effectively obscured deepest iceberg echoes;

- iceberg sub-surface shape resulting from the slope near the keel being almost parallel to the direction of the pulse and therefore reflecting very little back to the receiver;

- large sonar-to-iceberg range near deepest draft;

- inaccessible areas of the iceberg waterline for safe profiling; and

- towfish inclination resulting in the beam not "looking" in a horizontal plane and therefore detecting the bottom giving most return at a depth different from the actual draft.

NORDCO concludes that there is, at present, no acceptable method of determining a realistic impression of the three-dimensional underwater shape based on side-scan sonar profiles. At best, this method can give accurate estimates of iceberg draft and may even reveal a two-dimensional underwater profile, but it is incapable, in its present form, of providing sufficient data for the generation of complete shapes.

In summary, the techniques that have been used for measurement of iceberg draft provide only a rough measurement of this parameter. The confidence limits of accuracy are at best 10 to 15% for draft measurement. These techniques are inadequate for the determination of the underwater shape.

Table 1

Comparison of remote-controlled vehicle (RCV) and side-scan sonar data

Iceberg no.	Measured draft (m) RCV	Side-scan sonar	Error (%)
1	115	107	-7
2	68	74	9
3	67	75	12
4	76	84	11
5	115	74	-36
6	100	97	-3
7	66	64	-3
8	161	154	-4
9	110	90	-18
10	97	87	-10
11	97	87	-10
12	53	46	-13
13	73	70	-4
14	85	71	-16

Source: NORDCO (1980).

NOTE: RCV data are assumed correct.

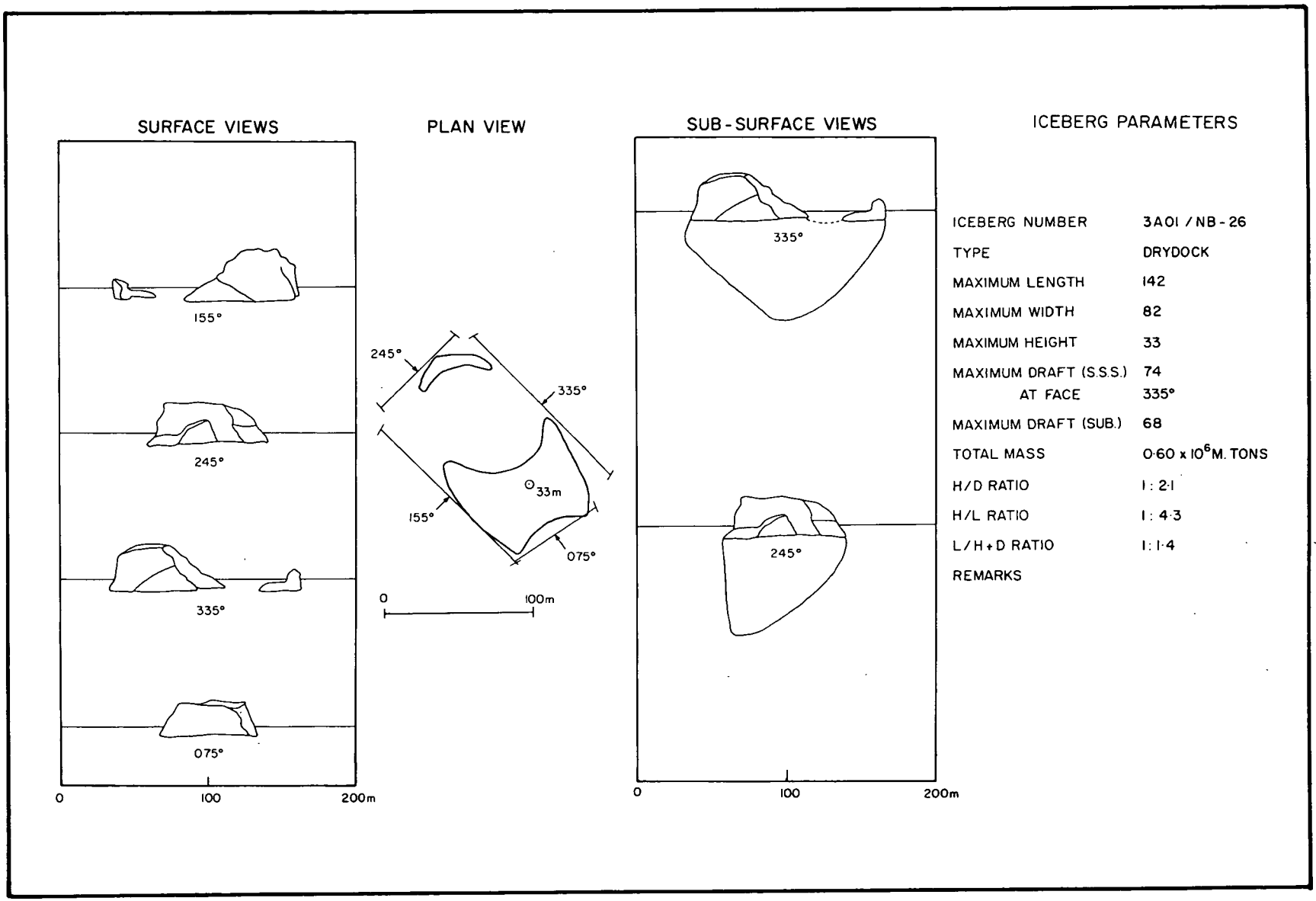

Fig. 4. NORDCO's typical format for data presentation (NORDCO 1980)

DESIGN AND OPERATIONAL CRITERIA

This section provides the design and operational criteria and defines the problem of determining the underwater shape of an iceberg. This information is to be used as a basis for the selection and design of the sensor, the development of a positioning technique, the examination of potential deployment schemes, the investigation of applicable data acquisition and processing systems, and the candidate conceptual system designs.

The current operational technique for measuring draft is not applicable to the determination of iceberg underwater shape because of errors inherent in the measurement system including attitudinal and positional errors, azimuth and vertical ambiguities, and detection problems.

Although the measurement of iceberg draft has been, and still is, a key requirement in assessing the immediate threat to a subsea structure, other requirements necessitate a knowledge of the underwater shape. These requirements include the need to develop accurate iceberg trajectory models, the need to assess the potential forces and their impact location on an offshore platform, and the need to ascertain accurate knowledge on the scouring characteristics associated with any given iceberg shape and size.

The operational requirements have been established through communication with the offshore oil and gas industry. A discussion of these requirements is followed by a thorough delineation and discussion of the problems to be encountered in designing a three-dimensional iceberg mapping system.

BACKGROUND

Traditionally, the main reason for measuring iceberg geometry has been to establish a maximum draft with which to evaluate potential damage to sea-bed installations in the path of a drifting iceberg. Although a number of conceptual approaches have been developed, a somewhat basic and standard technique has been adopted by most of the industry; namely, vertical profiling with a modified side-scan sonar. This method has been relatively quick and cost-effective and has generally provided measurements of maximum draft acceptable to the industry.

Basically, this procedure for measuring iceberg draft involves deploying the sonar fish vertically while the boat remains as stationary as possible. As the fish is lowered, it is forced to rotate by means of tilted fins attached to its upper body. Because the acoustic signal is emitted in a plane at right angles to the sonar fish, rotating the fish as it descends results in a scanning effect in the horizontal plane, thereby producing a picture of the underwater profile of the iceberg. The fish is lowered until the echo (return) disappears, when it is generally assumed that the bottom of the iceberg has been reached. The depth of the fish when the echo was lost is taken as the draft, the fish is then lowered an extra 15 or 20 m before commencing recovery, verifying draft. Usually, any doubt in the measurement is checked by profiling another side of the iceberg. Technical data for most of the side-scan sonar system used in iceberg draft measurement are given in Table 2.

Figure 5 shows a typical deployment technique. Figure 6 shows pictures of a modified Klein side-scan which has been used on the Labrador Shelf. Figure 7 shows a typical side-scan record obtained from this system. It is noted that a degree of skill and experience is required to interpret these records even for the measurement of maximum draft.

This technique has been used for obtaining information on underwater shape by collecting vertical profile returns from various positions around the iceberg (for example, Benedict, 1971). However, the potential errors render this almost a useless exercise. Most of these errors are inherent in draft measurement itself and are described as follows.

a) Transducer Attitude Error -- Other than a crude measurement of the cable angle in relation to vertical at the surface (which is not necessarily related to the orientation of the transducer package) no indication of the orientation of the transducer is available. Therefore, even if the transducer depth is known accurately (usually measured via a pressure transducer) the "look" direction of the sonar beam could be well outside the horizontal plane.

b) Transducer Positional Error -- Even though the vessel may be reasonably stationary under certain conditions in relation to a known point on the iceberg, the same may not hold true for the location of the sonar transducer. Only depth information from the pressure transducer is available and the disposition of the cable (attitude) at the surface

TABLE 2

Technical data for currently available side-scan sonar systems

Data (units)	Klein Hydroscan	Klein Hyroscan	ORE	EG&G Mark 1B	Edo Western	Wesmar
Standard towfish model	4225-001A	4225-001G	1098	272 Saf-T	606A-602	500SS
Frequency (kHz)	100	50	97	105	100	105
Horizontal beam-width (°)	1	1.5	2	1.2	1	1.2
Vertical beam-width (°)	40	10/20	28/14	20/50	25	35
Maximum range (m)	400	600	400	500	400	400
Pulse width (ms)	0.1	0.2	0.1	0.1	0.1	0.1-.5
Source level	228	228	225	228	N/A[a]	228
Band width (kHz)	10	10	15	10	N/A	3
Receiver level	1 volt	1 volt	-17dB	-100 dB	N/A	N/A
TVG	75dB	75dB	40 dB(4-400 m)	N/A	N/A	N/A
Recorder	521	521	EPC1600/3200	259-3	606A	-
Number of channels	2	2	2	2	2	2
Paper						
Type	wet(ALFAX)		dry(electronsen)	wet(ALFAX)	dry	dry
Width (cm)	49		49	28	49	20
Scanning range (m)	25-660		VAR.[b]	50-500	50-400	20-480
Paper feed rate(lines/cm)	20-110		VAR.	40/60/80	100-200	N/A

[a] N/A = Not available

[b] VAR. = Varied

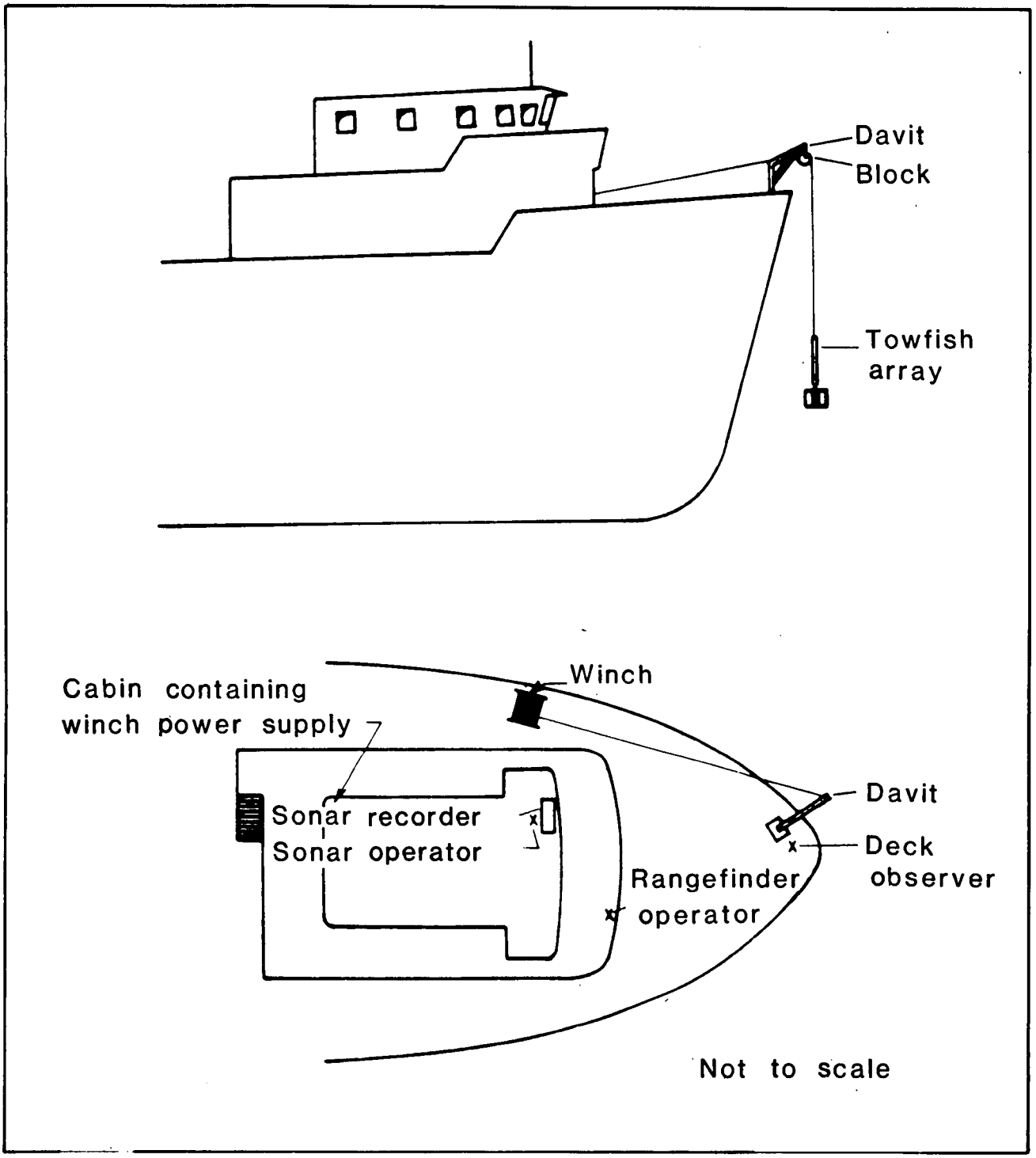

Fig. 5. Typical vertical deployment technique for side-scan sonar measurement of draft.

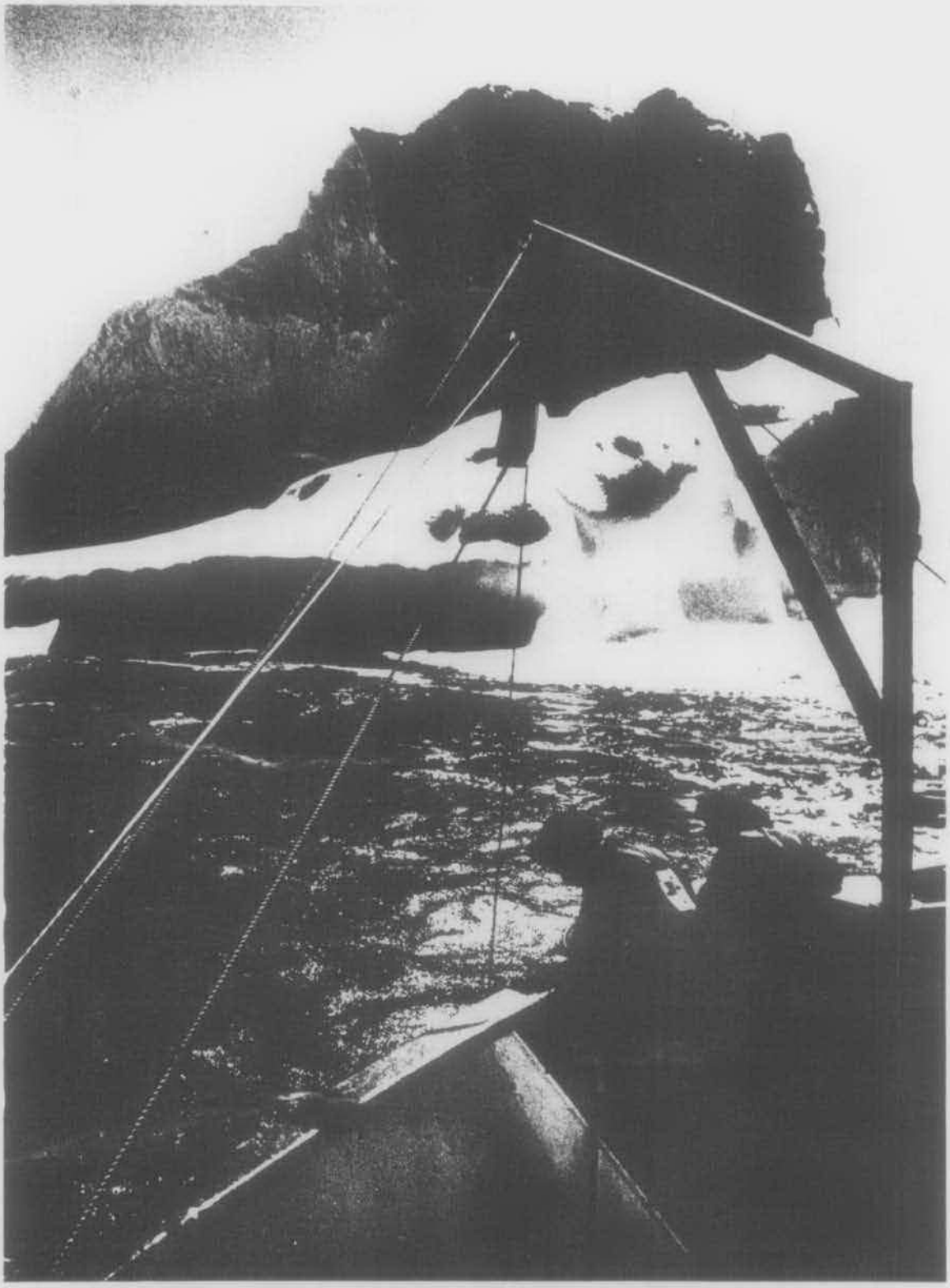

Fig. 6. Typical operation in side-scan sonar measurement of draft.

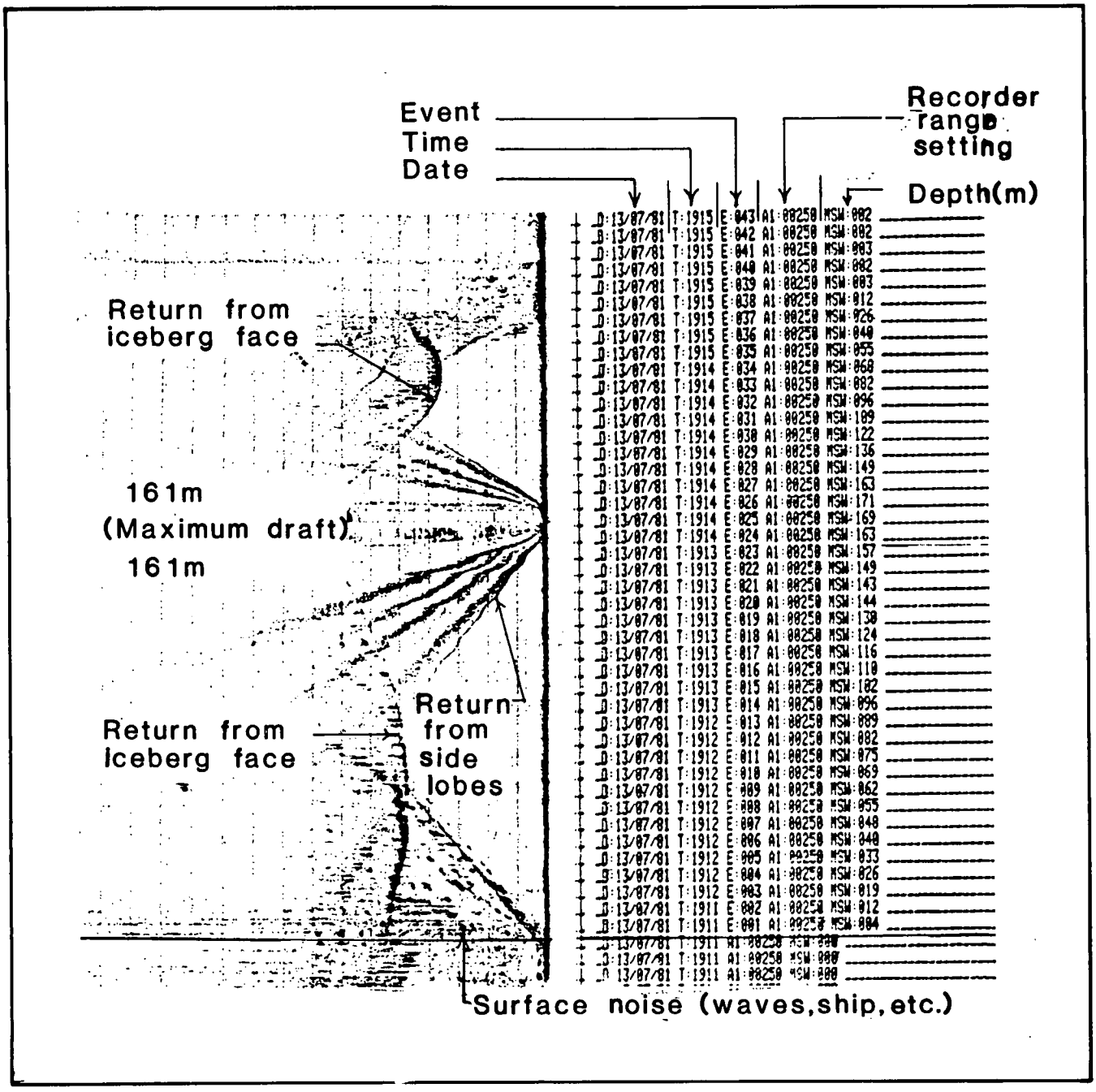

Fig. 7. Typical record of side-scan sonar measurement of iceberg draft.

is, by no means, a good indication of the sonar transducer's location in relation to that of the vessel and, in turn, to the reference point on the iceberg. In a practical situation the vessel is moving and its position relative to a point on an iceberg is not accurately monitored. Indeed, the distance between the ship and the iceberg is the only stringent requirement for draft measurements with the ship maintaining as close a position as possible (within reasonable safety limits of 50-100 m) to the iceberg to ensure that the sonar transducer is within its maximum detection range limit. This situation compounds the problem of monitoring the position of the sonar transducer. The inability to monitor the position relative to one point makes it practically impossible to monitor the position of a number of points on the iceberg relative to each other, making any extrapolations of shape meaningless.

c) Azimuth Ambiguity -- The side-scan sonar transducers scan (spin) in the horizontal plane. Thus, the true azimuth direction of the reflected signal cannot be derived. Also, most systems used to date consist of two transducers with beam-widths of about 35-40° in the horizontal plane (when deployed vertically). This wide beam-width results in a the resolution cells on the iceberg surface being of large size (about 35 m wide at 50 m depth) and precludes the ability to resolve a geometric structure smaller than this. The wide beam-width also prevents any accurate directional information on the origin of the signal returns in the horizontal plane from being obtained.

d) Vertical Ambiguity -- The sonar transducer is in constant motion in the vertical direction. Theoretically, even when the vertical beam-width is very narrow (around 1°), the area of illumination on the iceberg surface will have a vertical dimension of about 1 m at a distance of 50 m from the iceberg. This vertical motion is such that the reflected signal may be coming from a lower or upper portion of the iceberg and not from the area opposite the transducer, depending on the direction of motion. For bottom surveys the normal technique is to resolve this problem for successive returns, but the transducer attitude error discussed earlier precludes the application of this technique here.

e) Detection Problems -- Towards the lower extreme of the iceberg, its surface slope is oriented at increasingly greater angles from the transducer, which presents two problems. First the slope may result in no energy being returned to the transducer. Second, the range to the

iceberg may increase dramatically resulting in non-detection because of weak signals or the sonar range setting being exceeded. Thus, even if the sonar transducer is oriented vertically there is a high probability that the iceberg draft will significantly exceed the measured value.

Previous techniques to measure iceberg draft have been designed essentially to measure draft only, and cannot be deemed adequate and acceptable for the present purpose. The preceding discussions demonstrate that the technique currently in use is, at best, a crude measurement (and in all probability an underbiased measurement) of draft subject to considerable errors. Any attempts to derive shape information is of questionable value. The measurement of the underwater dimensions of an iceberg in sufficient detail and accuracy to reconstruct its shape must be treated as a survey problem. A new approach is required which either eliminates, or attempts to account quantitatively for, the sources of error described.

USER REQUIREMENTS

From discussions with the offshore oil and gas industry and the scientific community, it appears that there are four main usages of underwater iceberg geometry data.

a) Iceberg Trajectory Models -- One critical element in all deterministic iceberg trajectory models has been the determination of the underwater shape and draft of icebergs, parameters essential for the calculation of drag coefficients.

b) Structural Engineering Design -- In regions where collision between an iceberg and a structure is a possibility, the depth at which collision will occur and the characteristics of the iceberg's underwater shape are of prime concern to the design engineer. Therefore, it is necessary to determine depths at which contact is likely to occur and to describe the three-dimensional shape of the collision surface.

c) Scour Modelling -- In regions where it is required to protect bottom structures and submerged pipelines from iceberg scouring, it is necessary to know the characteristics of the bottom portion of the iceberg's keel. This knowledge will allow good estimations of the

maximum scour depth and resulting pressure distribution into the surrounding sediments.

d) Operational Subsea Threat Assessment -- In an operational situation (exploratory or production) it is necessary to be able to determine the threat to a well-head structure. Therefore, an accurate measurement of the draft is required to assess the threat and to minimize the potential for false alarms.

System requirements to generate these data sets differ considerably. The trajectory models require that the system generate an accurate cross-section of the underwater portion of the iceberg with no emphasis on its detailed morphology. The structural design engineer is interested in the detailed morphology of icebergs in the vicinity of any structure, and thus requires a high degree of accuracy in generating a three-dimensional model of their underwater shapes. Also, the area of interest on the iceberg's surface differs; to protect bottom installations from scouring, knowledge of the bottom portion of the iceberg is essential, whereas for collision protection, contact is more likely to occur near the mid-water depth of the iceberg.

To determine user requirements for a system capable of obtaining three-dimensional underwater measurements of icebergs, a brief questionnaire was forwarded both to the offshore oil and gas industry and to the interested scientific institutes. A tabulated copy of the questionnaire is enclosed in Appendix 5. Generally, the offshore industry is interested in developing such a system although its urgency has diminished somewhat because little exploration activity is planned for the Labrador Sea and the Arctic in the immediate future. Consequently, a system that is able to measure the iceberg's draft in real-time and to generate the iceberg's underwater geometry in non-real-time is required. The same system might also be capable of performing other tasks such as locating well-heads and other bottom structures.

Based on discussions held with industry representatives the following preliminary specifications are proposed as guidelines for the system design:

- system should be portable and transportable by aircraft, if possible, although this is not essential;

- mobilization of the system should take a maximum of one day;

- real-time iceberg draft should be measurable within one hour;

- three-dimensional measurement should be complete within four hours, although generation of the iceberg model could take place after the field program;

- system should be operational in Beaufort 5 sea conditions;

- system should have an accuracy of 5% for all essential parameters, such as, draft, mass, and cross-sectional shape;

- maximum acceptable downtime is one or two days per month, so reliability and durability of the system should be very important;

- operations should be performed by one technician with the assistance from the vessel's crew;

- daily operational costs should be minimized as high costs will only be considered if significant improvements in measurement are made;

- system should be able to operate in water depths to 300 m.

- system should be deployable in the meteorological and oceanographic environments prevalent in the Grand Banks area, Labrador Sea, Davis Strait, and Beaufort Sea.

- system should be operable when deployed 100 m from the iceberg as support vessels will not usually approach an iceberg closer than 100 m or, in some cases, 50 m; and

- all system monitors should be located on the bridge to ensure excellent communication between system operator and the vessel's master while undertaking potentially hazardous manoeuvers around an iceberg.

PROBLEM DEFINITION

The objective is to develop a conceptual measurement system (or systems) capable of mapping the underwater shape of an iceberg. To locate any given point on an iceberg within a known accuracy relative to an established three-dimensional frame of reference is a significant problem when the physical situation is considered. Three bodies come into play: the iceberg, the vessel, and the sensor package. The iceberg is usually very large in comparison to the vessel, is potentially

unstable, may roll or break up at any given time, and moves in an unpredictable (although usually slow) pattern of rotation and drift trajectory. The vessel motion is controllable to some extent, but, except in very calm seas, is subjected to significant motion in terms of the accuracy required. Also, the vessel is moving independently of the iceberg. The sensor package, once deployed underwater, will not be seen visually and is again subject to motions virtually unrelated to the other two bodies (even though it may be tethered to the vessel). Not only is knowledge of its position essential but also its rate and direction of movement around that position, and the attitude of the sensor itself ("look" direction).

Thus, the three bodies, although, close in proximity, exhibit characteristics of virtually independent motion. There is no fixed, land-based, reference point from which to obtain accurate positional information for each body or for any point on one of them. The iceberg, has a complex geometric structure and the condition of the ice surface itself is not condusive to positioning of objects upon it or to marking (besides the risk to personnel attempting to undertake such a task). However, to generate information on underwater shape, the data collected have to be referenced ultimately to a known point on the iceberg. If two or more points are required, their positions relative to each other must also be known. The vessel itself may be used as an intermediate point of reference.

To address the problem effectively and efficiently, the various fundamental aspects need to be investigated before considering an overall system approach. These include:

a) A sensor should be selected that can survey the iceberg in an acceptable time period (maximum four hours) with a known degree of accuracy.

b) A reference system should be established on the iceberg.

c) The sensor system should be linked to the reference system such that an accurate position in relation to the iceberg can be calculated in absolute terms within a given co-ordinate system.

d) A deployment platform should be chosen such that will give the sensor as much manoeuverability as is required to complete the survey accurately.

e) The deployment platform should be stabilized or its motion should be monitored, sampled adequately, and recorded throughout the survey. Sensor attitude (or "look" direction) is a key requirement of this monitoring package.

f) An on board data acquisition, display, and processing system for the generation of the underwater shape is necessary.

Sensor Selection

It has been determined that deployment of the present side-scan sonar system in a vertical mode is not adequate for mapping the three-dimensional shape of icebergs. To date, alternate sensor techniques such as impulse radar, low-light optics, and electromagnetic sensors have not been investigated adequately. It is apparent from the industry survey that even with the most commonly used sensors for this type of application, the factors affecting the performance of an acoustic mapping system needs to be examined.

Establishment of a Reference System

One of the major reasons why the traditional method of generating three-dimensional shapes is impossible is that the sonar data have not been referenced to known points on the iceberg. Attempts have been made to measure the water-line distance from the vessel to the iceberg by both optical and radar methods. However, the measurements have been fraught with numerous operational problems and the readings obtained are of questionable use. Also, these range and bearing readings only determine the vessel's position relative to the iceberg and in no way could they be used to reference the acoustic sensor to the iceberg. Consequently, what is needed is the establishment of a reference system using a point on the iceberg as the origin such that all sensor range and bearing readings are related directly to a known base-line.

The establishment of such a reference system around the iceberg has numerous associated problems. At any one time the sensor must always be located via at least two known reference points on the iceberg surface to make the range and bearing readings valid. Consequently, the number of reference points is specifically related not only to the size of the iceberg and but also to the sensor range to the iceberg.

The attachment of reference beacons onto, and their recovery from, an iceberg is in itself a major problem, whether they are marks or active beacons of some sort. The motions of these beacons, if not taken into account, will lead to positional errors which are addressed later.

Integration of Sensor and Positioning System

Specifically to relate the platform location to the established frame of reference, all the positional information recovered from the platform, along with the sensor data, will require integration and time referencing. An acoustic system, for example, will require a sonar transducer to map the iceberg target and a transducer to detect the reference beacons. Each transducer will operate at different frequencies to avoid interference. Consequently, the deployment platform will have not only the sonar and positional transducers, but also the associated control electronics such that simultaneous readings can be obtained.

Deployment Vehicle Design or Selection

The selection of a deployment vehicle will depend to a large extent upon the selected sensor and positioning systems. The options available range from vertical deployment to the use of a remotely controlled vehicle. It is recognized that the vehicle must have sufficient manoeuverability to complete the survey and that a trade-off between costs and overall system accuracy will have to be made.

Sensor Platform Motion Monitoring or Stabilization

Because the system requires that both the iceberg target sensor and the reference sensor be located at the platform, motion monitoring or stabilization of this platform is essential to reduce measurement errors. Two approaches could be used; either use a stabilized sensor platform or monitor the platform motion and compensate for it in the processing. Both of these techniques, for which products are readily available, are used throughout the marine industry with each having inherent advantages and disadvantages.

Onboard Data Acquisition, Display and Processing System

The many data that will be collected at the platform originate from a number of sensors. Synchronization of data between sensors is imperative to allow cross-correlation and, consequently, to determine the iceberg's underwater shape. Because of the vast variety of signal and power sources these data will have to be sampled at appropriate rates and multiplexed for transmission to the vessel's data processor, ensuring no loss of data and minimizing cable costs.

As a minimum the onboard system should:

- provide the operator with sufficient information to locate the fish and to assess data quality
- record data at such a rate that no loss of data occurs
- provide a quick estimate of the iceberg's draft.

It is anticipated that the following data products will be required:

- three-dimensional contour view of the underwater shape of the iceberg
- contour plan view of any likely underwater collision surfaces
- cross-section views of the overall iceberg shape from any reference point.

Additionally, the data set on the underwater shape of the iceberg should be able to be incorporated into the data set obtained from a simultaneous survey of the above-water portion of the iceberg thereby completing the three-dimensional model of the iceberg.

EXAMINATION OF SENSORS

A crucial part of an iceberg mapping system is the sensing device used to provide range measurement to the iceberg. To date, active acoustic devices have been used primarily and the suitability of other sensors has never been addressed adequately. In this section, a systematic analysis is made of a variety of sensing devices spanning a wide spectral range.

Using three general spectral regions -- acoustic, electromagnetic, and optical (or electro-optical) bands -- each is examined for potential sensors that may meet the necessary requirements of this application. A detailed theoretical assessment is undertaken where necessary, and the various parameters affecting the overall performance and accuracy are addressed. These include, but are not limited to, range of operation, propagation problems, resolution cell size, and motion effects. Many details are relegated to Appendices 6, 7, and 8.

SENSOR OPERATIONAL RANGE AND RESOLUTION REQUIREMENTS

To assess the utility of the various sensors certain required specifications have to be established. The design and operational criteria dictate that the accuracy of the essential parameters, such as, the draft, mass, and cross-sectional shape, should be 5% or less. Also, it is required that the sensor package be deployable 100 m from the iceberg at the surface as well as having the capability of operating to a depth of 300 m. For the purpose of sensor evaluation, it is assumed that icebergs will have maximum dimensions of 300 m. Using the preceding, it is possible to derive resolution and range requirements for the sensor package. If the volume is to be measured to within a 5% accuracy, any linear dimension must be measurable to within an accuracy of 1.64%. For a spherical iceberg having a diameter of 300 m, the resulting possible dimensional error in diameter is ± 4.9 m. For a spherical iceberg having a diameter of 10 m, the allowable dimensional error is ± 0.165 m. During an actual measurement the errors may average out and the net error will be much less than the maximum possible, and for this reason, sensing devices giving less measurement accuracy may still be acceptable.

Again, considering the largest iceberg to be spherical with a diameter of 300 m, the requirement that the sensor package be deployed 100 m from the iceberg at the surface, necessitates

that it have a maximum detection range of 206 m to detect at the maximum draft location. Because of incidence angle problems the sensor would have to be deployed to a depth below this point and a more realistic maximum range of detection would be about 250 m.

ACOUSTIC SENSING

Resolution and Range Considerations

The resolution and maximum operating range requirements determine the acoustic system pulse length and beam-width necessary. For a spherical iceberg having a 10 m diameter, the accuracy required is $\pm$0.165 m and translates to a pulse length of approximately 0.2 ms. The beam-width required depends on the maximum range. For the largest iceberg this figure is 300 m and for a maximum error of 4.9 m, this translates to a beam-width of about 0.9^{o}. For the 10 m iceberg (assuming a 100 m range) the beam-width required is about 0.095^{o}. Thus the pulse length and the beam-width requirement for the largest iceberg are technically feasible, whereas the beam-width requirement for the 10 m iceberg is probably not achievable.

The tabulation of the errors associated with acoustic ray bending (see Appendix 6), shows that positional and range errors could be in the order of metres, unless the acoustic velocity profile is known precisely and can be accounted for, which is probably not the case. Realistically, errors associated with the uncertainties could be in the range of 1 to 3 m. The practical limitations preclude the need to design a sonar system to meet the accuracy requirements detected. Thus, a pulse length in the range of 1 to 4 ms and a beam-width of around 1^{o} are all that is necessary in practice. These ranges are quite adequate to meet the accuracy requirements for the largest iceberg but will give a considerable error in the case of the smallest iceberg.

Having established that the accuracy requirements can be met at least for the larger icebergs, (using the pulse length of 1 ms and beam-width of 1^{o}) it is necessary to examine the other sonar characteristics needed to undertake iceberg profiling.

System Consideration

Operating frequency. The band-width of a standard sonar system using pulsed continuous wave (CW) is determined by the pulse

length (1 ms) which, in this case, is 1 kHz (see Appendix 6). Usually, the operating frequency is at least a factor of ten times the band-width and thus, in this situation, will be 10 kHz. The lower limit on the operating frequency has now been established.

The upper limit on the operating frequency is determined primarily by the maximum operating range, which is in turn a function of transmission loss, the target strength, and noise levels. The transmission loss is inversely related to frequency (see Appendix 6), whereas the reflection coefficient (which is a key parameter in the target strength determination) is independent of frequency. Figure A-10 in Appendix 6 shows the various sources and levels of noise as a function of frequency. Minimum noise levels can be expected at 100 kHz under normal conditions whereas at higher frequencies thermal noise becomes a dominating factor (see Appendix 6).

In considering transducer size considerations, a frequency higher than 40 kHz is attractive. For a given conical beam-width a 100 kHz transducer will be a factor of 2.5 smaller than that of a 40 kHz unit. Detection ranges of 250 m have been achieved using 100 kHz systems during routine measurements of iceberg draft. Therefore, the maximum operating range of 250 m should easily be achievable with a 100 kHz system, which, in practice is likely to be the upper limit for the transducer size.

A lack of measured data on the acoustic back-scatter of icebergs limits the confidence in which a given optimum frequency can be selected as well as the actual maximum range of detection that can be achieved.

Source level requirements. The source level limitations are dictated by the onset of cavitation at the high end and ultimately by the operating range requirement on the lower end of the source.

Most commercial systems operate at an upper limit of 225 dB re 1 μ Pa (decibels relative to one micropascal) and this has been identified as an exceptable upper limit. Sidelobe levels may pose some problems, but certain techniques can be used to reduce them significantly (see Appendix 6).

The lower limit is dependent on a number of factors including the target strength, the transmission loss, and the ambient noise level. These factors translate to the maximum range at which the sonar system will detect the iceberg. Most high-frequency (50 to 100 kHz) sonars have maximum operating source levels of around 220 dB re 1 μ Pa. It is therefore felt that the source level should be maximized with its lower limit being in this range.

Beam-width. One problem with any standard sonar system beam pattern is the presence of sidelobes, which are secondary lobes produced by the transducer or transducer array. These lobes radiate energy in directions other than that of the main beam. If there is sufficient energy in these lobes, reflections from their directions will cause ambiguities in the profile measurements. Sidelobes may be reduced by adjusting the transmitting characteristics of each element of an array (shading).

The use of parametric sonar to produce a beam pattern virtually sidelobe free was investigated. This source allows a narrow beam to be produced by a small crystal. However, the signal-to-noise ratio is significantly lower than for a conventional source. The highly directional beam advantage is produced at the expense of poor energy conversion. Thus, signal strength is ultimately a deciding factor in favour of a more conventional system because a narrow beam transducer can still be produced through careful design and operation in the high-frequency range of 100 to 500 kHz. The stronger signal will be an important asset in being able to discriminate true echo returns from the surrounding effects of ambient noise.

It is now possible to produce beam-widths in the range of 1.0^{o} (as specified earlier) and shading techniques can be employed to reduce the undesirable effects of sidelobes.

Pulse length. The requirement of a 1 ms pulse length is well within the capability of standard technology. In fact a 0.1-ms pulse length can be generated for the higher-frequency systems.

Wideband "chirp" or coded pulses can also be employed to generate much smaller resolutions even though the pulse length itself can be very long in time. These require sophisticated processing capability and are assumed to be unnecessary in this application.

Other Factors Effecting the Performance of an Acoustic Sensor

Iceberg surveying time. Iceberg mapping can be accomplished by repeated soundings. For an iceberg of 200 x 200 m and an assumed average sounding density of one sounding per square metre, 40,000 soundings are required. For a conventional sonar operating at a distance of 200 m from the target, each sounding requires 0.27 s using the two-way travel time. Therefore, about 3 hours is required to complete the survey. In practice, more than one sounding per point may be required and therefore the total survey time will be increased. However, sophisticated techniques can be used to overcome this problem.

Platform stability. Narrow-beam acoustic systems require special considerations be given to the platform stability. For a beam-width in the order of 1^{o}, the angular motion of the platform during the two-way pulse travel time may easily exceed the system beam-width. This motion will cause beam misalignment if both the transmitter and the receiver have narrow conical beams.

During the iceberg mapping, sensors should be used to monitor the motion of the platform and the profiles obtained should be corrected accordingly. This approach may be more feasible than trying to stabilize the platform.

ELECTROMAGNETIC SENSING

Radio echo-sounding is an active electromagnetic sensor which has been deployed on helicopters and used to measure maximum iceberg draft. The earliest application of this technique was in the measurement of glacier thickness and since then it has been used to sound of peat bogs, and to measure the thickness of permafrost, sea ice, and iceberg draft. Appendix 7 provides a description of the principles upon which the various relevant systems operate and an assessment of the radio echo-sounding technique as a practical tool for this purpose.

It appears that iceberg draft measurement is possible through radio echo-sounding of Arctic icebergs. More testing and improvement is required to make the technique operational. The determination of the underwater shape of an iceberg using radio echo-sounders or impulse radars appears considerably more complex and difficult, requiring a significant effort. Also, the accuracy of such measurements, which has yet to be determined, may not be adequate to suit the requirements stated.

Optical Sensors

A study of the literature regarding the measurement of iceberg draft and underwater shape indicates that optical techniques have not been employed to obtain this information.

Optical sensors include photo-optical sensors, such as conventional cameras, and electro-optical sensors, such as a regular television or a low-light-level television (LLLTV). In addition to these passive sensors, optical sensors also include active sensors such as a Lidar (laser radar) and an active TV or LLLTV (e.g., laser-gated LLLTV). Some of these sensors have been used underwater, mostly for photographic or visual inspection work.

The successful use of optical sensors is dependent on the availability of sufficient illumination relative to the sensitivity of the sensor under consideration. For passive sensors, the illumination can be provided by such artificial sources as lasers. In either type of sensor, the underwater application is largely dependent on the attenuation coefficient of water, which determines their range or distance of operation. The light available at the water surface and its subsequent attenuation with water depth is of prime interest in the operation of passive sensors. For active sensors, the main concern is the provision of enough energy to overcome the anticipated energy attenuation in water.

Several other factors determine the practical feasibility of an optical sensor to provide underwater dimensional or shape measurements, including: for example, field of view; resolution; scanning time and detector response time; scene and image stability (target, sensor, and background motion); image display and image recording; and data processing to deduce dimensional or shape parameters of a target in an efficient and accurate manner. Because some of these factors are interrelated, considerable trade-offs are involved in their selection.

A detailed examination of the factors affecting the performance of optical sensors for underwater iceberg shape determination is provided in Appendix 8. A summary of the crucial results are presented in the following section.

Passive Optical Sensors

A detailed theoretical analysis of the maximum detection range capability of passive photo-optical (camera and film) and electro-optical (LLLTV) system shows that at a depth of 10 m, ranges of 10 m and 40-50 m, respectively, are achievable. This range decreases with depth and this restriction virtually precludes the use of passive optical sensors. Also, such devices need an independent measurement of range (with another sensor) to provide the capability of making quantitative measurements. It is noted that the ability to provide an image may make such devices attractive as interpretative tools to be used in conjunction with a profiling sensor.

Active Optical Sensors. Active optical sensors use a laser or some other artificial source of light to illuminate a target (in this case only a laser is considered). The active optical sensors investigated were the lidar and the active LLLTV. There follows a summary of the results of a detailed analysis which is provided in Appendix 8.

Lidar. Lidar (light detection and ranging) is an active system as it supplies its own energy with which to illuminate the scene or target and measures the energy reflected or scattered back from an object. Thus, Lidars are not dependent on ambient light conditions or natural sources of illumination. The energy in lidars is traditionally provided by a laser (an acronym for light amplification by stimulated emissions of radiation), although other artificial sources of radiation (such as a lamp) may be used as well. Lasers provide optical radiation which is monochromatic (at one wavelength or within a very narrow wavelength band) and is coherent. These properties provide several advantages and lasers have been used in numerous applications.

Lidars are also known as laser radars. Lidars are more suitable for underwater applications because lasers provide radiation at optical wavelengths (at which there is low attenuation in sea-water) relative to microwave wavelengths available with conventional radars. Because of their short wavelength or high frequency, very small beam-widths (angular resolution) and small pulse lengths (time or range resolution) are possible with lasers. Moreover, being active sensors lidars provide a direct and accurate measure of range or distance between the target or object and the sensor.

A lidar sensor is subject to the same detection range restrictions as a passive LLLTV system. Although it easily meets the beam-width requirements (0.05^{o} is achievable) and its range resolution capability is at least comparable to that of the acoustic sensor, this range restriction virtually eliminates it as a potential profiling sensor.

Problems similar to those that may be encountered using an acoustic sensor are also common to a Lidar system. These are the problems with sensor motion (platform stability) and the long time needed to map the shape using conventional techniques.

Active - LLLTV. Unlike a radar, the low-light-level television (LLLTV) is considered as both a detector and a receiver. The main advantages offered by such a system are the relatively wide fields of view, but small resolutions, and the ease of video image generation, display, and recording. such an active imaging system has been considered before (Juliano and Bricks, 1976). The back-scatter from the intervening medium (sea-water), as in any other active system, is not a problem because of the pulsing of the laser and the gating of the LLLTV, so that it detects a return signal only from a limited range

around the target of interest. Appendix 8 contains a detailed evaluation.

As with the Lidar, a laser-gated LLLTV is limited to a maximum operational range of about 50 m. Its resolution is comparable to that of a lidar and the wide field of view virtually eliminates the problem of sensor stability. Some development work is necessary to expand the divergence of the laser beam to fields of view between 50^{o} and 90^{o} and to ensure uniformity of laser illumination and high average power within such a large field of view. This necessary development work and the limited range of operation results in this sensor being unattractive as an underwater profiling device.

DISCUSSION OF SENSORS

Clearly, an acoustic sensing system can be designed to obtain iceberg underwater shape information, although the accuracy requirement can only be achieved with the larger icebergs. Significant errors (up to 30%) in the volume measurements of small icebergs are possible.

The performance prediction of a system cannot be assessed reliably without measured data on iceberg back-scattering and the acoustic velocity profile regime in the immediate vicinity of an iceberg, both of which necessitate a field measurement program. Velocity variation can be corrected if it is measured during the determination of an iceberg shape. However, the velocity profile may vary spatially, in which case corrections based on one vertical velocity profile may be insufficient.

The discussion on surveying time requirements using conventional methods suggests that new or innovative techniques for drastically reducing the survey time need to be employed.

Platform motion is also shown to present a significant problem in the determination of look direction and misalignment of the receiving transducer with the direction from which reflected energy is returning. Again methods must be employed whereby these problems are eliminated.

None of the sensors investigated can provide both the resolution and range requirements necessary. The only sensor that is proven operationally and has the capability of at least partially meeting the resolution requirements is the acoustic sensor. It is concluded therefore that the acoustic sensor is the only device with the potential to perform operationally in determining the underwater shape of icebergs.

There are some problems that still need to be overcome to produce an operational unit. These are the long time required to map the iceberg using conventional methods and platform motion. Both have to be addressed in a system design.

POSITIONING SYSTEMS

In defining the problem of three-dimensional mapping of the submerged portion of an iceberg, it was stated that the data collected by a remote sensor package must ultimately be referenced to a fixed point on the iceberg. The system approach to the problem identified several aspects to be considered here:

- a reference system must be established on the iceberg;
- the sensor system must be linked to the established frame of reference; and
- the positioning system employed must be operable when deployed about 100 m from the iceberg with maximum operating distance of about 400 m.

Previous attempts to determine the geometry of the underwater portion of an iceberg usually employed a spinning side-scan sonar deployed from a survey vessel. In general, little success has been achieved, mainly because of the inability to specify the position of the sensor package in a frame of reference fixed to the iceberg. In past surveys, it was necessary to assume the location of the sensor with respect to the ship and the attitude of the sensor in relation to the iceberg while attempting to maintain the vessel motionless relative to the iceberg. Optical range finders, ranging on natural cracks and crevasses on the iceberg or dye markers applied with an archers bow and arrow have been employed to maintain vessel position. Radar ranges have also been used but have been found to be less reliable than the visual method.

Acoustic sensors have already been recommended for mapping the submerged portion of an iceberg. Acoustic positioning systems are also recommended for defining the iceberg frame of reference and for specifying the position of the hydrophone array within that frame. Two options are available: either the position and attitude of the sensor package can be linked directly to a frame of reference established on the iceberg, or the sensor can be referenced to the position of the survey vessel which is known accurately with respect to the iceberg. As background, the following section contains a general discussion of acoustic positioning systems.

ACOUSTIC POSITIONING SYSTEM

Three basic types of acoustic navigation systems are available today. The salient attributes of each system were described recently by Langford (1984). These systems are classified as:

. super-short base-line (SSBL) -- approximate frequency range 60-120 kHz

. short base-line (SBL) -- approximate frequency range 16-36 kHz

. long base-line (LBL) -- approximate frequency range 8-16 kHz.

General characteristics, accuracies, and equipment of these systems are discussed in the following sub-sections.

Short and Super-Short Base-Line Systems

Short-base-line (SBL) systems generally use a single transponder on the seafloor or on the object to be tracked and an array of hydrophones consisting of two to four sensors deployed about the hull of the surface vessel. Measurements of the slope distance and bearing to the transponder are made using phase comparisons of the signal received at each of the hydrophones (Figure 8). Super-short base-line (SBL) systems employ a single hydrophone containing multiple receivers, which may be deployed on the survey vessel or on a towfish; the position relative to the transponder is determined using phase comparisons as with the short base-line systems. In operation, both systems may employ pingers or responders rather than transponders. Figure 9 illustrates various configurations of these systems. The operational range of either of these systems is limited to about 1,000 m.

Primarily, SSL and SSBL systems are used to locate and re-locate drilling units over well heads for dynamic positioning, to track submersibles in diving operations, to position objects being lowered to the seabed, to position points along a seismic streamer, or to navigate within limited distances from the seabed transponder. They are also used in pipe laying, dredging, and salvage operations.

Hydrophone sensor positions are determined relative to the transponder by signal incidence angle, slant range, and depth. In operation, position is established by measuring two angles relative to the frame of reference of the hydrophone array

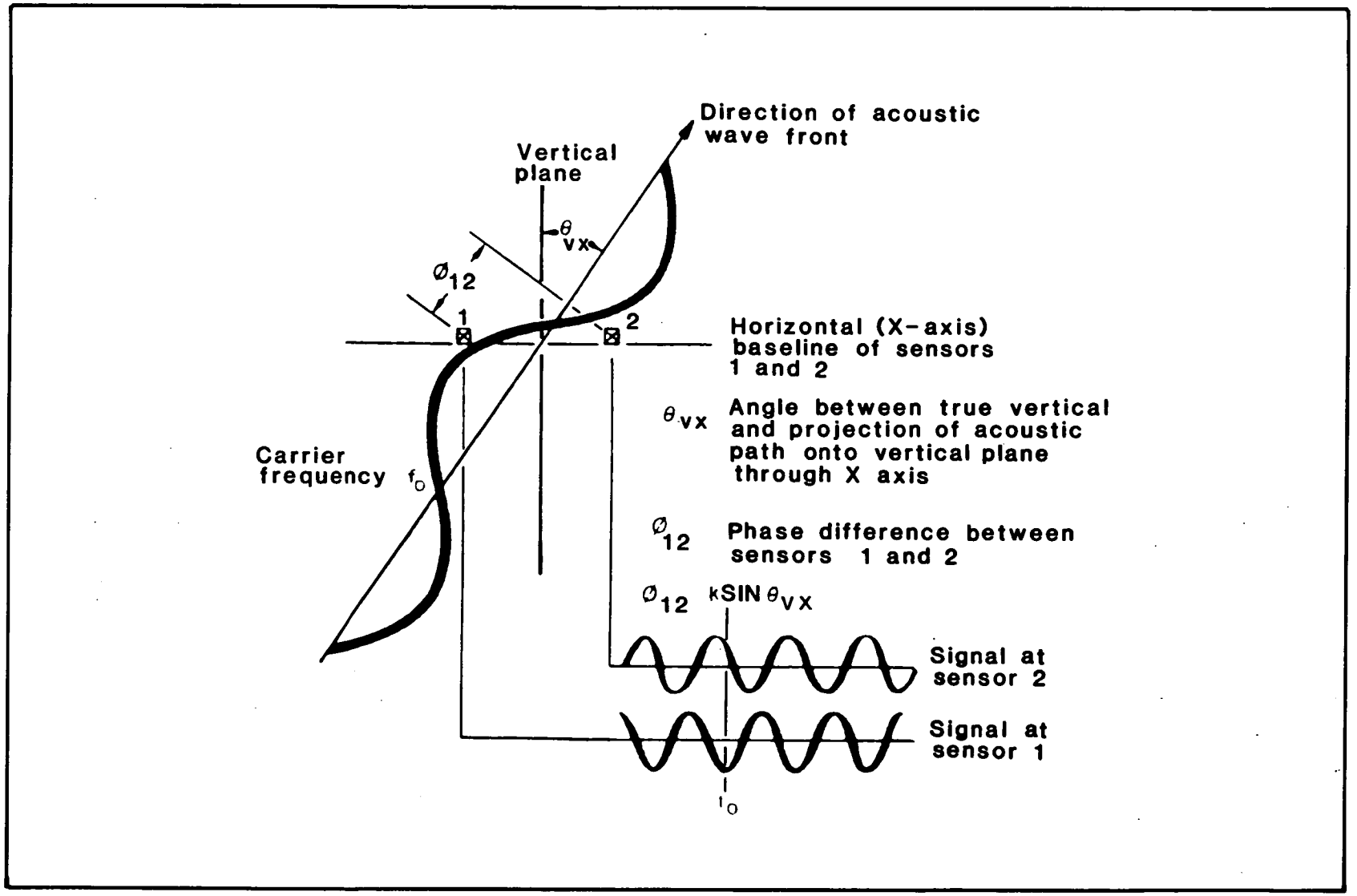

Fig. 8. Phase relationship of an acoustic wave at the hydrophone.

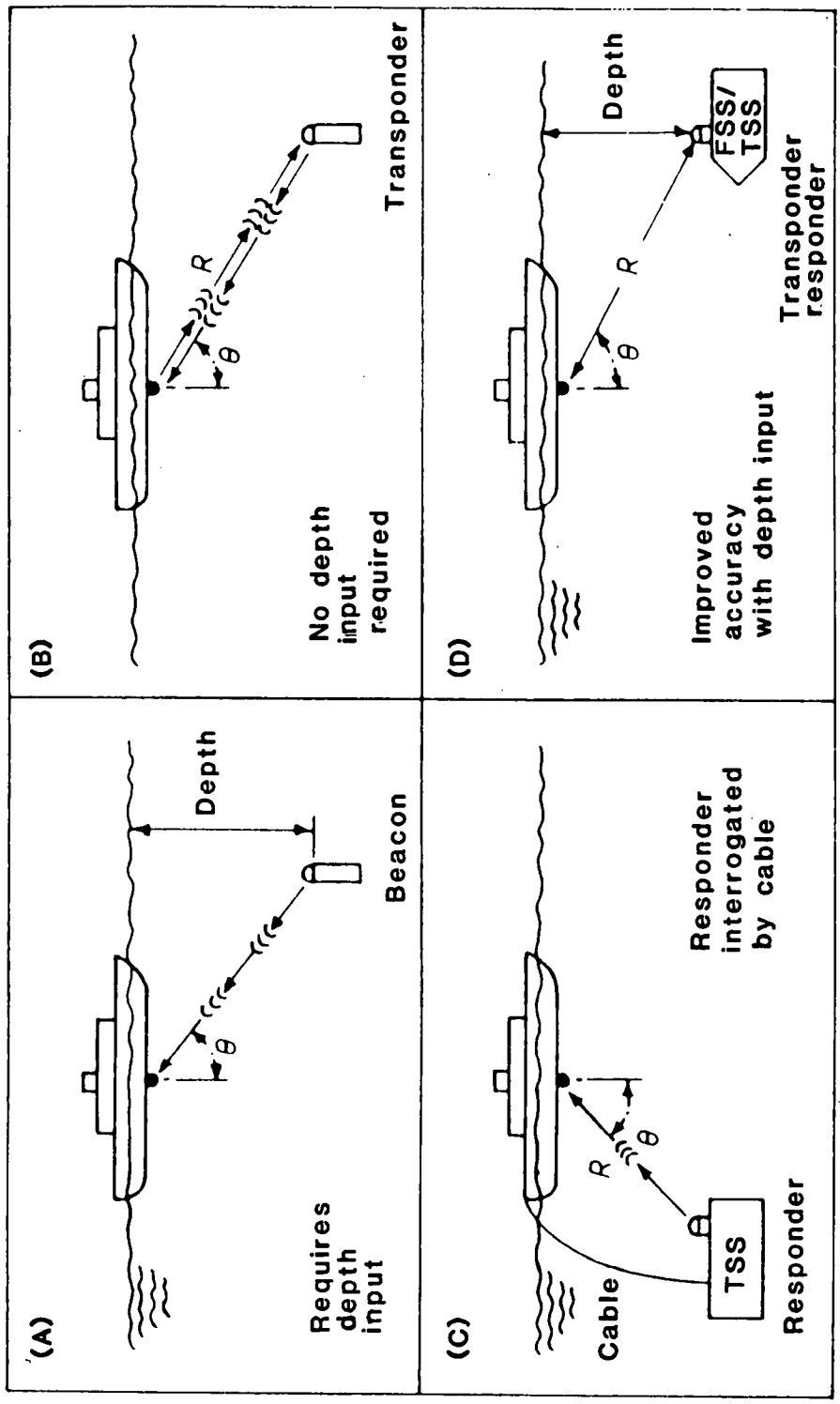

Fig. 9. Short base-line modes: (A) pinger mode; (B) trans ponder mode; (C) responder mode; and (D) transponder/ responder mode.

(angles θx and θy) and the slant range (R) as shown in Figure 10. The importance of establishing accurately the depth of the transponder on the position determination is illustrated in Figure 11 in relation to uncertainties in measurements of vertical angle of incidence and slant range.

Accuracies of these short and super-short base-line systems are reported to be generally 1% of the water depth up to horizontal offsets equivalent to water depth and 2% up to twice the water depth of horizontal offset. At greater offsets, accuracies drop off dramatically (Langford 1984). With operating frequencies of 100 kHz at distances of 180 m accuracies of $\pm$ 5 cm are reported for super-short base-line systems ranging on several transponders. For short base-line systems with an operating frequency range of 19 to 36 kHz, accuracies of $\pm$ 20 cm can be achieved over the same distance. To obtain these accuracies measurements of temperature, conductivity, and depth are required to apply sound velocity corrections to the results.

Errors and corrections to which acoustic measurements are subject, besides salinity and temperature of the water column, are vessel roll and pitch, hydrophone offset from the vessel reference point, and transducer offset from the reference point.

With a fixed hydrophone or hydrophones some element of uncertainty exists with the primary measurements which have to be resolved mathematically. However, with the advent of electronic beam steering coupled with mechanical training of the hydrophone, higher accuracies at longer ranges are achieved. This latter development is of significant benefit when operations require the tracking of manned or unmanned submersibles. In this technique, a series of narrow acoustic beams is steered in discrete steps from the surface to the nadir out to about 45° on each side of the centreline. Beam steering in a particular direction is performed by inserting delays at the different transducer elements to compensate for the relative propagation delays of the acoustic signal arriving from that direction; then the signals are summed. In this procedure, the signals arriving from the particular direction are added in phase and are amplified, whereas signals such as noise and reflections are added out of phase and are damped. A mechanical training function is provided for the transducer which enables continuous tracking in the horizontal plane to be performed for one or more transponders.

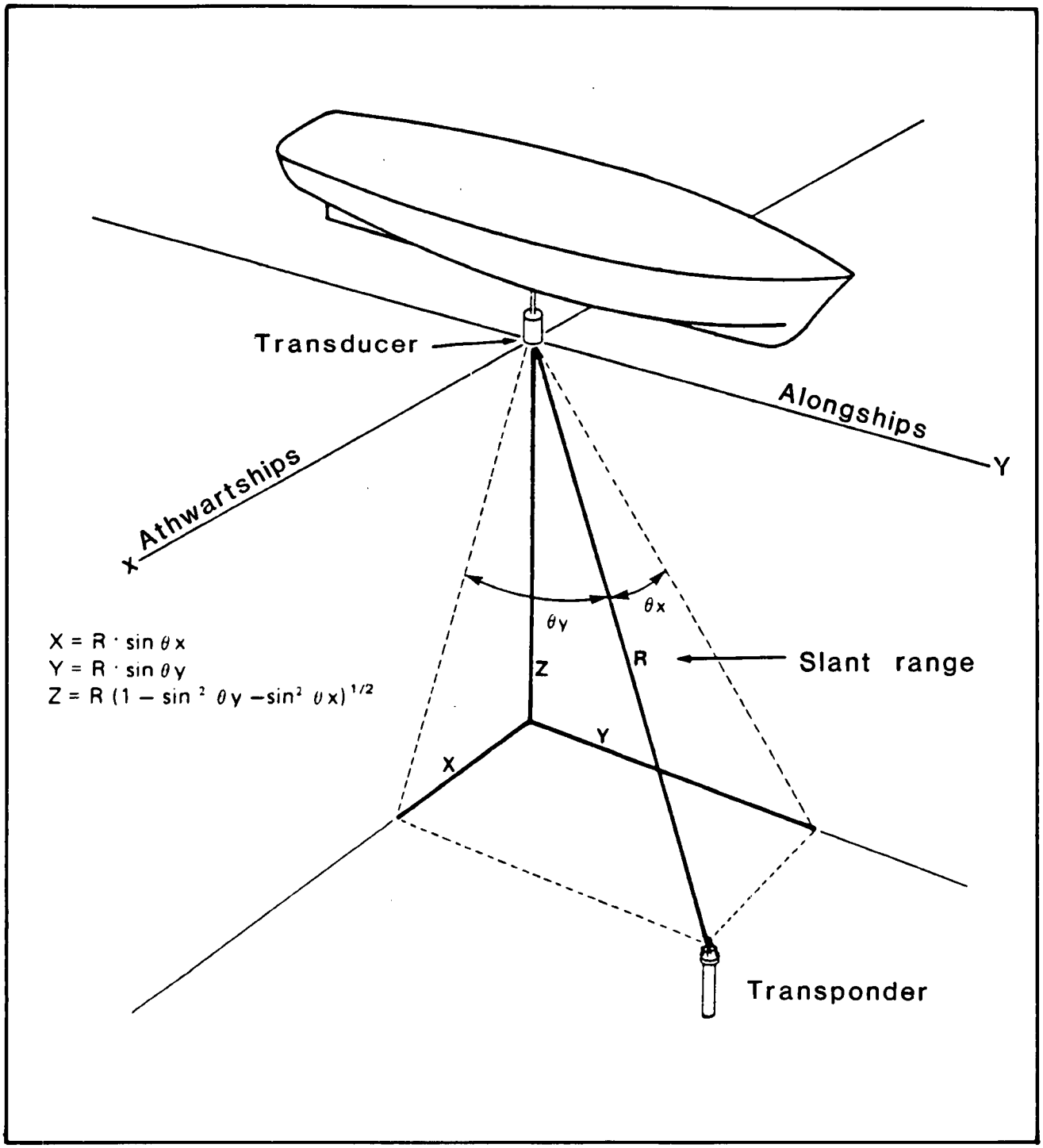

Fig. 10. Position determination in short and super-short base-line systems

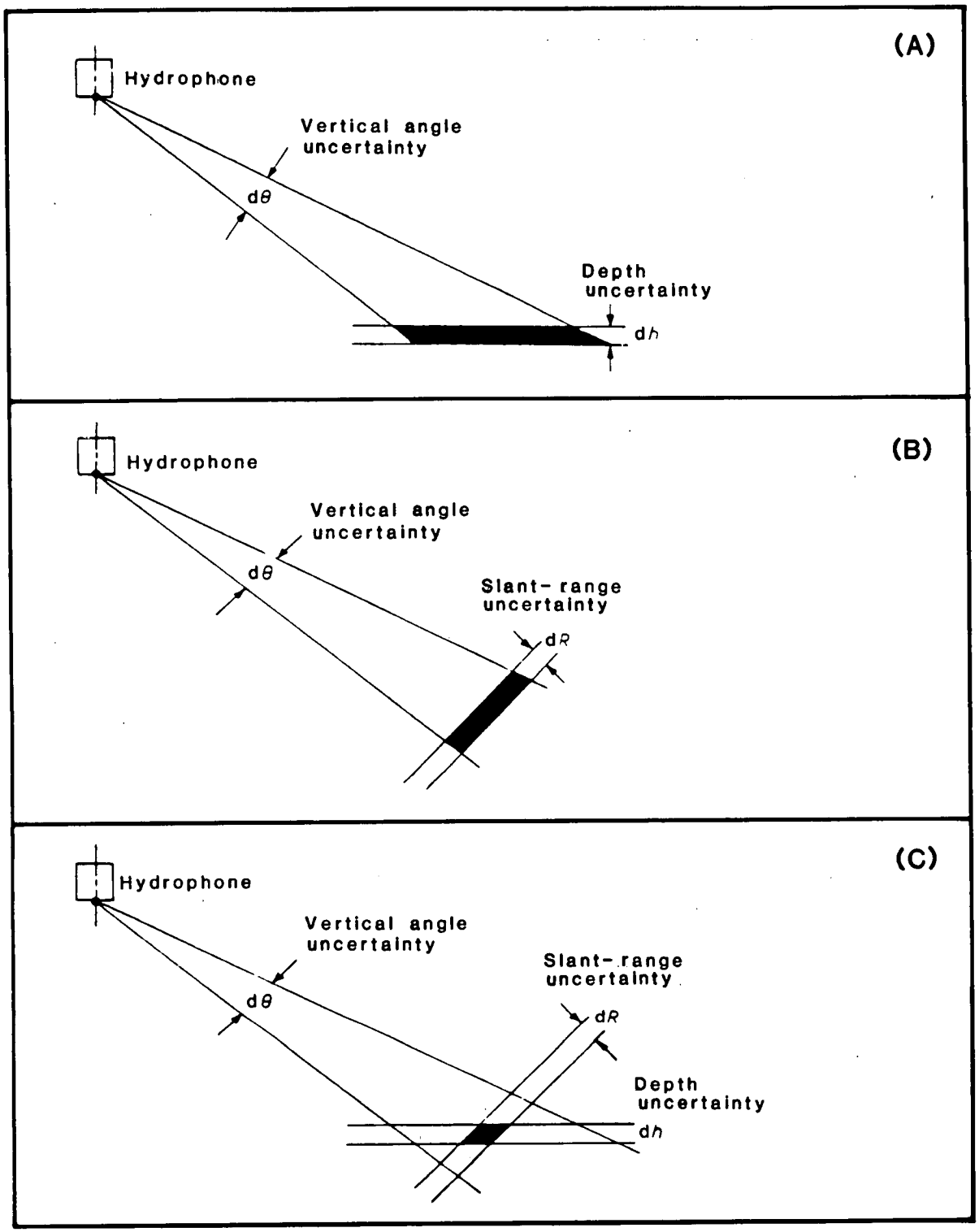

Fig. 11. Short base-line position determinations: (A) incidence angle and depth information (A-mode); (B) incidence angle and range information (T-mode); (C) incidence angle, and depth informatin (TH-mode) (after Neudorfev, 1978).

Long Base-Line Systems

The long base-line systems use an array of four or more transducers deployed on the seabed and a single hydrophone at the surface vessel which ranges to the transponders to fix its position in space. Besides covering most of the activities of a short base-line system, it can provide navigation at distances of 3-6 kms from the transponders. The transponders are normally set out in a grid configuration on the seabed to cover as large a portion of the area of interest as possible. Additional transponders may be added to this network to enable the surface vessel to navigate over a wider area.

The long base-line systems may be used as stand alone navigation systems, but are generally employed as back-up systems in situations where regular surface navigation cannot maintain the project accuracy requirements. As an example, a pipeline-laying operation may use a system in a "stand alone" mode, whereas the pipeline route survey may use an acoustic navigation system integrated with surface navigation techniques to improve the accuracy and reliability of the position data.

These systems are used for well-site surveys, pipeline surveys, pipe-laying operations, three-dimensional deep seismic surveys, and for general purpose positioning work in oil field operations.

In these applications, however, it is necessary to integrate the acoustic system to surface electronic, or to satellite navigation systems, or to both, to obtain the geodetic position of the transponders on the seabed. Subsequent positions acquired from the long base-line acoustic system are thereafter referenced to the geographical grid. Figure 12 illustrates typical geometry of a four-transponder, long base-line system. In Figure 13 the position measurement geometry of a typical submersible tracking operation is shown.

Transponder grid calibration. Intelligent transponders are currently available for use in long base-line systems. They enable self-calibration of the grid network to be carried out within one hour of system deployment. Some transponders are capable of measuring temperature and salinity at the seabed to correct measured distances to actual distances. With these units, determination of the geographic positions of two transponders using an external navigation system fixes the entire network. The transponder grid may also be calibrated by measuring base-line distances between transponders in combination with numerous ranges to all transponders from the

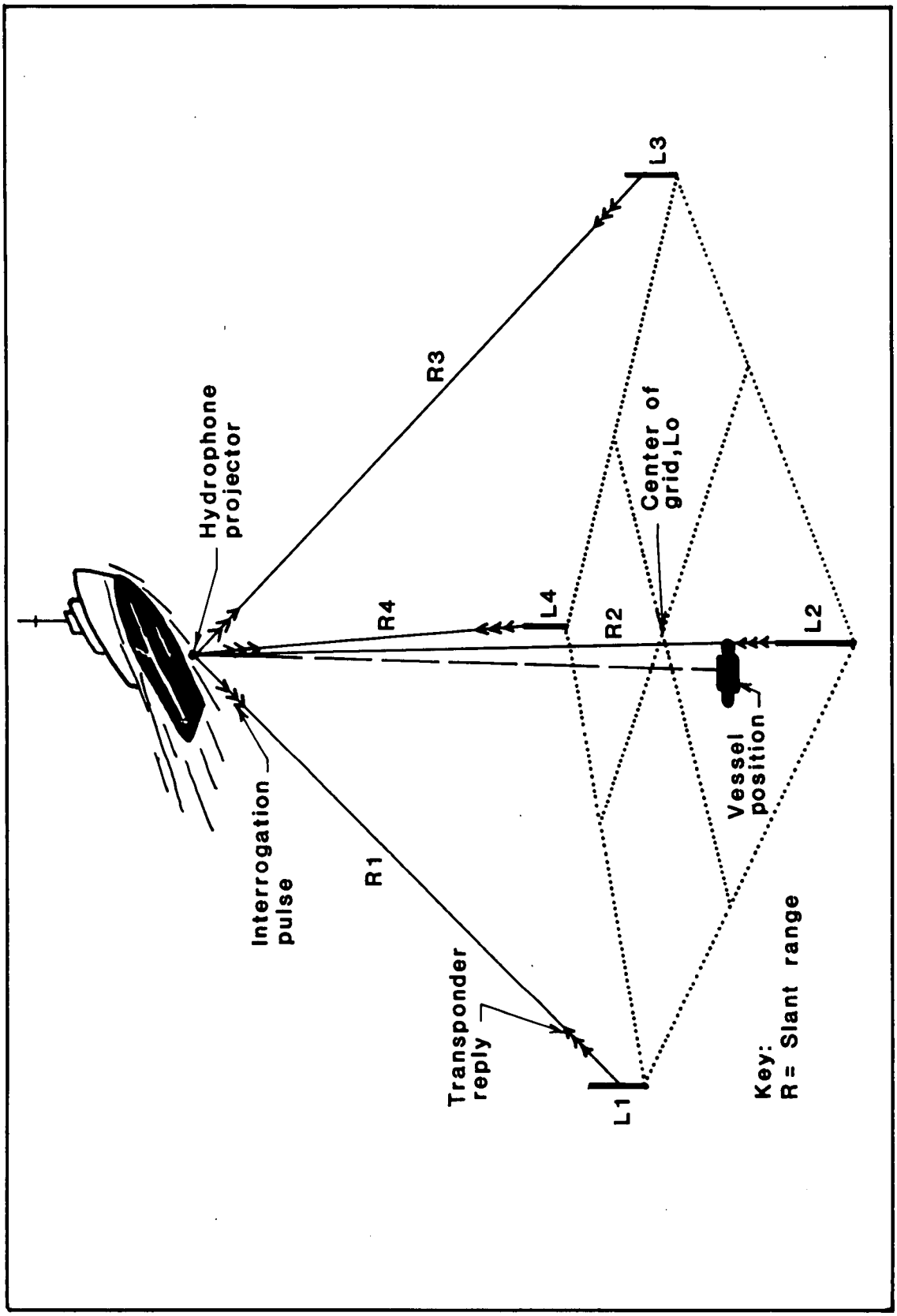

Fig. 12. Typical four-transponder, long base-line geometry.

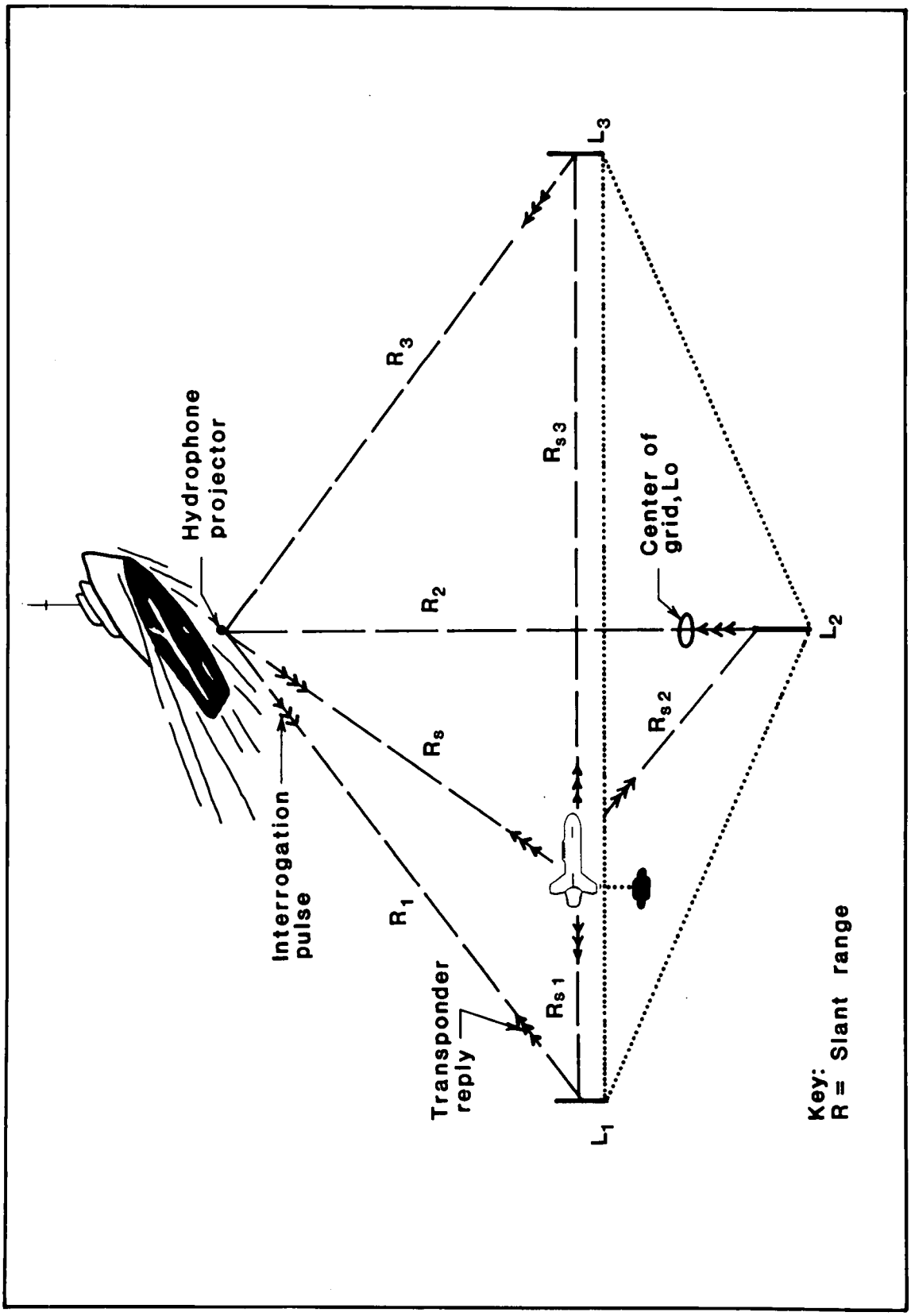

Fig. 13. Position-measurement geometry for typical long base-line submersible tracking operation.

survey vessel during random manoeuvering within the grid. Improved results with this technique may be obtained by steering the vessel directly over each transponder in the grid and measuring the depth accurately. The time required to calibrate a transponder grid using this procedure may exceed four hours. The shadowing of transponders as a result of seabed relief and turbidity of the water will adversely affect the grid network calibration.

Optimum calibration results require a carefully laid out grid network that avoids acute angles and extremely short distances between transponders combined with the use of intelligent transponders to establish quickly a preliminary calibration and range measurements obtained during field operations. These latter measurements can be used to adjust transponder location grid co-ordinates for a braced quadrilateral network using a least-square algorithm programmed for a microprocessor on board ship. For a two-dimensional fix, a minimum of four transponders is recommended; a good three-dimensional fix requires at least five transponders. Fix accuracy is directly proportional to the thoroughness with which the calibration of the transponder array is conducted.

Systems accuracies. Realistic accuracies of long-range acoustic positioning systems are reported to be about 1-3 m at a range of 3 km in Canadian waters (Langford 1984). The effective range is limited by attenuation of the acoustic signal by absorption mainly because of the conversion of kinetic energy of the sound signal to heat as a consequence of the viscosity of the water and to scattering of the signal by dissolved gases, air bubbles, and turbidity matter. System accuracy is influenced by ambient noise levels, surface and bottom reflections, and by acoustic refraction of the ray path.

Ambient noise in the oceans tends to be below 5 kHz. Therefore, the lowest frequency used with long base-line positioning systems is 7-12 kHz, which avoids spurious signals. Acoustic noise at the operational frequencies or their multiples is largely eliminated by electrical filtering. Similarly, the reception of multiple signals can be reduced and the correct signal identified through the means of signal discrimination circuitry.

Sound velocity varies both horizontally and vertically as well as with time within a stratified ocean because it is dependent on temperature, salinity, and pressure (Figure 14). Acoustic signal refraction can be accounted for by velocity corrections based on routine measurements of conductivity, temperature, and depth collected during the operating period. Overall accuracy of the system will be a function of the system calibration and error corrections applied as a result of the ambient oceanographic conditions during the survey period.

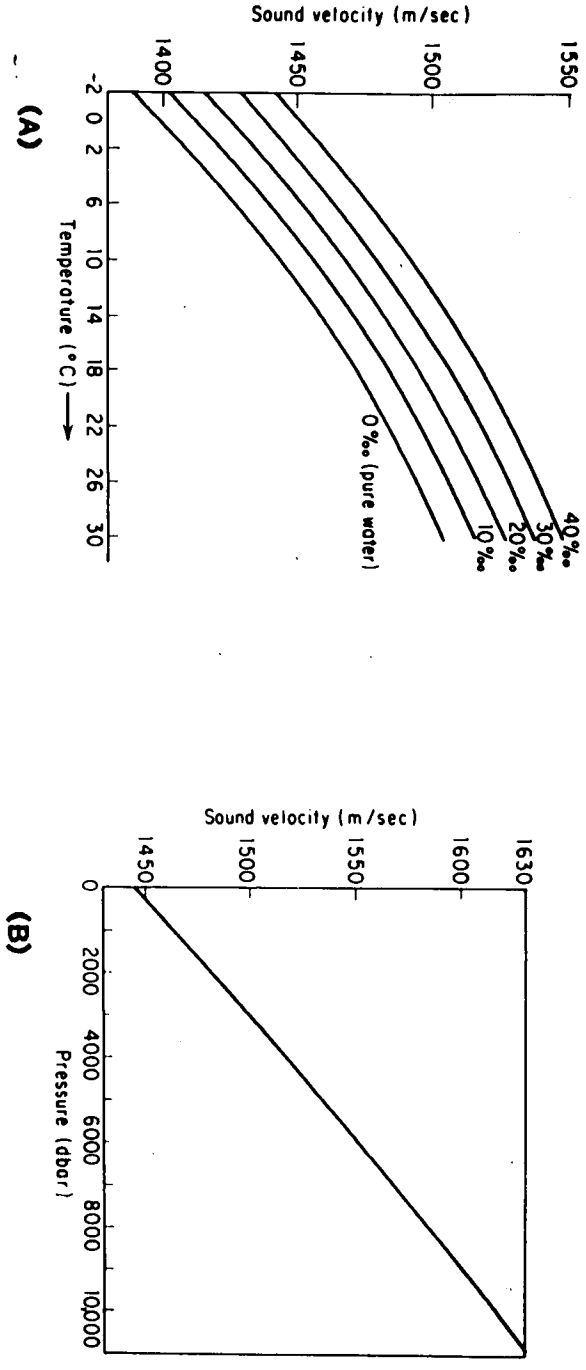

Fig. 14. Dependency of sound velocity on salinity, temperature, and pressure: (A) velocity of sound in pure water and sea water of different salinity at atmospheric pressure as a function of temperature; and (B) sound velocity in sea water of 35 percent salinity at $0^{\circ}C$ as a function of pressure.

System equipment components

In this sub-section, the various deployment modes for hydrophones are described and the general characteristics and uses of pinger, responders, and transponders are given.

Hydrophone. Four methods of hydrophone deployment are commonly used.

a) For super-short base-line systems, the multi-element hydrophone is commonly mounted on a rigid support within a sea chest inside the hull of the survey vessel. When in use the hydrophone is projected about 1-3 m below the ship's hull and retracted upon completion of the survey. Frequently hydrophones installed in this manner are directional, incorporating a trainable feature, which not only adds significantly to the range attainable but also provides the bearing of the transponder being interrogated.

b) Omni-directional or directional hydrophone arrays may be deployed on a rigid support over the side of the vessel and extended a few metres below the hull.

c) Omni-directional hydrophones may be hung over the side of the vessel supported on a connecting cable with or without a safety wire or rope.

d) The hydrophone unit may be housed in a tow-fish which is towed over the stern of the vessel. The tow-fish, which may weigh 100-250 kg, can be maintained at a reasonably constant depth below the ship's stern where ship- and sea-created noise is less of a problem.

To adjust the acoustic range measurements resulting from vessel movement, a vertical reference unit consisting of pitch and roll sensors is installed as close as possible to the centre of pitch and roll of the vessel. Altitude measurements from the unit are fed directly to the navigation computer; these measurements are of particular importance in short base-line operations where a high degree of accuracy is required.

Pingers. Pingers that transmit a continuous acoustic signal are used primarily in short-base line system applications having small horizontal offsets and a known depth. Usually, a multi-element hydrophone is employed to receive the signal.

Responders. Responders transmit acoustic signals when interrogated electrically through a connecting cable from the

tracking vessel. They are used principally for tracking tethered submersibles and yield better accuracy than acoustic interrogation. Once again, multi-element hydrophones are normally used to receive the signal.

Transponders. Transponders transmit acoustic signals upon acoustic interrogation from the tracking vessel and are employed for both short and long base-line positioning systems. With multi-element hydrophones, phase comparison is used to determine transponder range, whereas with a single-element hydrophone, a calibrated transponder network is used to determine positions.

Transponders with the capability to measure temperature conductivity, depth, and tilt are available, and when incorporated into the range computations, greater accuracy is achieved.

Acoustic Positioning System Comparisons

A summary comparison of some of the major components of various super-short, short, and long base-line systems currently available on the market is given in Table 3.

SURVEY CONTROL

Establishment of planimetric control of the transponder array fixed to an iceberg requires a series of acoustic bearing and ranges on at least three transponders concurrently as the survey around the iceberg is carried out. The usual practice in calibrating a transponder grid in a long base-line acoustic positioning system involves minimizing distance errors in a braced quadrilateral using a least-square software routine. The problem at hand differs in that distance measurements between transponders are not available because of the intervening ice mass; in this case, polygon side lengths and interior angles calculated from the range and bearing data are unlikely to close and will require a suitable adjustment scheme to determine the most probable co-ordinates of the transponders. Appropriate algorithms are required which can be built into existing software packages for on board processing of positional data in near real-time.

TABLE 3

Comparison of Acoustic Positioning Systems

System

	Acoustic Navigation & Positioning System	MARAC L/F	SONARTRACK II	ATNAV II	PAN/COMPATT	RS/906 Acoustic Position Indicator	HPR Hydroacoustic Position Reference System
SUPPLIER	OCEANO INSTRUMENTS	OCEONICS	SONARTECH WC	E.G. & G.	SONARDYNE	HONEYWELL (SBL-LBL)	SIMRAD (SSBL)
VESSEL UNIT	RM 201, 16 ch Receiver TT 101, Telecommand Unit AM 1X1, Acoustic Module RX/TX X'ducer	019A Oceanlink Ranging Unit, 12 ch, Switching Unit, X-ducer. Millisecond or tenths, Display 4 rng.	NS-011, 16 ch Receiver, DP-010, Position Processor. Tow Fish X'ducer.	706 16 ch. Rang. Recvr. 701, Digital Acoustic Command System 702, X'ducer Tow hous.	PAN 7145 Type, Program. Acoustic Nav. Recvr, Tx Command Module, Microcomputer driven, 4 Rng.	Display, Sig. Processor Pwr. Amp V.R.U. Hydrophone Projector 18 ch.	HPR 309 Display/Control Unit Transceiver HPR 300, VRU, X'ducer Assy.
OPERATING FREQUENCY	8-16 khz	Tx 9-11 khz, Rx 10-15 khz. Sensitivity 85 db re 1 uPa.	Tx 7-11 khz, Rx 7-15 khz Sensitivity $\leq$-70 db re 1 uPa.	7.5-15.0 khz Sens. -81 db re 1 uPa	18-36 khz (STD) Sensitivity -0 db re 1 microbar	6.25-14.75 khz. L/F 22-30 khz (SBL/LBL)	24-30 khz
TRANSPONDER	RT 1X 1, 2-8000 m Recoverable	*0198 Oceanlink, disposable or recoverable. 1500 m depth. Sensitivity 85 db ref. 1 uPa.	*NT-018, Recoverable, 6700 m, 5 Yr MTTF, Sensitivity $\leq$ 70 db re 1 uPa. External magnet controls.	711/3A 1-6000 m. Recoverable. Rx 9-11 khz, Tx 7.5-11 khz.	*Compatt 7100 Type. 7250 L/F 2000 m CTD data.	RS/906 Transponders 2 - 600 m Recoverable	*
NETWORK	3-7 (STD) up to 16 (ETD)	up to 12 (STD)	up to 16 (STD)	up to 16 (STD)	3 and up	3+	up to 14
INTERFACE	IEEE 488/RS232	IEEE 488	IEEE 488/RS232	RS232/EEE 488/20 ma	IEEE 488/RS232	RS-232	RS232/20 ma.
COMPUTER	HP 9826-36-45	HP 9826s and others	DEC LSI 11/23	PDP 11/04	HP9845B	Basic Microcomputer. Nav. computer required	Required
SOFTWARE AVAILABLE	Calibration, General Nav., D/R, Precise Nav, Track, pos'n 4 remotes, Geodetic Pos'n, Way Pt. Nav., Tilt, Sat/Nav Integration, Post Processing. Volume Calc, Position/orientation 16 pnts in streamer. Secured programs.	True power-fail run-up, Auto interface status, 3 Nav. systems pos'n fits, choice recording media, choice recording format, choice track plot, lease sq. fit residual display, cont. nav. geog. coords, display page selection, cycle time 0.5 sec. update.	Sound velocity, ray path analysis, system status, self calib., std. calib, operational nav., error analysis, recompute, simulation.	Calibration, general nav., D/R Auto Edit, Smoothing, Post Plot, Ray tracing, Geodetic Positions.	Auto Calibration, LBL Pos'n Calc., Submersible tracking. Navigation etc. req'd via master computer.	Simulation, X-Y Coords, Slant Range, Test, Calibration, Mobile Pos'n. Navigation Software required.	Transponder Pos'n, Calibration, Test, Error Analysis, Geodetic Co-ords.
CALIBRATION TECHNIQUE	Random Manoeuvering	Parallel ranging to four other transducers	Self calibration and random manoeuvering NT 32 transp.	Random Manoeuvering	Automatic calibration	Random Manoeuvering	Thru SSBL techniques
RANGE/ACCURACY	10 km, 1-3 m	10 km, $\pm$1 m (0.1 m Res)	20 km, $\pm$1 m	10 km, $\pm$1 m	3.5 km, <1 m 10-15 km, 1-3 m (STD)	3 km, $\pm$1-3 m	0.5-3% of Slant Range
DATA LOGGING	All, Cassettes	All, 9 track or choice	Winchester flexible disc. 12 hrs. ops. per disc. All data.	Required	Required	Required	Required
INTEGRATION	IM 100 Interface Module 16 Systems, Argo, Syledis, Trisponder etc.	Scope III Multiple Interface, HP1B to Host computer, 7 external devices, signal processing, smoothing, etc. Argo, Maxiran, Syledis, etc. Multiple compass, streamer alignment.	2 Quad RS232 serial. All Nav. status reports Loran, Satnav, Gyro, doppler log, positioning in local grid.	Required	Required	Required	Required
TRANSPONDER FLOTATION	4 Hyper 6, Floats 6000 m	Required	Required	Required	Flotation collars 1000-1500 m	Required	Included
STREAMER HYDROPHONE	CH 111 Cable Hydrophone receiver 8-16khz, trans X twisted pair, 300 m max. horizontal dist.	--	Microtransponder NT-030 Range Freq. 14-15 khz	--	Type 7153/4	--	--
REMARKS	In Canada, McElhanney, B.I.O. Marinav, Cansite	Multiuser operation	--	No video, Plotting only, Dome, Mobil own	User choice of software Used extensively North Sea. SSBL, SBL, LBL Systems.	Tilt, Depth Meas. Used for SSBL, SBL, LBL, Ops. Beaufort Ops. Instaltns on drill ships/rigs	Extensive use in North Sea.
SPECIAL FEATURE	Modular design concept	Well developed & proven interface & software packages.	Cable transmission to tow fish, Expandable Rx to 32 ch. Baffle X-ducer greater directivity. Transducer (CFAR) Constant False Alarm Rate, eliminates noise spikes.	Ray tracing program	DMT Dual Mode Transponders. Simult. or sequen. response. Sing-around, Improved calib. & submersible tracking. DAS Data Acquisition system transponders (CTD).	Self Test, Easy Operation.	Variable beam width X-ducer. 150°, 60°, 30° Tracking X-ducer.

RECOMMENDED SYSTEMS

From the previous discussion, either a short, or a super-short base-line acoustic position system appears to be appropriate for the surveying of the submerged portion of an iceberg. However, the inconvenience and expense of establishing and calibrating a fixed transponder network on the seabed virtually precludes the use of a long base-line system for this purpose. Of the two options for positioning systems both require the establishment of a series of acoustic transponders fixed at known depths around the iceberg. Ideally, the transponders will be capable of measuring conductivity, temperature, and pressure.

It is recommended that the survey vessel should be equipped with a retractable super-short base-line hydrophone array housed in a sea chest. Beam steering and mechanical transducer training are also recommended. Acoustic interrogation of the transponder array fixed to the iceberg should provide the range and bearing of each transponder relative to the ship. Because of the possible large temperature and salinity gradients in the vicinity of melting icebergs (see Figure 14), temperature and salinity should be measured at the survey vessel as well. Data processing incorporating the effects of temperature and salinity variations and vessel motion, to determine the position of the vessel with respect to the iceberg should be done with a microprocessor on board. With multiple-range and bearing measurements on at least three transponders at any one time, closure of the transponder network can then be affected by imposing minor corrections to distances and interiors angles using an appropriate algorithm. With closure, the position of the vessel relative to the iceberg should be known at any time during the survey.

It is also recommended that distances to the iceberg surface should be measured acoustically from a hydrophone transducer mounted in a tethered submersible sensor platform deployed from the survey vessel. Ideally, the transducer package should be operable either in a stationary or in a towed mode. A responder on board the tethered tow-fish would be interrogated electrically to determine its position relative to the ship. Pressure, conductivity, and temperature data measured at the tow-fish and incorporated in the analysis would then allow optimum position assessment of the transducer sensor package with respect to the iceberg frame of reference.

During a survey, the attitude, or more specifically the look direction, of the sonar transponder should be controlled and monitored continuously while the fish is towed at various depths, or while the sensor platform is lowered when operating in stationary mode. The problem of determining the look direction or orientation of the transducer may be solved by the following methods:

. designing a highly stable sensor platform

. monitoring the motion of the tow-fish

. employing a combination of these two

It is further recommended that the platform should be designed to achieve as much stability as possible to give a reasonable measure of confidence in the transducer orientation. Additionally, the sensor package motion should be monitored during the survey using an inertial reference system. Compact systems are available commercially which, although costly, are recommended for an experimental prototype.

DEPLOYMENT OPTIONS

In this section deployment options for various iceberg survey systems are discussed.

AIRBORNE DEPLOYMENT OPTIONS

Airborne surveys of icebergs have, in the past, primarily involved the use of impulse radar to collect underwater iceberg data. Both helicopters and fixed-wing aircraft have been used for this purpose. As well, side-scan sonar systems have been successfully deployed by helicopter. The advantages of mobility and speed to obtain large amounts of data in a relatively short time are offset by the high cost, the need for a service base, and their limited operating capability in conditions of reduced visibility and icing. Helicopter operations require a support vessel or drilling platform equipped with a heli-deck because high fuel consumption from a shore base will, in general, be unacceptable. This requirement may not be necessary, however, if helicopters servicing offshore platforms are equipped with impulse radar. Survey of icebergs could then be done on an opportunity basis with an incremental increase in operating cost. Mitigating against this choice would be the inability to gather iceberg data during periods between helicopter service flights.

Fixed-wing aircraft offer the advantage of extended range capability, but their inability to hover severely limits their use as a platform from which to survey the submerged portion of an iceberg. Airborne survey of icebergs from both fixed-wing aircraft and helicopters does, however, allow for the determination of above-water shape using standard photogrammetrical techniques.

SUBSEA DEPLOYMENT

Submarines

Submarines have been used to collect data ice profiles using a variety of sonar configurations. The exorbitant cost precludes the use of a submarine as an operational survey platform, but they may be suitable for the collection of scientific data at minimal extra cost on a pre-scheduled mission. The advantages of using a submarine are many:

- provides a stable platform which would be largely unaffected by sea state
- makes deployment of a remote sonar sensor package unnecessary
- allows adequate space for onboard real-time data processing.

Serious disadvantages make impractical the use of submarines as a survey platform:

- extremely high cost
- availability
- difficulty of deploying a series of transponders around the iceberg to establish a reference co-ordinate system.

Bottom Mounted Installations

Another subsea iceberg measurement system has been proposed by Desbartes (see Appendix 2). The system employs a grid or array of bottom-mounted transducers. Icebergs drifting over the array would be surveyed by the array by a non-real-time remote recording system. Advantages include:

- risk free other than during deployment and recovery
- virtually unaffected by sea state
- no surface support required except for maintenance checks.

There would be a number of disadvantages to this technique, mainly stemming from the fact that to ensure that icebergs pass over it, the array would have to be fairly large. Thus, the deployment and recovery operation would be tricky and labour-intensive. Also the water depth would have to be no greater than the transducers effective range. This requirement introduces the risk of damage from icebergs, which may scour at the array location. Also, there would most likely be no way of determining damage or malfunctions until system recovery.

SURFACE VESSEL DEPLOYMENT

Surface vessels have been the primary support platform for virtually all underwater measurement programs for icebergs undertaken to date. Their advantages and disadvantages may be summarized:

Advantages:

- a support/survey vessel working in the vicinity of an offshore well-site may be available on short notice when the opportunity to survey an iceberg arises at a minimal additional cost
- operation may proceed under conditions of poor visibility
- space and equipment will be available for computing facilities and sensor platform handling
- crew members are usually available to lend assistance.

Disadvantages:

- undesirable movement in a seaway during an iceberg survey
- relatively slow transit time limiting range and consequently the number of icebergs that can be surveyed in a given time
- costly if large amounts of data are to be gathered
- possible lengthy delays waiting for, or obtaining, repair components.

Stationary Mode

To date the most common method of surveying the underwater portion of an iceberg involves the use of a spinning side-scan sonar deployed vertically from a "stationary" surface vessel at a distance between about 50-250 m from an iceberg. Typically, the side-scan sonar units are lowered over the side or bow of the vessel by a Kevlar-strengthened multi-conductor electrical cable from a rotatable davit under the control of an electrically driven winch. The unit is designed to rotate during descent and ascent to ensure that the iceberg is scanned by the acoustic signal. This rotation is usually achieved by the action of "tilted" fins attached to one end of the sonar unit. Slip rings are employed at the winch but not at the rotating sensor.

These surveys can be carried out by one skilled individual assisted by one or two crew members. The use of bow thrusters and over-the-bow deployment is advantageous to maintain a near-vertical wire angle; also, the vessel may assume an appropriate heading to minimize undesireable vessel motions in a seaway. Lack of control of the side-scan sonar unit resulting from leeway, pitch, heave, and instability of the sensor package design is a major short-coming of the technique; the position and attitude of the sensor have not been monitored during past work.

Mobile Mode

Underwater surveys of iceberg geometry have not as yet been undertaken while the support vessel is underway. To accomplish

this requires the use of a tow-fish containing the sonar unit and other essential instrumentation. The location of the tow-fish relative to the vessel can be determined using standard techniques developed for seismic seabed surveys: slope distance and bearing from the vessel determined from time differences and phase comparisons of an acoustic signal transmitted from a responder onboard the tow-fish.

Tow-Fish. Operationally, the tow-fish must maintain a stable attitude at all depths and range of towing speeds, incorporate some manner of depth control, and be capable of supporting the required instrumentation. Passive lightweight tow-fish are available commercially in which depth maintenance is achieved primarily as a result of towing speed and cable length. Typical vehicles achieve vertical and horizontal stability through the action of dihedral-oriented fins which also act to develop a hydrodynamically induced depressing force varying as a function of square of the velocity. A double steel-armoured coaxial electrical cable is recommended, the careful selection of which is essential. The overall performance of the underwater towed vehicle is dependent on cable weight in sea water, on diameter, and on operating and breaking strengths. System design must consider the effect of the downward-directed force resulting from cable weight and the opposing lift due almost entirely to the pressure drag. Serious consideration should be given to the use of a "faired" cable to reduce hydrodynamic drag or strumming; the efffectiveness of cable fairing is a function of cable angle (eg. Brainard 1976) and speed. A balance must be made between the design operating cable tension and breaking strength. Impulse loadings resulting from vessel heave, pitch, and surge must be minimized through the use of stabilizers and possibly by incorporating a weak link at the tow-fish. Breaking the weak link should result in a sudden re-positioning of the tow point on the tow-fish thus causing a radical change in angle of attack which drastically reduces the depressing force generated by the flow over the vehicle.

Two other types of towed vehicles should be considered; in each case the instrumentation and cable requirements are basically the same as those already described. The tow-fish could be designed with remotely adjustable fins so that the system operator could manually control the depth of the instrument package. Alternatively, a servo-mechanizer could be employed to maintain a pre-selected depth automatically. This feature may be desirable, particularly because the survey requires circumnavigation of an iceberg rather than a straight course. Mitigating these advantages are the increased mechanical and electrical complexity with the attendant increase in cost. A third possibility to be considered is the use of a relatively simple and inexpensive passive tow-fish which carries the instrumentation coupled with a commercially

available depressor fin hung close below the instrument package. This unit would be designed to be hydrodynamically stable. Additional stability and the depth control would be provided primarily by the depressor fin. As discussed earlier for depression-type instrument packages, depth control will be a function of depressor design, tow speed, cable length, cable weight and diameter, and cable fairing, and instrument package design. This option should be decidedly less costly than the previous two, however, it would be slightly more difficult to deploy from the survey vessel.

Instrumentation. The tow-fish should be designed to support the following instrumentation and equipment:

- a controllable, and monitored, narrow-beam sonar to measure distance to the iceberg
- an inertial reference system
- pressure, conductivity, and temperature sensors
- a responder.

Relatively small and lightweight inertial reference systems are now available commercially (for example, Humphrey, Inc. Inertial Reference System Model CF32-0201-1) which could be adapted to be carried aboard a tow-fish. Such units provide continuous measurements of position and rate output for pitch, roll, and yaw in addition to three axes of linear acceleration. Power from the survey vessel can be transmitted through a coaxial tow cable with a step-down transformer or converter on board the fish to meet system requirements. Output data can be multiplexed through the same coaxial cable to the computer on the vessel.

Pressure, conductivity, and temperature measurements at the tow-fish can be obtained, if required, with instrumentation such as the Guildline CTD which provides accurate data on a continuous basis from a small sensor package. Although these units are usually used for vertical sounding of the water column, they have been used successfully when deployed on towed underwater vehicles. The inclusion in the underwater instrument package of a responder to determine the vehicle's position completes the system.

Deployment. The required instrumentation is expected to have a mass of about 50 kg. A suitable vehicle or vehicle and depressor combination is expected to range between about 200 and 400 kg. An electro-mechanical, or electro-hydraulic, variable-speed winch of appropriate size and fitted with an

integral A-frame is required to deploy the tow-fish. The winch would be mounted at the stern of the vessel with the A-frame designed so that the underwater unit can be conveniently secured during transit. The winch drum should be capable of carrying about 600 m of 1-cm diameter, double steel-armoured, coaxial cable.

Field operations of an instrumented tow-fish would simply require lowering the unit from the A-frame and towing it in a series of relatively straight segment courses at constant depth around the iceberg at a distance between 100-200 m while continuously monitoring and recording the data.

Unconnected Mode

Complexity of the survey methodology is significantly increased with the use of a tethered remote controlled vehicle (RCV). In addition to the instrumentation required in a tow-fish, the RCV requires position and orientation monitoring and control systems. Commercial RCVs are normally equipped with a low-light television system.

The major advantages of using a tethered RCV are that:

- it is capability of supporting a large number of sensors
- it is able to obtain accurate position and orientation when equipped with suitable instrumentation
- it may be operated close to an iceberg without endangering the survey vessel
- it is unaffected by vessel motion during operation and may operate in higher sea states than towed systems.

The primary disadvantage of using a tethered RCV is cost arising as a result of:

- the requirement for a specialized operating crew
- heavy-duty lifting equipment for deployment and recovery
- high power consumption
- the need for a relatively large amount of deck space on the survey vessel.

An articulating hydraulic crane is used to place the submersible over the side and in the water. Immediately after being released from the crane, the submersible is piloted away from the ship using a remote control unit. The crane is then used to place the umbilical cable guide sheave over the side and to support the sheave during operations.

At this point, buoyancy hose is attached to the umbilical as it is being payed out by the winch. The length of buoyancy hose used depends on the size of the iceberg being measured and the anticipated distance of the ship from the iceberg, which in turn is a function of wind and sea conditions and of iceberg shape. With the umbilical cable continuing to be payed out, the submersible is piloted away from the ship toward the iceberg. When the installation of the buoyancy hose is completed and the submersible is close to the face of the iceberg, control is passed to the operator control unit and the control station.

Once the control station has assumed full command and a final instrument check confirms that all systems are working satisfactorily, the submersible is driven down the face of the iceberg, using sonar to avoid obstacles, and commences its measurement procedure.

After the measurement process is completed and the project team is assured that all necessary data have indeed been obtained, the recovery of the submersible is begun.

The ship now moves off slowly while maintaining an orientation broadside to the iceberg. As the submersible moves out from underneath the iceberg and begins to surface, the umbilical cable is gradually reeled in on the winch and the buoyancy hose is removed. Upon reaching the surface, and as the umbilical cable continues to be reeled in, the submersible is manoeuvered to the side of the ship, is removed from the water, and is secured on deck.

ICEBERG TRANSPONDER ARRAY DEPLOYMENT

The establishment of a reference co-ordinate system on an iceberg according to the recommended methodology would require the deployment of a series of acoustic transponders around the iceberg. The number of transponders required will be a function of the water-line circumference of the iceberg with the stipulation that the establishment of survey control demands the ability to obtain ranges on at least three transponders concurrently. Each transponder would be fitted with a buoyancy device to maintain the unit near the surface. The transponders would be linked together with a buoyant line and their deployment could be carried out directly from the survey vessel by lowering one end of the string into the water and steaming around the iceberg at a safe distance. A large float-drogue combination secured to the end lowered into the

water would facilitate recovery. Upon recovery, the float could be replaced with a standard acoustic release which would be used to join the line. The release would be lowered into the water and the bitter end drawn taut allowing the transponder string to tighten around the iceberg. Details would be worked up with the prototype design.

An alternative deployment method would involve the use of a small skiff or inflatable craft powered by an outboard motor. The transponder string would be put aboard the boat and a crew of two individuals wearing immersion or perhaps wet suits would deploy the gear as they navigated around the iceberg. In this case, it would be desirable to have a second inflatable and crew available at a moment's notice to ensure rescue capability.

After deploying the transponders, establishment of survey control would be done, and then an acoustic survey of the iceberg would be made. Upon completion, the acoustic-release would be triggered and the transponder string would be recovered as it floated free of the iceberg.

CONCLUSION

It will be apparent from previous sections that a surface vessel will be required to support the recommended survey technique. Despite obvious inconvenience such as relatively slow travel-time and undesireable motions in a seaway, a surface vessel will be required from which to deploy the acoustic transponders on the iceberg, to deploy and operate the subsea instrument package, and to provide a suitable platform to process the incoming data.

DATA ACQUISITION, DISPLAY, AND PROCESSING

In reviewing the requirements for a data-processing system to support a three-dimensional iceberg mapping system, two types of field-based acoustic systems are considered here. The first, a form of which has been field tested, makes use of acoustic beacons attached to an iceberg to determine an absolute co-ordinate system which is fixed to the iceberg. The second system uses an increased rate of data acquisition and interactive graphics to avoid having to attach beacons to an iceberg. Requirements on a field-based system include those associated with signal processing, data storage, field determination of iceberg draft, system error and accuracy, and quality control of data at the collection stage. With respect to a laboratory-based system for later processing of data, the main requirements are associated with having software suitable for generating the data products.

Various design and operational criteria have already been developed for the total system, five of which relate to the acquisition and processing of data in the field as follows:

- draft of an iceberg must be measurable within one hour and available in real time;
- total measurement time should not exceed four hours;
- system accuracy should be within 5% on all major parameters, including mass and draft;
- operating distance for the system should be about 100 m from the iceberg;
- quality control for the system should exist in the field.

DATA PROCESSING FOR A SYSTEM EMPLOYING ACOUSTIC BEACONS

The first of the two field systems discussed employs acoustic beacons attached to the iceberg. The main purpose of the beacons is to provide a co-ordinate system which is fixed to the iceberg. The data processing portion of the system will receive data from several subsystems, which based on an existing system at a minimum will include:

- an acoustic sensing system to produce data on distance to the iceberg;

- an internal orientation monitoring system to produce a continuous record of the attitude of the system relative to an arbitrary, but fixed, three-dimensional co-ordinate system; and

- an external positioning system to produce a continuous record of the position of the sensing system relative to the iceberg and the depth of the system in the water column.

In the alternative system which does not make use of acoustic beacons, the requirements would be the same except that data would be acquired from a depth sensor. The alternative system is discussed later.

Whether there are beacons attached to the iceberg or not, it is essential that the iceberg does not undergo a significant roll during the data-gathering process. Were this to happen it would necessitate re-deploying the marker beacons, and beginning the data collection process again. Otherwise, it would be impossible to have confidence in the quality of the data collected. In the following discussions it is assumed that the iceberg remains stable during the process of data collection.

Signal Processing

In the schematic diagram of the required signal processing system (Figure 15), raw acoustic data in analog form enter the system. In the simplest possible case, these data arise as returns of groups of pulses which are emitted simultaneously. Pulse rates must be slow enough to permit the acquisition of returns before the next pulse is emitted; this makes keeping track of which echo is associated with which pulse easy, although other, more complicated, sensing schemes are possible. Depending on the operating distance, pulse rates could vary between 3 and 10 Hz. To obtain a range resolution of about 0.5 m, the length of each pulse would have to be approximately 0.5 ms, corresponding to a bandwidth of 2 kHz. At a maximum operating distance of 200 m, the return time is less than 0.3 s, whence even if the sensing system were being towed it would move less than 1 m parallel to the iceberg. Given basic facts governing the raw acoustic data, there are two possible courses for dealing with these data.

The first option is to record the data directly on tape in analog form in the field, and to process them in a laboratory. Systems for collecting these data on a real-time basis have been available for many years. However, no information can be gleaned from the data without further processing. Moreover, a great deal of information is saved which has no value to the problem. Nevertheless, given the costs of ship time, it may be worth-while to have this type of system on line so that all raw data collected in the field are saved for future study.

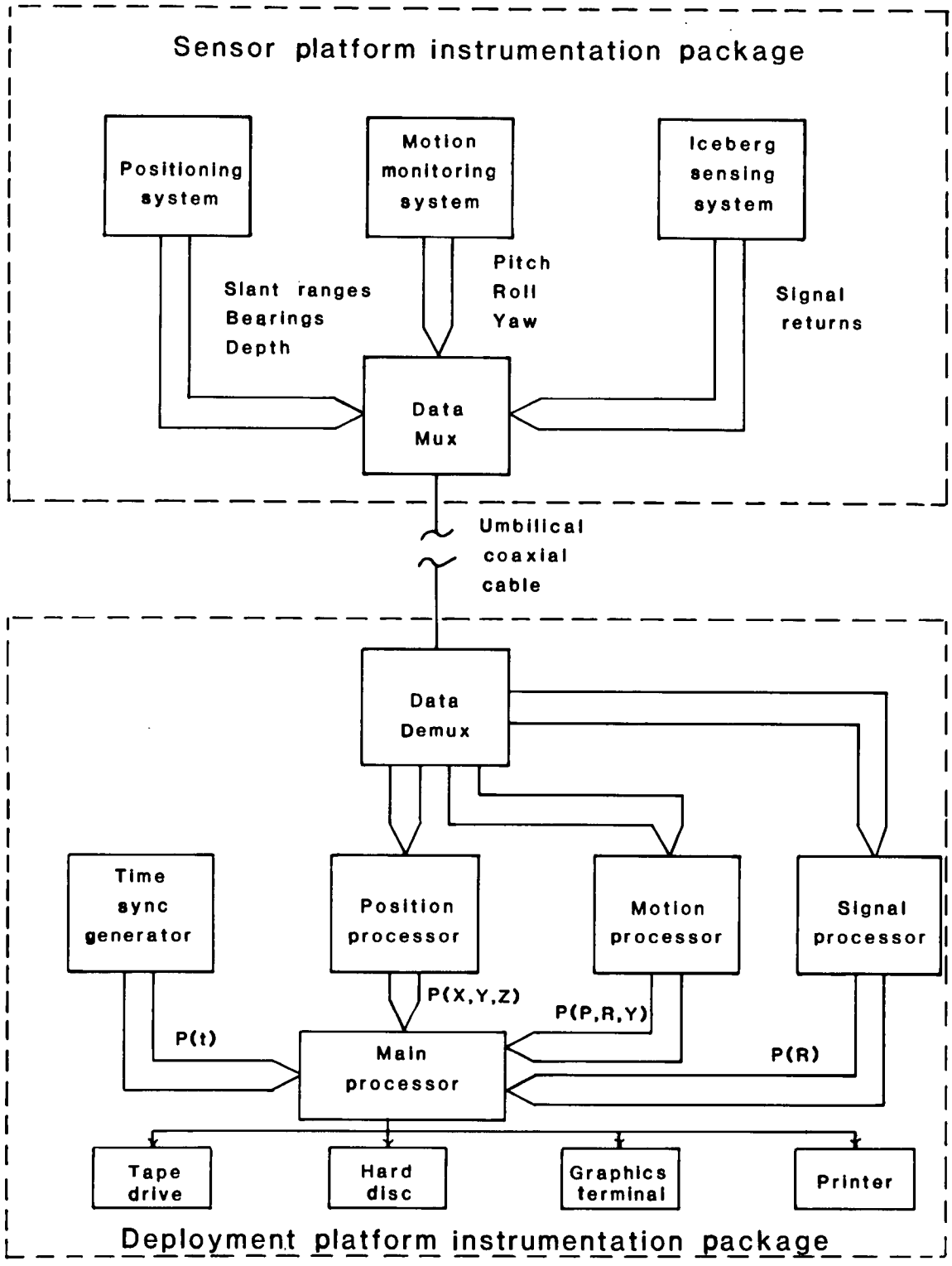

Fig. 15. Data acquisition processing and display system block diagram.

The second option involves processing the data in the field by digitizing the analog signal on the spot. This method would generally create a great mass of data. However, because the only fact of interest is the distance of the sensing system to a point on the iceberg, the mass of digitized data could be discarded, leaving only the distance to the iceberg. Because calculation of at least some distances is required, the system will have to be able to extract distances from the analog signals in the field, and thus, this option is the recommended one. Further, if it is possible to extract digitized distances from the analog data at all, it will be because the iceberg has a clearly identifiable signature in the analog signal from which time lags, and hence distances, can be determined. It would appear possible to have sufficient processing power available in the field that the analog signal could immediately be converted to a single digitized distance which would then be passed to the main processor. This course is recommended (see Figure 15). Thus, for example, data on distances to marker buoys and depth would be processed by the positioning system and, in addition to the distance data, absolute x-y-z co-ordinates would be passed to the main processor by the positioning system. To see what difficulties may be anticipated in extracting digitized information from the returned signal, the reader is reminded of the "Examination of Sensors".

The signal-processing problem does not end with the interchange of the analog signal to a digitized distance. Considerable problems remain. To elucidate this problem associated with collating data from these various subsystems, consider how the data is to be used. All the data entering the main processor will be in digitized form. Figure 16 shows an acoustic sensing system in relation to an iceberg. Dashed lines indicate that three ranging signals must simultaneously be recorded and synchronized. The synchronization of these signals is simple, because all will have been initiated simultaneously as part of the same pulse. Indeed, there will be instances when three of the external positioning buoys (B_1 to B_4 in Figure 17) will simultaneously be within range of the system; thus, the requirement will be for four range signals to be recorded and synchronized. From the two range values, d_1 and d_2, and from the depth of the system, the absolute co-ordinates of the system relative to a central axis through the iceberg may be calculated provided the depth of the sensing system and the six distances are known (see Figure 17). In Figure 17, the central axis is vertical and passes through A, the point of intersection of d_{24} with d_{13}. Thus, the depth of the system must be obtained in concert with the distance measurements from the positioning point. It is proposed to obtain this measurement by interrogating the depth sensor on first receipt of a return from the last pulse. The time

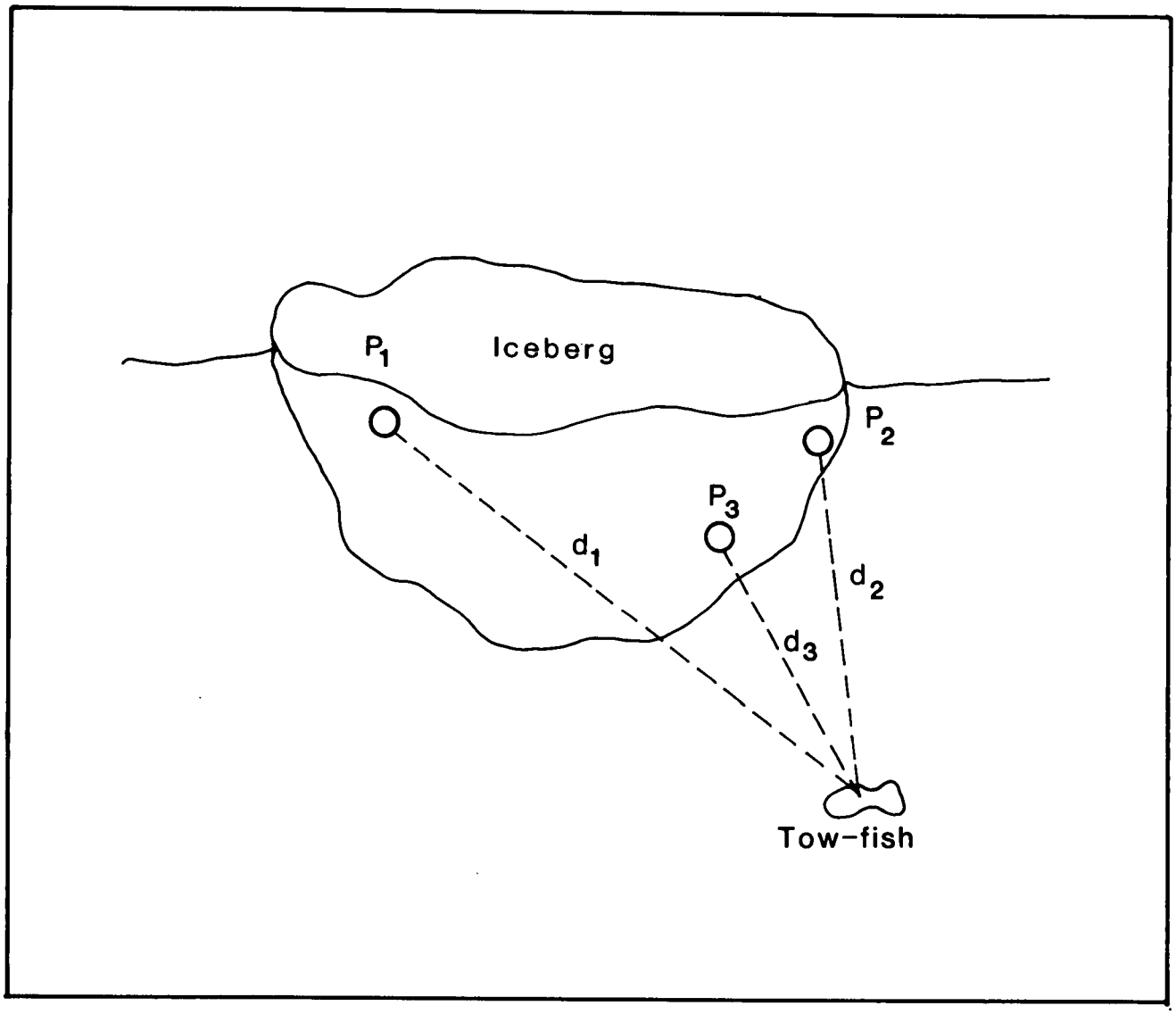

Fig. 16. Schematic diagram showing tow-fish receiving acoustic positioning information from an iceberg.

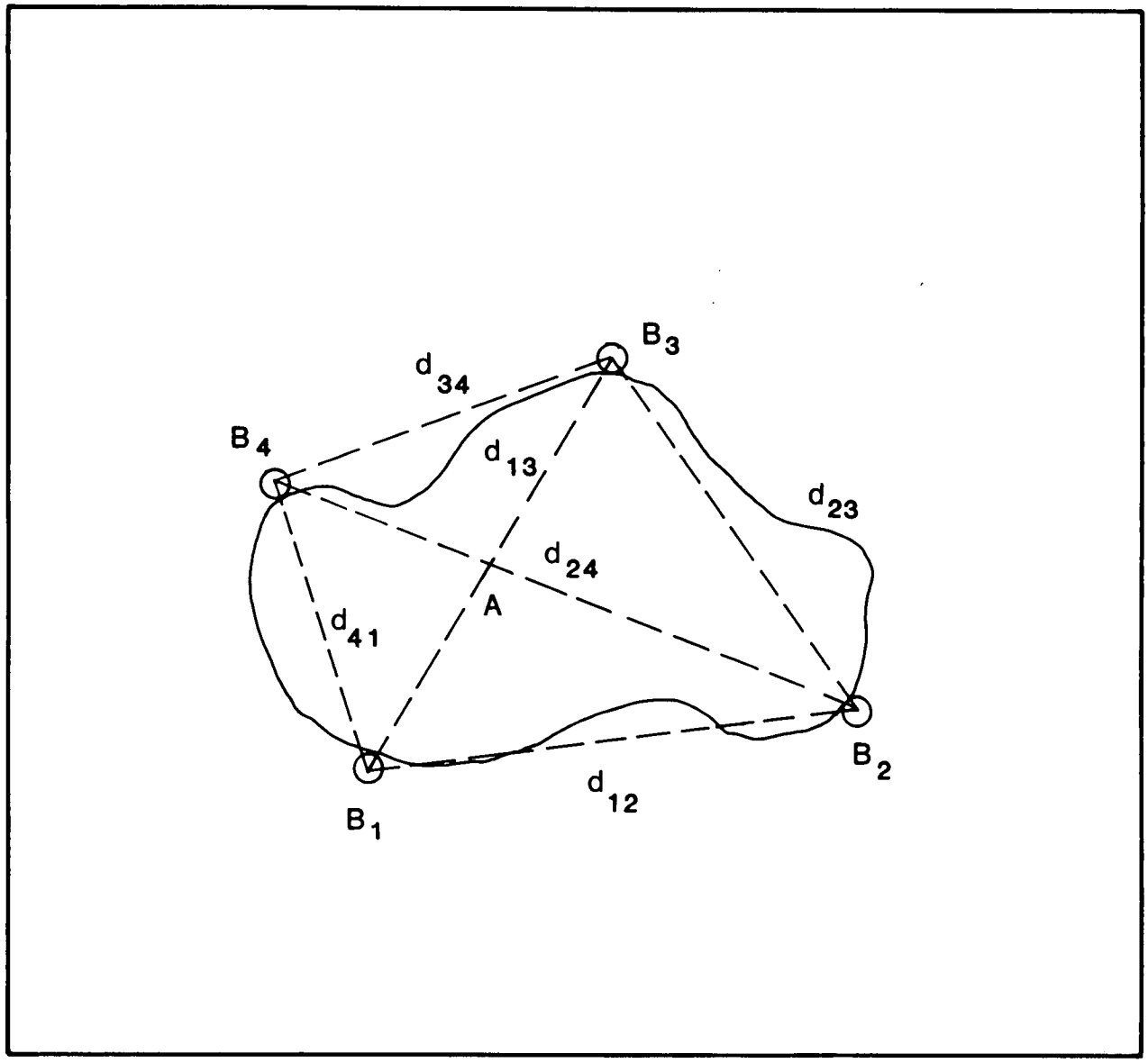

Fig. 17. Plan view of absolute buoy positioning system attached to an iceberg.

interval involved in obtaining this value will lead to negligible errors. However, the absolute position of the system, considered as a point, is insufficient to define the absolute position of the point P_3 (see Figure 16) on the iceberg relative to the fixed central axis. To obtain the absolute position of P_3, it is necessary to know the orientation of the system with respect to any fixed, but arbitrary three-dimensional co-ordinate system as a function of time. For a system that delineates the insonified cell by use of a pair of orthogonal transducers, it is necessary to know the orientation of the sensing system at the initiation of a pulse and also on the return of a pulse. Again, synchronization can be accomplished merely by interrogating the orientation system at the initiation of a pulse and again at first receipt of a return.

Thus, the digitized data must consist of records containing a minimum 11 numbers. The first four of these numbers would be distances, three of which are indicated as d_1 - d_3 (see Figure 16). The fourth would be the depth of the system at the instant the three distances were received. The next three numbers would define the orientation of the system at the initiation of the pulse generating the distances. The remaining three numbers would describe the orientation of the system at the instant the three distances were received. Some system designs might record multiple ranges to different points on the iceberg simultaneously. In the remainder of this discussion, it is assumed that the record length is 11, and that recommendations for other record lengths can be easily generated.

Data Storage Requirements

A nominal requirement of the system is that the total measurement time be restricted to four hours, which limits the amount of data collected during a mapping run. For the type of system described in Figure 15, data could propably be acquired at a rate of 100 records per second. This suggests that about 50 megabytes of hard disc storage be available. This calculation is based on each record requiring 32 bytes of storage and continuous data acquisition for four hours.

The storage requirement can be sharpened considerably by an examination of the rate at which data are generated by the sensing system. Data are obtained by firing a sound pulse and waiting for a return. Typical time intervals between pulses at an operating distance of 100 m exceed 0.1 s. Thus, a maximum rate of record generation is 10 records per second, which gives a rough minimum storage requirement of five megabytes of disc.

Many "off the shelf" micro-processor systems are available which offer a hard disc with a capacity of between 10 and 50 megabytes. It is expected that a system permitting 20 to 30

megabytes of storage will be adequate to store the data from a single mapping run. The reason for recommending a greater-than-minimum capacity will be clear later.

Disc storage is recommended as the initial storage device because the transfer of data to disc is considerably more rapid than to tape. However, as it is anticipated that many mapping runs will be conducted during the course of a field experiment, alternate data storage devices must be available. Thus, it is recommended that a magnetic tape drive be available using compact cartridges. Such devices have a single cartridge capacity of 40 megabytes.

Real-Time Determination of Draft

The real-time determination of draft can be quite easily accomplished with relatively limited processing power. By this, it is understood that the processor would have the capacity to accept a collection of 11 numbers as described to compute the depth of P_3, and to compare it to, and possibly replace, a test value within the time lapse to the next pulse of approximately 0.1 s. Given this level of processing power, the system would simply calculate a potential draft value each time a new record is received. The deepest value seen on completion of the scan would measure the draft.

Such a calculation is not particularly onerous from the point of view of processing required for its completion. However, the calculation must be seen as being part of the total processing requirement, which could be substantial -- depending on the computational requirements associated with extracting ranges from returned sound pulses.

Sources of Error

The overall system is composed of three subsystems; the absolute positioning system, the internal attitude system, and the iceberg sensor system each of which can be easily identified from the schematic diagram of the system (see Figure 15). Each of these subsystems collates signals of various types, some of which are common to more than one subsystem. Thus, both the iceberg sensor and the absolute positioning system employ an acoustic ranging system. Thus, this discussion considers the types of errors associated with the most basic types of measuring devices employed and how the errors associated with the devices affect the mapping of the underwater surface of the iceberg.

The first source of error is associated with the echo-ranging system. This type of sensor is part of the absolute positioning system and the iceberg mapping system. It is

assumed here that the ranging system records echoes from a 1^{o} by 1^{o} cell, which at an operating distance of 100 m, yields a 1.75 m radius circular cell on the iceberg, known as the insonified cell. The total error in the ranging system (Figure 18) results from two effects: the error associated with the time lag on which the distance is calculated, and the error resulting from bending of the sound ray. The total error depends not only on the error inherent in the ranging system, which is small, but also on the shape of the iceberg in the sampled cell. Here, the sampled cell is meant to take in all those points on the iceberg which could have been the true source of the returned echo. However, if an unknown amount of ray bending takes place, then to know the true position of the insonified cell on the iceberg becomes impossible, rather, all that can be said is that it lies somewhere within the sample cell. If the iceberg has a severely bent shape within the sample cell, the significant errors can result from lack of information about the true position of the insonified cell. Therefore, the size of the sample cell must be minimized. Note that the range error does not change the size of the sample cell, but the bending effect acts to increase the vertical dimension of the cell.

The second source of error is in the depth sensor, which is part of the absolute positioning system (Figure 19). The main effect of errors in this system will be to decrease our knowledge of the vertical position of the sensing system, which will have the effect of increasing the vertical dimension of the sample cell. As well, errors in the absolute position can occur through errors obtained by the acoustic portions of the system. The severity of this type of error on mapping performance will be determined by the shape of the iceberg in the sample cell.

The three remaining types of errors all relate to the internal attitude sensor of the system, which measures the three angles relative to some fixed co-ordinate system. All three angles can be important depending on the particular orientation of the sensing system to the iceberg. Given that these angles can be measured within 1^{o}, at an operating distance of 100 m the size of the sample cell would have to be increased by about 1.75 m in both the vertical and horizontal directions. In Figure 20 this type of error is illustrated by tilting the instrument package through a roll angle. Again the severity of this error on the iceberg mapping data will depend on the iceberg shape in the sample cell.

Figure 21 illustrates the cumulative increase in the sample cell from the various errors. However, it should be emphasized that this figure illustrates the optimal case of a sample cell projected on a flat surface.

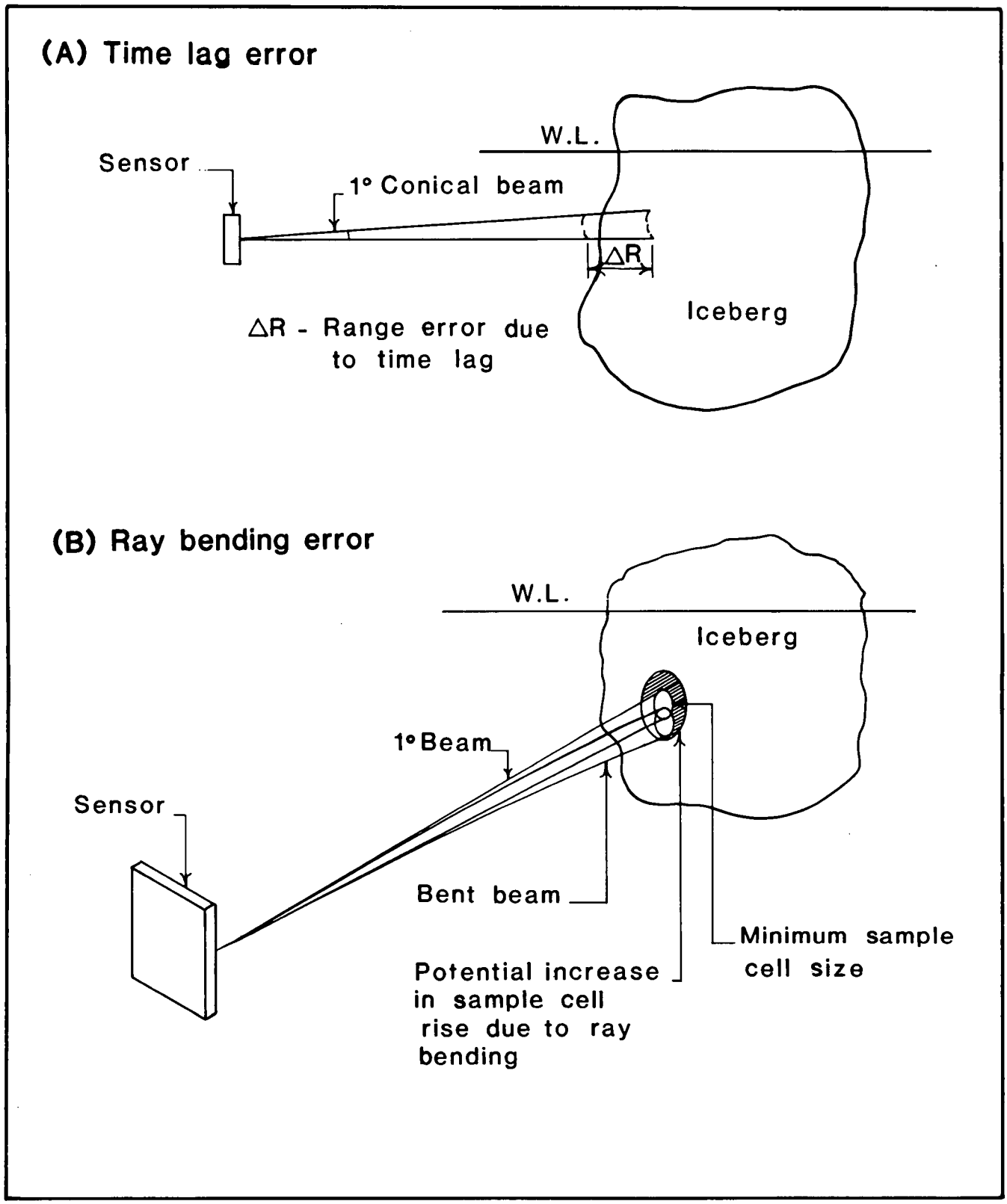

Fig. 18. Errors associated with an acoustic sensing system: (A) time lag error; and (B) ray-bending error.

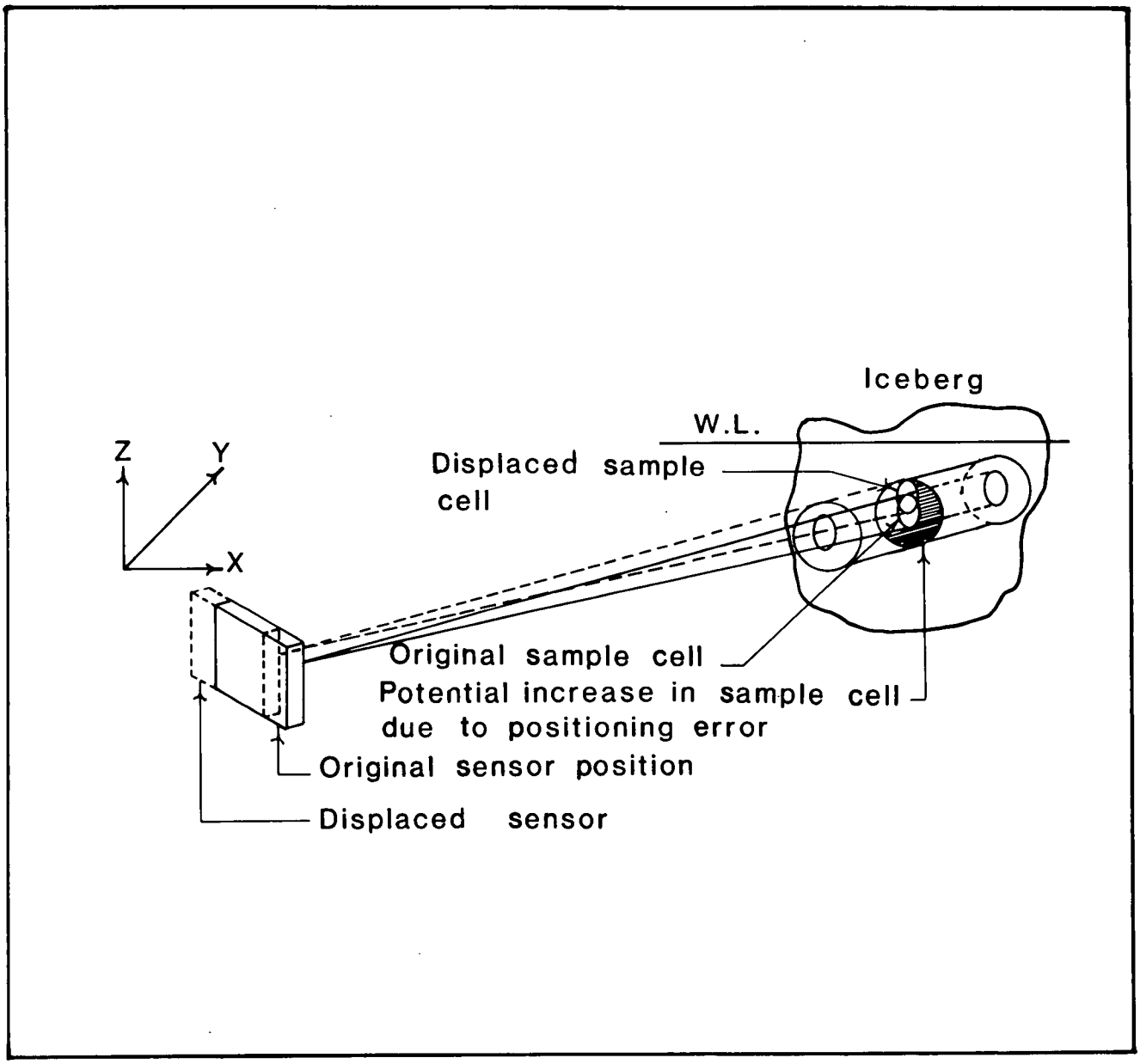

Fig. 19. Error associated with positioning system.

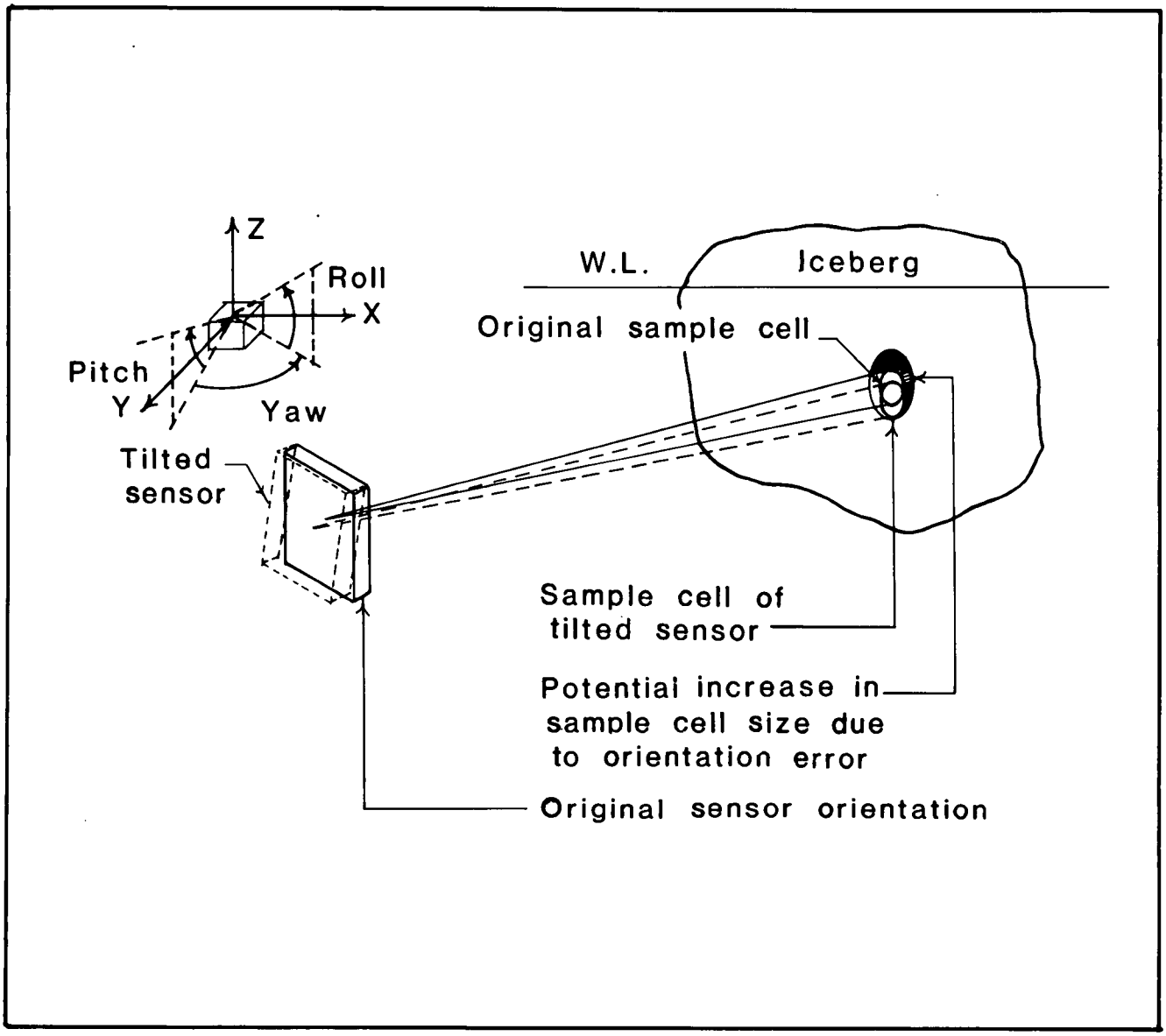

Fig. 20. Error associated with sensor orientation.

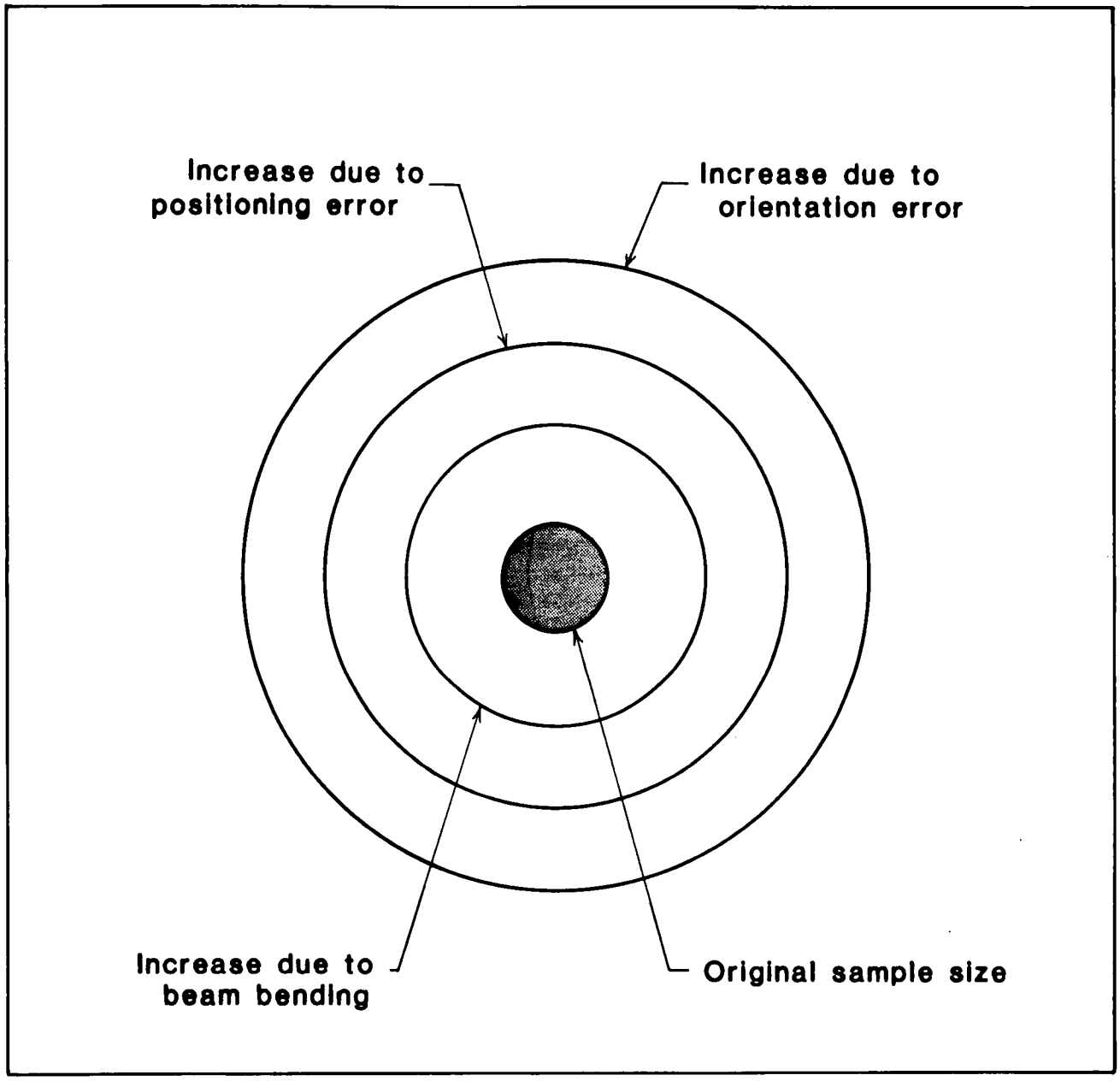

Fig. 21. Cumulative effects of error on the iceberg mapping system's sample cell.

In Figure 22, a sketch of the sensing system sampling an iceberg, errors associated with the distances d_1 and d_2 should be consistent with those derived earlier. In this way the absolute position of the system relative to the iceberg can be found very precisely. However, the error associated with d_3 can be much larger because of the large size of the sample cell. Thus, data relating to the surface boundary may suffer for reasons already discussed. Without actual experimental work, it is impossible to estimate the final residual error of a fully functional iceberg mapping system. It is important to note that the error associated with the range to the centre of a given sample cell is not completely controlled by system parameters, because many of the errors are affected by the shape of the iceberg in the cell.

The analysis shows that the intrinsic quality of the data acquired by the system would be effected by the stability of the platform to which the sensor is attached. If the sensor is undergoing rapid non-uniform motions with six degrees of freedom, the quality of the data would be decreased, whereas a very stable platform would enhance their quality. Thus, deploying the sensor system via a cable attached directly to a stationary or anchored support vessel would yield poor data unless the sea were extremely calm or some other means for increasing platform stability were adopted. For this reason it is recommended that the platform be towed, which by appropriate platform design will lead to relative stability, even in moderate seas. An immediate consequence of this recommendation is that the system sensor be designed to acquire data over the whole face of an iceberg on each pass.

Overall System Accuracy

If, as already stated, the system is required to have an accuracy of 5% on all major parameters, in particular for draft and mass, this degree of accuracy for draft measurements requires that each measured range to the iceberg be within 5%. However, a more stringent requirement exists for the determination of mass.

The estimation of an iceberg's mass is based on its volume calculated by summing the volumes of a number of horizontal layers. The principal source of error is associated with the determination of the boundary of a layer in the horizontal plane. Given that a fixed percentage error of 5% exists for each range determination, then it is possible that a given width determination could be out by as much as 2 x 5% or 10%. At an operating range of 100 m, each length, or width, could then be long, or short, by 10 m. Thus, for the case of long estimates, the error in the calculated area assuming a rectangular shape becomes:

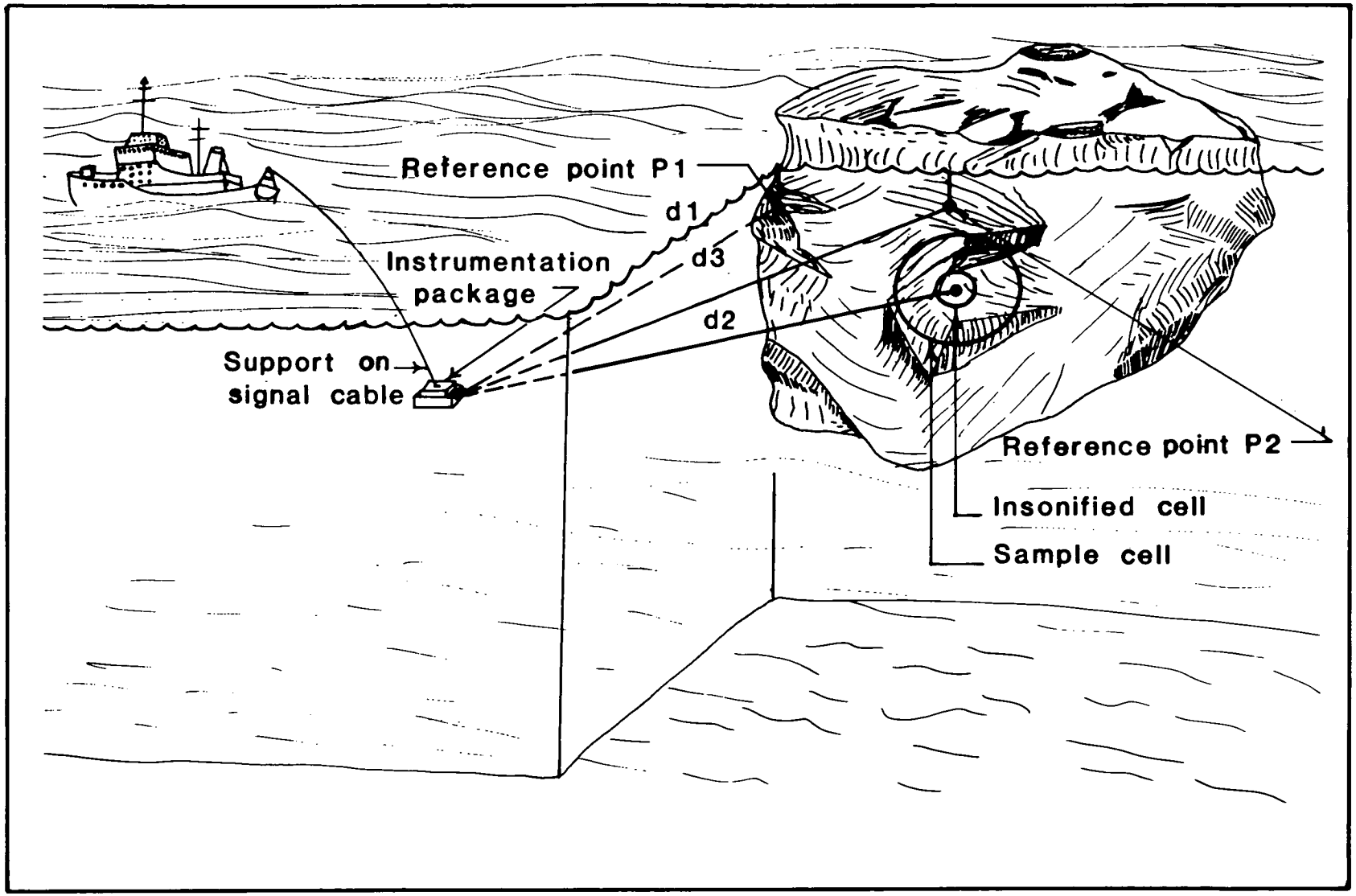

Fig. 22. Artist's concept of an iceberg mapping system in operation

$$\text{Error} = \frac{10\,w + 10\,l + 100}{lw}$$

where l and w are the true length and width of the iceberg. Since range errors depend only on the operating range of the system, the error will be small for very large icebergs. (For an iceberg whose length more than doubles the width, the error is less then 10% if the width is a bit over 150 m.)

The system's accuracy during a particular survey run on a given iceberg will affect its overall accuracy. As there is no way to control the shape of the iceberg, this type of error cannot be completely controlled. However, significant reductions in error can be accomplished by multiple measurements of the positions of various cells on the iceberg. Although, the system will be unable to pick individual cells on the iceberg and repeatedly to sample their position, repeated positions will be obtained by virtue of the fact that sufficient data are collected to ensure that they exist. The question then arises: how many data should be collected to achieve the required sampling rate?

The underwater surface area of an iceberg having a length of 200 m could easily exceed 100,000 m^2. To sample one record per square metre of iceberg would require about four hours of mapping time at a record acquisition rate of 7.5 records per second. Thus, to ensure multiple records, the sampling rate must be increased. Increased sampling can be achieved with no increase in mapping time and with a minimal cost in the amount of data to be stored merely by increasing, in the system, the number of sensors used to determined distances to individual cells on the iceberg. Other available means are discussed under "System Designs" but a firm recommendation of the number of sensors required to ensure a given level of accuracy may have to await the outcome of studies recommended earlier.

Quality Control of Data in the Field

The simplest, most direct method for quality control of data would be to link the acoustic sensors directly to a grey-scale recorder. This link would provide immediate feedback on the data being received from the acoustic sensors; gross errors would immediately be detectable. This method is recommended as a first step.

Optimal quality control of data involves the comparison of one set of measurements against another set obtained independently. Several types of quality control checks suggest themselves here.

First, the distances between the various buoys used for determining absolute positions (see Figure 17) can be

calculated based on data returned from the sensing system. These values can be compared with values determined by other means, such as, radar ranges to the iceberg. Also, the position of buoys will have to be very carefully determined by independent means for use in computations at a later date. A real time determination, even if not highly accurate, of the distances between the buoys would provide a useful means of real-time quality control.

A second method for the quality control of the data would be to deploy some test buoys at fixed depths at the side of the iceberg. Their positions would be known independently known and could be used to check positions determined by the sensing system.

The third method for quality control involves alternate methods of computation of the absolute position of the sensing system relative to the centre of the iceberg. Three methods exist for doing this, involving different subsystems contained in the sensing system. For example, the absolute position can be calculated from the distance to any buoy and from data for the internal attitude system, provided the absolute position of the buoy is known. By comparing the values in pairs it should be possible to ascertain the functionality of the various subsystems associated with positioning in the field.

DATA PROCESSING FOR A SYSTEM WITHOUT ICEBERG-FIXED CO-ORDINATES

Although, the existence of a system of buoys would increase the accuracy of the co-ordinates, its optimization is not without price. First, deployment of such buoys can be hazardous, unless limited to relatively calm weather. Secondly, deployment of such buoys adds significantly to the length of time required to complete a mapping operation. It is estimated that the deployment of acoustic beacons under ideal conditions would require a minimum of one hour. Such a system would therefore have limited application as an operational tool.

The remainder of this section considers the data processing aspects of whether it is possible to develop a three-dimensional iceberg mapping system that does not employ buoys attached to an iceberg and that could be used operationally?

Shape Recovery Without External Positioning

With buoys fixed to the iceberg, the co-ordinates of the centre of an insonified cell can be calculated without ambiguity.

Without the use of buoys attached to the iceberg, the nature and use of the data set collected must be re-evaluated.

The problem is to come up not only with a data set but also with a method for employing it which will lead to an accurate three-dimensional map.

The data set proposed here is a list of distances obtained as a ship tows a sensor passed an iceberg. The distances are assumed to be taken at a fixed depth and at right angles to the path of the sensor. It is further assumed that the sensor travels in a straight line from the moment of first return from the iceberg until no further returns are recorded. A total of eight runs are proposed (Figure 23).

To determine how accurately the actual iceberg contour can be recovered from this data set an experiment was carried out. A sample closed curve was generated which purported to represent an iceberg contour (Figure 24). From the closed curve a collection of numerical data was developed and is presented in Table 4. In constructing the data set some data were omitted based on situations where no return might be the result from insonifying an actual iceberg contour of similar shape. The numerical data were then transmitted to an individual who had no previous knowledge of the shape of the original closed curve, and who was required to reconstruct the curve.

In the process of reconstruction each of the eight data sets (see Table 4, Run 1 to Run 8) was used to generate one or more curve segments (Figure 25). In cases where data were missing, more than one segment resulted; but the multiple segments were treated as one rigid curve with an unseen piece. Each segment was labeled to establish relative positions with respect to the closed curve. Reconstruction was accomplished by overlaying one segment onto another and by sliding the segments until a satisfactory match was achieved. A portion of the reconstructed curve showing overlaying segments is presented in Figure 26 and an overlay of the two curves (original and reconstructed) in Figure 27. The total time for the reconstruction process, with no computer assistance, was two hours. With suitable computer assistance the result could probably be accomplished in about 15 minutes.

The assertion of feasibility of this type of method is given further credence by noting the following. The curve used in the experiment was drawn at a scale of 1 cm to 10 m. The sampling rate used in the experiment would be equivalent to a field rate of once per 10 m. As a reasonable towing speed for this type of system would be 2 m/s and a plausible pulse rate would be once per second, an actual sampling rate for such a system would be once per 2 m. Thus, the density of data collected in the field would be as much as five times greater than that of the experimental case above, whence an actual reconstruction of the contour from the individual pieces should be much easier than it was in the experimental case.

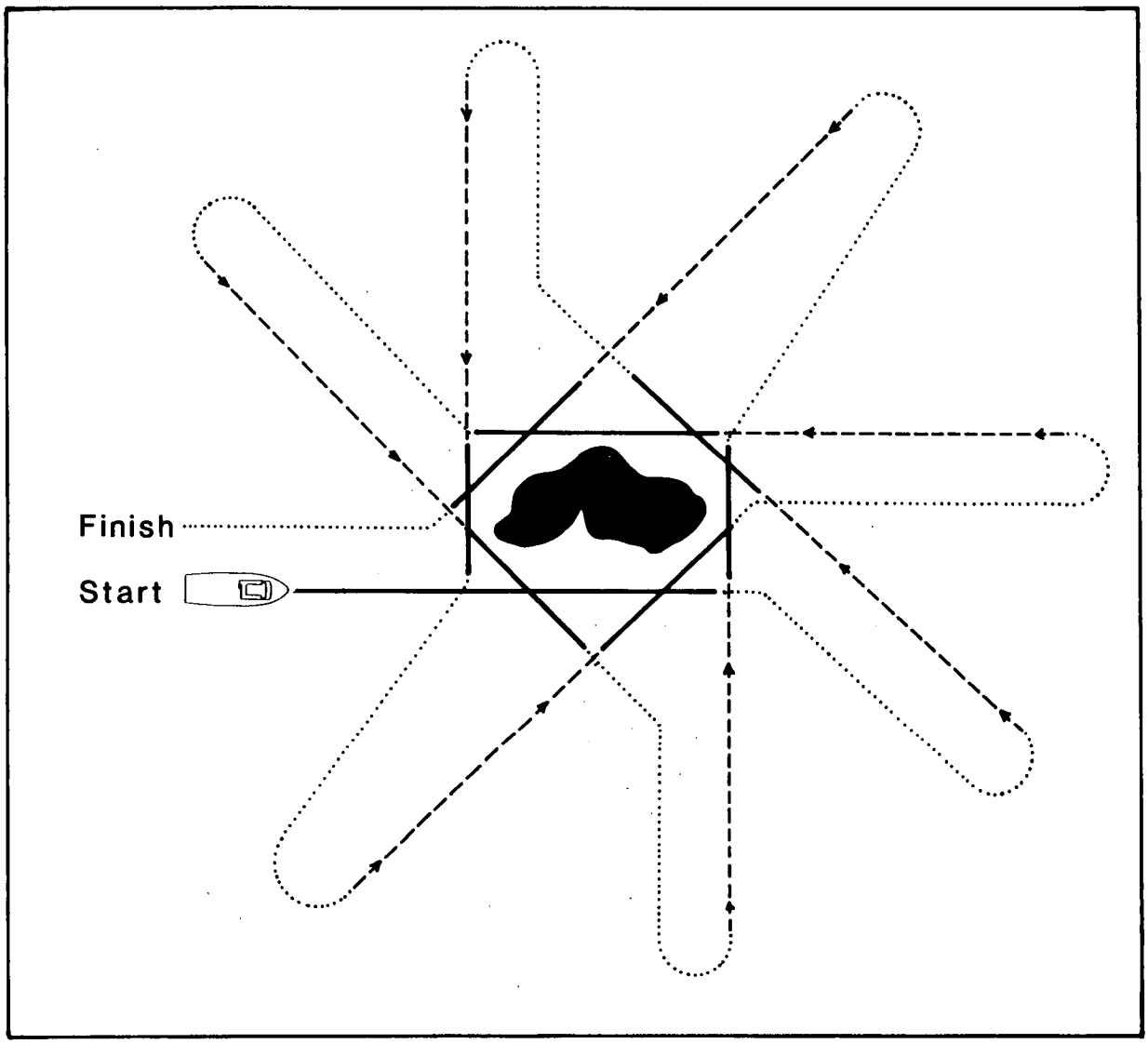

Fig. 23. Vessel's survey pattern during iceberg mapping.

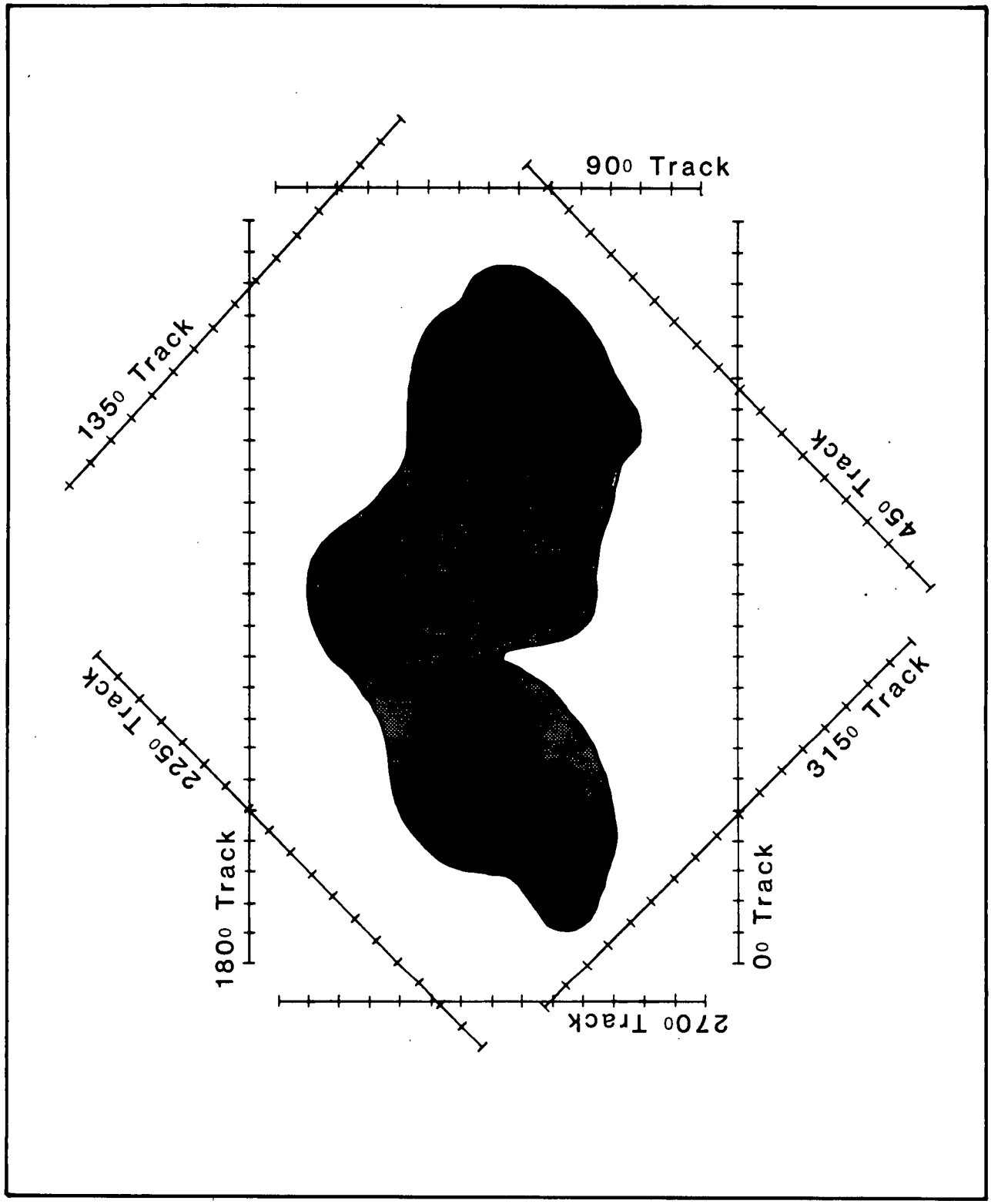

Fig. 24. Experimental iceberg shape representing a slice through the iceberg at approximately mid-water draft.

TABLE 4

Test data for reconstruction of experimental closed curve

RUN[a] 1	RUN 2	RUN 3	RUN 4	RUN 5	RUN 6	RUN 7	RUN 8
48[b]	128	55	55	73	60	109	41
43	121	40	52	63	55	M	11
40	117	31	53	56	55	M	13
41	114	25	51	54	54	49	20
43	113	26	54	53	50	43	28
47	113	37	62	52	45	42	M
53	80	44	72	49	38	37	M
62	M	101	76	40	34	24	80
77	M	108	76	28	33	27	80
M[c]	28		75	21	35		87
47	27		74	20	42		95
46	23		75	21	46		100
45	21		80	27	45		107
41	21			37	46		108
39	22			42			
32	26			45			
33				47			
39				50			
44				58			
51							

Notes: a) Data collected every 10 m during collection run.

b) Scale is 1 cm = 10 m.

c) M designates missing data.

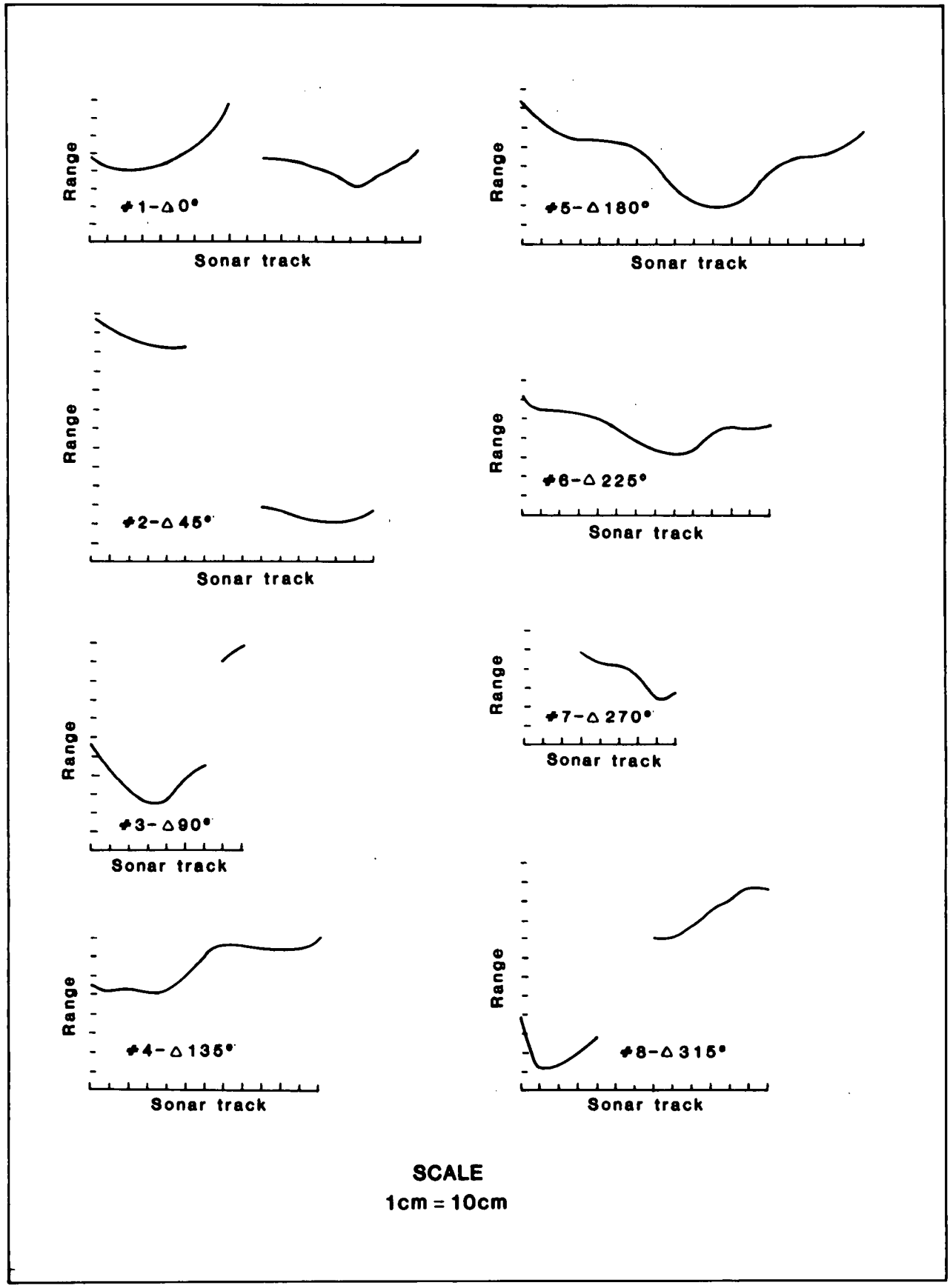

Fig. 25. Individual iceberg underwater curves (derived from Table 4).

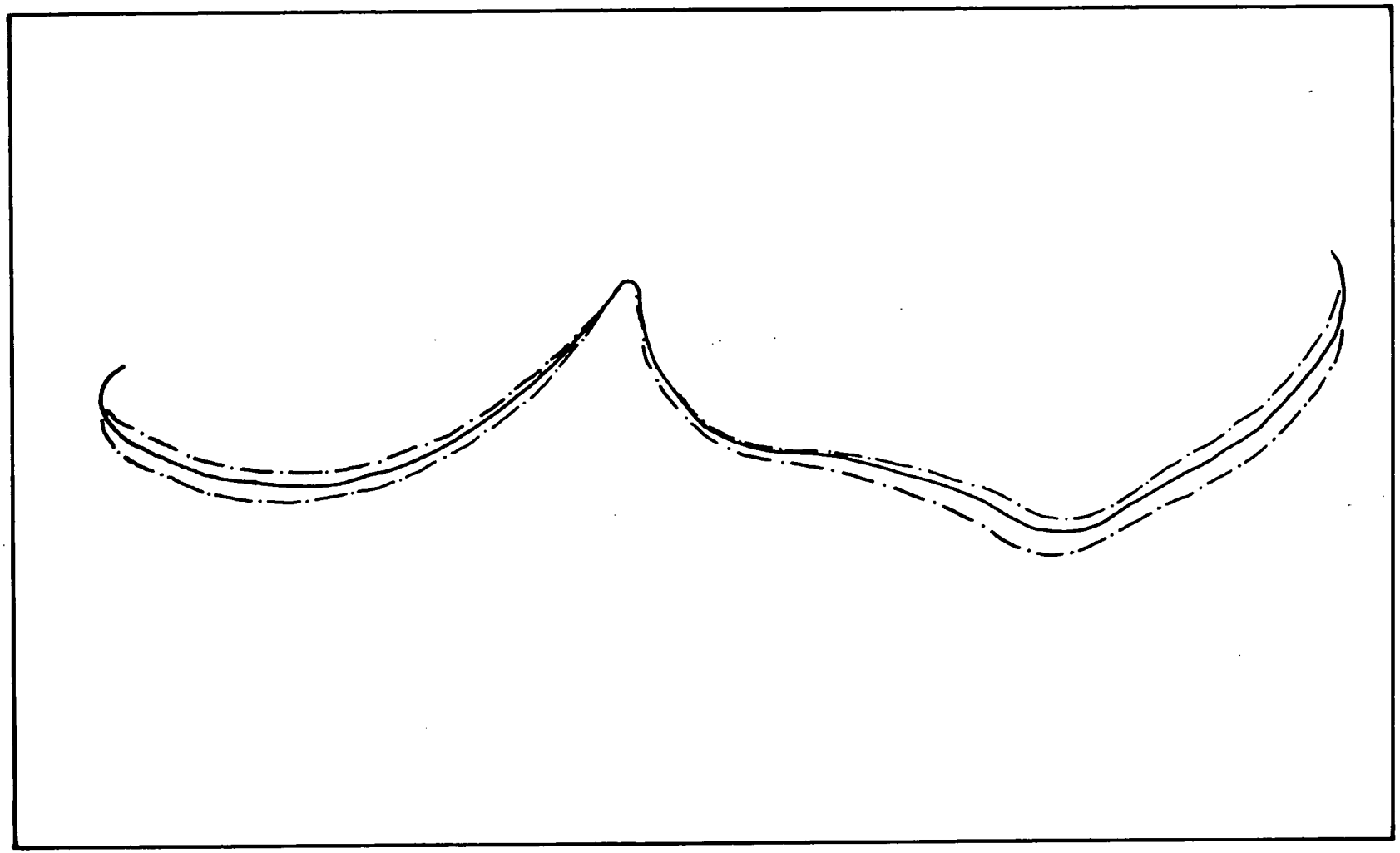

Fig. 26. Recovered iceberg shape (from individual curves presented in Figure 25.

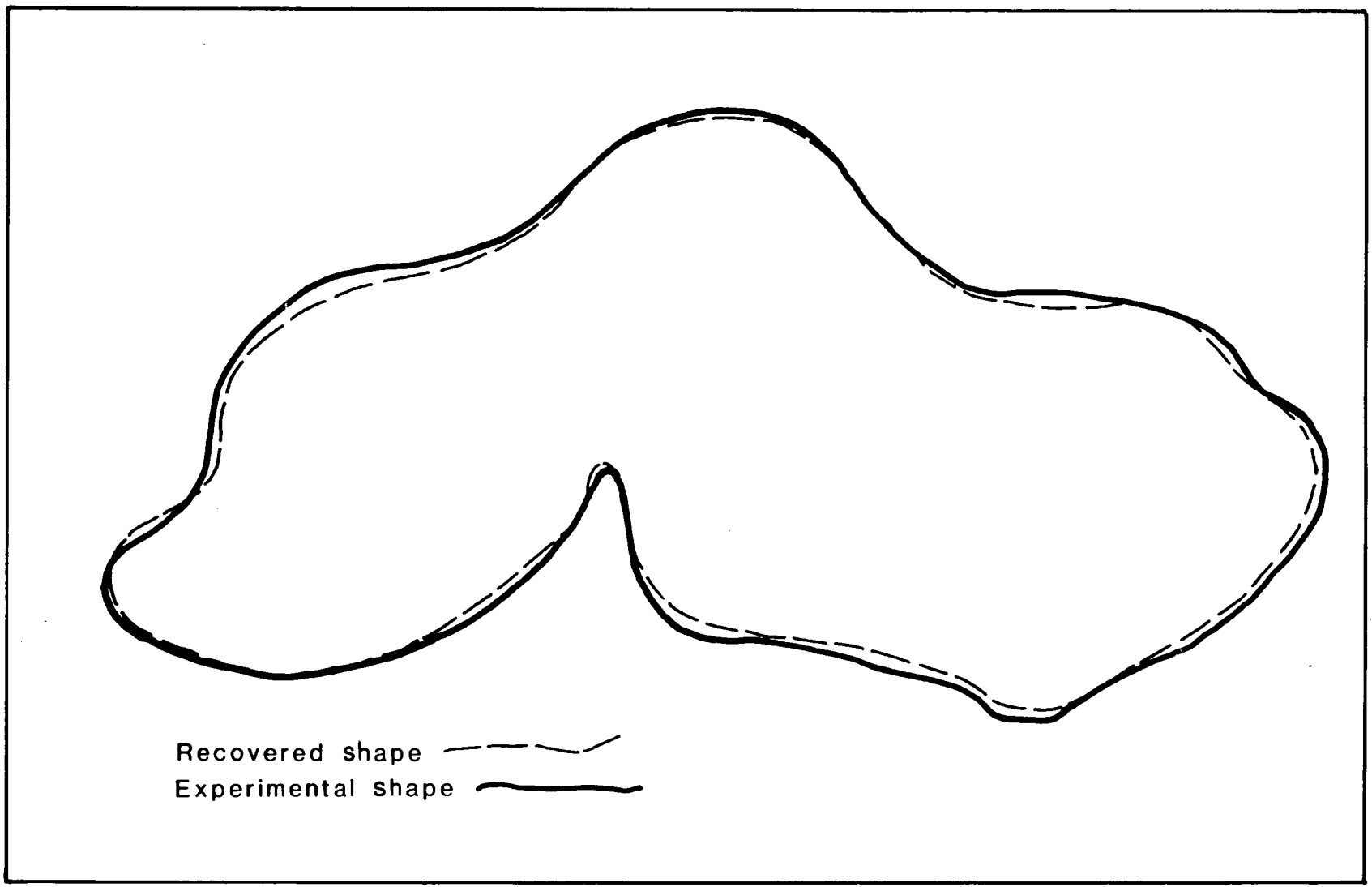

Fig. 27. Overlay of experimental shape versus recovered shape.

A major problem remains in matching the reconstructed contours from different depths so as to produce the total shape. The simplest solution to this problem would be a sensing system that insonified the whole side of an iceberg on each straight line run. Design specifications for such a system are proposed later and such a system is assumed to be possible. Under this type of scenario, one whole vertical strip of the iceberg would be insonified every second. One contour at a known depth would be pieced together by a person aided by a computer using an interactive graphics package, and this contour would then determine the remaining shape. This last step could be performed by the computer because each point on the recovered contour would be linked to a vertical strip of points.

Signal Processing and Data Storage Requirements

The signals that must be processed for a system without buoys are essentially identical to those for a system using buoys attached to the iceberg. The main difference is that more data would be transmitted from the sensor to the data storage unit during each pulse cycle because the whole side of the iceberg would need be insonified on each pass of the sensor. Under the contemplated scenario, in addition to data from the internal attitude sensor and the depth sensor, it is assumed that distances to as many as 22 points in a vertical strip on the iceberg would be transmitted for processing during each full duty cycle. This number would require a longer duty cycle so as to prevent misinterpretation of the insonification data, and thus, a cycle length of about 1 s is therefore contemplated. The data would be processed in real time, as with the system discussed earlier.

System Errors and Quality Control

The errors in this system would arise from all the same sources as those discussed previously with one extra. The additional source of error arises from the piecing together of a single contour from eight separate parts. In the experimental case, the total error, as determined by the difference in areas between the two contours is minimum. Although it may be negligible, field determinations of the amount of this error would be useful. This could be done by using the proposed system with acoustic marker beacons. The beacons would simply provide an absolute frame of reference from which careful determinations of the error associated with this technique could be determined.

Without acoustic beacons attached to the iceberg, the only method of quality control would be to link the system to a

grey-scale recorder, which would provide a means for detecting gross errors associated with system disfunction. As such it is recommended as a means of quality control in any case, but it would not provide a method for checking one subsystem against another, because to do so requires a fixed frame of reference.

An Operational System

Exclusive of the time required initially to deploy the sensor, it is expected that the eight passes of a 90 m iceberg following a track similar to that shown in Figure 23 could be made within a period of 2-3 h. The remaining time required would be associated with recovering the primary contour and with further processing of graphical data. This would be accomplished in three steps.

Step 1. The portion of each of the eight data sets associated with the primary contour would be turned into a sequence of curves, or curve segments, or both displayed on a graphics screen. Portions of curves missing as a result of incomplete data, would be left blank. The totality of each curve would be treated as a rigid body.

Step 2. Using a light pen, an operator would piece together the curves by matching features.

Step 3. The generated contour would then be passed back to the computer where it would be linked to the missing vertical portions of the data set. The complete data set would then be processed into a total three-dimensional shape which would then be available for display using suitable graphics options.

This system has a variety of useful features in an operational setting. If a requirement exists to determine the shape and depth of any collision surface on one side of an iceberg, it could be done by making one run with the system past the appropriate side of the iceberg. The total time for the operation would be about one-half hour and a complete three-dimensional picture of one side of the underwater portion of the iceberg could be obtained. Indeed, data on draft, stability, and a general profile could be obtained during one run. The only parameter which would require measurements to be taken all around the iceberg is the mass of its underwater portion. Thus, this type of system would be very useful in an operational setting.

PROCESSING FOR DATA PRODUCTS

A computer system must have the capacity to deliver a spectrum of data products. If, as already discussed, most of the data processing, i.e. taking raw data and turning it into digitized data files of manageable size, will already have been accomplished in the field, it is recommended that an idential processor be used in the laboratory. The only difference will be in the set of peripherals available to the processor, which would use a suitable software package together with the peripherals to generate the required data products. Additional peripherals would include:

. a graphics terminal with light pen

. a flat bed, or other, plotter.

For this concept to be workable and useful, a complete set of data products should be available in real time. The concept is considered feasible, and, by careful selection of equipment, a complete system could be installed on the bridge of a support vessel.

Additional Processing

A number of algorithms would have to be generated to produce the required data products. The main algorithm would have to produce a surface boundary point on the iceberg in each of a series of resolution cells. This algorithm would take as input data obtained in the field and have as output a three-dimensional underwater boundary for the iceberg. Some smoothing and other statistical techniques will have to be applied to produce a reasonable surface.

A second algorithm would interface the above-water data to the underwater data. At present, this aspect of the mapping process could not take place in real time, because there is no current method for inputting data obtained on the above-water portion of the iceberg directly into the computer. If this problem were solved, a method would have to be developed for linking the above- and below-water data sets to produce a single contiguous shape. One method might be to employ a marker that can generate data for both above- and below-water data sets.

A third algorithm would produce a total surface boundary for the iceberg. These algorithms would be used to produce a collection of data files which would be accessed by the graphics software package described below. The below-water portion of the surface could be generated in real-time.

Data Products

The main data product would be in the form of a three-dimensional graphics display on a graphics terminal. This product would be generated by an interactive, menu-driven graphics package in several steps.

Step 1. The user would select a given iceberg from whatever icebergs were in a master file.

Step 2. The user would then declare a point in space the "viewing point," or "view from" point from which to view the iceberg, and would then declare a "look at" point, and the dimensions of a window through which to view the iceberg.

Step 3. The user would then declare a plane for contouring, i.e., x-y, x-z or y-z, as the presentation of the iceberg would include both slices and contours.

Step 4. The portion of the iceberg which could be seen would be drawn on the screen. (This type of presentation implies the use of hidden line removal in its construction.)

Step 5. If a hard copy of the graph of the iceberg presented on the screen was required to be saved, the graph would be dumped to the plotter.

In schematic diagram (Figure 28) the user chooses a point on the iceberg to look at, and a place in space from which to view the iceberg, the view from point. Then a window size is selected; with small windows, the user would view the details of the iceberg near the point being looked at; with large windows, the user would see less detail, but would view greater portions of the iceberg. Because the co-ordinate system is fixed in the iceberg, by changing the look at and view from points all sides of the iceberg can be seen. In a sample graphics product, presented as Figure 29, both contour lines and slice lines are shown. The presence of both types of lines leads to a much better sense of the three-dimensional shape of the iceberg. It is emphasized that the software would be interactive and the graphics initially generated on a screen; hard-copy graphics would be produced only after the user was satisfied with the product.

In addition to the graphics products, the user could obtain a cross-sectional area for the iceberg in any plane, as well as any specified linear dimensions. Lastly the user could obtain a calculated mass, and the above- and below-water volumes.

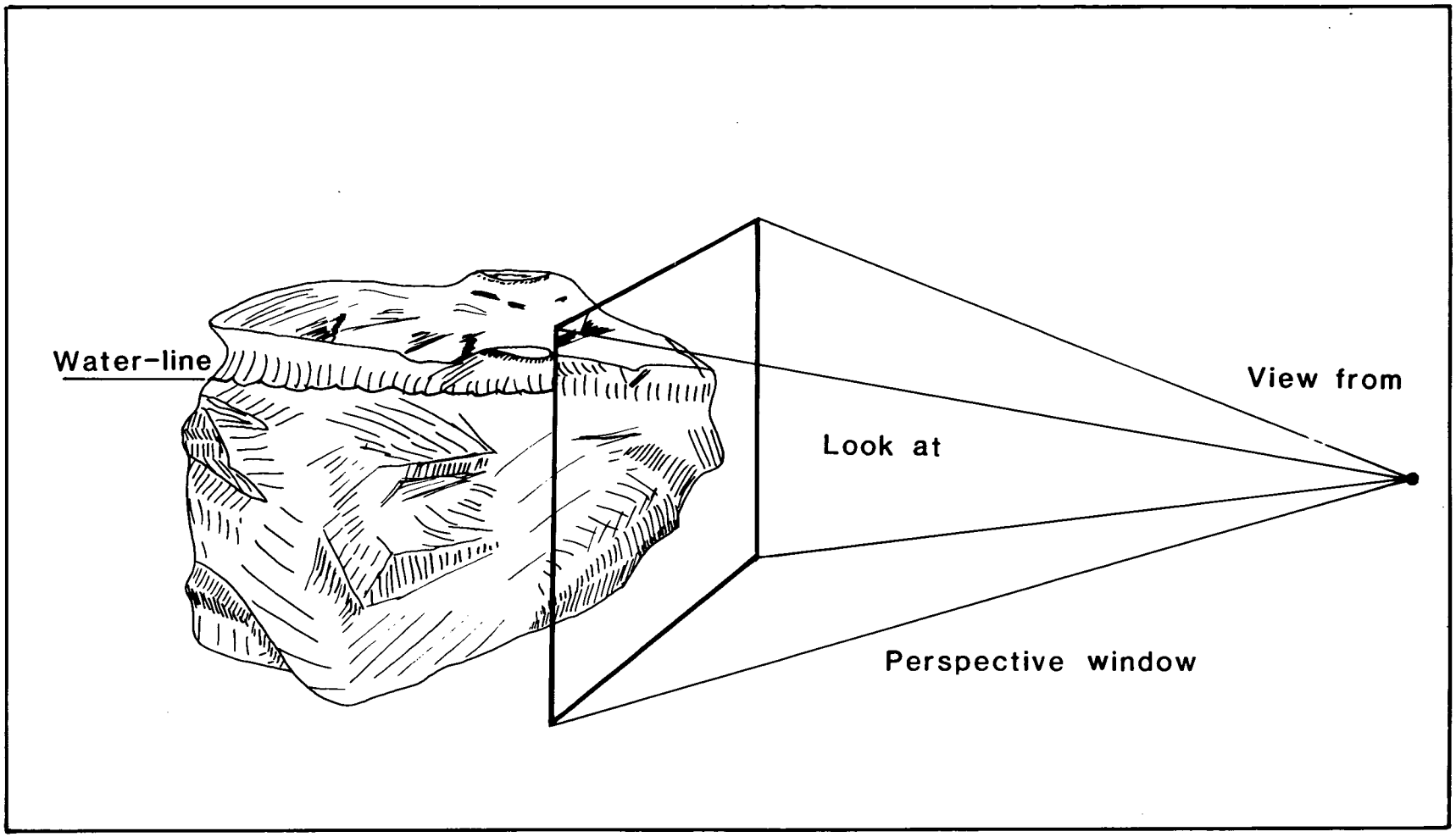

Fig. 28. The operations of an interactive graphics program.

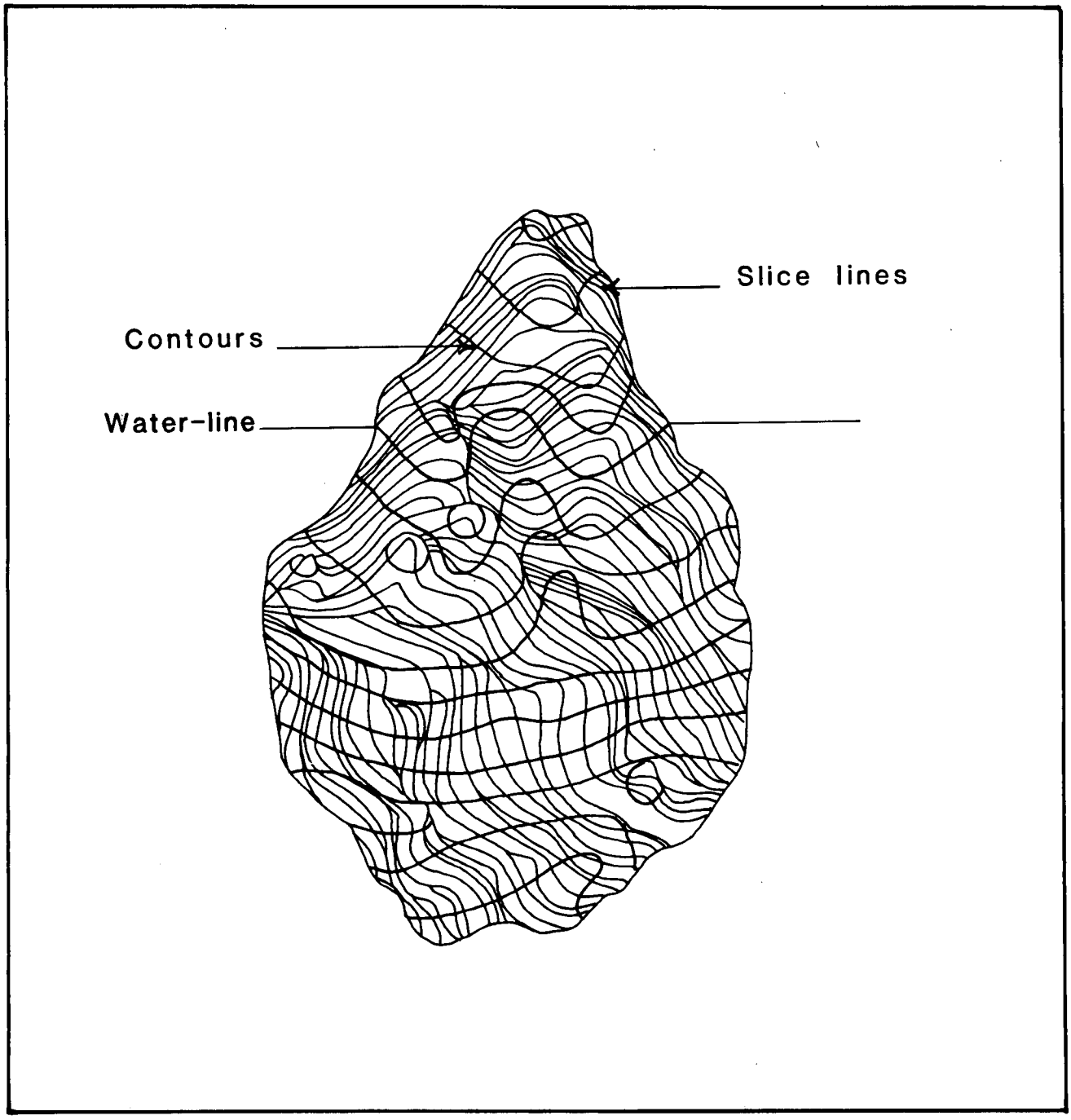

Fig. 29. Sample graphics product.

SYSTEM DESIGNS

The earlier discussions point to two possible types of systems being used for iceberg mapping. The first type involves pencil-type beam-scanning of the iceberg with these data being supplemented by an internal positioning system physically attached to the iceberg with an attitude-monitoring system attached to the sensor. The system generates individual co-ordinates on the surface of the iceberg and the family of these individual co-ordinates is used in generating a map of the iceberg's geometry. Such a system under the trade name, Polarscan, was employed for iceberg mapping in the spring of 1984.

Clearly, the requirements for iceberg mapping require rapid measuring techniques. Conventional side-scan sonar systems are used for mapping the seabed by imaging in time and space. There is no doubt that side-scan sonar can see the iceberg effectively. Consider Figure 30 which shows a sonogram obtained by towing a bottom looking sonar fish near a grounded iceberg. Repeat passes showed the same shape. However, conventional side-scan sonar records, although satisfactory for many applications, have three major scale distortions that limit the use of these systems for iceberg mapping.

a) A typical sonar record has a different scale in one axis than in the other axis (i.e. imaged in time and space). Thus features are distorted. Accurate correction of the axis along the vessel's track requires the integration of the navigation system with the sonar system.

b) The attitude or look direction and position of the side-scan sonar fish in water column fluctuates during scanning. Both require monitoring and correction during the scanning operation to provide true measurements.

c) The standard sonar system measures the distance from the tow-fish to a point on the seabed rather than true distance from a known frame of reference. To do slant range correction, the conventional system basically solves the equation for a right triangle. This solution assumes a flat target, which is a reasonable approximation for the seabed in most situations. This assumption is no longer acceptable for the vertical face of an iceberg. With the fan-shaped beam of the standard transducer, the sonar data that is obtained includes only azimuthal angle and range (time) to a particular target; it does not contain the vertical angle of the target relative to the transducer. Thus, with imaging in time not space, two points because they are the same time (or range) away, appear together in

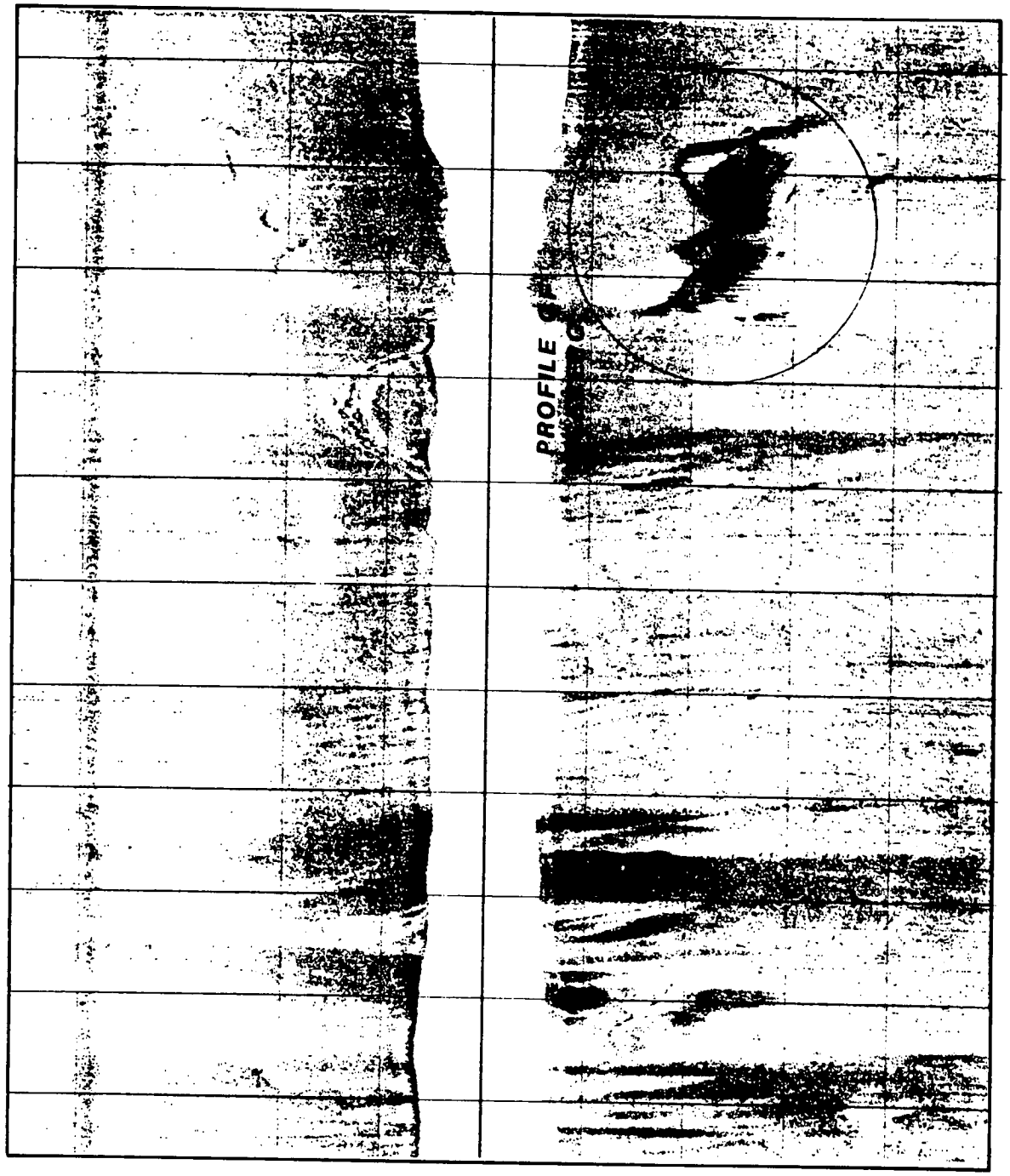

Fig. 30. Iceberg profile obtained by bottom-looking, side-scan sonar (courtesy Mobil Oil Canada, Ltd.).

the sonar record even though they may be separated widely on the vertical face of the iceberg. There is no known technique with which to correct this.

The second type of system that offers a practical solution to iceberg mapping involves imaging techniques. Although three-dimensional imaging has been developed for military applications, the degree of sophistication required for such a system and its overall cost make two-dimensional imaging techniques the more-attractive alternative.

OSPS OPERATIONAL SYSTEM

The system design described in this section is operational. It was developed by Offshore Survey & Positioning Services Ltd. under the trade name Polarscan and was employed during the 1984 ice season to produce underwater three-dimensional images of icebergs. Based on these field experiences significant improvements have been made in the iceberg imaging and profiling sonar data acquisition system which are outlined below.

The Polarscan system was originally developed as a support tool for the Polar Gas Project. Its main purpose was to serve as a means for detailing precise bottom topography information for use in construction of underwater pipelines. It was also used to survey the underside of the Arctic pack, as described by Good et al. (1984).

The disadvantages of this system are:

- the length of time required to completely survey the iceberg's underwater surface (estimated at 1 day per iceberg);
- the absolute requirement that a positioning system be attached to the iceberg itself. An operation that is difficult even under ideal environmental conditions;
- data is not available in real time; and
- the cost of each iceberg surveyed would be high (probably in the range of $5,000 to $10,000 per iceberg).

The system is comprised of the following components:

. an imaging sonar system
. an acoustic positioning system.

Imaging Sonar System

A Mesotech Model 971 imaging sonar is employed to insonify the face of an iceberg. Its specifications are listed in Appendix 9, Table A-13. This scanning sonar operates on the principle of mechanically rotating a transducer array through a vertical or horizontal plane. Based on data products, presented in Figures 31 and 32, it is concluded that profiling took place in a horizontal mode. The narrow pattern of the conical beam (2.1^{o}) and the azimuthal angle of scanning permit the determination of the slant range to the sonar target. A stepping motor positions the transducer through successive rotary steps of 0.225 degrees. A full transmit pulse cycle is repeated between each rotary step. Two modes of operation of this component are available, an image and a profile mode. The image mode produces displays that show selected areas surrounding the sonar transducer. The profile mode displays the same images with the addition of a plotted profile line derived from the first strong sonar return. This profile data is available through a serial output port. The installation of a compass in the sonar head allows the absolute orientation of sonar images and targets relative to magnetic north to be determined.

Acoustic Positioning System

The system consists of a Mesotech model 411/412 acoustic navigation system and four (4) Mesotech Model 501AR acoustic release transponders. Resolution of the system is about 1 m. OSPS provides special EPROMS to make it possible to collect data at 1 s intervals. This system allows the iceberg's geometry to be defined through a technique of superimposing corrected adjacent images.

Software controls data acquisition, display, and storage. Position and track is displayed on a CRT graphic screen and hard copy is available on plotters. System components include an HP 9825A computer and an HP 9872B plotter.

Features of the Iceberg Imaging System

The following are features of the iceberg imaging system:

- a magnetic compass internally mounted in the transducer head provides accurate heading and accurate reference bearing calibration directly;

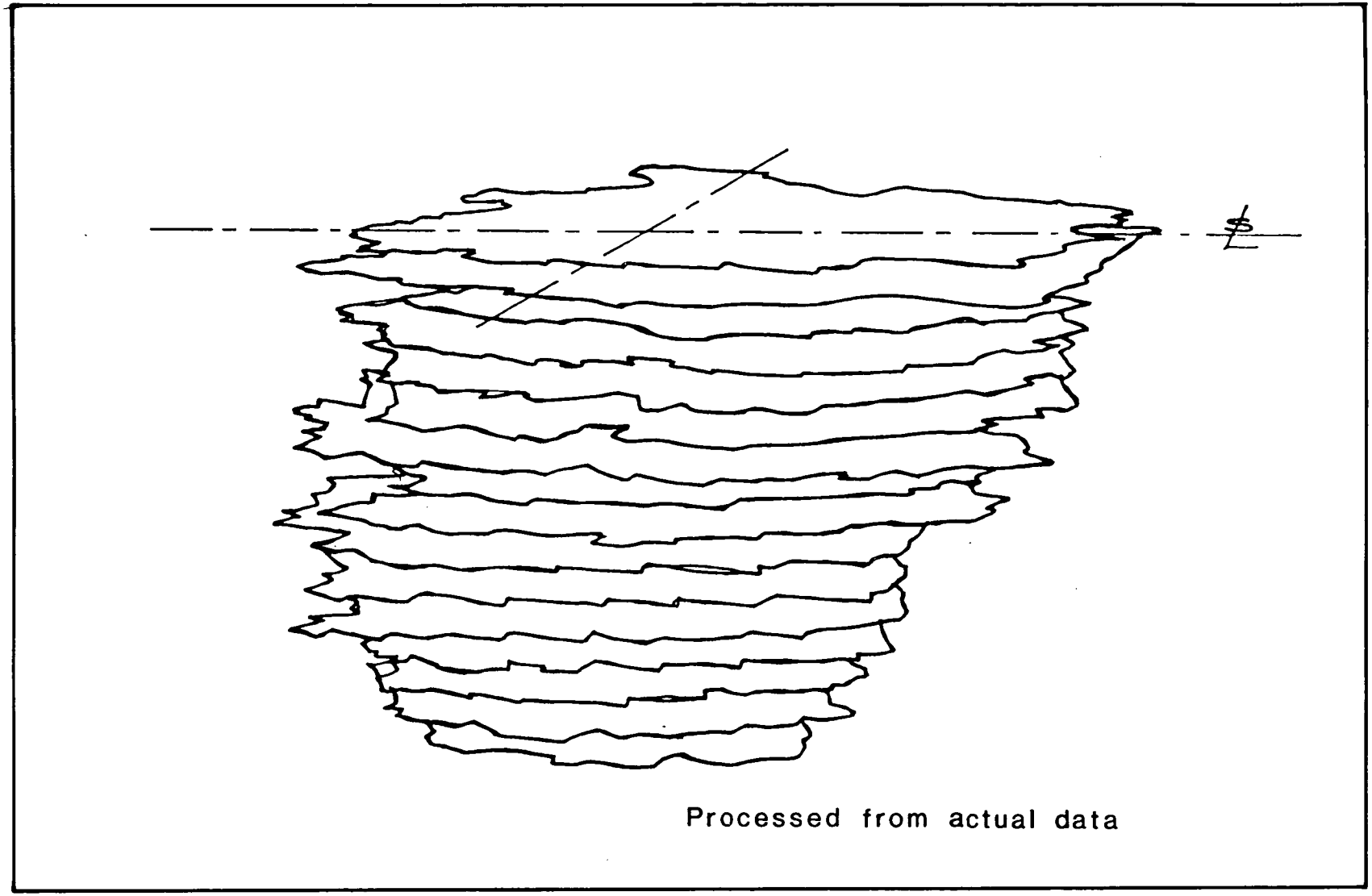

Fig. 31. Typical stacked horizontal cross-section of an iceberg (courtesy of Offshore Systems Ltd. 1984).

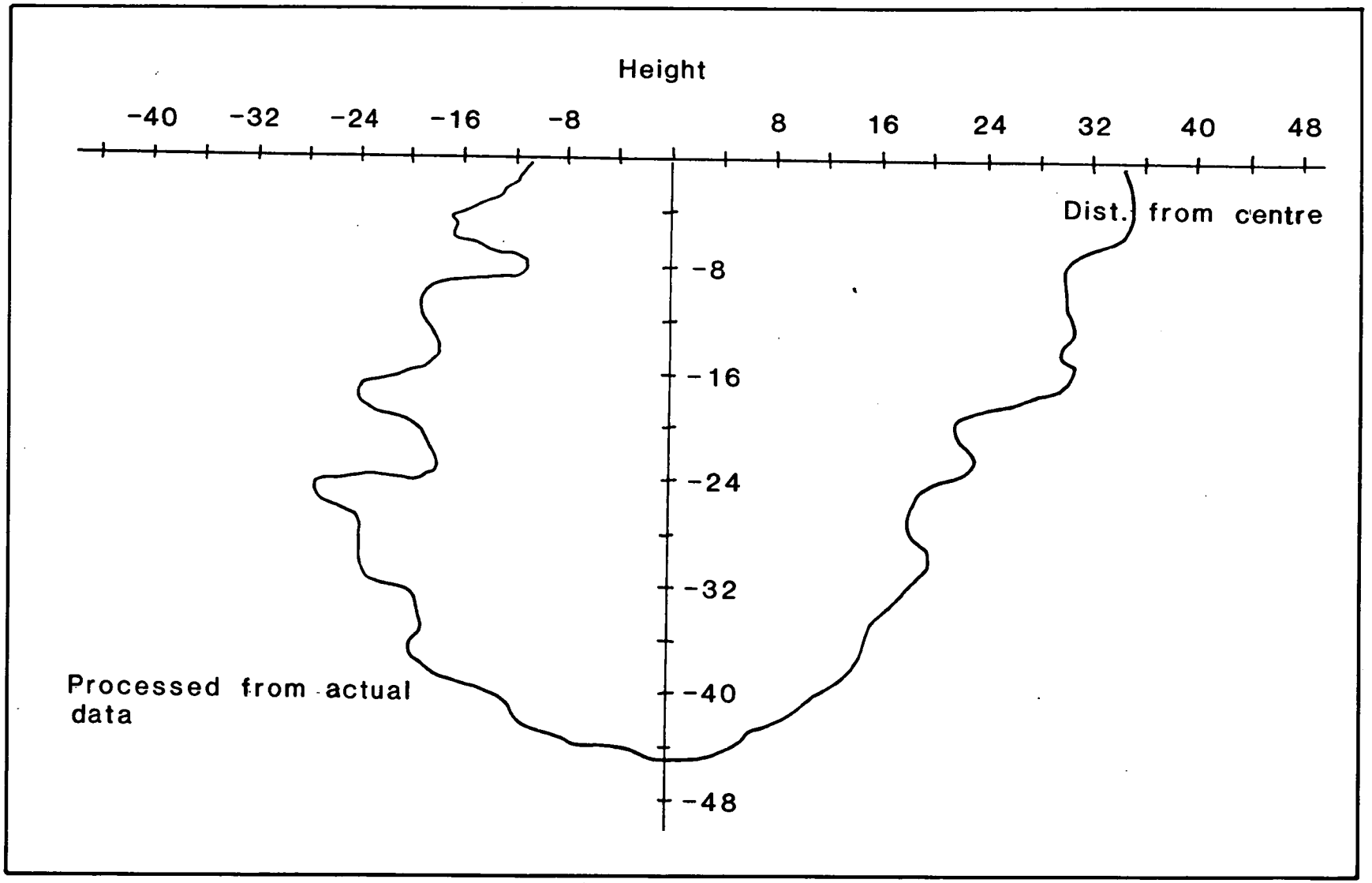

Fig. 32. Typical vertical section of an iceberg (courtesy of Offshore Systems Ltd. 1984).

- an improved 330 kHz combination transducer OSPS specially designed for the project achieves extended ranges to 280 m. Modification for the pulse repetition rate allows data to be collected in almost half the time of a standard or conventional Mesotech transducer;

- special improvements in the acoustic interrogation system make it possible to collect acoustic positioning data at 1 s intervals, which increases the data density to five times that of the previous project. This feature now permits continuous tracking of the vessel's position during data collection and greatly enhances the reliability of the positioning information;

- a custom-modified OSPS-Mesotech transducer beam pattern effectively reduces ship's noise; and

- data-processing software make it possible now to verify the quality of the raw data as it is acquired.

Data Acquisition

The OSPS high-resolution iceberg mapping and profiling sonar data acquisition system will allow determination of orthogonal three-dimensional underwater profiles of at least four sides around the perimeter of an iceberg with the sonar also providing water depth at each value of the profile obtained. Both the depth and shape of any underwater protrusions or indentors are determined directly.

The system also allows the determination of three-dimensional grid of the underwater iceberg shape of the peripheral of the iceberg. The grid points can be spaced no further than 10 m in the horizontal and vertical such that length, width, and depth of the iceberg are calculated directly to produce estimates of the mass.

Operational Methodology

The survey vessel approaches the iceberg and deploys four acoustic reference transponders as a positioning control system while monitoring and recording ship's gyro heading. After all transponders are deployed, the vessel circumnavigates the iceberg while taking ranges to each of the transponders. These ranges are processed using advanced Kalman filtering to determine the absolute geometry of the four positioning transponders. This method requires the system to survey each

quadrant of the iceberg separately. A constant on-site positioning update, calibration, and quality control of the raw data directly and instantaneously with the acoustic ranging system are provided. Iceberg data output would include a real-time CRT monitor displaying iceberg view, plan, or section as required.

Through circumnavigating the iceberg in stages, each iceberg's geometry is defined through a technique of superimposing corrected adjacent images.

Data Analysis

Acoustic positioning system range data are calculated using a least-square adjustment to obtain the best estimate for the transducer position. Profiler data are tested for outlines and the corrected are manipulated to fit individual iceberg profiles and used to generate cross-sections. Output includes horizontal and vertical cross-sections, and three-dimensional graphic representations (stacked profiles).

Numerical processing of some data is possible in the field, although production of a complete underwater image is not available in real time. Typical data products, which are produced by mosaicing data sets from horizontal scans at various depths, are contained in Figures 32 and 33. Basically, these consists of contours at each depth. However, the alternate data products of the type suggested earlier would also be available.

Quality Control

Calibration of the acoustic system. The acoustic system is calibrated using a self-calibrating least-square adjustment before and after the data collection period and will detect the presence of motion in the reference acoustic network.

Error sources. The major sources of error in an iceberg profiling system are alignment error, azimuth error, and attitude error mainly from sea state conditions that create roll, pitch, and heave of the profiler. The alignment error between the positioning transducer and the sonar profiler is eliminated by co-locating the transducer-profiler on the same boomed cable system. The azimuth error is reduced by incorporating the ship's gyro and the profiler's magnetic compass to obtain relative direction information to better than 5^{o}. Attitude error of the transducer-profiler assembly is minimized by attaching a weight to dampen the effects of undesired motion.

Minor sources of error include, but are not limited to, positioning calibration errors, speed of sound variation, data intermittency, beam-width data corruption, transponder network motion, and vessel drift.

Finally, operation is contained to sea state conditions ranging from a preferred calm to a maximum sea state of 4 on the Beaufort scale.

System Accuracy and Performance

The results of the 1984 field program are not available at this time and thus it is not possible to comment on data accuracy or system performance achieved.

It is suggested by the designers of the system that both horizontal and vertical sectors can be scanned to better than 10 m (accuracies of $\pm$ 2 m have been obtained previously). Interval accuracy depends on sea state conditions.

CONCEPTUAL DESIGNS FOR ICEBERG MAPPING SYSTEMS

Conceptual designs are presented for two iceberg imaging systems. Both systems use the combined effect of the directionalities of the transmitter and receiver to generate a series of searchlight-type beams on a narrow area of the iceberg representing the vertical profile of the iceberg (see Figure 33).

Operational constraints require that the iceberg mapping should be accomplished in a relatively short time and from a safe distance. A conventional, single-pulse sonar would require (apart from other problems) excessive time to complete the survey. The two designs described here as Towed Iceberg Mapping System 1 and 2 are a continuation and further development of the original system conceived by Zielinski (1980) for which a patent is pending. The systems proposed can be used for other diverse applications such as bathymetric surveying, dredging operations, and active-passive target detection.

These systems are two-dimensional, real-time imaging systems. They are complete, computer-linked, data acquisition systems designed to accumulate and collate information suitable for automatic generation of an underwater iceberg map. The systems would generate rectilinear profile views of the iceberg in real time and the data would be stored digitally.

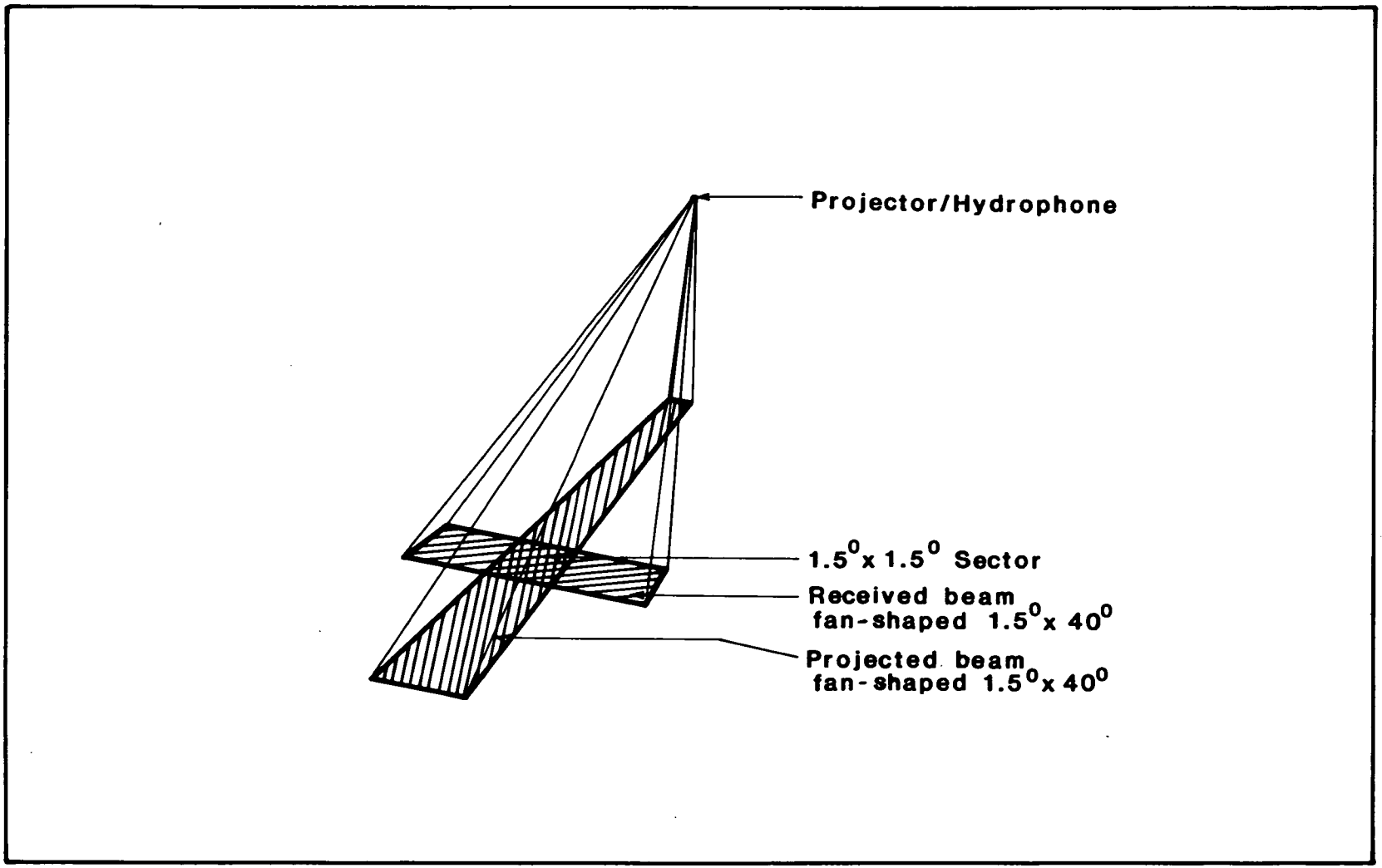

Fig. 33. The effective insonified area formed by the intersection of the projected and received beams.

Both systems have an internal inertial positioning system from which data on sensor orientation and its relative position in the water column are obtained. These data would be used to normalize the acoustic image to a true three-dimensional reference. Although the quality of the acoustic image is not especially dependent upon platform stability, the overall system design would seek the most stable sensor platform available.

TOWED ICEBERG MAPPING SYSTEMS 1

At the basis of the Towed Iceberg Mapping System 1 (TIMS-1) are the two acoustic transducer arrays, T_1 and T_2, as shown in Figure 34. Transducer, T_1, functions as a projector with a narrow (in the horizontal direction) fan-shaped beam which can be steered from its horizontal position by mechanical rotation of the transducer. Transducer, T_2, is a fixed receiver with a narrow (in the vertical direction) fan-shaped beam. The two arrays can be physically identical. In combination, these two beams create a narrow, searchlight-type beam.

The fish is towed along the side of an iceberg as shown in Figure 35. The projector beam scans the iceberg in the vertical direction by constantly changing its angular position and by transmitting a short pulse at the selected positions. During a single vertical scan the last pulse is transmitted before the first echo from the iceberg is received by the receiver. This requirement imposes a restriction on the duration of the transmitted pulse sequence for a given target range as discussed later. The received echos are generated by reflection from a small rectangular resolution cell as shown in Figure 35.

Echos resulting from different projected beams (angular directions) are distinguished by their order of arrival. It is assumed that echo resulting from the earlier transmission arrives before the echo from the subsequent transmission. To avoid ambiguity, which can potentially arise from a complicated iceberg profile, a proper time-spacing, between transmitted pulses must be provided. Alternatively, different frequencies can be used to mark (colour) the adjacent pulses. To allow separation of signals coming from the different pings it is possible to colour these pings in frequency (i.e. first ping 100 kHz, second 101 kHz, third 102 kHz, pattern repeated).

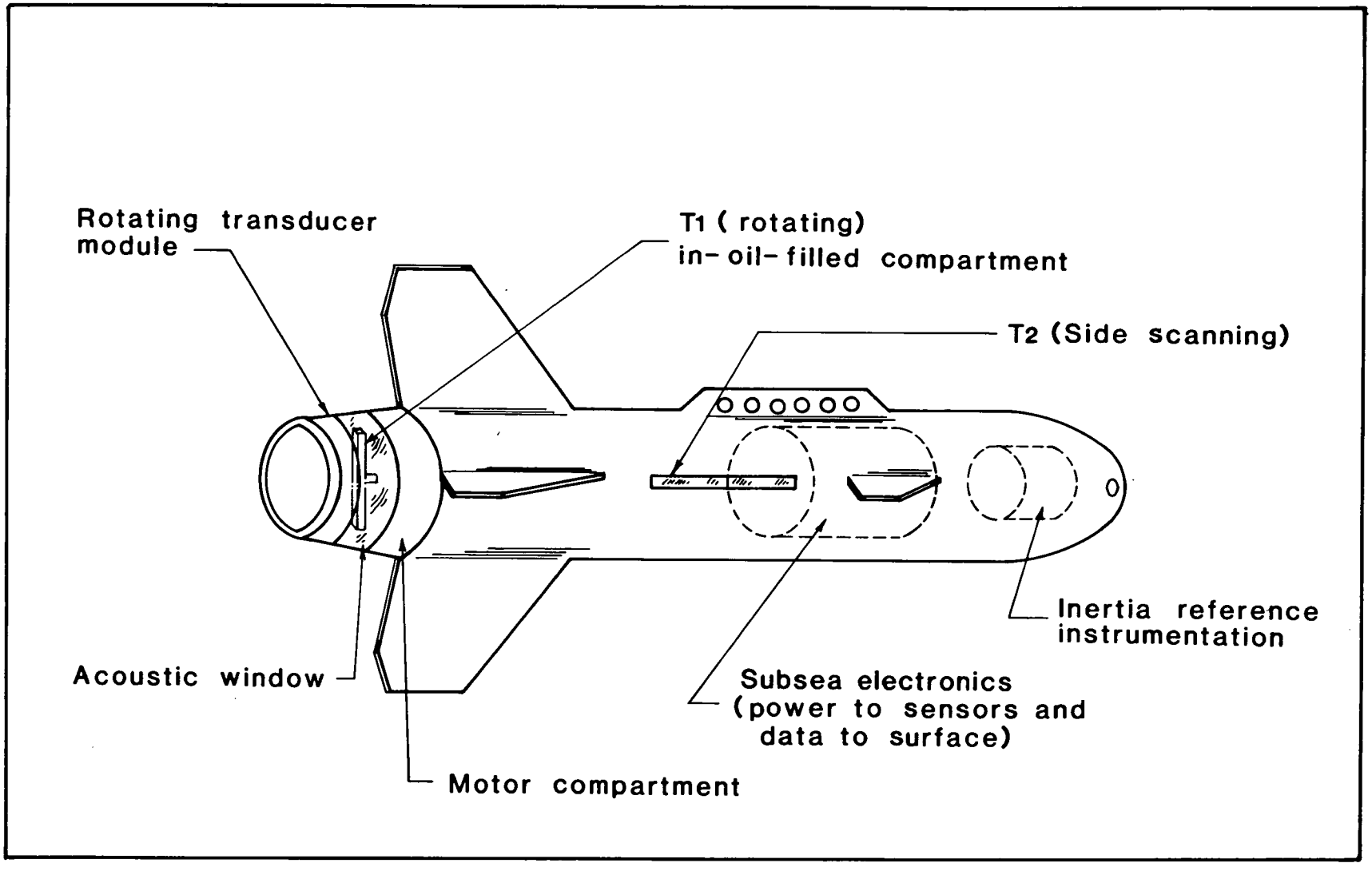

Fig. 34. Configuration of acoustic transducers.

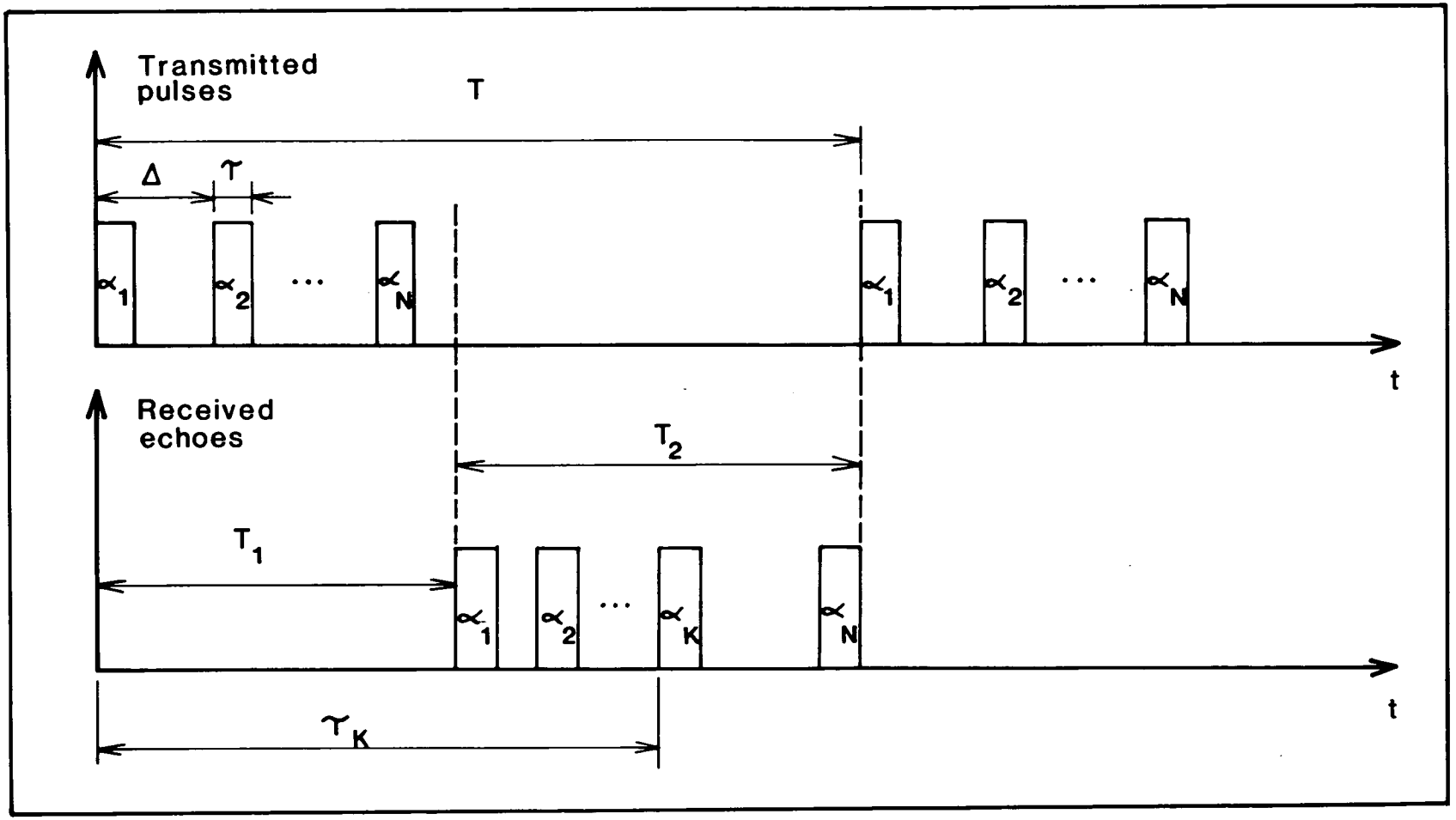

Fig. 35. Geometry of iceberg scanning.

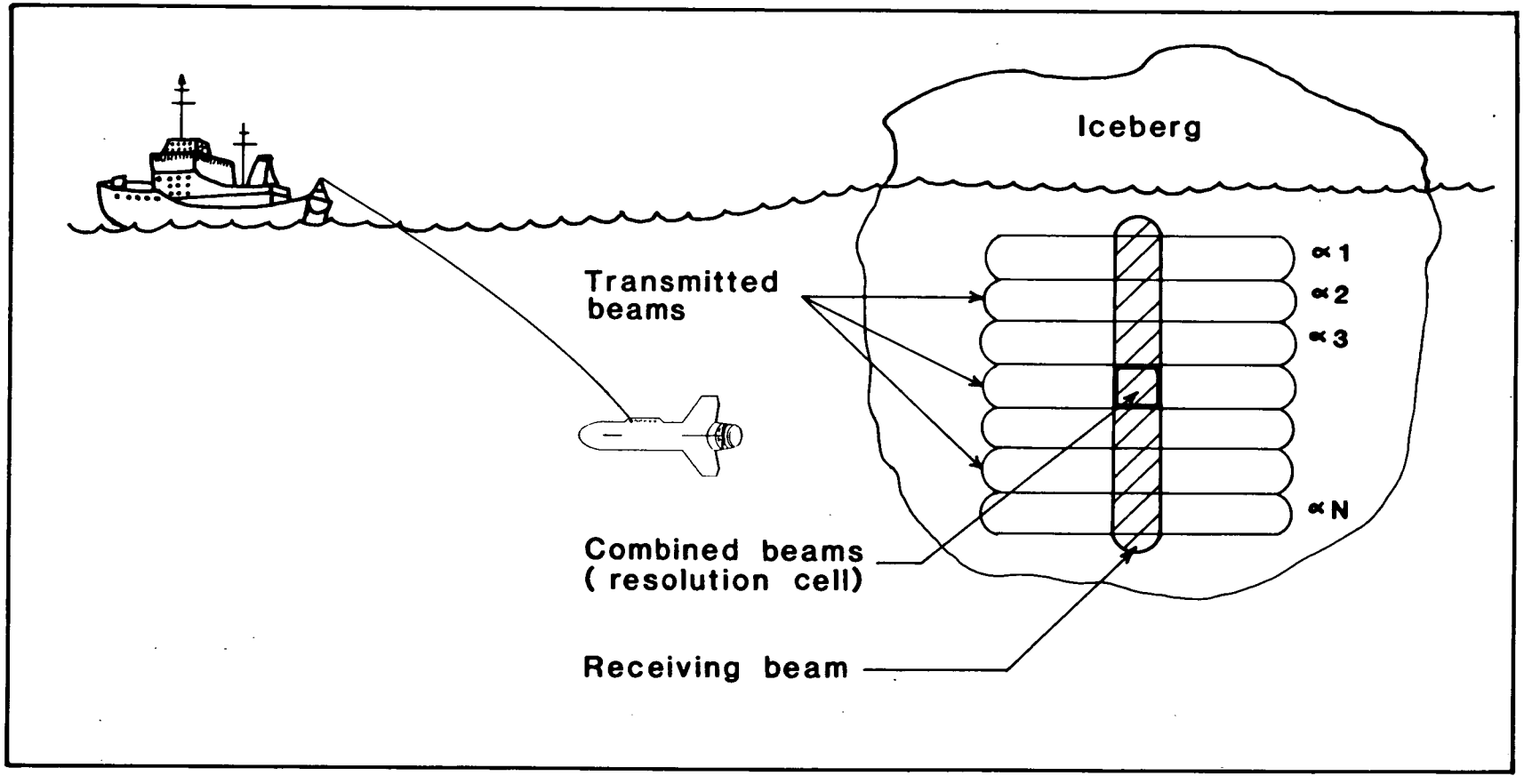

Fig. 36. Sequence of the transmitted and received pulses.

The sequence of transmitted pulses and received echoes is shown in Figure 36. The minimum radial distance, r_{min}, from the sensor and to a target must satisfy

$$T_1 = \frac{2r_{min}}{c_1} > (N-1)\Delta + \tau \quad (1)$$

where:

N = number of pulses in the transmitted sequence,

Δ = separation between pulses (large enough to avoid ambiguity), and

τ = pulse duration.

The minimum repetition period of the probing sequence is related to the maximum radial distance, r_{max}, to a target, that is:

$$T > T_1 + \frac{2(r_{max} - r_{min})}{c_1} \quad (2)$$

The delay of each echo is related to an iceberg vertical profile by:

$$x_k = D - \frac{c_1 \tau_k}{2} \sin \alpha_k \quad (3)$$

$$y_k = \frac{c_1 \tau_R}{2} \cos \alpha_k - r_o \quad (4)$$

where:

k = 1,2..... N

τ_k = two-way travel time of a pulse transmitted in the λ_k direction,

y_k = distance between an iceberg at depth x_k and the reference plane and,

r_o = distance between the sensor towed, at depth, D, and the reference plane.

A complete, three-dimensional scan of one side of the iceberg is accomplished by combining the vertical scans obtained during a survey track along the side of the iceberg.

Technical Considerations of Acoustic Sensor

The technical parameters for TIMS-1 are presented in Appendix 9, Table A-14.

Operating Frequency. The 3-dB beam-width of a linear transducer, $\emptyset$, is approximately related to its length, L, and operating frequency, f_o, by:

$$\emptyset \text{ (deg)} = 50 \ \lambda/L \tag{5}$$

where wavelength(λ), is given by:

$$\lambda = c/f_o \tag{6}$$

The selection of operating frequency is a compromise between system's angular resolution and range, and transducer size. The 100 kHz pulses have been successfully used for iceberg draft measurement at ranges exceeding 300 m. For these reasons the operating frequency f_o = 100 kHz and beam-width $\emptyset$ = 1.5^o are postulated as sensible choices for the system. Several commercially available side-looking sonars operating at this frequency have relatively narrow beam-widths of approximately $1\text{-}2^o$ and reasonable transducer size.

In view of the errors associated with a finite beam-width and the ray-bending problems discussed earlier, the justifiable system radial resolution should be approximately 1.5 m. This resolution is achievable by the 2 ms probing pulse and corresponding 0.5 kHz system bandwidth.

Beam patterns. System performance will be degraded if excessive side-lobes are present in the projector or receiver beam patterns. A linear, uniform transducer, for example, has

its first side-lobe attenuated only by 13 dB with respect to the main beam. Thus, precise shading is required to increase the amount of attenuation. It is recommended that transducers with side-lobes attenuated by at least 30 dB be used. The length of a shaded transducer is about 25-35% larger than given by Equation 2 (Burdic 1984).

Beam scanning. The number of pulses in the transmitted sequence corresponding to the number of beams is a function of the assumed minimum radial distance of the target as given by Equation 1.

For N = 22 pulses in the sequence (or 22 beams), the separation between adjacent pulses Δ = 9 ms and pulse duration $\uparrow$ = 2 ms, the minimum radial distance to a target, r_{min}, as calculated using the Equation 1 is 143 m. Assuming maximum target range r_{max} = 400 m, the minimum repetition period of the probing sequence is (according to Equation 2), T = 0.53 s. With the proper rotation of the acoustic projector during transmission of the probing sequence, a desired angular sector can be scanned. For the 22 contiguous 1.5° beams the required transducer scanning speed is 167°/s (within the 33° sector).

Mechanical Consideration. The projector will be enclosed in an oil-filled dome. Methods of rapid mechanical scanning (continuous versus steps) should be investigated in consideration of accuracy, vibration introduced, and effects on fish stability (a counter-balancing dummy transducer may be required). A provision can be made for a controllable tilt of the projector. This feature can be also used to stabilize the beam variation caused by the rolling of the tow-fish.

Positioning System

It is proposed that three-dimensional reference be provided by incorporating an inertial reference system in the sensor body, such as the Humphrey's Model CF32-0201-1. This system provides continuous, precise measurements of position and attitude (pitch, roll, and yaw) and is compatible with nearly all telemetric and recording systems. The system has been used in monitoring the response of underwater towed vehicles, which would eliminate the need of attaching transponders directly to the iceberg. Estimated total cost of this system is about $35,000. Specifications are included in Appendix 9, Table A-15.

Tow System

It is anticipated that sensor platform will be towed at two depths at least. First, the mid-water depth of the iceberg would provide maximum coverage. For the Grand Banks area it is anticipated that this would be between 40 and 50 m. Secondly, at or below the draft of the maximum keel depth of the iceberg would provide the clearest image of this portion of the iceberg and would improve returns from an area of the iceberg that would usually be insonified at a near-grazing angle.

The advantages of a towed system are many. A separate tow body behind and below the ship almost eliminates ship noise and, if properly designed, generates very little noise of its own. The acoustic path variability problem at large angles can be reduced to insignificance by positioning of the transducers. The platform, towed at depth, will exhibit much less yaw, pitch, and roll because it avoids ocean surface disturbances. The disadvantages of a towed body are its launch and recovery difficulties and its vulnerability while being towed.

Other features that should be incorporated in the deployment platform design are:

- a decoupling of the tow body from the heave of the towing vessel, and

- recovery system in case of failure of the two cables.

Tow Cable

The system is to be deployed and operated through an armoured coaxial cable. All power and telemetry signals are multiplexed onto the coaxial cable (or cables). Frequency division multi-plexing is recommended to permit flexible use of numerous analog and digital data channels. Data from high-precision sensors can be digitized with high accuracy and can be sent to the surface via an expandable digital channel. The highly flexible multiplex telemetry capability of the system also allows additional sensors or systems to be easily incorporated.

Deck Equipment

The tow cable would be stored on, and towed from, a simple winch with drum and slip-ring assembly. The tow-fish would be launched and recovered with either a davit or an A-Frame. The entire deck-handling system and shipboard electronics will be

transportable for use on ships of opportunity. Adequate hydraulic or electrical power for the deck-handling equipment should be readily available and a free area on the fantail must be available.

Data Processing, Recording, and Display

The received acoustic signal, after amplification, will be transmitted through a coaxial cable to the receiver on the towing ship, where it is to be converted to the baseband signal with a band-width of approximately 500 Hz. The baseband signal will then be digitized at the minimum sampling rate of 1.0 kHz for computer analysis.

Additional data channels will contain other pertinent data such as the sensor attitude, the vehicle depth, surge and sway, and navigation signals. A computer interface will supply all slant range corrected acoustic image data and precision positioning data from the inertial reference system to the computer-controlled logging and storage devices.

As a back-up system, all signals can be recorded on a conventional tape recorder. Real time audio tape recordings of analog data and other operational parameters can be post cruise analyzed and re-digitized to ensure that real time computer failure will not jeopardize cruise success.

A conventional grey-scale recorder can be used for quick assessment of signal quality and as an additional means for signal interpretation (particularly for noisy signals).

Vessel Requirements

The TIMS systems are flexible enough to operate from a broad range of vessels. However, the handling and sea-keeping characteristics of the ship have a significant effect on the quantity and quality of data that is collected. As a minimum, a vessel which is capable of manoeuvering at slow speeds (1-2 knots) and has sufficient deck space for deployment and on-board operational instrumentation is required. On large, more-stable vessels the system should produce good-quality data in sea states up to Beaufort 5. On smaller vessels, the motion of the deployment platform will probably increase drastically with a corresponding deterioration in data quality in sea states greater than Beaufort 4. In fact, the combined effects of wind current and waves may make it impossible for a small or less-manoeuverable vessel to achieve the desired course. Vessels with two thrusters, active rudders, twin screws, and

experienced personnel increase the probability of successfully carrying out a desired survey under adverse environmental conditions.

TOWED ICEBERG MAPPING SYSTEM 2 (TIMS-2)

General scanning scenario and tow-fish is similar to that of TIMS-1. Transducer T_2 (see Figure 34), however, functions now as a narrow-beam transmitter, whereas transducer T_1 is a multi-element linear receiving array. By proper delays and addition of signals sensed by each element of the array, it is possible to synthesize several narrow beams pointing at different directions simultaneously. By measuring echo delays from a specific angular direction a vertical iceberg profile can be computed using Equation 8.1. Unlike TIMS-1, no moving parts are required and vertical scanning can be accomplished by transmitting a single probing pulse. The system is, however, much more complex because of the acquisition and processing of signals from each element of the receiving array.

Technical Considerations of Multi-beam Forming

The synthetic beam pattern changes depending on the look direction of the main beam (steering angle). The main beam broadens with the increase of the steering angle and side-lobe structure changes as well (see Figure 35). Using these curves and assuming parameters as for the TIMS-2 system (that is beam-width of 1.5° and 33° scanning sector) one can find the required array to wavelength ratio $L/\lambda = 35$. Assuming that the separation between array elements and their length is $\lambda/2$, and allowing for 35% increase in the array size to accomodate shading, the required number of array elements is found to be 90. To reduce this number, broader beams scanned over larger sector are chosen, which will require a closer pass to the scanned iceberg than using TIMS-1.

For beam-width of 4° and scanning sector of 60° the number of array elements is reduced to 41 and the total array length at 100 kHz is approximately 31 cm. Such an array can be used to produce 15 contiguous beams pointing in different directions.

Multi-beam formation can be accomplished by summing (with proper weights) delayed signals from each element of the array. The delays required to steer the beam into $\emptyset$ direction are given by:

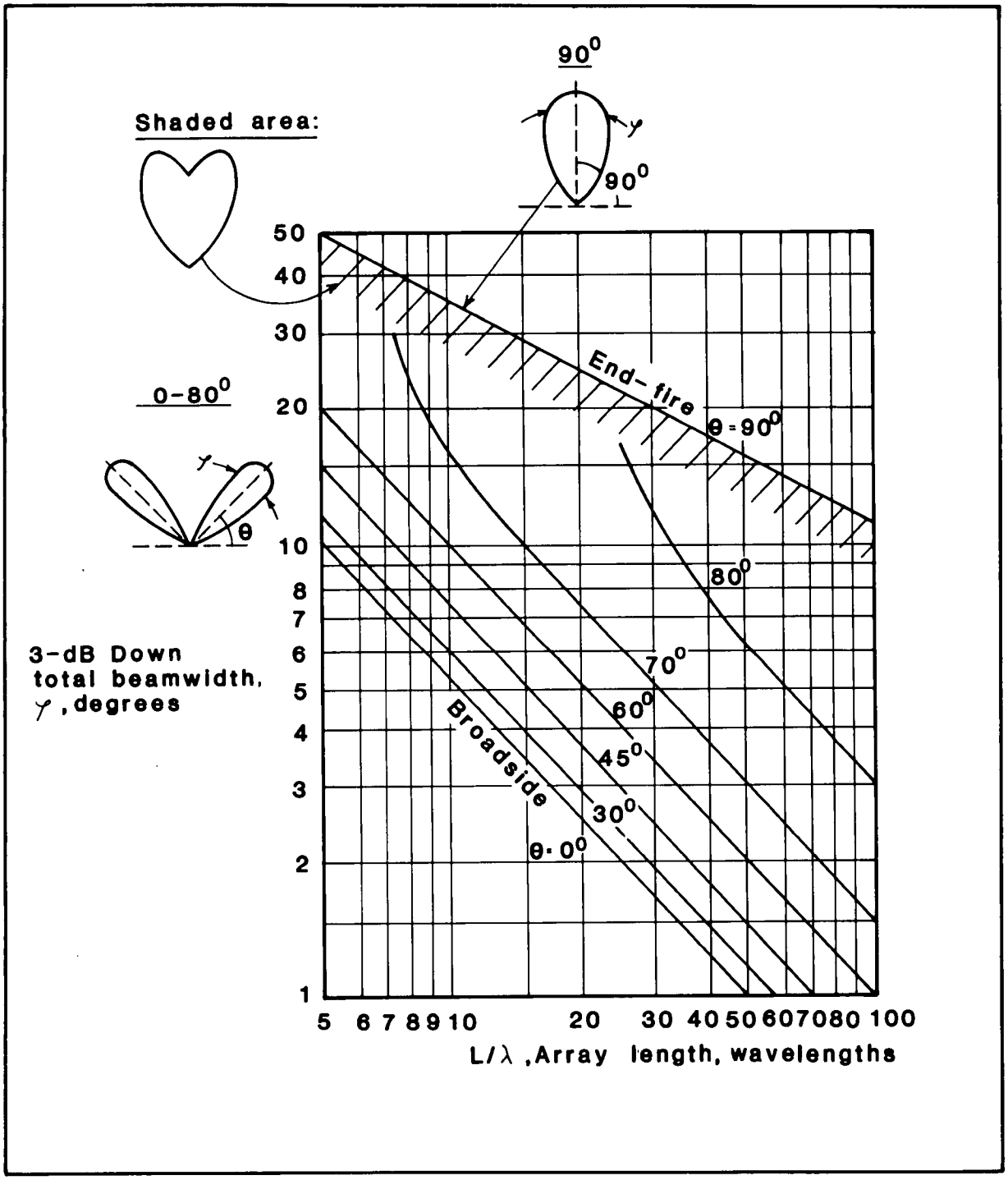

Fig. 37. Beam-width of a line array of elements $\lambda/2$ apart at various steering angles to broadside.

$$\tau_n = \frac{nd \sin \phi}{c_1} \qquad (7)$$

where:

n = number of the array element
(n = -20, -19, ..., 0, 1, ...20)

d = spacing between elements (d = /2).

Assuming small ϕ such that:

$$\sin \phi \cong \phi = m \Delta \phi$$

where:

m = beam number (m = -7, -6, ... 0, 1, ...7)
$\Delta\phi$ = beam-width

Equation (7) becomes,

$$\tau_{nm} = nm\tau \qquad (8)$$

where:

$$\tau = \frac{\lambda \Delta \phi}{2c_1} \qquad (9)$$

For the λ = 1.5 cm and $\Delta\phi = 4^{\circ}$, τ = 34.9 μs.

It follows from Equation 8 that hardware implementation of multi-beam receiver requires 36 tapped delay lines, each with 252 taps providing maximum delay of 8.8 ms. Commercially available tapped delay lines (Recticon TAD-32) have 32 taps and therefore 288 devices would be required at the cost of about $8,500.

Data Recovery and Display

The cost and complexity of the hardware implementation suggests that the beam forming should be accomplished by a suitable signal processing (software). All 41 signals can be frequency multiplexed for transmission to an on-board processor over a single coaxial cable. The multiplexed signal will occupy a bandwidth of about 40 kHz. This multiplexed signal can be recorded on a conventional analog recorders as well as digitized for further processing. The minimum sampling rate required is 80 kHz but 50% oversampling is usually desired bringing the sampling rate to 120 kHz.

Assuming the difference in the maximum radial distance of the profiled iceberg to the sensor to be 100 m, a 133 ms signal has to be digitized at 120 kHz sampling rate. This rate leads to 16,000 samples per one vertical profile. At a towing speed of 2 m/s (4 knots), scanning frequency of one profile per second, iceberg size of 100 m and 2 bytes/sample, 1.6 Mbyte of computer memory will be required for each pass.

Demultiplexing and beam forming can be accomplished by suitable digital processing. In particular, the frequency demultiplexing can be performed by digital filtering using Fast Fourier Transform algorithms (FFT). (A 1024-point FFT using ASYST Scientific Software and an IBM-PC computer with 8087 co-processor takes less than 3 s.)

VERTICAL DEPLOYMENT ICEBERG MAPPING SYSTEMS

Both TIMS-1 and TIMS-2 can be used to map an iceberg from a stationary platform when deployed vertically. At a given depth a horizontal iceberg profile is obtained. Scanning of the iceberg is accomplished by lowering the sensor from the platform and by collecting several horizontal profiles at the different depths.

During scanning, the acoustic sensors has to be stabilized such that the beam is pointing towards the iceberg. This stabilization can be accomplished by monitoring the angular direction of the sensor and by mechanical rotation of the transducer assembly. The angular direction of the assembly can be sensed by a flux gate compass and the assembly position control can be accomplished by a controllable vane subjected to water currents induced during lowering or raising the system. Alternatively, an electric motor with vertical-blade propellor can be used.

By combining features of TIMS-1 and TIMS-2 it is possible to achieve a three-dimensional iceberg scan from a stationary platform using only one probing sequence (a snap-shot mapping).

Beam forming can be accomplished by suitable digital processing.

Extensive efforts will be required to optimize necessary algorithms for speed, accuracy, and use of memory.

APPENDIX 1

GENERAL INFORMATION ON ICEBERGS

APPENDIX 1
GENERAL INFORMATION ON ICEBERGS

A1.1 ICEBERG DRIFT

The vast majority of icebergs found in the western North Atlantic originate from the glaciers of West Greenland, particularly those located in or around the periphery of Melville Bay.

There are about 100 glaciers along this coast, of which 21 are principal iceberg producers. It is believed that as many as 40,000 icebergs can calve annually, although an average of only 380 eventually drift south of 48°N.

The system of ocean currents in Baffin Bay, the Davis Strait, and the Labrador Sea is the major factor in the transport of icebergs from Baffin Bay to the Grand Banks of Newfoundland.

Icebergs which complete this journey do so in eight months or longer. They drift south along Baffin Island most of the year and by mid-December there is a scarcity of icebergs south of the Hudson Strait as a result of heavy disintegration from warm sea temperatures and lack of sea ice during late summer and early fall. During this time iceberg limits are at their minimum in the western North Atlantic. Later, protected by growing and advancing sea ice, the iceberg limits gradually move south reaching a peak in late April or mid-May on the Grand Banks. Along the Labrador coast, this peak is reached in May-June.

Drift speeds vary from region to region, but can be as high as 3 knots, when gale or storm force winds acting in the same direction as the main current flow.

Average speeds on the Grand Banks are in the order of 0.5-0.7 knots, whereas in the main stream of the Labrador Current average speeds usually range from 0.7-1.0 knot.

Figure A-1 is a map showing general iceberg drift patterns.

A1.2 ICEBERG DETERIORATION

To date, no one has been successful in developing an accurate model of iceberg deterioration which would be extremely useful in forecasting iceberg sizes. What is known, however, is that it appears to be somewhat random, leading one to conclude that a statistical model would be most appropriate. Several factors affect the way an iceberg melts. These include

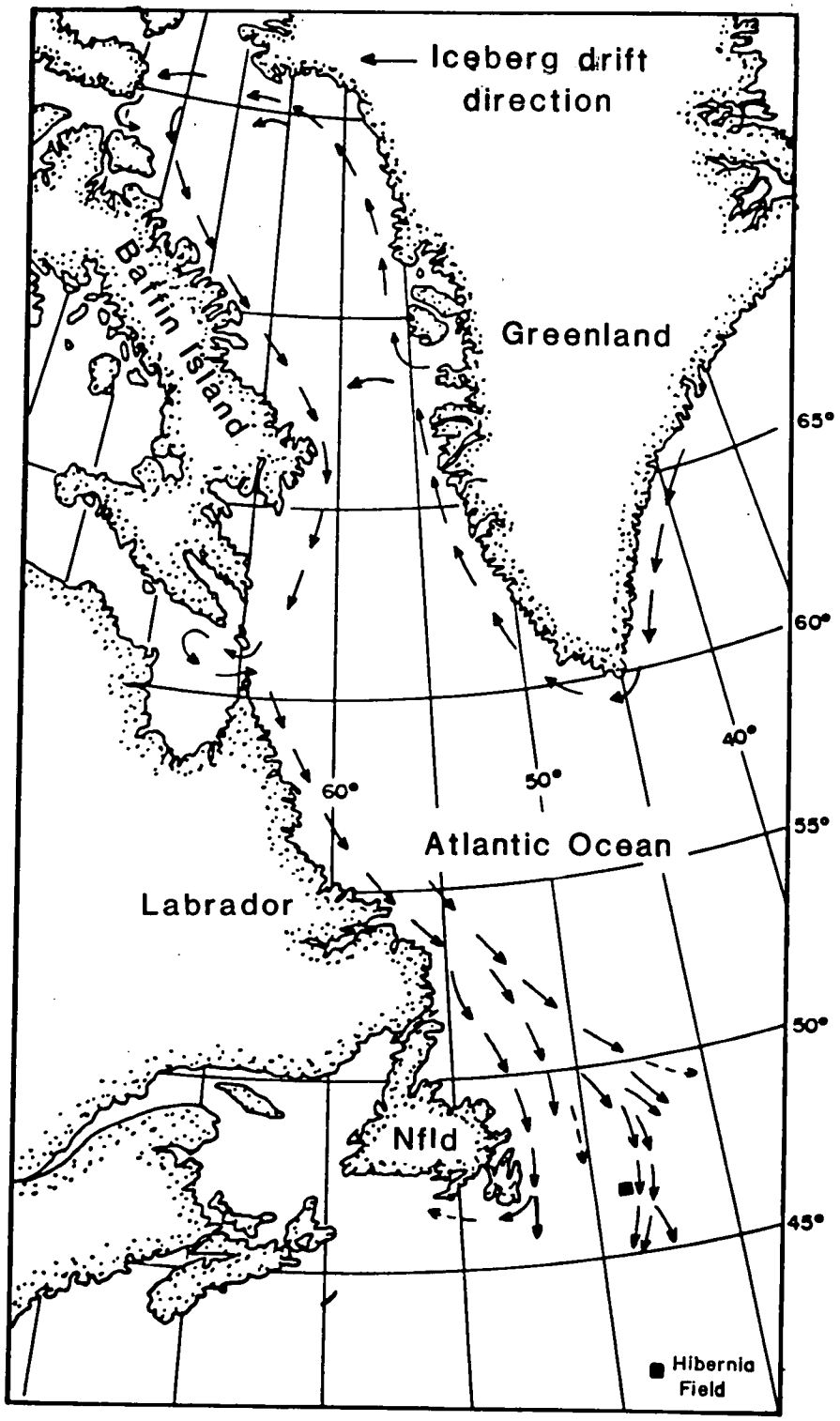

Fig. A-1. General iceberg drift pattern off the east coast (adapted from Royal Commission on the Ocean RAnger Marine Disaster 1984).

unequal temperature distribution and density throughout the iceberg. The underwater configuration also plays a major part in the variance in deterioration rates by presenting different surface areas for a given mass. Calving is also a significant factor in iceberg deterioration and, again, is virtually impossible to predict. These many factors all contribute to an explanation of why iceberg shapes are virtually infinite in number.

A1.3 ICEBERG DISTRIBUTION

Research done on the distribution of icebergs reveals that coastal areas (within about 100 nautical miles of the shore line) of Labrador and northern Newfoundland typically have the highest iceberg concentrations. Particularly high concentrations exist in an area extending from about 100 nautical miles north of Hopedale on the Labrador coast to the tip of the Great Northern Peninsula in Newfoundland. Off Newfoundland, itself, iceberg concentrations are not as high in coastal areas, but tend to be fairly high off the northeast coast and on the northern Grand Banks. Figure A-2 shows the distribution of icebergs, given as total sightings for the Labrador Sea and Grand Banks area. Ultimate limits can be as far as 250-300 nautical miles offshore, but sightings are rare at these distances.

Certain locations act as pre-season indicators, others as traps that can effectively deter further southward drift of icebergs. This type of information is also useful when planning iceberg field studies.

A1.4 ICEBERG SIZE AND SHAPE CLASSIFICATION

The shape of the above-water portion of icebergs is, in general, random. However, the International Ice Patrol (IIP) has devised a shape classification system by which they can be categorized as one of the following basic shapes; tabular, dry dock, domed, blocky, and pinnacled. Icebergs are given size classifications based on above-water dimensions according to guidelines laid out by the IIP. The measurements used to determine size classifications are usually obtained by photographic or sextant techniques which are now fairly standardized.

The size and shape guidelines are summarized in Tables A-1 and A-2.

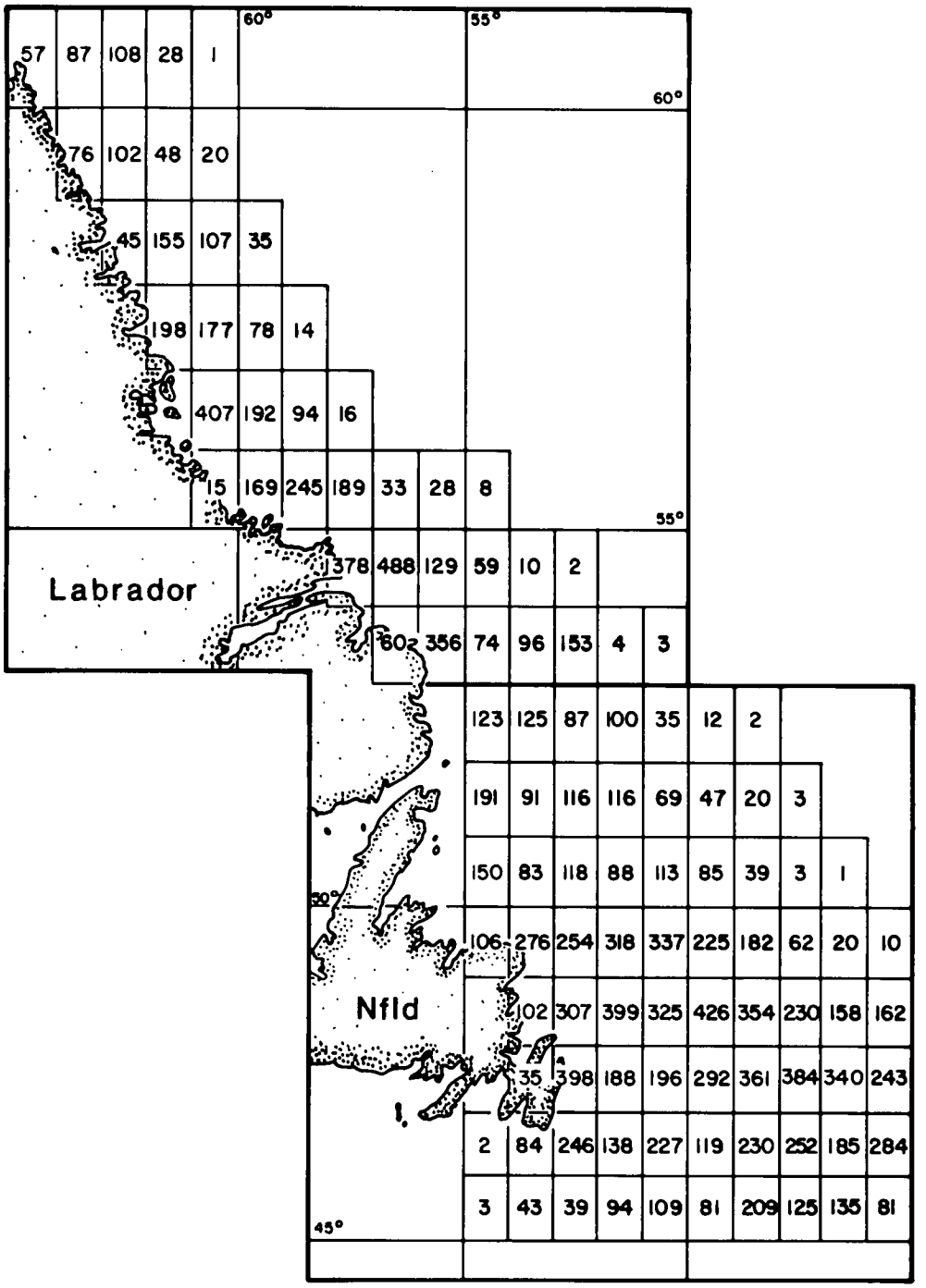

Fig. A-2. Distribution of iceberg sightings per degree square 1963-67 by International Ice Patrol for the Newfoundland and Labrador Sea area (Murray 1969).

TABLE A-1

Iceberg size classification

Type	Height(m)	Length (m)	Size
Tabular	6 or less	90 or less	Small
	6 - 15	90 - 215	Medium
	15 or more	215 or more	Large
Other	15 or less	60 or less	Small
	15 - 45	60 - 120	Medium
	45 or more	120 or more	Large

TABLE A-2

Iceberg shape classification

Name	Description
Tabular	Horizontal or flat-topped with length:height ratio of 5:1 or more
Blocky	Steep precipitous sides with near-horizontal top and length:height ratio of less than 5:1
Domed	Smooth round top
Dry Dock	Eroded such that large U-shaped slot is formed with twin columns or pinnacles. Slot extends into the water-line or close to it
Pinnacled	Large central spire or pyramid or one or more spires dominating shape
Bergy Bit	A mass of glacial ice smaller than an iceberg but larger than a growler, typically 8-12 m long; small iceberg or large growler is the preferred usage
Growler	A mass of glacial ice that has calved from an iceberg or is the remains of an iceberg; typically less than 2.5 m high and less than 6 m long

APPENDIX 2

HISTORICAL DEVELOPMENT OF ACOUSTIC TECHNIQUES FOR SENSING ICE

APPENDIX 2
HISTORICAL DEVELOPMENT OF ACOUSTIC TECHNIQUES FOR SENSING ICE

Acoustic echo-sounding (sonar) is not new. It has been used extensively since its development in World War II as a means of underwater navigation for submarines and as a means of detection of underwater features for ships. The advent of offshore hydrocarbon discovery accelerated the development of various applications of underwater measurement techniques, and, as a result, sonar is used today for a wide variety of tasks. Then, with the frontiers of exploration being pushed back by drilling operations in ice-infested waters, a need arose for underwater measurement techniques that could be applied to ice (sea ice and icebergs). Once again, sonar was the most obvious choice.

Perhaps the first acoustic measurements of the underwater portion of ice took place in the Arctic Ocean when, in February 1960, the U.S. submarine, Sargo travelled 1,500 km across the very shallow waters of the Bering and Chukchi Seas (Lyon 1967). The sonar system was used successfully to pilot USS Sargo between the deepest ice ridges. The upward-looking sonar recorded a continuous profile of the under surface of the ice. Specific information on the sonar system used is scanty, but apparently the ice-profiling unit operated on a frequency of 22 kHz. For high speed (15 knots) and (122 m) deep cruising under ice by nuclear submarines, it was necessary to use a much sharper-beamed, higher-frequency (150 kHz) sounder than used in previous work by diesel-battery submarines.

A series of submarine cruises followed during the next five years (Lyon 1961), with the SSN Seadragon performing cruises in 1960 and 1962 and the SSN Skate in 1962. In all, thousands of kilometres of under-ice profile data were obtained from these early expeditions.

The next underwater ice measurement work appears to have been carried out at Prudhoe Bay, Alaska (Breslau 1970). There, in April of 1969, the underwater geometry of a grounded ice island was mapped using a narrow beam sonar. Vertical section profiles were obtained by lowering a sonar transducer through the pack ice at 11 sites surrounding the ice island.

The sonar used to make the echo ranging measurements was a Kelvin-Hughes transit sonar. This commercially available unit was used without any alteration other than mechanically attaching the transducer to a long aluminum pipe, which was lowered through a hole in the sea ice adjacent to the ice island. It consisted of a shipboard console and the underwater transducer. The shipboard unit included a transmitter, a receiver, and a recorder. The power input was 40 watts at 24

volts dc. The sonar output was a 1 ms pulse at 48 kHz, with a transmission rate of either 160 or 80 pulses per minute, for the 275-550 m range scales, respectively. The transducer measured 15 X 10 X 112 cm and weighed 24 kg. The beam was fan-shaped and measured 1.5° by 51° between its 3-dB points, with the wide-beam direction being in the horizontal plane. The operation ran fairly smoothly, with only minor mechanical difficulties being encountered. Satisfactory results were obtained and a conclusion was reached that the sonar was effective in defining underwater ice shapes.

The next incidence of underwater ice measurement was again by a submarine under the Arctic ice (Swithinbank 1972). In March 1971, the HMS Dreadnought, a British nuclear-powered submarine, steamed to, and surfaced at, the North Pole. Upward-looking conventional echo sounders were used to record continuous profiles of the ice canopy from the ice edge at latitude 79°15'N to the pole on a track between longitudes 1°E and 8°E. A Kelvin-Hughes Type 776 echo-sounder operating at a frequency of 48 kHz, was coupled to a magnetostrictive transducer mounted in the upper casing of the submarine. The beamwidth of the instrument was such that it illuminated a circle of about 24 m in diameter at sea level.

In June of 1971, the first attempts were made to measure the underwater portion of a free-floating iceberg (Allen, 1971). On a scientific cruise off the coast of labrador aboard the CSS Dawson two systems for measuring the underwater portions of icebergs were tested by the Ocean Engineering Division of Memorial University of Newfoundland (MUN):

- an experimental device constructed for the cruise, consisting of a standard echo sounder (Furuno F602) with its transducer mounted on a 1.25 cm thick steel plate and lowered by a hydrowire (the barium titanate transducer had a vertical angle of 10° to 12°, and its operating frequency was 50 kHz); and

- the ship's Simrad SB2 sonar with a 360° horizontally and +5° to -25° vertically trainable transducer (vertical beam angle was 11°, and it operated at 24 kHz).

The steel plate of the latter had two 10-cm wide fins attached at an adjustable angle. These fins imparted a spin about the vertical axis to the transducer when it was raised or lowered. The wire to the sounder was payed out as the transducer was lowered. No trouble was experienced with wire twisting or with recovery of the instrument. The actual distance from the ship to the iceberg at the surface was monitored, "although not very satisfactorily," with a range finder.

The ship's sonar had the disadvantage of interference from ledges on the ice surface. Many "soft" echos and double echos were obtained making interpretation difficult. However, the echo received from the Furuno experimental device was very clear and simple to interpret, leading to the conclusion that the basic idea was sound, and the next step was to design a more sophisticated mechanical system.

In April 1972, before further field work by MUN, a survey was conducted by the University of Wisconsin in a pack ice field near Fletcher's Ice Island (T-3, then at 84°N, 84°W) (Kan 1974). The field work comprised an under-ice sonar survey and a surface survey. A modified Kelvin-Hughes transit sonar was used for the under ice portion of the work. The sonar transmitted 1 ms pulses at 48 kHz with 250 watts of acoustical peak power. The beam measured 1.5° by 51°. The transducer was lowered through the ice and the direction was changed incrementally until the unit had been rotated through a full 360°. Data was taken in two orientations; vertical and horizontal. Strong under-ice echoes were obtained and a complete under-ice map was constructed by converting the data into polar co-ordinate mosaics.

Shortly after this project, additional work on Fletcher's Ice Island was carried out by the University of Washington while testing a system they had developed (Francois 1973). This system, known as UARS (Unmanned Arctic Research Submersible System) comprised two major elements: the submersible, which served as a mobile instrument carrier; and an acoustic tracking, command, and recovery system. The vehicle's first free run in the under-ice environment was on 3 May 1972. This run lasted slightly over 1 hr and almost all acoustic systems indicated some problem areas. These problems were resolved and a final run on May 9 was a complete success.

The quality of the data from the profiler was judged to be outstanding. Fine grain resolution of the ice surface elevation was possible. In fact, it was observed that on five of the many traverses made near the launch and recovery hydrohole (0.91 by 2.74 by 6.4 m deep) the UARS profiler defined the water surface of the hole as it passed some 37 m beneath.

In August 1972, further work was carried out on the CSS Dawson when Project ICE (Iceberg Cross-Section Echo) was being conducted by MUN (Allen 1972; and Benedict 1972). This was essentially a follow-up to the work performed the previous summer. The objective was to obtain a complete profile of the submerged portion of an iceberg using sonar techniques.

The sonar array comprised of a modified Klein Associates Model SA-350 transceiver, a Model 402 towfish, and a single channel Hydroscan Recorder. Thirteen icebergs were insonofied

by a series of stations taken around the icebergs at a minimum radius. By this time, the system had been perfected to the extent that the measuring technique had become routine.

The next report of iceberg underwater measurement is from the 1973 cruise of the CSS Dawson again by MUN Ocean Engineering (Allen 1973). The technique was by now becoming fairly standardized. Basically, the only changes implemented in 1973 were:

- a dual-channel side-scan unit was used with operational amplifiers to add the two channels and display them on one side of a paper recorder; and
- a high-frequency transducer (100 kHz) was deemed to be preferable to achieve narrow beam-widths with a manageable sized transducer. Because of the short ranges involved the high attenuation at this frequency was not considered a problem.

Six icebergs were successfully profiled using the new equipment and technique.

In July 1974, the U.S. Coast Guard used a sonar transducer deployed 1 m below the surface to measure iceberg draft (Robe 1976). These measurements were taken with a Kelvin-Hughes Transit Sonar during a cruise aboard the CGC Edisto. The Edisto was operating in the Davis Strait area and along the west coast of Greenland. The sonar was deployed vertically and produced a beam 0.5^{o} wide in the horizontal and 52^{o} wide in the vertical, between 3 dB points. The transducer was pointed down at an angle of 26^{o}, so that the top of the fan-shaped beam would just pass under the surface of the water and the bottom of the beam would be depressed at 52^{o}.

The system was originally designed to be used in a small boat with a low freeboard. However, this virtually eliminated measurement in anything but the calmest weather. It was subsequently modified to work aboard the Edisto. the ship was positioned such that the beam of the sonar was completely intercepted by the iceberg. As the vessel circled the iceberg, it increased its range until at some point the sonar beam passed under the iceberg. The assumption was made that the last return from the iceberg comes from its deepest portion. In all, measurements were obtained for a total of 30 icebergs.

Also in the summer of 1974, sonar was first used in a drilling support operation for Total Eastcan, offshore Labrador (Brooks 1979). The method developed by Memorial University's Ocean Engineering Division was used. Total Eastcan also used this method in 1975 and 1976. Although little specific information about the system and techniques employed was

available at the time of this writing, it is known that in the three drilling seasons a total of about 50 icebergs were measured.

In March 1975, the University of Helsinki tested a sonar they had developed the previous year to measure successfully the submarine profile of an ice ridge (Pousi 1975). The equipment consisted of two parts: the immersed portable scanning sonar head; and the central unit, containing the graphic recorder and a 220 V generator. The sonar head consisted of two separate 750 kHz, 2.4° beam-width transducers; one for transmitting and one for receiving. This configuration was considered useful in eliminating ringing effects in the receiver after the transmitted pulse. The transducers were lowered through a hole in the ice using a metal pipe and the underside of ridges were scanned.

In October 1976, the nuclear submarine, HMS Sovereign, was sent into the Arctic Ocean on a voyage to the North Pole (Wadhams 1977). Its mission was to obtain, for the first time, an underwater sea-ice profile which would correspond to an above-ice profile on the same route, providing a complete topography. Sovereign was fitted with a sonar transducer having an overall beam-width of 17° fore-and-aft and 5° athwartships, and was interfaced to a Kelvin-Hughes MS45 recorder operating at 45 kHz. More than 4,000 km of profile was obtained.

The submarine was also equipped with an experimental side-scan sonar. The transducer was from Offshore Acoustics, Ltd., and it was interfaced to a Klein recorder. The transducer was bolted to the forward casing under a protective cage of steel tubing. Unfortunately, owing to water penetration, the side-scan produced data for only two hours and on one channel only. However, the data obtained were easily correlated to the MS45 profile and many features were clearly distinguishable.

Similar cruises were carried out in 1977 by SSN Flying Fish and USS Gurnard. Little is known about the specifics of these cruises, but it is known that a 1,400-km profile was obtained by the Gurnard using a narrow-beam, upward-looking sonar.

Also, in the period 1976-77, a significant amount of underwater iceberg measurement work was conducted through the Greenland concessionaires and the Greenland Technical Organization (GTO). Technical details of the work were not available at the time of this writing, but a summary is provided (Brooks 1979).

In 1976, the petroleum company, Total Greenland A/S, used a commercial side-scan sonar to profile icebergs in support of their exploratory drilling offshore West Greenland, and as part

of the Greenland concessionaires environmental studies. The sonar, modified similarly to that used by Total Eastcan, was deployed from a support vessel, and six icebergs were measured.

In 1976, the Greenland petroleum concessionaires sponsored development of a sonar system to profile icebergs offshore West Greenland from a chartered weathership. The transducer was deployed on a 200 m cable and emitted a 360^{o} horizontal and 2^{o} vertical acoustic signal. This omnidirectional horizontal beam eliminated the need for the transducer to spin as in previous sonar systems. However, this beam pattern meant that, for a given total power, it yielded less radiated power in the desired direction. As with previous systems, the transducer was lowered until no echo was detected, and the length of cable deployed was assumed to be equal to the iceberg's draft. Seventy-two icebergs were measured with this system. In 1977 the Danish Hydraulic Institute used this same system to measure 13 icebergs for the Greenland Technical Organization, Ministry for Greenland.

Also in 1977, the Greenland concessionaires sponsored development of another sonar system for deployment from supply boats in support of three drillships offshore West Greenland (Brooks 1979). This system was a commercial scanning sonar mounted in gimbals for vertical reference and stability and deployed in a sound dome on a 150 m cable. The 6^{o} conical beam was trainable in both azimuth and elevation. Twenty-two icebergs were measured with this system. Little technical information on this system is available at this time.

Sukhov (1977) proposed a method of iceberg draft measurement involving delivery of instruments and sensors to a point below the iceberg via a submerged instrumentation platform, although no actual measurements were made.

Sukhov considered four types of submersible platforms:

. towed body
. manned submersible
. military submarine
. unmanned submersible a) untethered b) tethered

but concentrated on manned and unmanned submersibles for operational, economic, and safety reasons.

Sukhov's proposed method for use of a manned submersible is essentially as follows:

- submersible launched about 1 mile from iceberg;
- submersible scans horizontally with forward-looking narrow-beam sonar as it approaches iceberg and descends;

- submersible, maintaining checks on distance to sea-bottom, locates iceberg's deepest point; and
- submersible then passes under deepest point with upward-looking sonar and depth meter activated.

The proposed method for an unmanned, untethered submersible was identical to this.

However, the method proposed for the use of an unmanned, tethered submersible was somewhat different. The procedure was as follows:

- Submersible launched over stern of vessel from a position up-current of the iceberg;
- using up-, down- and forward-looking sonars the unit is directed under the iceberg;
- when submersible is downstream of the iceberg, it is directed in a pendulum-type motion, laterally; and
- as the iceberg moves relative to submersible several lateral profiles of the bottom of the iceberg are obtained.

Sukhov stated that the accuracy of the method would depend on the accuracy of the depth meter and echo sounders used, and that with proper selection of instrumentation absolute errors of as low as 0.2-1.0 m could be achieved.

In 1977-78, Exxon Production Research Company used subsea profiling, in conjunction with aerial reconnaissance, to obtain quantitative information on sea ice characteristics relevant to structure design and to the planning of offshore operations in ice-covered portions of the Bering Sea (Deily 1979). Subsea profiling was conducted over a 10-month period using bottom-mounted upward-looking sonar instruments. Three of these instruments were deployed about 65 km west of Nome in 33 m of water in September 1977, and were recovered in July 1978. The instruments were set out in an approximate 183 m equilateral triangle array. The instruments sent a 200 kHz pulse upward every 30 s and recorded the travel time to and from the ice bottom (or ocean surface) on an internal tape-recording system. Interpretation of the travel time yielded information on ice keel depths. The data obtained were considered to be of consistent quality and yielded significant quantitative and qualitative information on sea-ice conditions.

Additional work, discussed only briefly here because of insufficient information, was also carried out in 1978 when ICE Engineering Ltd. used a helicopter-based sonar and aerial photography to measure 35 icebergs in Baffin Bay. These data were collected for Petro-Canada Exploration Ltd. as part of the Canadian Eastern Arctic Environmental Survey. The sonar had 1.8^{o} vertical and 15^{o} horizontal beam-widths and was made to spin on the deployment cable.

A project was undertaken by NORDCO Limited on behalf of Total Eastcan in the summer of 1979 (NORDCO 1980) to do systematic draft measurements using the conventional side-scan sonar technique and a remote-controlled submersible (RCV) to obtain exact values. The side-scan sonar used was a standard Klein system modified for vertical deployment, whereas the RCV used was the Scorpio made by Ametek, Straza Division. Sonar scanning by the RCV was performed in the horizontal mode until the unit was below the keel. Then the sonar was set in the vertical mode and the deepest keel located. This method is similar to that suggested by Sukhov in 1977.

The drafts of 14 icebergs in the Labrador Sea were measured by both methods, with the accuracy by RCV judged to be about 2%. Using its measurements as references showed that the side-scan system, on the average provided a draft measurement which was within 11.4% of the actual draft. However, in a number of cases this error exceeded 10% either way, and in one case the side-scan method undermeasured the draft by 36%. In the majority of the cases the drafts measured by side-scan were less than the actual draft.

Since 1979, many underwater profiles and draft measurements of icebergs have been obtained in support of drilling operations offshore Labrador, using various conventional side-scan systems. Almost all of the work has been carried out by four contractors - Fenco (formerly MacLaren Plansearch), NORDCO Limited, ICE Engineering Ltd., and Geomarine.

On 17 June 1980, a U.S. patent was granted to Robert Desbrandes of the Institute Francais du Petrole, France for a method and device for determining the geometrical outline and draught of the underwater part of icebergs. The method comprises laying a line of acoustic transducers on the sea bottom which are energized when an iceberg approaches. The transducers are activated sequentially and the reflected echoes from the iceberg sensed by receivers located on both sides of the transmitter. The iceberg shape is determined by drawing the geometrical envelopes of a system of ellipsoids whose foci are the transmitter and the different receivers. Because the transducer array is fixed onto the sea bed any iceberg which crosses the line could be measured. It is claimed that the invention gives a good approximation of the iceberg outline and this approximation improves by increasing the number of transmitter-receiver pairs.

APPENDIX 3

HISTORICAL DEVELOPMENT OF ELECTROMAGNETIC ICE MEASUREMENT TECHNIQUES

APPENDIX 3
HISTORICAL DEVELOPMENT OF ELECTROMAGNETIC ICE MEASUREMENT TECHNIQUES

Radio echo-sounding has been used for measurements on glaciers and large Antarctic icebergs. Perhaps the first significant work was done when a pulsed-CW system was used for measuring the thickness of Antarctic icebergs, primarily very large tabular types (Swithinbank 1977). The system had a 60 MHz carrier frequency with a pulse length of 0.3 μ s and a peak pulse power of 1.2 kW. It was mounted on a Twin Otter aircraft and soundings were made as the plane flew over the icebergs at the altitudes between 5 and 3,000 m. It was said that the icebergs were so easy to measure that little was to be gained by flying low over them. Altitudes of 19 to 350 m were given with data samples. However, it is noted that the icebergs reported in the work are tabular icebergs, and even, so called small icebergs would be very large in comparison to Arctic icebergs. Iceberg thicknesses ranging from 30 to 280 m were said to have been measured in earlier studies. Unfortunately, because of the pulse length (0.3 μ s), the minimum resolvable thickness accuracy is theoretically about ± 25 m. Swithinbank was able to detect fractures and crevasses within the icebergs.

In 1977, the results of radio echo-sounding of an Arctic ice island and an Antarctic iceberg were reported (Kovacs 1977a and 1977b). An impulse radar system was used having a centre frequency of 100 MHz and a 100 MHz bandwidth. Unfortunately no other system characteristics were provided. The ice thickness resolution of the system, based on the band-width, was about ±1.7 m. Measurements were made by towing the system on the surface with a sled. The average calculated thickness of the iceberg was 72 m, whereas the thickness of the ice island was found to be between 22 and 24 m (which was confirmed by auger measurements). Kovacs concluded from his results that for large tabular icebergs, impulse radar could be used to determine thickness, to provide mesoscale bottom relief, to find cracks and crevasses, and to detect internal layers.

Radio echo-sounding was also used, more recently again, to measure the thickness of a very large (3,630 by 1,740 m) tabular iceberg in the Antarctic (Kristensen et al. 1982). Thicknesses of between 100 and 150 m in a longitudinal traverse across the iceberg surface were obtained. The system used was the same as that employed by Swithinbank in 1977 and was deployed on a helicopter. In 1983, overlapping work using the same system was reported (Wadhams and Kristensen 1983). A detailed contour map of the thickness of an iceberg was constructed. The maximum thickness shown was 320 m. Again the iceberg was a very large tabular type having sides averaging around 1,000 m in length.

Other early work reported on attempts to measure iceberg thicknesses in the Labrador Sea (Goodman et al. 1977). The system used was a 840 MHz pulsed-CW system having a 50 nanosecond (ns) pulse length and a peak transmitter power of 40 kw. This peak power was effectively reduced considerably by a 40 dB attenuator placed in the system to prevent receiver overloading by strong reflections from short ranges. The radar was mounted on a helicopter and measurements were made while it flew over, hovered, and landed on the icebergs. Although no actual iceberg thickness data were provided, the authors did state that thickness measurements were "consistent with the observed freeboard of the icebergs." The echograms were found to be free of internal scatterers. It was pointed out that the echogram from an iceberg is complicated because of scattering from the ice-water interface, multiple reflections within the ice and refraction at the ice-air interface. It was also noted that single spot echograms are often uninterpretable because of multiple reflections.

The authors also discussed the possibility of inverting the echograms from icebergs to obtain underwater shape information. The method suggested is the same as that developed for the enhancement of seismic data. The technique was demonstrated using a synthetic echogram. Work is now being initiated at the University of British Columbia to develop this technique fully (Clarke 1984).

In 1977, an 80 MHz impulse radar system was tested for its capability in measuring iceberg thickness (Rossiter and Gustajtis 1978 and 1979). The system had a peak transmitter power of 53 watts (W) and a 20 ns pulse length. The transmitter-receiver and antenna assembly were slung in a net about 6 m below a helicopter.

One small iceberg was sounded and the result (18.0 $\pm$ 0.9 m) was verified by simultaneous measurements with side-scan sonar. The echogram showed reverberations and multiple reflections. In a discussion of the results the authors suggested that airborne radar could be used as a quick, safe, and accurate means for obtaining iceberg drafts. Because of the problem of multiple reflections and reverberations the authors felt that this technique might be easier to use on larger icebergs. A reference was made to the work of Goodman et al. (1977) stating that the technique proposed by this work may be used to delineate underwater shape.

A major project was undertaken in 1978 in which nine small and medium sized icebergs of various types were sounded by airborne radar (Rossiter et al. 1979). All the icebergs were located in the Labrador Sea. Two radar systems were used; the 840 MHz unit employed by Goodman et al. (1977), and the 80 MHz radar used by Rossiter and Gustajtis (1978). Of 10 icebergs, 8

were successfully sounded by impulse radar. One of the two that were not successfully sounded was a small tabular-like iceberg that was said to have given only a faint bottom echo, whereas the other was a small tabular iceberg in which multiple echoes prevented identification of the bottom echo. The impulse radar system well outperformed the pulsed-CW system, with the latter reporting only two draft measurements. Both units were deployed from helicopters. The poor performance of the pulsed-CW system probably resulted from its low resolution and slow scan rate. There was no alternate verification technique used to confirm the draft measurements but the height to draft ratios did come within the expected ranges.

As a result of this work, the authors suggested that it should be possible to measure the draft of the largest icebergs that might be encountered in the Arctic waters, with the major limitation being internal scattering resulting from irregularly shaped icebergs. The need for verification work (the use of an alternate measurement technique) to confirm the operational ability of radio echo-sounding was emphasized. The speed at which measurements can be made was said to make the technique potentially very attractive as a tool to build up a large statistical data base. It was noted that in this case the error associated with one measurement may not be critical.

Reviews of this work agreed with the need for more data collection along with further instrument development (Kovacs 1979) and agreed that the radar technique could provide a large statistical data base (Brooks and Sabins 1979). It was felt that because of the uncertainty regarding the maximum draft, the technique should be employed as a research and development tool. Again, reflection was noted as a possible significant problem in the relatively small, irregular Arctic icebergs. Also the need for further verification work was stated.

In 1981, an impulse radar, specially designed for deployment from an airborne platform (in this case a helicopter), successfully measured a grounded iceberg draft off the Labrador coast (Bazeley 1982). The centre frequency was 120 mHz, the pulse length was 10 ns, and the peak transmitter power was 50 W. A check with hydrographic charts confirmed the measured draft of 83 m.

In 1983, the thickness of a large tabular iceberg was measured using a sled-mounted, 300 MHz, impulse radar system manufactured by Geophysical Survey Systems Inc. (Christian et al. 1984). The iceberg was grounded in Freshwater Bay just outside the entrance to St. John's Harbour. The draft measurement of 70 m was confirmed by hydrographic chart readings. Some problems were encountered with coupling the antenna to the surface. The presence of multiple reflections suggested that a

draft of 210 m might be measurable, at least with the antenna directly coupled to the iceberg surface.

In 1982, a comprehensive assessment of impulse radar as an iceberg draft measurement tool was undertaken (Remotec Applications Inc. 1982). Based on a detailed literature review, some data analysis, and theoretical considerations it was shown that impulse radar, operating in the range 80-300 MHz, should be able to measure iceberg thicknesses up to 250 m. Reflection was indicated only to be a problem for the smallest icebergs. Tabular, blocky, and large domed icebergs (which probably have the maximum drafts in a given size class) were said to be the most favourable for sounding. Suggestions for operational and research deployment modes were described encompassing the type of platform as well as the flight pattern above the iceberg. It was recommended that work be continued towards investigation of the underwater shape determination technique proposed earlier.

APPENDIX 4

DRAFT ESTIMATION FROM ABOVE-WATER SHAPE REVIEWED

APPENDIX 4
DRAFT ESTIMATION FROM ABOVE WATER SHAPE REVIEWED

The drafts of 30 icebergs in the Davis Strait and along the west coast of Greenland were measured during a cruise aboard the CGC Edisto July 1974 (Robe 1976). It was concluded from this data base that there was no significant relationship between the above-water iceberg classification and the draft to height ratio. The distribution (Figure A-3) was not linear and was represented by the power curve:

$$D = 49.4\ H^{0.2} \qquad (A4.1)$$

where: D = draft
H = height.

Later investigators (El-Tahan 1982; Hotzel and Miller 1983), working with significantly larger data bases, have concluded that this ratio is a poor predictive tool. However, work with a data base collected by Fenco Newfoundland Limited on a total of 214 icebergs measured between latitudes 49° N and 75° N between 1973 and 1979 indicated that there was a significant relationship between above-water iceberg classifications and draft to height ratio (El-Tahan 1982). The distributions were not linear and the plots had significant scatter (Figure A-4). Their derived relationships, based on above-water classification, were as follows:

$$\text{Pinnacled and Dry dock: } D = 2.2\ H \qquad (A4.2)$$

$$\text{Domed: } D = 111.04\ H^{-0.111} \qquad (A4.3)$$

$$\text{Tabular: } D = 198\ H^{-0.235} \qquad (A4.4)$$

Based on the graphs of the Fenco data base and the theoretical relationships obtained by the least-squares method of fitting power curves of the form $y = ax^b$ for domed and tabular icebergs, it is evident that this is also a poor prediction tool. Additionally, the domed and tabular relationships are not supported by stability theory, as it seems highly improbable that draft would decrease with increased above-water height.

The Danish Hydraulic Institute (DHI) (DHI 1979) analysed a data base of about 115 icebergs collected during 1976 and 1977 off the west coast of Greenland in support of exploration work. They plotted height versus draft for each iceberg type as well

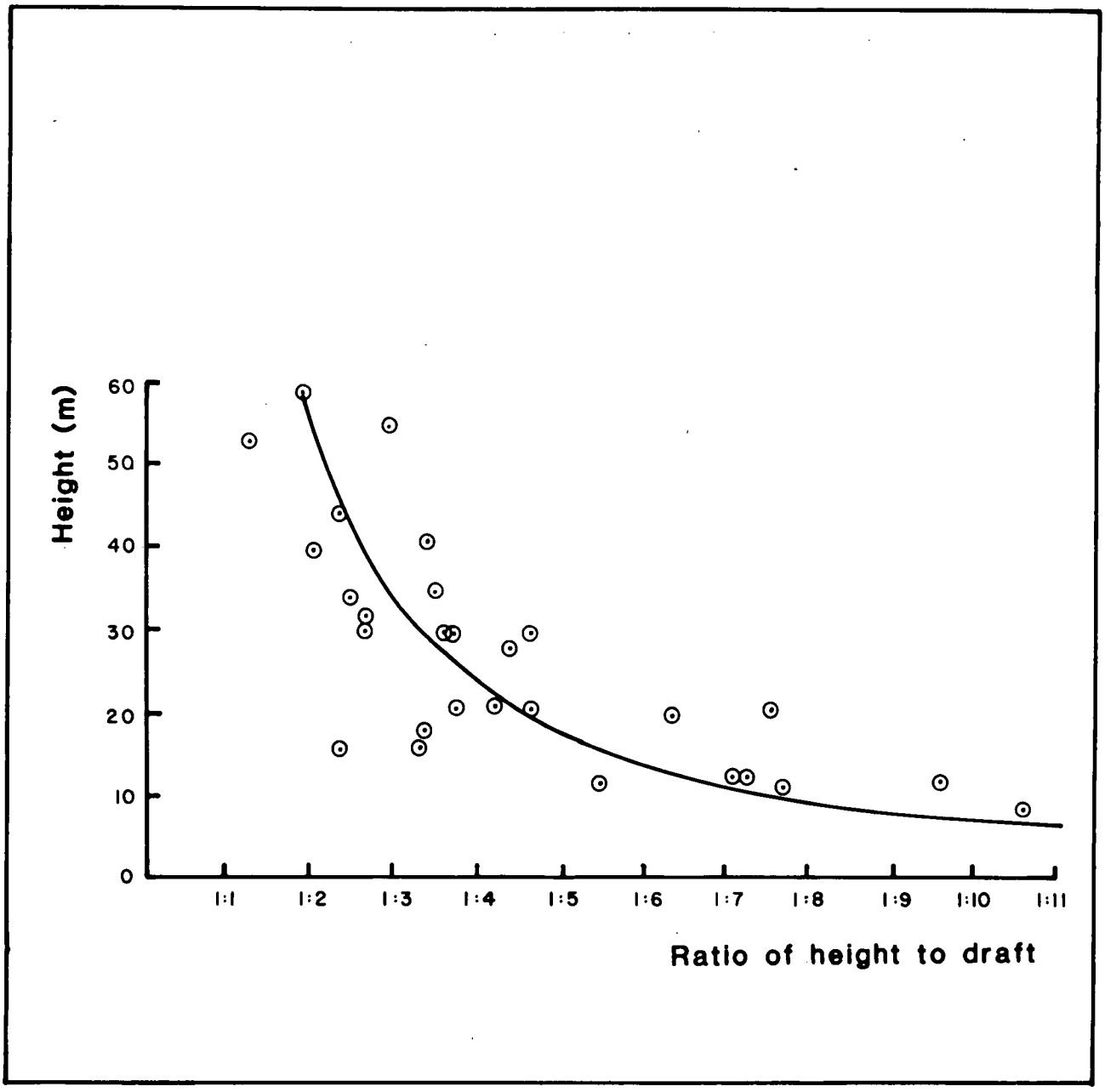

Fig. A-3. The distribution of height to draft ratios of icebergs as a function of iceberg height (Robe 1976).

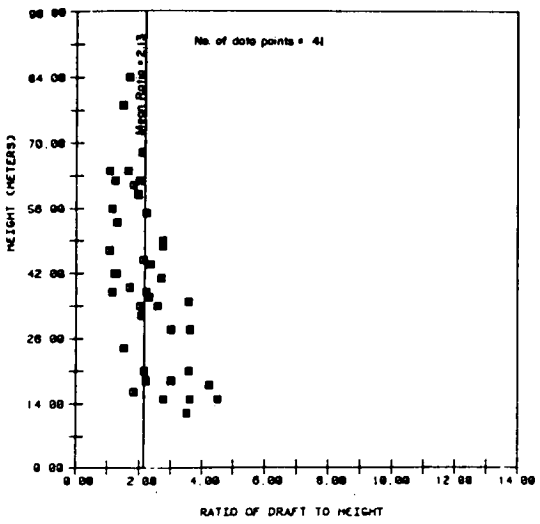

(A) The distribution of draft to height ratios of dry dock icebergs as a function of iceberg height

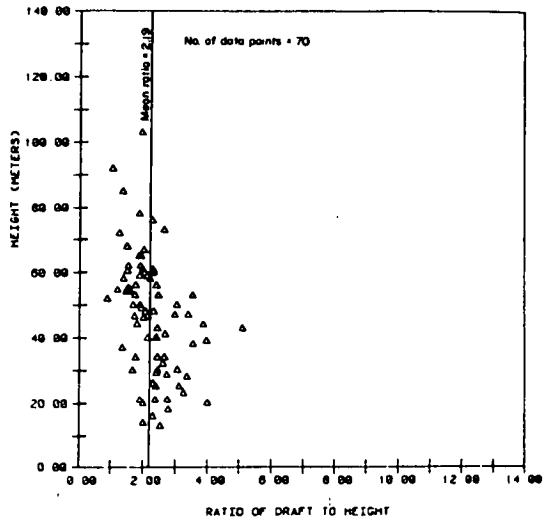

(B) The distribution of draft to height ratios of pinnacled icebergs as a function of iceberg height

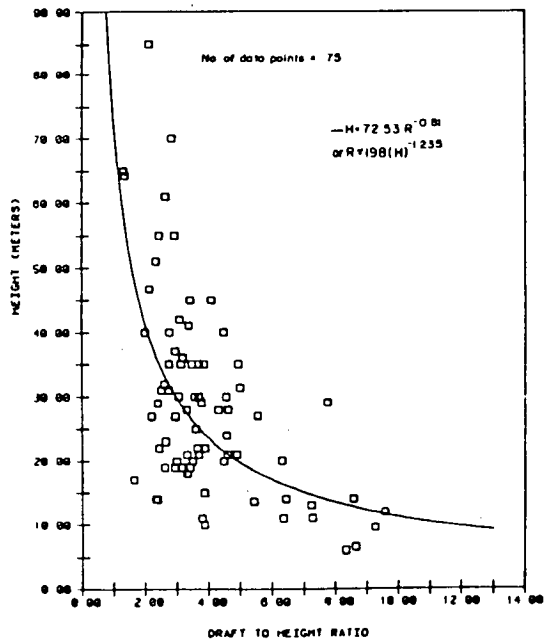

(C) The distribution of draft to height ratios of tabular icebergs as a function of iceberg height

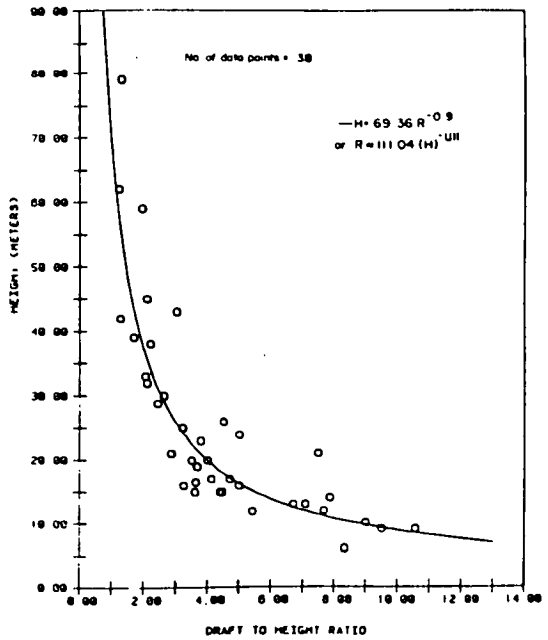

(D) The distribution of draft to height ratios of domed icebergs as a function of iceberg height

Fig. A-4. The distribution of draft to height ratios of drydock, pinnacled, tabular, and dome icebergs as a function of iceberg height (El-Tahan 1982).

as for all types combined (Figure A-5) and concluded that, as the plots show considerable scatter, an estimate of iceberg draft based on an average height to draft ratio would have a very limited accuracy. Iceberg width and draft data was subjected to the same analysis (Figure A-6). They argued that an iceberg has its maximum stability for an axis of rotation approximately parallel to the longest side and thus it appears that the stability of an iceberg is highly dependent on the width (W) and the draft (D) and that it is independent of length. There was a significant reduction in the scatter of these plots, however they still showed a high degree of randomness.

Hotzel and Miller analysed a data base collected by the Labrador Group of Companies in support of exploratory drilling activity in the Labrador Sea during the period 1973 to 1978. This work examined the functional relationships between various iceberg dimensions. They concluded that height to draft probably varies not only with mass but also with shape, making height-to-draft relationships a poor predicting tool.

They argued that length (maximum water-line length) is the simplest and probably the most accurate dimension which can be measured for an iceberg. Thus, they suggest a first approximation of draft based on length. Relationships between measured dimensions of icebergs are presented in Tables A-3 and A-4. These relationships are in the power curve format ($y = ax^b$). Also included are the correlation coefficients and number of observations.

Table A-5 shows the comparison of the various iceberg draft estimation techniques based on iceberg height. The estimations in most cases are closely centred about the mean value of the draft and in two cases actually decrease with increasing height. These data are presented graphically in Figure A-7. The most reasonable relationship was obtained by substituting the relationship for height to length into the relationship of draft to length from the work of Hotzel and Miller, although these authors do not agree with the concept of relating draft to height.

Although the maximum water-line length is an easily measured dimension from aerial reconnaissance, it is difficult to measure parameters from a vessel. From a vessel, and especially a drilling unit, the most accurately measured parameter is the height.

In discussions of efforts to determine a functional relationship for predicting iceberg draft, two important problems appear to have been neglected. First, lack of attention is given to the techniques used to measure iceberg draft. These techniques are often imprecise and rely

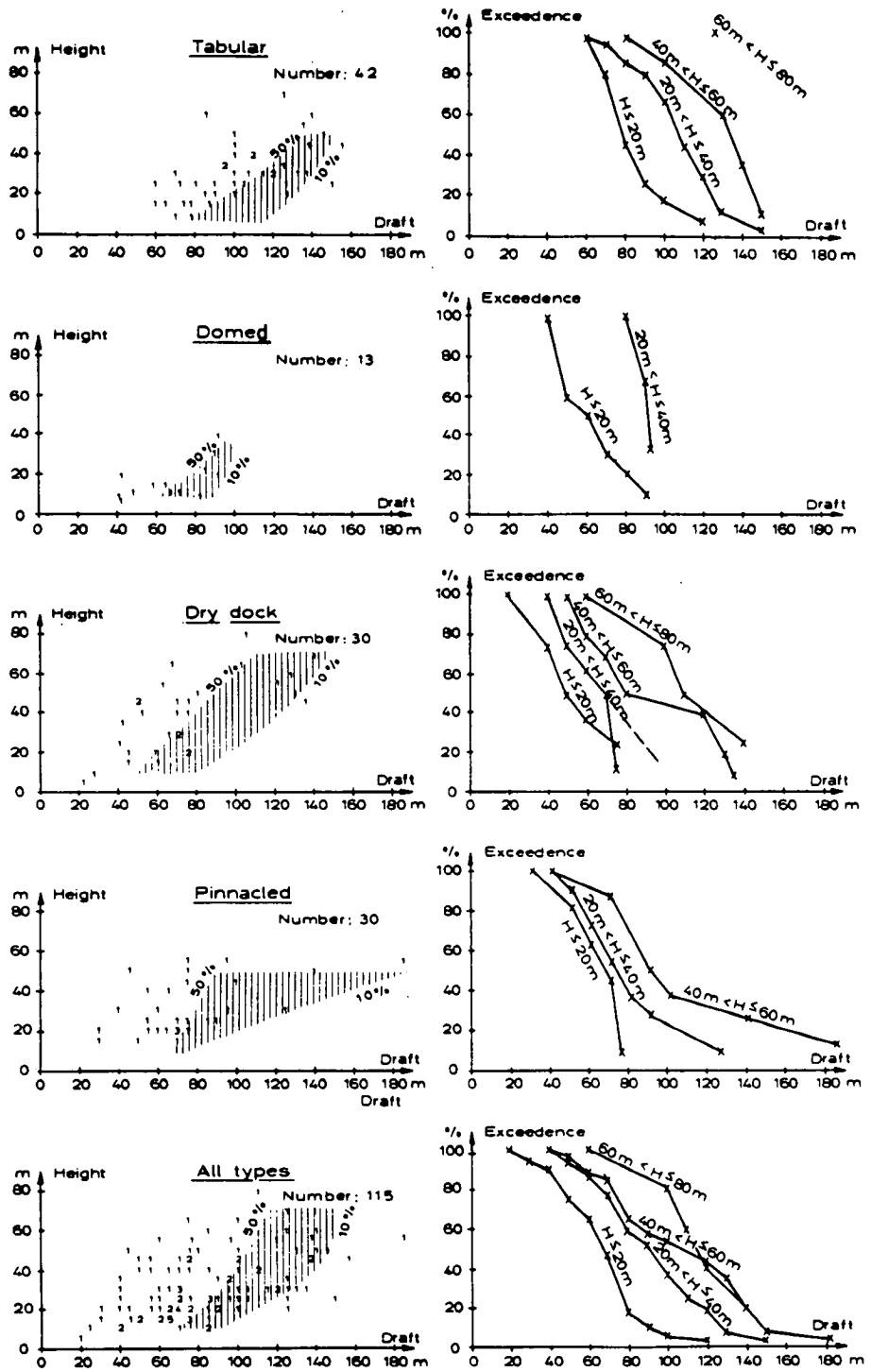

Fig. A-5. The correlation between iceberg height and draft for tabular, dome, drydock, pinnacled and all type icebergs (DHI, 1979).

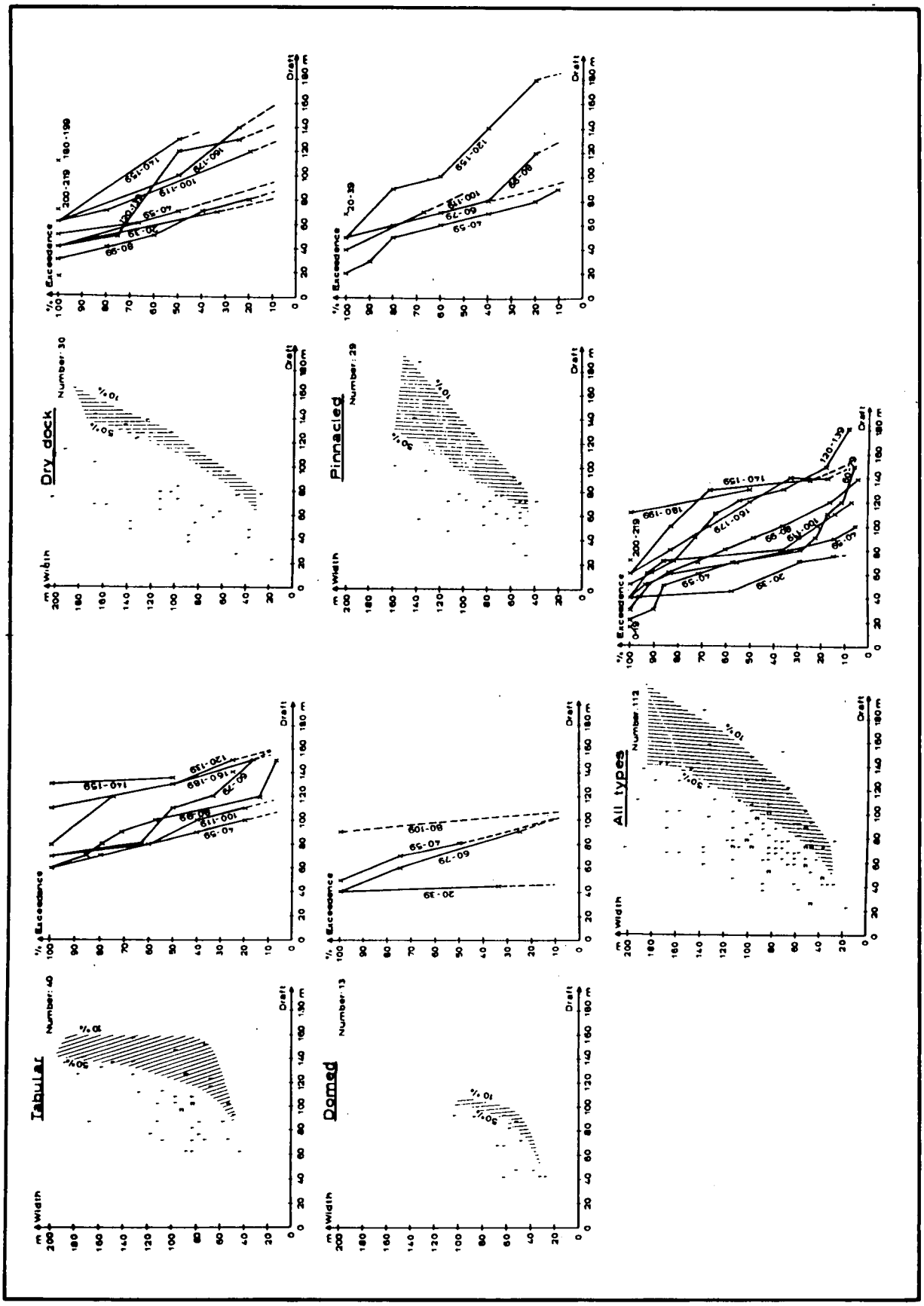

Fig. A-6. The correlation between iceberg width and draft for tabular, dome, drydock, pinnacled, and all type icebergs (DHI 1979).

TABLE A-3

Statistics for iceberg ratio data

Ratio	Mean	Mode	Median	Standard deviation	Range	Maximum	Minimum	No. of Observat.	Mean Sq. Value
Width/Length	0.74	0.85	0.77	0.21	1.17	1.45	0.29	67	0.60
Draft/Length	0.67	0.70	0.63	0.32	1.49	1.69	0.19	74	0.55
Height/Length	0.28	0.30	0.32	0.18	2.26	2.29	0.02	230	0.11
Mass/Length	10.81	5.00	4.29	17.15	130.43	130.43	0.01	168	410.92
Draft/Width	0.93	0.70	0.81	0.42	2.20	2.59	0.39	48	1.04
Height/width	0.36	0.35	0.32	0.16	0.96	1.08	0.12	68	0.15
Mass/Width	17.61	5.00	8.20	27.00	166.67	166.67	0.10	66	1,039.15
Height/Draft	0.41	0.35	0.35	0.18	0.93	0.97	0.04	75	0.20
Mass/Draft	25.10	5.00	11.40	34.32	166.13	166.67	0.54	55	1,807.95

Source: Hotzel and Miller 1983

TABLE A-4

Functional relationships between parameters of iceberg dimensions

Type	Y	X	N	R	A	B
All icebergs	Draft	Length	75	0.74	3.781	0.63
	Width	Length	67	0.94	0.7118	1.00
	Height	Length	230	0.83	0.4025	0.89
	Mass	Length	168	0.90	0.002009	2.68
	Mass	Draft	55	0.78	0.01470	2.50
	Draft	Mass	55	0.78	17.245	0.232

Note: Y, X = Iceberg parameters
A, B = Regression equation parameters
N = Number of data pairs
R = Correlation coefficient
$Y = AX^B$

Source: Hotzel and Miller 1983

TABLE A-5

Comparison of estimated drafts based on height

Height	DHI*	El-Tahan			Robe	Hotzel & Miller**
		Pinnacled & drydock	Domed	Tabular		
10	70	22	86	115	78	37
20		44	80	98	90	60
30	90	66	76	89	98	80
40		88	74	83	103	98
50	110	110	72	79	108	115
60		132	70	76	112	131
70	115	154	69	73	116	146

* These numbers are from the exceedence diagram for the iceberg types (Figure A-5). Exceedence curves are presented for four ranges of iceberg height (2 m intervals, up to 80 m) and the sole exceedence values for the middle of each range are given here.

** The equation used here is $D = 7.2\ H^{0.708}$. This equation was derived by substituting the functional relationship for height to length into the relationship of draft to length.

significantly on operator judgement. Additionally, the measurements often skew on the side of under-estimating draft, because the instruments may be operating at maximum range at iceberg keel depth. Also the arrangement of the transducer is a factor. In the case of spinning transducers, the probability is less than 20% that the keel would be "seen." Secondly, no clear theoretical relationship between the draft and the above-water parameters or mass has been proposed.

APPENDIX 5

TABULATED QUESTIONNAIRE

APPENDIX 5

TABULATED QUESTIONNAIRE

1.0 PRELIMINARY INFORMATION

1.1 Company name and address:

1.2 Name and title of person(s) providing requested information:

2.0 ASSESSMENT OF INDUSTRY DESIRES

2.1 What is your opinion of iceberg underwater measurement systems (sidescan) currently used?

10 Useful (scientifically)
7 Useful (operationally)
0 No use
1 Other_____

2.2 Which do you see as being the more important benefit of underwater iceberg information?

7 Operations
10 Scientific Research
Specify_____

2.3 Are you interested in the development of a system to allow determination of the entire 3 dimensional underwater shape of an iceberg, rather than just draft?

12 Yes
2 No

2.4 If such a system were developed would you desire it to be able to perform the following additional functions:

a) underwater sea ice measurement?

8 Yes
5 No

b) small-scale bottom surveys?

4 Yes
8 No

c) wellhead location?

4 Yes
8 No

2.5 What would you feel would be a reasonable mobilization time for such a system?

5 1 day
4 2 days
0 3 days
3 5 days

2.6 Would you prefer that the system be aircraft carriable so that it can be flown to and installed on site?

9 Yes
2 No

2.7 Would you have any objection to a system requiring more than one operator?

5 Yes
7 No

2.8 What, in your opinion, would constitute acceptable times to complete:

a) draft measurement only

10 less than 1 hour
1 1 to 2 hours
1 greater than 2 hours

b) complete underwater shape determination

3 1 to 2 hours
4 2 to 3 hours
3 3 to 4 hours
2 greater than 4 hours

2.9 Would you desire to have these measurements in real-time?

a) draft measurement

10 Yes
2 No

b) complete 3-dimensional underwater shape determination

5 Yes
6 No

2.10 What accuracy would you realistically desire from the system?

2 2%
4 5%
1 7%
5 10%

2.11 What would be the worst environmental conditions you would expect the system to be operable in?

5 Beaufort 5 (17-21 knot winds with 2.5 m seas)
4 Beaufort 6 (22-27 knot winds with 4 m seas)
3 Beaufort 7 (28-33 knot winds with 5.5 m seas)
0 Other (specify)_____

_____

2.12 What would you consider as acceptable monthly downtime for this system?

3 less than 1 day
4 1 to 2 days
4 3 to 5 days

2.13 What, in your opinion, would constitute a reasonable day rate for such a system?

1 < $250
7 $250 - $500
1 $500 - $750
2 > $750

If you have any comments to add, please do so in the space provided.

APPENDIX 6

ACOUSTIC SENSING

APPENDIX 6

ACOUSTIC SENSING

A6.1 INTRODUCTION

Acoustic methods are used extensively for diverse underwater applications. The standard techniques used operationally for the measurement of iceberg draft provide at best a crude measurement of draft and are is totally unsuitable for shape measurement. However the results do show that an acoustic sensor can be used to detect icebergs from reasonable ranges (in the order of 200 m or less at high frequencies of 50-100 kHz). Indeed, the problem with the current technique is not within the acoustic sensor itself, but rather the ambiguity associated with the lack of information regarding the location of the area insonified and the resolution problem associated with the use of wide beam-width systems. It is therefore worthwhile examining the factors affecting the performance of acoustic sensors as a tool for an iceberg mapping system. Various types of sonar systems are used to detect an underwater object (target) and to determine its position. In the simplest case a short acoustic probing pulse is transmitted toward a target and the travel time of the reflected acoustic echo is used to calculate the target range.

The angular position of a target can be determined using echo arrival times observed from one or more locations. In the design of a sonar system for a specific application, several factors associated with the generation of the acoustic pulse, its propagation in water and the echo reception must be considered. Acoustic energy generated by an acoustic transducer propagates in several directions as determined by the transducer radiation pattern. A practical search-type acoustic beam is always accompanied by finite sidelobes. Also, acoustic waves do not propagate along straight lines but are refracted because of the variation of sound velocity propagation with depth. Finally, reception of the echo can be severely impaired as a result of noise from several different sources.

Several different schemes can be considered for an acoustic iceberg profiling system and it would be undesirable at this stage to restrict our attention to any particular one. On the other hand, a general scenario as dictated by operational and technical constraints with emphasis on the problems to be discussed, is useful for a

proper selection. As a the general scenario it is therefore assumed that the iceberg profiling will be accomplished by a steerable, searchlight-type, acoustic beam (such a system has apparently been used successfully for draft measurement (Brooks, 1979)). Such a beam can be produced by suitable acoustic arrays, by analog-digital signal processing, and by mechanical array rotation or linear translation. Several different iceberg profiles (scans) are required to produce a three-dimensional image of its underwater portion. It is postulated that, because acoustic ray bending, operational constraints (size of an array), and technical considerations (precision required), the minimum acoustic beam-width will be in the order of 0.6° to 1°. Operational considerations suggest that, most likely, both transmitting and receiving arrays will be located in proximity to each other at a maximum distance of several hundred metres from the scanned iceberg.

In the subsequent paragraphs, the general parameters associated with a search-type sonar system are introduced and specific problems of iceberg profiling are discussed in more detail.

A6.2 BASIC DEFINITIONS AND UNITS

A6.2.1 Units

SI units based on metres (m), kilograms (kg), and seconds (s) will be used.

Force: $1N = m.kg/s^2$	(N - Newton)
Pressure: $1Pa = 1N/m^2$; $1\mu Pa = 10^{-6}$ Pa	(Pa - Pascal)
Energy: $1J = 1N.m$	(J - Joule)
Power: $1w = J/s$	(w - Watt)

A6.2.2 Sound Pressure and Intensity

Sound pressure, p(t), is proportional to the particle velocity, u, or

$$p(t) = zu(t) \qquad \text{(A6.1)}$$

where:

z = specific acoustic impedance (rayls), $z = c\rho$,
c = sound velocity of propagation, and,
ρ = water density.

The average pressure level is expressed in terms of its root mean square value:

$$P = \overline{p^2} = \left[\lim_{T\to\infty} \frac{1}{T} \int_{-T/2}^{T/2} p^2(t)dt\right]^{1/2} \quad . \qquad (A6.2)$$

Power carried by a sound wave per unit area (w/m^2) is called wave intensity and is proportional to p^2, that is,

$$I = \frac{p^2}{z} \quad . \qquad (A6.3)$$

A6.2.3 Logarithmic Scale

Sound intensity is expressed using a logarithmic scale (decibels or dB) referenced to a reference intensity I_o,

$$\begin{aligned} I(\text{dB re } I_o) &= 10 \log(I/I_o) \\ &= 10 \log(p^2/z/p_o{}^2/z) = 10 \log (p/p_o)^2 \\ &= 20 \log (p/p_o) \end{aligned} \qquad (A6.4)$$

The reference currently used is p_o = 1 μPa and a pressure expressed in dB re 1 μPa is equivalent to its intensity expressed in dB re I_o, as given by equation A6.4.

For a given pressure, p, (in dB re 1 μPa) the sound intensity (in W/m^2) in water is given by:

$$I = 6.49 \times 10^{0.1p - 19} \quad . \qquad (A6.5)$$

A6.3 ACOUSTIC TRANSDUCERS

A6.3.1 Beam Patterns

An acoustic transmitter (projector) is used to generate an acoustic pressure waveform. The parameters of the transmitter are derived using steady-state sinusoidal pressure waveforms at a certain frequency. The pressure generated by the acoustic transmitter (or transmitting array) varies according to its normalized radiation pattern, $v(\theta,\phi)$, as observed at a constant distance far away from the transmitter, and is given by:

$$v(\theta,\phi) = \frac{R(\theta,\phi)}{R(0,0)} \quad , \qquad (A6.6)$$

where $R(\theta,\phi)$ represents the actual pressure generated by a transmitter in the polar directions, θ and ϕ.

The beam pattern, or pattern function, $b(\theta,\phi)$, is the square of v, or:

$$b(\theta,\phi) = v^2(\theta,\phi), \text{ and ,} \qquad \text{(A6.7)}$$

$$B(\theta,\phi) \text{ in dB} = 20 \log v(\theta,\phi) \text{ in dB} \qquad \text{(A6.8)}$$

The direction (0,0) is usually taken to be the direction of the maximum response. For a symmetrical beam pattern this direction is referred to as the acoustic axis of the transmitter.

A three-dimensional beam pattern for a circular piston transducer is illustrated in Figure A-7. A beam pattern consists of the main lobe and several undesirable side lobes. The angular width (beam-width) of the main lobe is inversely proportional to the physical dimensions of the transmitter or transmitter array, relative to the wavelength.

The sidelobes can be reduced by, so called, shading of the array; that is, by a proper adjustment of the transmitting characteristics of each element of the array. Acoustic lenses and reflectors can also be used to modify the beam pattern. Particularly impressive beam patterns can be obtained by parametric arrays where the nonlinearity of sound propagation in water is used. In this case, a transducer is driven by two high-power, high-frequency signals each of which propagates along a very narrow beam. As a result of nonlinear interaction of these two signals in water a low-frequency signal is produced which propagates along a highly directional beam without sidelobes (Figure A-8). The main drawback of this method lies in the very low efficiency of the electric-to-acoustic energy conversion (a few per cent).

A discussion of the transmitter beam pattern applies directly to the receiving hydrophone (or hydrophone array). The pattern function $b(\theta,\phi)$, describes, in this case, the directional sensitivity of the receiver when receiving a pressure wave from a (θ,ϕ) direction.

A6.3.2 Transmitting Directivity Index

The transmitting directivity index, DI_T, of a projector is a difference, measured or calculated at a point on the axis of the beam pattern, between the level of the sound generated by the given projector and the level that would be produced by a omnidirectional projector radiating the same total amount of acoustic power, W.

The pressure level, SL, (in dB re 1 μPa) 1 m away from the transducer is given by:

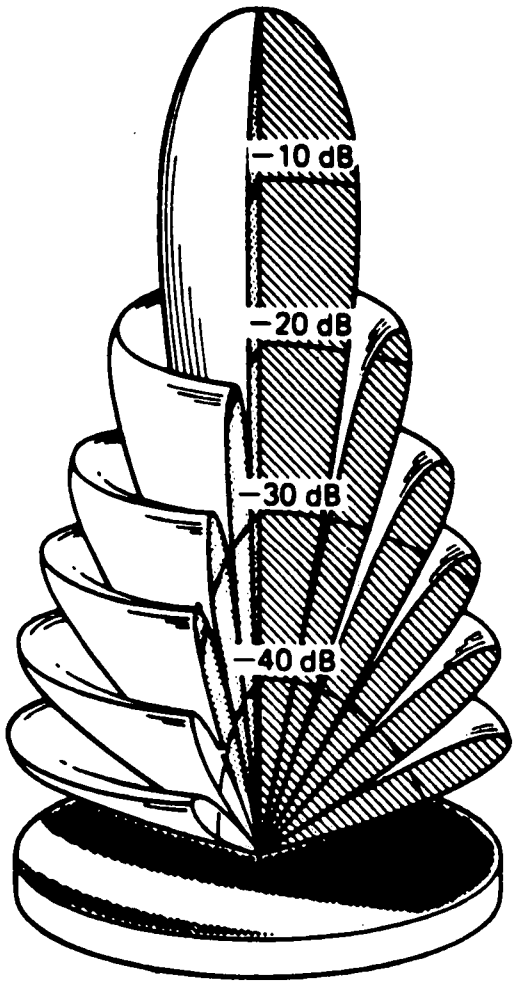

Fig. A-7. Three-dimensional beam pattern for a circular piston transducer (Clay and Medwin 1977).

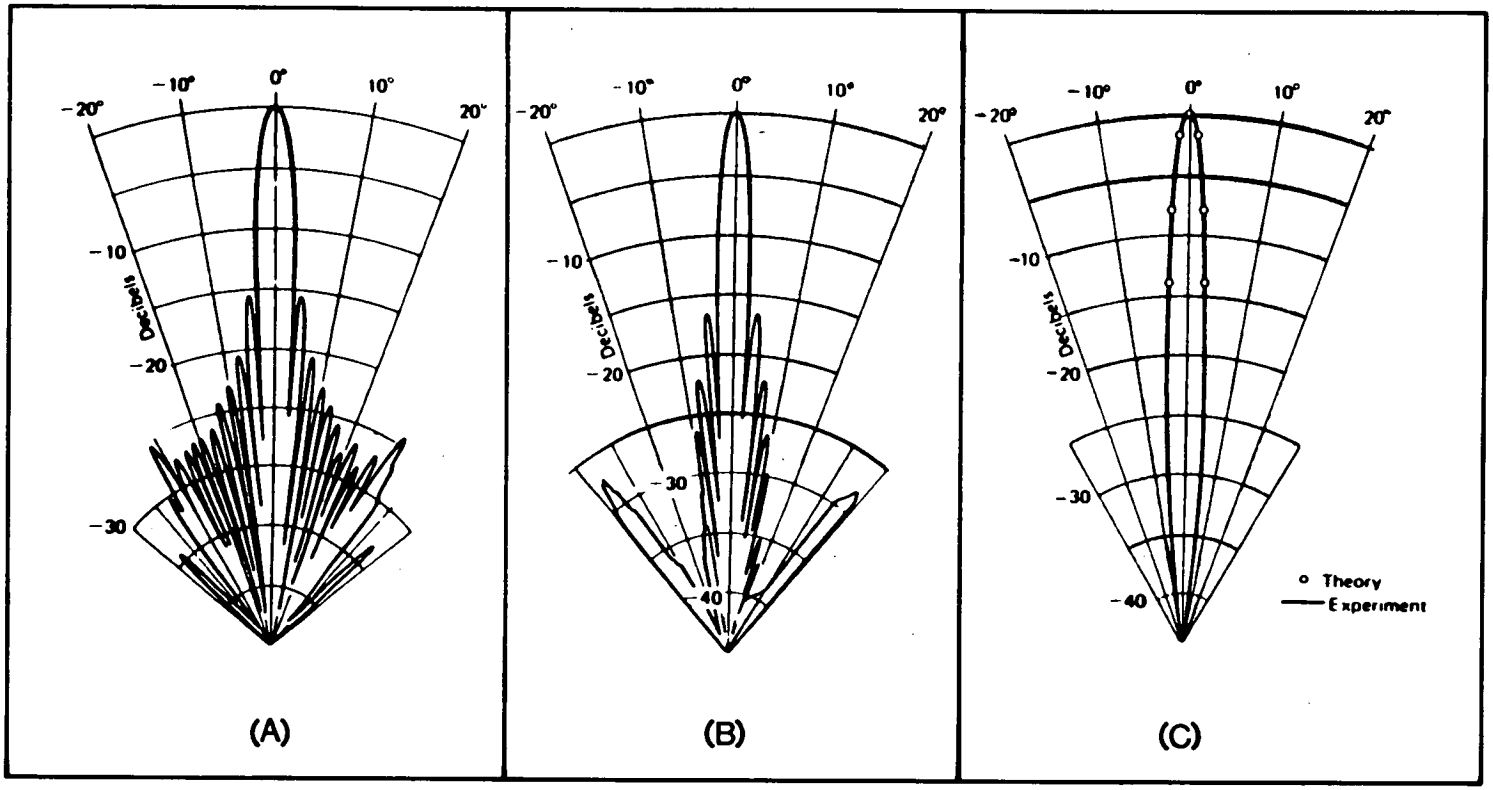

Fig. A-8. Parametric transmitting array directivity patterns. (A) Beam pattern of 418 kHz primary. (B) Beam pattern of 482 kHz primary. (C) Difference frequency beam pattern. (Clay and Medwin 1977).

$$SL = 170.88 + 10 \log W + DI_T \qquad (A6.9)$$

and is called the source level. Typical values of SL for side-looking sonars are in the 216-228 dB re 1 μPa range and are limited by cavitation effects.

A projector can usually operate within a range of frequencies, B, centred around a frequency, f_o. The Q-factor of a transducer is defined as the ratio:

$$Q = f_o/B \quad . \qquad (A6.10)$$

Typical values of Q vary from 2 to 10. Electric power to acoustic power conversion efficiency increases with Q and varies from 20 to 70% for most piezoelectric transducers.

A6.4 SONAR OPERATION AND PARAMETERS

A6.4.1 System Bandwidth and Resolution

The concept of an acoustic beam is valid for a CW (continuous waveform) sinusoidal signal. However, it can be applied as a useful approximation to bandpass signals such as sinusoidal pulses providing that their bandwidth, B, is much smaller then the central frequency, f_o. For practical applications the following inequality should be satisfied:

$$f_o /B > 10 \quad . \qquad (A6.11)$$

The duration time of a sinusoidal pulse, τ, is inversely proportional to its bandwidth. For the Gaussian shaped envelope of a sinusoidal pulse the following equation applies:

$$B\tau = 0.664 \quad , \qquad (A6.12)$$

where B and τ are the 3-dB bandwidth and 3-dB duration time, respectively.

As a convenient rule of thumb, it is assumed that for a simple sinusoidal pulse of duration, τ, the minimun bandwidth occupied by such a pulse satisfies the equation:

$$B\tau = 1 \quad . \qquad (A6.13)$$

The signal duration is closely related to the sonar radial resolution, δ, given by:

$$\delta = \frac{\tau c}{2} = \frac{c}{2B} \quad . \qquad \text{(A6.14)}$$

A conical acoustic beam diverges proportionally to the distance, r, between a projector and a target (iceberg). At the target, the beam has a circular cross-section with a radius, R, given by:

$$R = r \tan \frac{\phi}{2} \quad , \qquad \text{(A6.15)}$$

where ϕ is the beam-width. This circular cross-section is then projected onto the random surface of the target where an echo is formed. The azimuthal resolution dictated by the beam-width is 2 R.

The insonified area on the target has a certain radial depth which will vary randomly depending on the position of the insonified area on the iceberg. It can be expected that (on average), this depth will increase with the increase of R. For this reason it is sensible to limit the required radial resolution of the system, δ, to a certain fraction of R. It may be arbitrarily postulated that:

$$\delta = 0.2 \; R \quad . \qquad \text{(A6.16)}$$

As an illustration, if it is assumed that $\phi = 0.6°$ and r = 200 m, using equations (A6.15) and (A6.16) then R = 1.05 m and δ = 0.21 m. Using equation (A6.11) and (A6.13), the minimum bandwidth and central frequency of a system are 3.6 kHz and 36 kHz respectively.

A6.4.2 Source Level

The power of an acoustic pressure pulse generated by the transmitter is described by a source level (SL) as measured or calculated at 1 m away from the transducer (actual measurements are usually done at longer distances but are corrected to 1 m distance). The source level is expressed in dB re 1 μbar (microbars) at 1 m, in which case 100 dB should be added to correct it to the 1 μPa reference. It may also be expressed in dB re 1μPa (or 1μbar) at 1 yd, in which case 0.82 dB should be subtracted to correct for the 1 m reference.

A6.4.3 Transmission Loss and Target Strength

As the transmitted acoustic pulse propagates through the water its amplitude decreases because energy is spread over an increasingly larger area and by absorption of sound energy by water. At a target r metres away from

the transmitter, the signal level is reduced and the transmission loss (TL) is expressed as:

$$TL = 20 \log r + \alpha r \ , \qquad \text{(A6.17)}$$

where the absorption coefficient, α, is expressed in dB/m. The variation of α versus frequency for different temperatures and a salinity of 35 ppt (parts per thousand) is shown in Figure A-9.

A portion of the incident sound energy is reflected or scattered back toward the receiver and is expressed as a target strength (TS). On its way back the signal is further weakened by the transmission loss given by the equation (A6.17). Finally, the acoustic pressure signal reaching the receiving hydrophone is given by:

$$SR = SL - 2TL + TS \ . \qquad \text{(A6.18)}$$

A6.4.4 Noise and Receiving Directivity Index

Even in the absence of the transmitted pulse the receiving array registers random pressure fluctuations, termed ambient noise. In general, the noise field is characterized by the directional function $N(\theta,\phi,f)$ representing noise power per unit solid angle Ω in a 1 Hz band-width at frequency, f, in a (θ,ϕ) polar direction with respect to the receiving hydrophone array. The total noise power admitted to the system by the hydrophone array with a beam pattern, $b(\theta,\phi)$, is given by:

$$\overline{n^2} = \frac{1}{4\pi} \int_{f_o - \frac{B}{2}}^{f_o+\frac{B}{2}} df \int_{4\pi} N(\theta,\phi,f)\, b(\theta,\phi) d\Omega \ . \qquad \text{(A6.19)}$$

When the noise is isotropic, that is, the noise power per unit solid angle is the same in all directions so that $N(\theta,\phi,f)=N(f)$, the equation (A6.19) reduces to

$$\overline{n^2} = \int_{f_o - B/2}^{f_o+B/2} N(f) df \cdot \frac{1}{4\pi} \int_{4\pi} b(\theta,\phi) d\Omega \ . \qquad \text{(A6.20)}$$

For narrow-band systems where N(f) does not vary much within a narrow band of frequencies, equation (A6.20) can be further simplified to

$$\overline{n^2} = BN(f_o)/D_i \ , \qquad \text{(A6.21)}$$

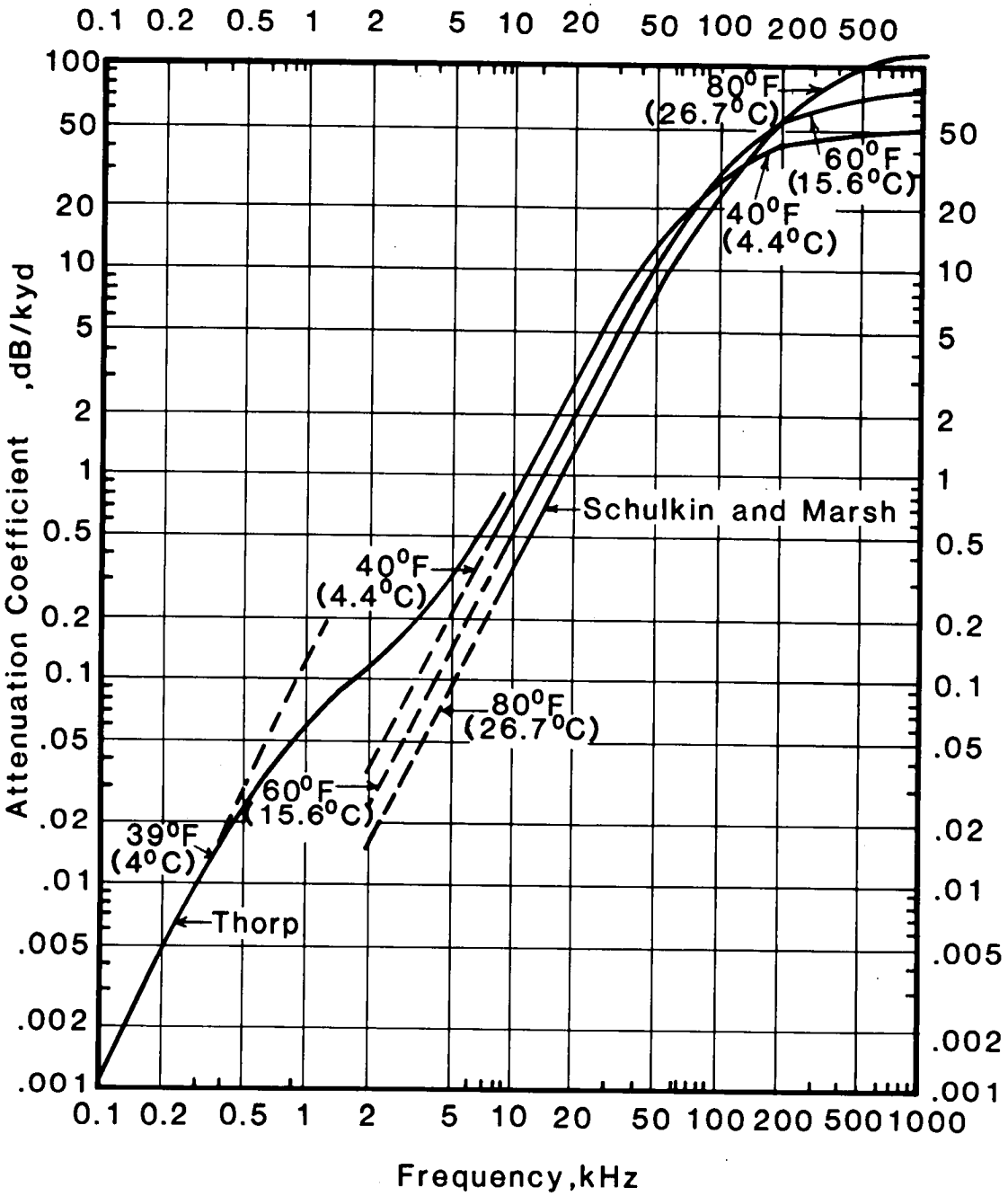

Fig. A-9. Attenuation coefficient in seawater as a function of frequency and temperature (Urick 1975).

where the directivity index, D_i, is given by:

$$D_i = \frac{4\pi}{\int_{4\pi} b(\theta,\phi)d\Omega} = \frac{\int_{4\pi} d\Omega}{\int_{4\pi} b(\theta,\phi)d\Omega}$$

$$= \frac{4\pi}{\int_0^{2\pi}\int_{-\pi/2}^{\pi/2} b(\theta,\phi)\cos\theta\, d\theta\, d\phi} \quad . \qquad \text{(A6.22)}$$

Equation (A6.22) provides for a physical interpretation of the receiver directivity index as a ratio of noise power received by a omnidirectional hydrophone ($b(\theta,\phi) = 1$) to the noise power received by the directional hydrophone. A useful approximation to the equation (A6.22) for a receiver with small sidelobes, is given by:

$$D_i = \frac{4\pi}{\theta_1\phi_1} \quad , \qquad \text{(A6.23)}$$

where θ_1 and ϕ_1 are the receiver beam-widths in azimuth and in elevation (expressed in radians). If several independent noise sources are present then superposition of powers applies, that is:

$$N(\theta,\phi,f) = \sum_{i=1}^{N} N_i(\theta,\phi,f) \quad . \qquad \text{(A6.24)}$$

Applying a logarithmic scale to equation (A6.21), the in-band noise level (NR) admitted to the system (expressed in dB) is:

$$NR = 10 \log \overline{n^2} = 10 \log B + NL - DI \quad , \qquad \text{(A6.25)}$$

where:

NL = 10 log $N(f_o)$ and is the ambient noise level at the central frequency, f_o, and

DI = 10 log D_i and is the directivity index expressed in dB.

The conclusion from the above discussion is that to reduce noise power a system with a narrow bandwidth and a high directivity index should be used.

Representative noise spectra versus frequency are shown in Figure A-10. It is noted that above 100 kHz, in moderate sea states, the thermal noise predominates over the sea state noise. Thermal noise level is described by the equation

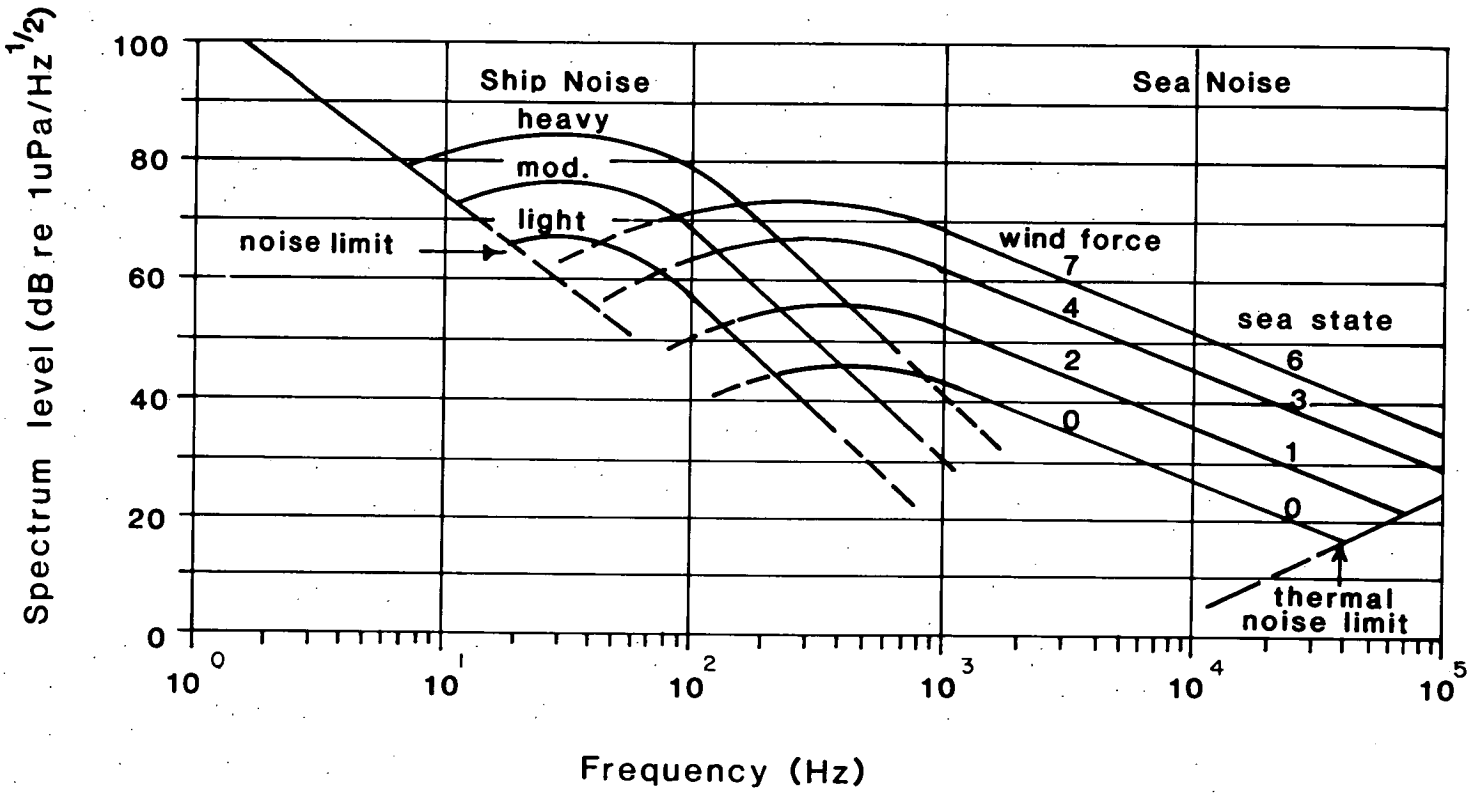

Fig. A-10. Average deep-water ambient noise spectra (Flemming et al. 1982).

$$NL \text{ (dB re } 1\mu Pa/\sqrt{Hz}) = -75 + 20 \log f \quad . \qquad (A6.26)$$

The ambient noise level shown in Figure A-10 is only a general indicator of the actual noise intensity. Several additional factors such as rain, biological noise, cracking ice, and others may change appreciably the encountered noise level, especially at the lower frequencies. Noise caused by rain for example can vary in level by up to 18 dB at 10 kHz (Urick 1975).

A6.4.5 Reverberation

Reverberation is a combined result of echoes from other than intended targets, such as the sea surface, sea bottom, fish and other organisms, suspended particles, and air bubbles. Prediction of the reverberation level has many similarities to a target strength evaluation but from the system performance point of view the reverberation is treated as a directional noise field with intensity and directionality linked to the transmitter radiation pattern and its source level. The basic difference between reverberation and ambient noise is that reverberation depends on the transmitter radiation pattern and source level, and its bandwidth is similar to that of the transmitted signal.

The main portion of the reverberation power is back-scattered along the acoustic beam of a directional transmitter and receiver. If the beam is pointing toward strong scatterers (such as the ocean surface or the bottom) the echo from a possible target will be most likely masked by the reverberation noise. Reverberation will also be admitted to the system from other directions off the main beam through the side lobes in the transmitter/ hydrophone radiation patterns. In the calculation of the total noise power admitted to the system the reverberation term should be added to the right side of equation (A6.21), that is,

$$\overline{n^2} = BN(f_o)/D_i + \overline{n_r^2} \quad , \qquad (A6.27)$$

where $\overline{n_r^2}$ represents the total reverberation power.

A6.4.6 Signal to Noise Ratio

The signal-to-noise ratio (SNR) in dB can be obtained by subtracting the total received noise level, as given by equation (A6.25), from the received signal level, as given by equation (A6.7):

$$SNR = SR - NR \quad . \qquad \text{(A6.28)}$$

The SNR may serve as a figure of merit of a sonar system and can be related to other operational parameters. The typical minimum required value for the SNR varies from 0 to 20 dB, depending on the application.

A6.5 ACOUSTIC RAY BENDING

The velocity of sound propagation in water is a function of water temperature, salinity, and pressure, as given by the empirical relation (Urick 1975):

$$c = 1492.9 + 3(T-10) - 6 \times 10^{-3}(T-10)^2 - 4 \times 10^{-2}(T-18)^2 + 1.2(S-35) - 10^{-2}(T-18)(S-35) + z/61 \quad , \qquad \text{(A6.29)}$$

where: c = metres per second,
T = temperature in degrees, centigrade,
S = salinity in parts per thousand, and
z = depth in metres.

Equation (A6.29) is said to be accurate to 0.1 m/s for T less than 20°C and for z less than 8,000 m. Because of the variation of sound velocity with depth the acoustic rays do not propagate along straight lines. An illustration of ray bending resulting from velocity variation with depth is shown in Figure A-11 for a velocity profile obtained in May 1978 in Placentia Bay off the Island of Newfoundland. The ray bending affects the performance of a sonar system in several ways. It may cause an appreciable departure from the predicted transmission losses, as given by equation A6.17 and, in an extreme case, may cause an acoustic shadow zone (Figure A-11).

In addition, ray bending causes an error in the determination of the angular position and the range of a target on the iceberg. These latter effects are considered in some detail for a simplified, linear velocity profile, and the situation as depicted in Figure A-12. A sonar transmits an acoustic pulse along a very narrow beam in the α_p direction with respect to the horizontal toward a plane target located at a distance, r, from the sonar. It is shown by Kinsler and Frey (1962), that for a linear variation in the sound velocity with depth, an acoustic ray propagates along a circular arc, s, with a radius, R_o, given by:

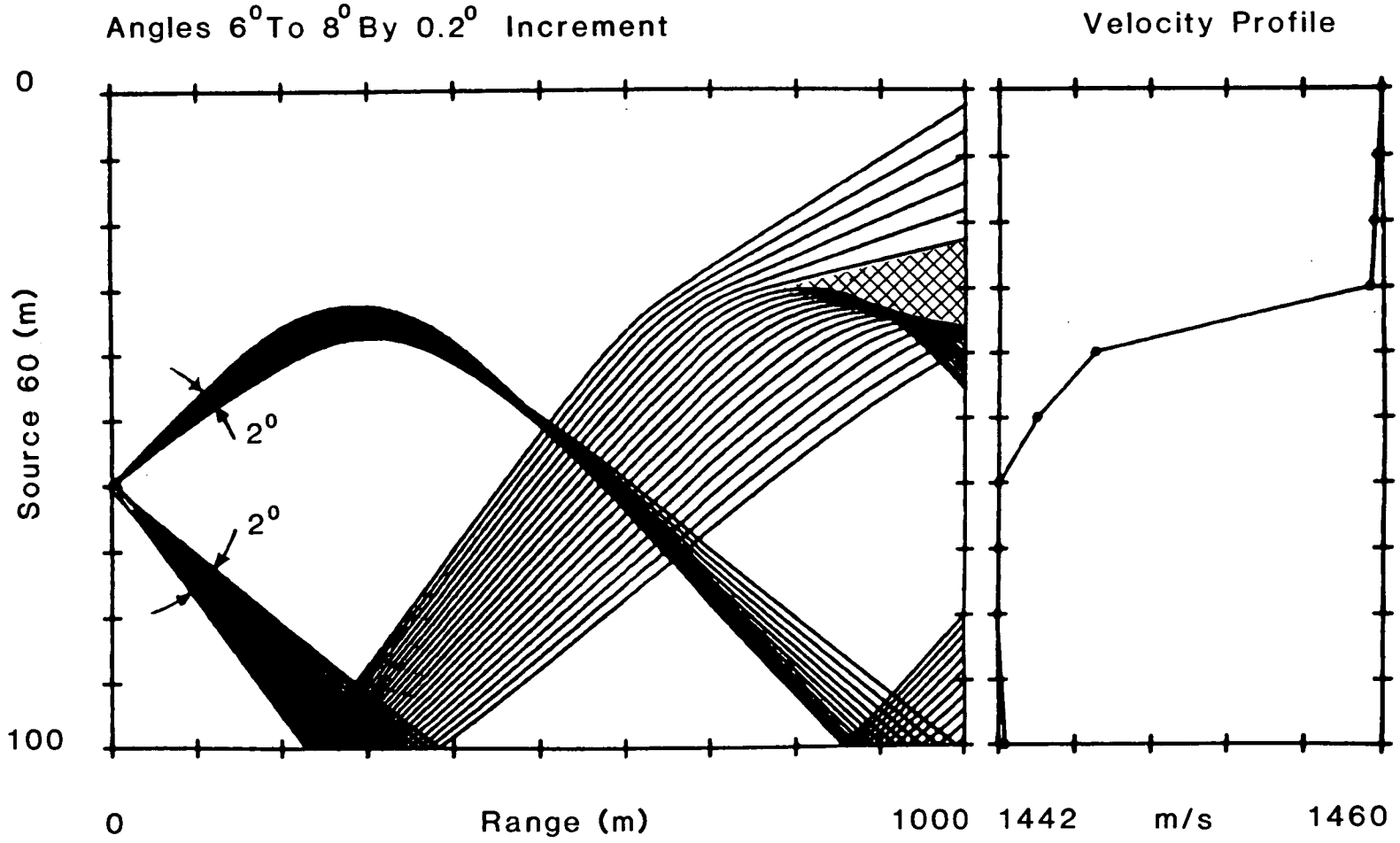

Fig. A-11. Acoustic ray bending due to sound velocity variation.

$$R_o = c_o/|g| \cos\alpha_p \quad , \qquad \text{(A6.30)}$$

where: c_o = sound velocity at the sonar depth, and
g = velocity gradient, $g = dc/dz$.

For a negative g the acoustic ray is bent downwards (as in Figure A-12), whereas for a positive g it is bent upwards.

A6.5.1 Position and Angular Errors

The point at which a straight-line ray (no bending), projected at an angle, α_p, by the transmitter, intercepts the target plane (with respect to the reference level shown in Figure A-12) is given by:

$$z_p = R_o \cos\alpha_p + r \tan \alpha_p \quad , \qquad \text{(A6.31)}$$

whereas the actual depth at which the target is intercepted by the bent ray is found to be:

$$z_a = \sqrt{R_o^2 - a^2} \quad , \qquad \text{(A6.32)}$$

where $a = R_o \sin \alpha_p - r$. (A6.33)

This point can be reached by a straight-line ray projected at angle, α_a, given by:

$$\alpha_a = \tan^{-1}[\tan\alpha_p - \frac{\Delta_p}{r}] \quad , \qquad \text{(A6.34)}$$

where the position error, Δ_p, is given by:

$$\Delta_p = z_p - z_a \quad . \qquad \text{(A6.35)}$$

The angular error (Δ_α) associated with the position error is

$$\Delta_\alpha = \alpha_p - \alpha_a \quad . \qquad \text{(A6.36)}$$

A6.5.2 Range Error

In addition to an angular error there is a range error equal to the difference between the straight-line slant range, r_p, which is found from the equation:

$$r_p = r/\cos \alpha_p \quad , \qquad \text{(A6.37)}$$

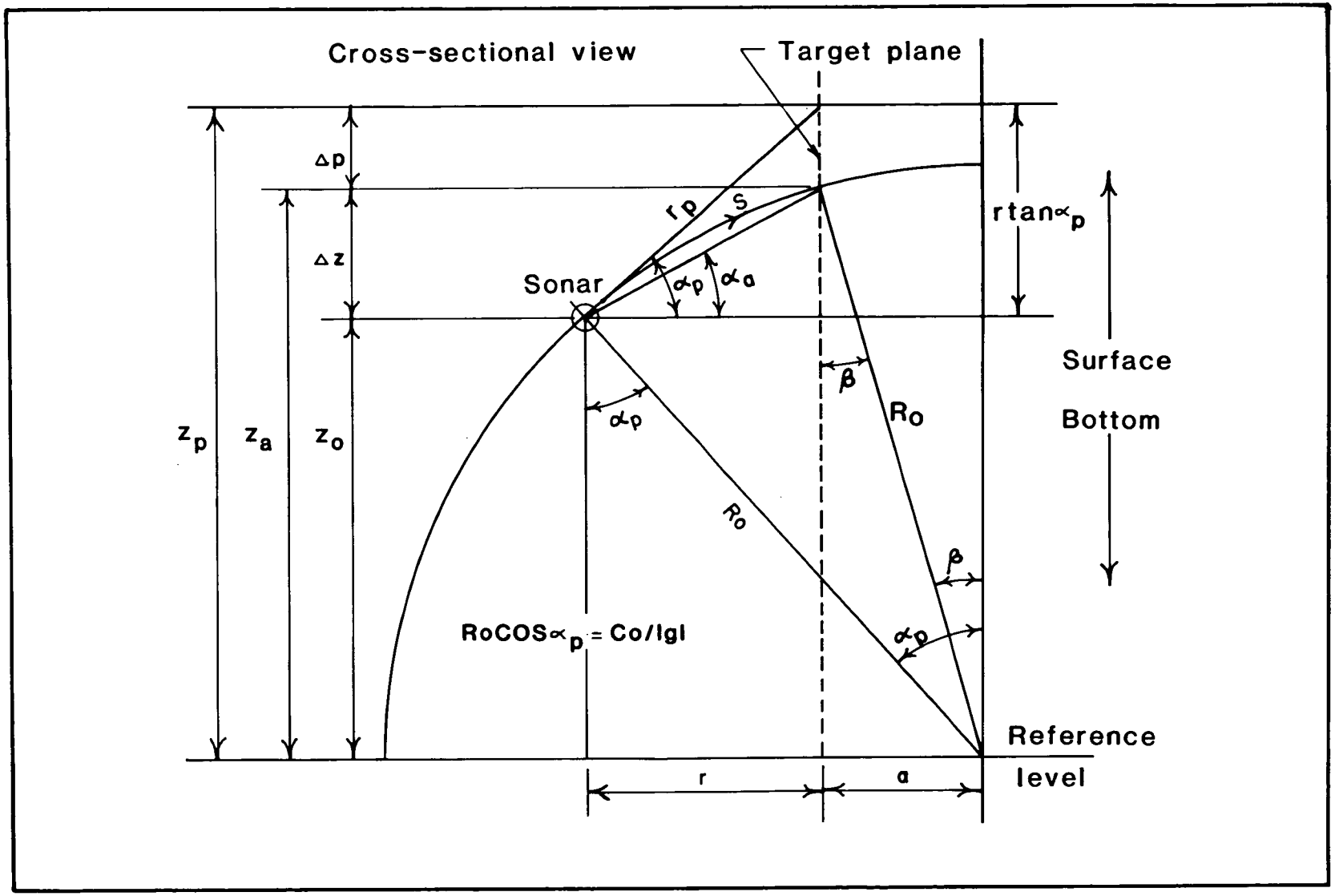

Fig. A-12. Errors caused by acoustic ray bending.

and the actual sound travel path along arc, s, given by:

$$s = R_o(\alpha_p - \sin^{-1}(a/R_o)) \quad , \tag{A6.38}$$

that is:

$$\Delta_r = r_p - s \quad . \tag{A6.39}$$

A6.5.3 Velocity Error

In situations when the velocity gradient is unknown, the estimate of a target range can be obtained as a product of the one-way travel time and sound velocity at the transmitter. Because the sound travels with a depth-varying velocity this estimate is an error. An exact expression for the travel time in water with a constant velocity gradient is given by Clay and Medwin (1977). An approximate expression is given here for the velocity error, using, for calculation purposes, the arithmetic average of the sound velocities at the transmitter and the target. This calculation leads to the following approximate expression for the velocity error:

$$\Delta_c = - \frac{sg\,\Delta z}{2c - g\Delta z} \quad , \tag{A6.40}$$

where,

$$\Delta z = z_a - z_o \quad , \tag{A6.41}$$

and,

$$z_o = R \cos \alpha_p = c_o/|g| \quad . \tag{A6.42}$$

A sample of the calculated errors associated with acoustic ray bending is shown in Table A-6 for the assumed values of r, g, and c_o. For this particular case, the dominating error is the position error due to the angular error. The range and velocity errors are smaller and are strongly dependent on the projection angle, α_p. If no correction is applied these errors will cause distortion in the measured iceberg profile. The actual velocity profile can be highly nonlinear with local gradients exceeding the assumed value in Table A-6 of -0.2 m/m/s. If a sound velocity profile is available the ray bending errors can be corrected using a ray tracing algorithm, which decomposes the complex profile into layers of constant gradients. An additional complication arises from local disturbances in sound velocity caused by the iceberg temperature and melting process, which affects the salinity of the

TABLE A-6

Errors associated with the acoustic ray bending

Errors	$\alpha_p = o°$	$\alpha_p = 25°$
Position error Δ_p(m)	2.7	3.2
Angular error Δ_α(°)	0.8	0.8
Range error Δ_r(m)	0.02	1.36
Velocity error Δ_c(m)	-0.03	1.32

Note: For r = 200 m, g = -0.2 m/m/s and C_o = 1500 m/s

surrounding water. Assessment of this effect will require the collection of experimental data.

A6.6 ACOUSTIC REFLECTION FROM A SOLID TARGET

When a compressional wave is incident on an elastic solid, part of the energy of the incident wave is reflected, part is transmitted as a compressional wave into the solid, and part is converted to a transmitted shear wave in the solid.

For a smooth liquid-solid interface, the angle of incidence is equal to the angle of reflection. The reflection coefficient, R_{12}, at this interface as derived by Tolstoy and Clay (1966), is (in modified form) given by:

$$R_{12} = \frac{A - B}{A + B} \qquad \text{(A6.43)}$$

where:

$$A = 4\gamma_2\delta_2\alpha^2 + (\delta_2^2 - \alpha^2)^2 \ ,$$

$$B = (\rho_1/\rho_2)(\gamma_2/\gamma_1)\ c_{s2}^{-4} \ ,$$

$$\alpha = \sin\theta_1/\ c_1 \ ,$$

$$\gamma_1 = \cos\theta_1/c_1 \ , \qquad \text{(A6.44)}$$

$$\gamma_2 = \frac{1}{c_{p2}}\left[1 - \left(\frac{c_{p2}}{c_1}\sin\theta_1\right)^2\right]^{1/2} \ ,$$

$$\delta_2 = \frac{1}{c_{s2}}\left[1 - \left(\frac{c_{s2}}{c_1}\sin_1\theta^2\right)^{1/2}\right] \ ,$$

c_1 = sound velocity in the liquid ,

θ_1 = angle between the incident ray and the normal to the interface surface ,

c_{p2} = compressional wave velocity in the solid,

c_{s2} = shear wave velocity in the solid, and,

ρ_1, ρ_2 = density of the liquid and the of solid, respectively.

According to Carlin (1960), the velocity of a shear wave is about 48% of the longitudinal (compressional) velocity. The density of ice is approximately 920 kg/m^3

and the compressional velocity is 3200 m/s. For sea water these parameters are 1,026 kg/m^3 and 1,500 m/s, respectively (Kinsler and Frey 1962). Using these data and equations A6.34 and A6.44 the reflection coefficient for the water-ice interface, and at normal incidence ($\theta_1 = 0$), it is found to be $R_{12} = 0.313$ or -10dB.

For a random surface the reflection is accompanied by scattering and the acoustic energy is re-radiated according to a certain beam pattern with an axis usually along the specular direction. For surfaces rough in comparison to the wavelength of the incident waveform the re-radiation pattern tends to be more omnidirectional. In this sense a back-scattering target strength is frequency dependent. No experimental data are available on iceberg back-scattering. One can expect, however, that for a narrow-beam system, the insonified portion of an iceberg may be smooth enough to result in specular reflection. Since, only some parts of the iceberg surface will be perpendicular to the beam, one would expect considerable fluctuations in target strength on a pulse-to-pulse basis. This effect may be minimized if a more complex pulse, such as a frequency modulated "chirp" pulse, is used.

A6.7 PARAMETRIC SONAR

The sidelobes of the acoustic array may cause degradation of the system performance since echoes from the surface or bottom admitted by them, may mask weak echoes from an iceberg. A parametric source produces an impressive beam pattern, virtually sidelobe free (see Figure A-8, for example). This source type uses the non-linearity of the medium to generate energy at the difference of two or more primary frequencies. The resultant beam has the characteristics of an exponentially tapered end-fire array, the exponential taper being caused by the water attenuation at the primary frequency, whereas the end-fire array is formed in the water column. As the beam-width is dependent on the length of the virtual array and not directly by the transducer size, a narrow beam can be produced by a small crystal.

It has been well documented by a number of scientists (i.e. Berktay 1967; Tucker 1965; Kritz 1977; Horton 1974; Konrad 1979) that the unique beam pattern of the parametric source provides a distinct improvement in the performance of active sonar under reverberation limited conditions. Two examples to illustrate the potential advantages of the parametric source for echo ranging in shallow or surface waters were described by Konrad (1979). He stated:

"...a comparison was made of conventional and parametric systems in an experiment at NUSC's Millstone Quarry Facility in 1971; each system used the same projector. The transducer depth was 4.5 m and the range to the target was 36 m. The source level was the same in each case. The target in each case was an LC-10 hydrophone (7.8 cm long by 1.3 cm diameter); target strength was -35dB. Note that the narrow parametric beam eliminates surface reverberation and the target is unobscured." (Figure A-13A).

"...on a larger scale, Figure A-13B displays a return from a 5 dB target at a range of 8.7 Kyd in Seneca Lake. The difference frequency was 12 KHz with a source level 221 dB re 1 μPa at 1 m and a conical 3° beam. Reverberation is just above the noise level for the parametric source. The much higher reverberation completely obscures the target for the convential source."

Other controlled experiments with fixed transmissions and reception platforms and between moving platforms at sea were conducted with available equipment from NUSC and Sperry Research Centre, Sudbury MA (Quazi et al. 1977 Bohman et al. 1975). They also showed the potential advantages of a carefully designed parametric source where a narrow beam remarkably reduced multipath distortion. This is not to say that the parametric source is the best source to use in scanning an iceberg or that such a source would prevent distortions in propagation.

There are many questions still unanswered regarding the use of parametric sources in turbulent waters or in an inhomogeneous medium. However, studies by Culberston (1979) have helped shed some light on the behavior of a parametric receiving array in turbulent waters and where thermal micro structure exists. Likewise, work performed by Muir et al. (1974, 1979) on propagation models for parametric sources in shallow waters have provided comparisons of mean propagation curves for linear and non-linear sources. When the problem of echo to reverberation becomes important the high directivity of the parametric source has been noted to weigh favourably against equivalent broad beam linear sources. Wide band-width capabilities (for signal processing) as well as Doppler considerations (Muir et al. 1976) also appear to favour parametric sources. Bjorno et al. (1977, 1979), have also shown encouraging qualitative results for the operation of an array (parametric) in a temperature and salinity stratified shallow water region, such as the Baltic Sea.

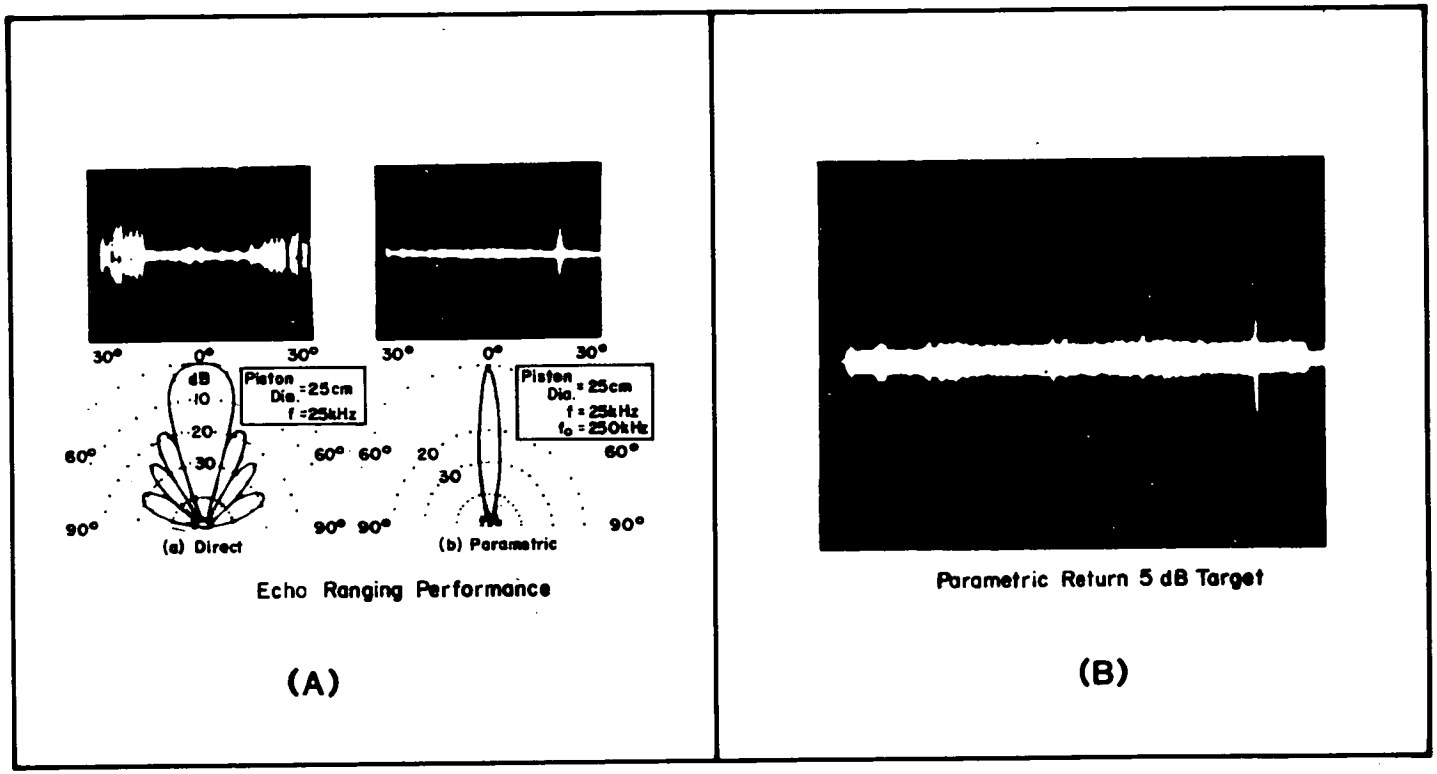

Fig. A-13. Potential advantages of the parametric source for echo ranging (Konrad 1979).

On the other hand, the signal-to-noise ratio is significantly lower for a parametric array than for a conventional source. The highly directional beam advantage is produced at the expense of a very poor energy conversion. This criteria of signal strength is ultimately a deciding factor in favour of a more conventional system since a narrow beam transducer can still be produced through careful design and operation in the high-frequency range of 100 to 200 kHz. The stronger signal will be an important asset in being able to discriminate the true echo returns from the surrounding effects of ambient noise.

If long distance scanning is required such as in ice hazard detection, the use of parametric arrays would become most attractive even with its lower energy level. However given that iceberg profiling is generally performed at close range (i.e., within 0.5 km) a conventional system would be a more effective approach.

APPENDIX 7

ELECTROMAGNETIC SENSING

APPENDIX 7

ELECTROMAGNETIC SENSING

A.7.1 PRINCIPLES OF OPERATION

A detailed assessment of radio echo-sounding for the measurement of iceberg draft and underwater shape was undertaken by REMOTEC (1982). This assessment included a comprehensive theoretical evaluation and of which only a general description of the operating principles is provided here. The reader is referred to that document for a detailed description of the theory.

There are two basic types of operational systems on the market: pulsed - CW (continuous wave) and impulse radars. Both have been used for sea ice, iceberg and glacier thickness measurments. Both systems provide thickness information by transmitting a pulse through the ice (medium). Whenever an abrupt discontinuity is encountered in the dielectric properties (air-ice, ice/water interface, etc.) a reflection occurs. The time delay, between transmission of the pulse and reception of the reflected energy at the ice-water interface, is used to determine the thickness. A knowledge of the dielectric properties of the medium (which provides velocity of propagation information) is necessary to convert the time delay into distance. Discontinuities in the medium for example, cracks or crevasses) which result in abrupt changes in the dielectric properties, can also be detected.

The rate of electromagnetic attenuation in ice increases with frequency, therefore, the lower the frequency the better. Lower frequencies, however, require larger antennas, especially if narrow beam-widths are required. The method of deployment (surface or airborne) dictates the maximum antenna size.

Conventional pulsed-CW systems transmit bursts of a number of frequency cycles at a known repetition rate (pulse repetition frequency). The minimum number of cycles in any given pulse is in the order of 5 to 10, which dictates the minimum pulse length and hence the optimal range resolution.

Impulse radars generate pulses that are very wideband, are carrier free, and approximate the shape of an impulse by exciting a wide bandwidth antenna with a voltage discontinuity. The transmit pulse length and shape are

influenced by the frequency response or characteristics of the antenna. In practice, the shape of the pulse is known and shorter pulse lengths are achieved than with a pulsed-CW system operating with a carrier frequency close to, or at the same frequency as the centre frequency of impulse radar. Impulse radars provide fine resolution in time (typically around 15 ns, range, and thickness (or depth). The practical resolving capability is influenced by dispersion in the medium (e.g., ice) and the nature of the discontinuity (e.g., ice-water interface geometry).

Other types of radars, including synthetic pulse radars, homodyne radars and holographic radars have been utilized primarily on a research basis to measure freshwater and sea-ice thickness. However, they have not been applied to glacier or iceberg sounding work and some have limitations, which prevent them from measurement of the thicknesses necessary to be of practical use.

A7.2 TECHNICAL ASSESSMENT

It is evident that radio echo-sounding techniques can be successfully used to measure glacial ice thicknesses up to 250 and 320 m, depending on the frequency. The work of Swithinbank (1977), Kovacs (1977a and b), Kristensen et al. (1982) and Wadhams and Kristensen (1983) demonstrates this capability relatively convincingly. However, these measurements were made on essentially giant sheets of glacial ice (very large tabular icebergs) and do not represent those icebergs which normally frequent the Arctic waters. These smaller, irregular-shaped icebergs present geometrical problems which, it is believed, may cause confusion due to multiple reflections from the inner surfaces of the icebergs. In the assessment undertaken by REMOTEC (1982) it is shown that multiple reflectors may not be a problem as the only return having a high probability of being captured are those from directly below the antenna. The results to date indicate that iceberg draft measurement is possible. Verification work is clearly required.

The potential for the determination of underwater shape, if proven positive, has enormous benefits. The major limitation is the wide beam-width of the various systems, which will no doubt cause ambiguity problems.

Although this does not seem to be a major problem for draft measurement from results to date, there is a fundamental problem which restricts the ability physically to design for narrow beam-widths. The beam-width is inversely related to frequency for a given antenna size.

At frequencies of around 100 MHz the antenna sizes which allow helicopter deployment prohibit beam-widths less than about 45° in any direction. The Instrumar Model 100 airborne impulse radar system, which has a centre frequency of 120 MHz, has a beam-width of 30° - 40° by about 60°. It remains to be seen whether the beam-width will in actuality preclude the ability to derive underwater shape

Pulsed-CW systems have an inherent problem with pulse length, which reduces the accuracy of the range (draft) measurement. A pulsed-CW system operating at 50 ns, for example, will only be able to resolve the draft to about ± 8 m. An impulse radar system, such as the Instrumar Model 100 unit, has the potential of resolving draft to an accuracy of around 1 m or less due to a pulse width of about 6 ns. This would seem to indicate that impulse radar systems have definite advantages over current pulsed-CW systems. The use of pulse compression techniques on the latter will likely improve their resolving capabilities considerably in the future.

APPENDIX 8

OPTICAL SENSORS

APPENDIX 8

OPTICAL SENSOR

A8.1 INTRODUCTION

A study of the literature regarding the measurement of iceberg draft and underwater shape indicates that optical techniques have not been employed to obtain this information, and the following subsections provide a detailed evaluation of their potential for this use.

Optical sensors include photo-optical sensors, such as conventional cameras, and electro-optical sensors, such as a regular television or a low-light-level television (LLLTV). In addition to these passive sensors, optical sensors also include active sensors such as a lidar (laser radar) and an active TV or LLLTV (e.g., laser-gated LLLTV). Some of these sensors have been used underwater, mostly for photographic or visual inspection work.

The successful use of optical sensors is dependent on the availability of sufficient illumination relative to the sensitivity of the sensor under consideration. For passive sensors, the illumination is provided by such natural sources as the sun, moon, and stars. The illumination in active sensors is provided by such artificial sources such as lasers. In either type of sensor, the underwater application is largely dependent on the attenuation coefficient of water, which determines their range or distance of operation. The light available at the water surface and its subsequent attenuation with water depth is of prime interest in the operation of passive sensors. For active sensors, the main concern is the provision of enough energy to overcome the anticipated energy attenuation in water.

Several other factors determine the practical feasibility of an optical sensor to provide underwater dimensional or shape measurements. These, for example, include field of view, resolution, scanning time and detector response time, scene-image stability (target, sensor, and background motion), image display and image recording, and data processing to deduce dimensional or shape parameters of a target in an efficient and accurate manner. Some of these factors are interrelated, and a considerable number of trade-offs are involved in their selection.

The primary factors involved in determining the practical feasibility of optical sensors are examined and discussed in the following subsections. These subsections attempt to establish anticipated typical ranges of operation for each type of basic active sensor; their likely operational limitations; and requirements for their satisfactory operation. The passive sensors are only discussed briefly from the point of view of natural illumination available as a function of water depth.

A8.2 OPTICAL PROPERTIES OF WATER

The optical properties of water of interest in the present study are:

- the complex index of refraction, η,
- the attenuation coefficient, α .

Both these parameters are dependent on the wavelength (λ) corresponding to the frequency (γ) of the radiation. These determine the following:

- suitable wavelength for operation
- range of operation and source power required
- ray path or beam spreading effects
- field of view.

The index of refraction can be written as:

$$\eta = (\varepsilon_\gamma - \frac{j\sigma}{\omega\varepsilon_o})^{1/2} \qquad \text{(A8.1)}$$

where:

ε_γ = dielectric constant of the medium (water) at the given frequency,
σ = conductivity of the medium (water),
ω = angular frequency ($2\pi\gamma$)
ε_o = the permittivity of free space, and,
j = $\sqrt{-1}$.

Typical values for the refractive index of water for selected wavelengths are given in Table A-7. It is known that the electrical conductivity of water, which determines the imaginary part of the refractive index, is a function of salinity, temperature, and pressure (see, for example, Bradshaw and Schleicher 1980). The electrical conductivity increases with increasing salinity, increasing temperature, and increasing pressure. Accordingly, the conductivity

TABLE A-7

Real (η_v) and imaginary (η_i) parts of the refractive index of water at selected optical wavelengths (λ) in micrometres (μm)

λ(um)	η_v	η_i
0.400	1.339	1.86×10^{-9}
0.425	1.338	1.30×10^{-9}
0.450	1.337	1.02×10^{-9}
0.475	1.336	9.35×10^{-10}
0.500	1.335	1.00×10^{-9}
0.525	1.334	1.32×10^{-9}
0.550	1.330	1.96×10^{-9}
0.575	1.333	3.60×10^{-9}
0.600	1.332	1.09×10^{-9}
0.625	1.332	1.39×10^{-9}

and, thus, the index of refraction of sea-water changes with water depth.

The electrical conductivity of water also determines the absorption coefficient, which provides for the loss of radiation resulting from absorption in passage through a unit distance or depth of water. The spectral absorption coefficient, $a(\lambda)$, is defined by:

$$T(\lambda) = \frac{I_\lambda(0)}{I_x(\chi)} = e^{-a(\lambda)x} \qquad \text{(A8.2)}$$

where:

T = transmittance at wavelength, λ, and distance, x,

$I_\lambda(0)$ = spectral irradiance at zero distance (incident radiation), and,

$I_\lambda(x)$ = spectral irradiance at x (transmitted radiation).

The spectral absorption coefficient for pure water falls to a very low value in the 0.4 to 0.7 micrometre (μm) wavelength range, so radiation can penetrate deeply into the water body and scatter from suspended particulates and from the bottom. The spectral absorption coefficient of sea water is higher (because of its salinity) than that of pure water, and is shown in Figure A-14 for the infrared, invisible, and microwave spectral regions. The absorption is low in the visible portion of the spectrum (0.4 to 0.7 μm) with a minimum at the wavelength of around 0.48 μm.

Natural water bodies contain both solutes and particulates in suspension. Thus, the combined effects of the absorption of the solution and particulates (as well as back-scattering due to particulates) in reducing the radiation is given by the extinction or attenuation coefficient, $K(\lambda)$. However, the attenuation coefficient is not necessarily the simple sum of the absorption coefficient of the solution and the back-scattering coefficient because of multiple scattering and particulate absorption. The spectral attenuation coefficient for natural water bodies is shown in Figure A-15. The attenuation coefficient for freshwater falls below that for distilled water, which may be an artifact of the experimental methods used.

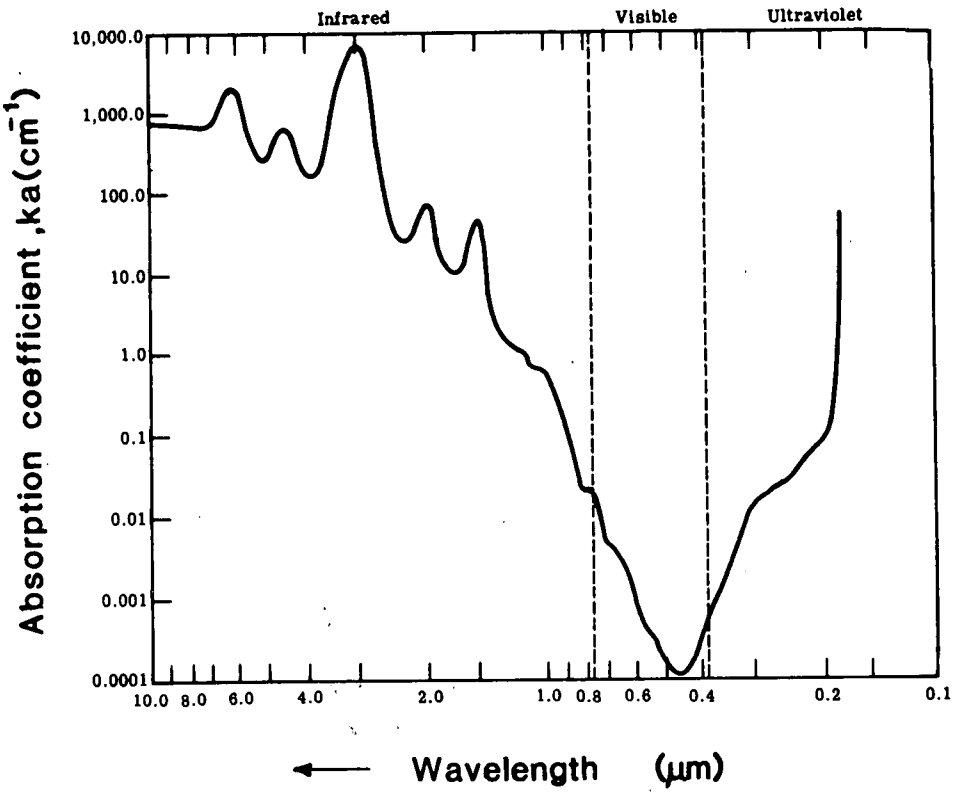

Fig. A-14. Absorption of radiation by sea-water (Ewing 1965).

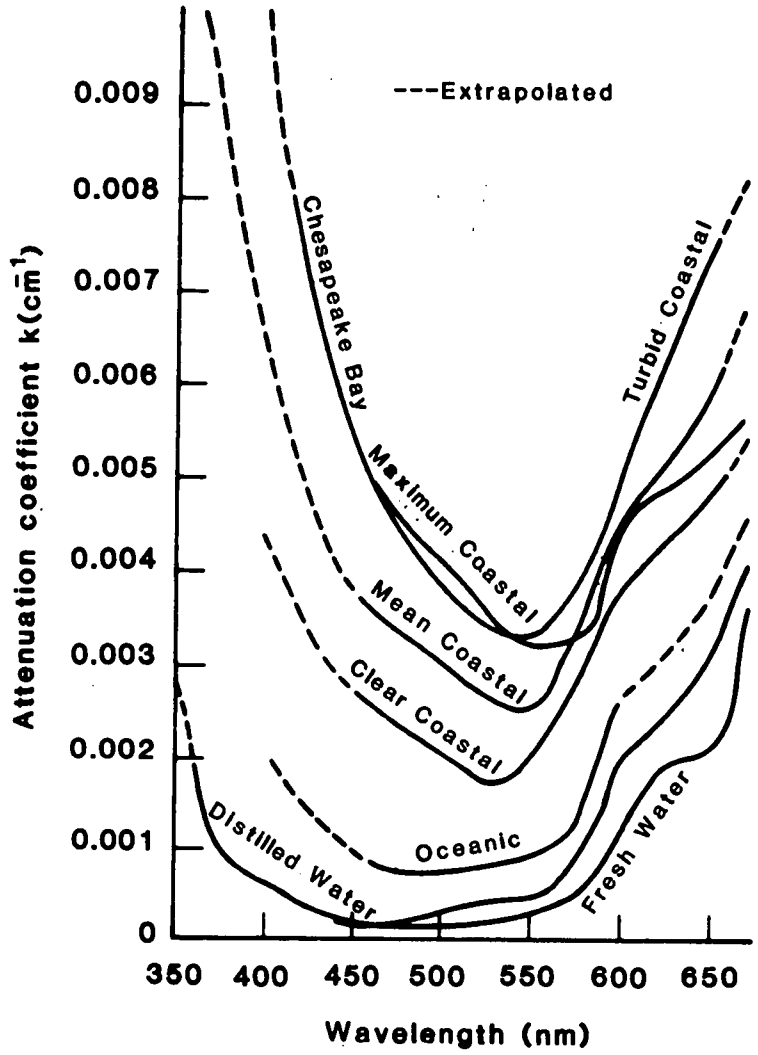

Fig. A-15. Attenuation coefficient, k, versus wavelength for distilled, fresh- and sea-water (Watson et al. 1969).

An examination of Figure A-15 indicates that there is a considerable difference in the spectral attenuation coefficient for different types of sea-water. The highest values are obtained for turbid coastal water, presumably because of the significant concentrations of suspended sediments, whereas clear coastal water has only half of this value. The wavelength of minimum attenuation appears to shift towards the longer wavelength with decreasing clarity of water.

These results can be summarized as follows.

1) The wavelength region of interest for underwater applications ranges from about 0.45 μm to about 0.58 μm, in which the attenuation of radiation is expected to be lowest.

2) The spectral attenuation coefficient, $K(\lambda)$, values of sea-water in the wavelength region of interest are likely to be between 0.001 cm^{-1} and 0.004 cm^{-1}. An average value of 0.0025 cm^{-1}, corresponding to average coastal conditions, is reasonable to use for calculating the operational range of various sensors. The minimum, average, and maximum values of attenuation loss using these coefficients are 0.434, 1.085, and 1.737 dB/m, respectively. Total one-way attenuation losses as a function of optical path length using these values are given in Figure A-16. The two-way path losses can be obtained by multiplying the one-way losses by a factor of 2.

A8.3 PASSIVE SENSORS

Passive sensors, such as a camera, a television, or a low-light-level television (LLLTV), rely on natural illumination to photograph or image an object. It is not possible to obtain dimensions of an object from its photograph or image unless the distance between the sensor and the object is known. Thus, passive sensors alone have limited value in the intended application. These sensors may be used to obtain relative dimensions of an object (its shape) and used in conjunction with other devices to obtain complete dimensional data.

In this section, primarily for the sake of completeness, the natural illumination at the surface of the sea and its subsequent attenuation with water depth are considered. These illumination levels are used to determine the feasibility of using passive sensors for

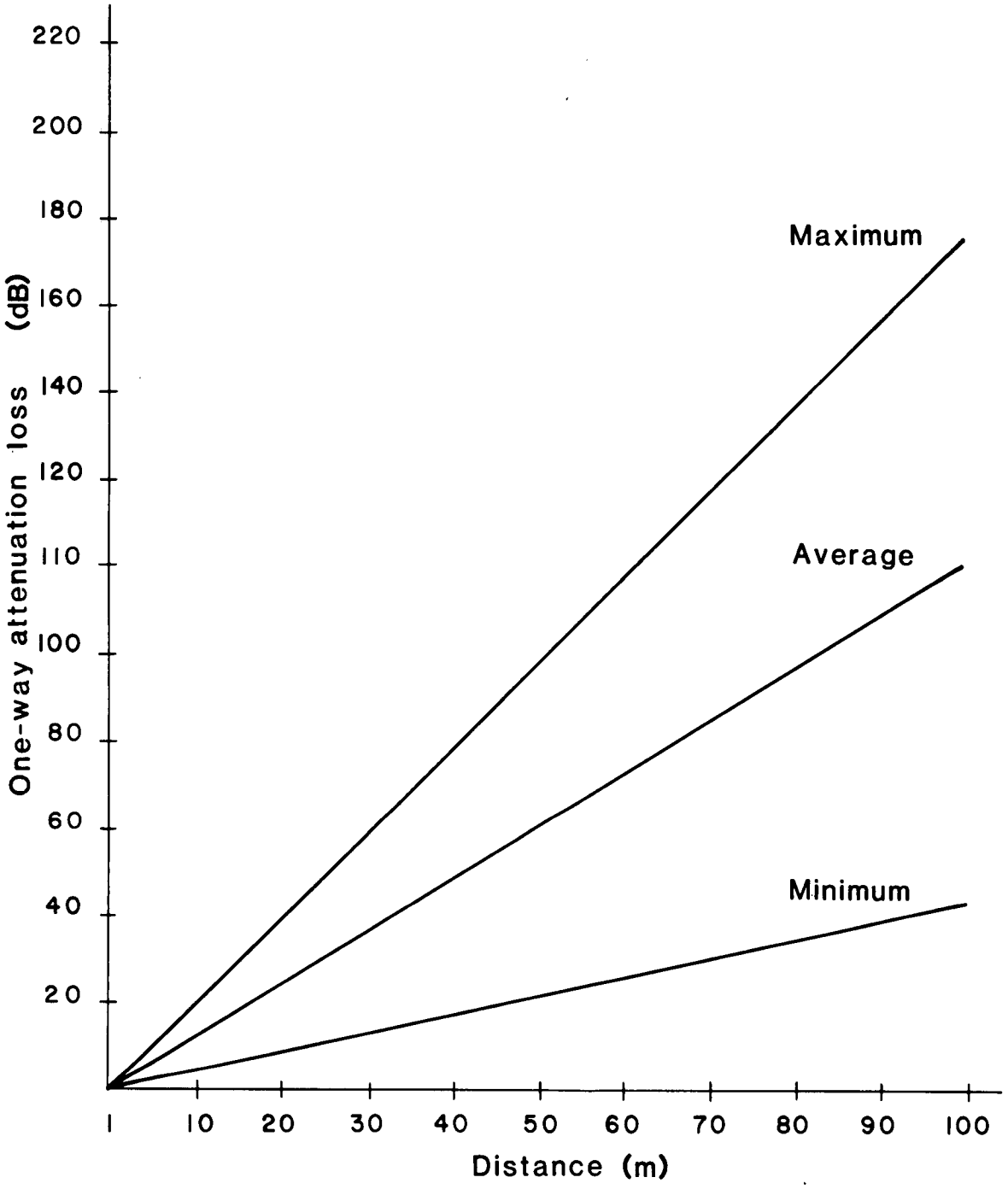

Fig. A-16. Maximum, average and minimum one-way attenuation as a function of path length through sea-water.

TABLE A-8

Typical illuminance levels at the surface of the earth

Condition	Illuminance, lm/m^2
Sunlight and skylight	
noon, clear day	$8\text{-}10 \times 10^{4}$
noon, heavy overcast	$5\text{-}10 \times 10^{3}$
sunset or rise, clear	$1\text{-}5 \times 10^{2}$
civil twilight, low limit (24 minutes past sunset or before sunrise)	$3\text{-}5 \times 10^{0}$
nautical twilight, low limit (48 minutes past sunset or before sunrise)	$1\text{-}2 \times 10^{-2}$
Moonlight and skylight	
full moon, clear sky	$1\text{-}2 \times 10^{-1}$
full moon, moderate cloudiness	$3\text{-}6 \times 10^{-2}$
7 days before or after full moon, clear sky	$1\text{-}2 \times 10^{-2}$
11 days before or after full moon, clear sky	$1\text{-}2 \times 10^{-3}$
Starlight and skylight, no moon	
clear sky	$0\text{-}8 \times 10^{-3}$
heavy overcast	$2\text{-}6 \times 10^{-5}$

imaging the underwater shape of an iceberg. The possibility of obtaining some dimensional information using these sensors alone is also discussed.

Typical natural illuminance levels for different conditions are given in Table A-8. These values are given in lumens/metre^2 where a lumen (lm) is the luminous limit of flux equal to 1/680 watts at a wavelength of 0.555 μm (peak response of the human eye), and is the radiant unit of flux or power. The lumen is a visual efficiency weighted flow of radiant flux (Suits 1975; Slater 1975).

The major source of natural radiation is from the sun directly or from its reflected or scattered radiation. The sun approximates a 6,000°K black body source and gives a peak spectral radiance at 0.5 μm. The sun's radiation remains within a factor of 2 of the peak value from a wavelength of 0.4 um to 0.8 μm. An average value of 1000 watt/m^2-micron or approximately 500 watt/m^2 is sufficient for calculation purposes (Skolnik 1970).

The attenuation loss values given in Table A-9 can be used to determine the illumination levels at various depths. By using the average attenuation loss the average downwelling irradiance due to the sun at various depths were calculated. These values are comparable to those measured in the field (Figure A-17). However, Figure A-17 illustrates that the down-welling spectral irradiance varies greatly with water composition.

The typical minimum exposure value needed for photographic films is about 0.01 lux-s (lux = lumen/m^2). The practical exposure times are usually of the order of 1 to 100 ms (Slater 1975). Thus, film sensitivity can be typically defined as 0.1 to 10 lux. Thus, theoretically, there could be sufficient light up to depths of 40 to 60 m to expose photographic films. However, these are the maximum depths corresponding to clear sunlight at noon. In general, the applicable depths would be considerably less than these due to a reduction in sunlight as a result of clouds or fog. Examining the illuminance values given in Table A-8 for other daylight conditions, an average value of 10^3 lm/m^2 for daylight appears reasonable. Accordingly, the usable depths sufficient for photographic illumination are reduced to 20 to 40 m.

The operational ranges (i.e., the distance between the object and the sensor) are considerably less than those described earlier because of the reduced efficiency of the optical system (e.g., lenses) and less than 100%

TABLE A-9

Down-welling irradiance (illumination) at sea-water depths for the sun on a clear day

Depth (m)	Down-welling irradiance (lm/m^2)	Down-welling Irradiance $Watt/m^2$
0	10^5	500
5	32×10^3	158
10	10^4	50
20	10^3	5
30	10^2	5×10^{-1}
40	10	5×10^{-2}
50	1	5×10^{-3}
60	1×10^{-1}	5×10^{-4}
70	1×10^{-2}	5×10^{-5}
80	1×10^{-3}	5×10^{-6}
90	1×10^{-4}	5×10^{-7}
100	1×10^{-5}	5×10^{-8}

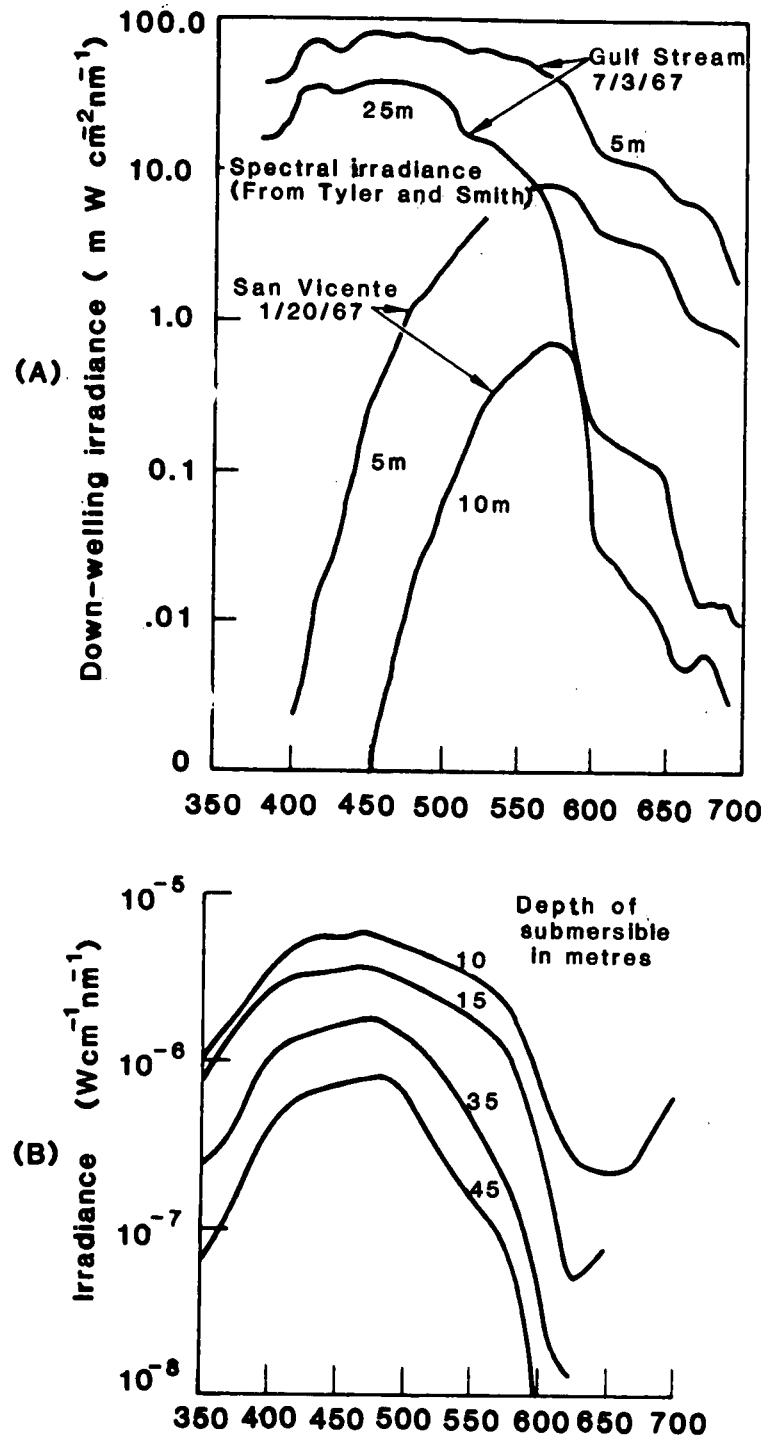

Fig. A-17. Measured down-welling spectral irradiance (A) at two different locations and different depths (B) at different depths by submarine (Spetcht et al. 1973).

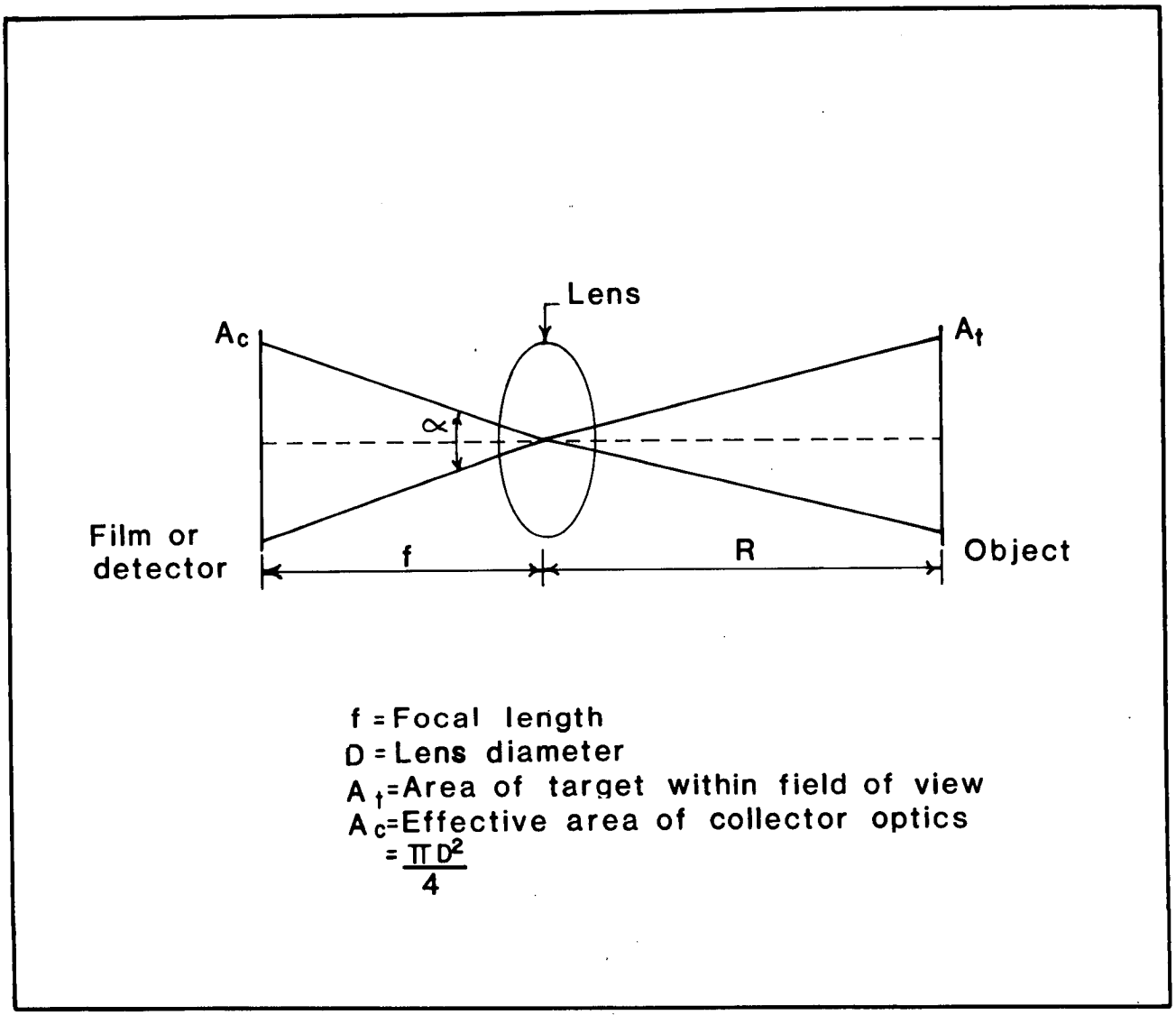

Fig. A-18. Simple viewing geometry with an optical sensor.

reflectivity of the target. The simplified geometry of observation is illustrated in Figure A-18. The spectral radiant power, P_λ, which enters the optical system and ultimately falls on a film or detector (Baker and Scott 1975) is given by:

$$P_\lambda = \frac{T_w(\lambda)\ T_o(\lambda)\ A_t\ A_c\ L_{e\lambda}}{R^2} \quad , \qquad \text{(A8.3)}$$

where:

A_s = area of the target within the field of view,

A_c = effective area of the collector optics,

D = lens diameter, $D^2/4$,

$L_{e\lambda}$ = spectral radiance of the object,

= $\rho(\lambda)\ E_{o\lambda}/\pi$ (for a lambertian object),

$E_{o\lambda}$ = illuminance in lumen/m^2 at the object,

R = distance to the object,

$T_w(\lambda)$ = transmittivity (attenuation loss) of intervening the water divided by $\Delta\lambda$,

$T_o(\lambda)$ = transmisivity of the optics directly by $\Delta\lambda$,

ρ = reflectivity of the object divided by $\Delta\lambda$, and,

$\Delta\lambda$ = wavelength band of interest.

From Figure A-18 it can be seen that the field of view is given by the solid angle, Ω, as follows (for a square law detector or film):

$$\Omega = \alpha^2 = \frac{A_t}{R^2} = \frac{A_c}{f^2} \quad . \qquad \text{(A8.4)}$$

Thus, the power per unit area (lumen/m^2) at the image plane is given by:

$$E_{I\lambda} = \frac{T_w(\lambda)\ T_o(\lambda)\ \rho(\lambda)\ E_{o\lambda}}{4N_1^2} \quad , \qquad \text{(A8.5)}$$

where, N_1 = f/D and is referred to as the relative aperture of the lens or the f-number. In complex lens systems a T-number is often used, which for a circular aperture, is given by:

$$T\text{ - number} = \frac{f\text{ - number}}{\sqrt{T_o(\lambda)}} \quad . \qquad \text{(A8.6)}$$

This equation assumes that there is no direct contribution from the down-welling irradiance. The reflectivity of icebergs, ice, or sea-ice, at the wavelengths of interest is usually around 0.7 whereas the reflectivity of the background ocean can be taken as 0.28. By using the typical f - number of 2.8 with $T_o = 0.64$, or a T-number of 3.5, $E_{I\lambda}$ is given as:

$$E_{I\lambda} = 1.42 \times 10^{-2}\ T_w(\lambda) E_{o\lambda} \quad . \qquad \text{(A8.7)}$$

The average value of the attenuation loss (from Figure A-16) is about 1 dB/m and the average value of the downwelling irradiance (diffuse) can be taken as 10^2 lm/m^2 corresponding to a depth of 10 m for an average daylight flux of 10^3 lm/m^2. Thus, the value of $E_{I\lambda}$, the power per unit area in the image plane, at various distances between object and sensor are, given in Table A-10. A conventional photographic camera can only capture the image of this object (iceberg) when it is within 10 m of the object (film sensitivity of 0.1 lm/m^2). On the other hand, an electro-optical sensor such as a LLLTV, which typically has a sensitivity between 10^{-4} to 10^{-5} lm/m^2, can image this object within a range of 40 m to 50 m. The sensitivity (minimum level discernible) of LLLTV is comparable to that of the human eye (Swift and Thompson 1972).

In summary, passive photo-optical or electro-optical sensors are dependent on natural illumination during the day time which can vary considerably due to clouds and fog. For average daylight levels of illumination photo-optical (camera-film) and electro-optical (LLLTV) systems may be able to observe an iceberg to a depth of 10 m up to distances of 10 m and 40-50 m, respectively. To photograph or image icebergs at greater depths considerably smaller ranges would be necessary. It may be possible to obtain dimensional measurements as opposed to shape information alone by moving the optical sensor across the target (e.g., on a vessel) or by measuring the range to the target with another sensor or by both. However, the following principle drawbacks of passive optical sensors make them impractical and unreliable:

- dependence on natural illumination which in turn can be highly variable and weather dependent, making only short ranges achievable;

TABLE A-10

Radiance received by a photo-optical or an electro-pptical system at a distance from the object for a natural illumination level of 10^2 lm/m^2

Distance, d m	Radiance lumen/m^2
10	1.42×10^{-1}
20	1.42×10^{-2}
30	1.42×10^{-3}
40	1.42×10^{-5}
50	1.42×10^{-5}

- variation of illumination or image radiance with depth;
- need for an independent measurement of range with another sensor.

A8.4 ACTIVE SENSORS

A8.4.1 Lidar

Lidar (light detection and ranging) is an active system as it supplies its own energy for scene or target illumination and measures the energy reflected or scattered back from an object. Thus, lidars are not dependent on ambient light conditions or natural sources of illumination. The energy in lidars is provided traditionally by a laser (an acronym for light amplification by stimulated emissions of radiation), although other artificial sources of radiation (such as a lamp) may be used as well. Lasers provide optical radiation which is monochromatic (at one wavelength or within a very narrow wavelength band) and coherent. These properties provide several advantages and lasers have been used in numerous applications.

Lidars are also known as laser radars. Lidars are more suitable for underwater applications because lasers provide radiation at optical wavelengths (at which there is low attenuation in sea-water relative to microwave wavelengths available with conventional radars). Because of their short wavelength or high frequency, very small beam-widths (angular resolution) and pulse lengths (time or range resolution) are possible with lasers. Moreover, being active sensors lidars provide a direct and accurate measure of range or distance between the target or object and the sensor.

The range to the target in a lidar is usually obtained by measuring the time elapsed between the transmit and receive pulses. Thus, range is given by:

$$R = \frac{c}{2T} \quad , \qquad \text{(A8.8)}$$

where c = speed of light in m/s in the medium-water (equal to 3×10^8 m/s in a vacuum and modified by the refractive index of the medium), and,

T = time elapsed (s).

The factor of 2 accounts for the two-way trip of the pulse; i.e., to the target and back.

Similarly for a pulsed system which transmit pulses of τ seconds duration, the range resolution, ΔR, is given by:

$$\Delta R = \frac{c\tau}{2} \ . \qquad \text{(A8.9)}$$

The range resolution is a measure of the minimum radial distance between two objects or points which can be distinguished, i.e., two points or objects separated by a radial distance equal to the range resolution can be separated by their individual returns. This resolution is small for lidars because of the very short pulses (in the order of several microseconds) which are achievable with lasers. The performance of a lidar can be determined in the same manner as used for a conventional radar such as a radio echo-sounder. The treatment given here is taken from Skolnik (1970) and Wolfe and Zissis (1978).

The geometry of the operation of a lidar is the same as shown in Figure A-18 except that illumination is provided by a beam from the lidar; energy travels to and from a target following the same path; and the returned energy is made to fall on a detector. In practice, separate optics may be used for the receiver and transmitter portions of a lidar. The fraction of the transmitted power returned to the receiver photo detector depends on the divergence of the transmitted beam, the attenuation of the propagation medium (water), the effective cross-section of the target, the attenuation of the optical system, and the receiver collection area. The general equation for received radiant power (watts) at the detector is:

$$P_r = \left(\frac{P_t}{\Omega t}\right) \left(\frac{\pi D^2}{4}\right) \left(\frac{\sigma_T}{R^4}\right) T_o \, T_w \ , \qquad \text{(A8.10)}$$

where; P_t = transmitter power in watts,

R = range to target in metres,

Ω_t = the transmitted beam solid angle ($\frac{\pi \alpha_t^2}{4}$ for the transmitted beam-width, α_t),

D = receiver diameter, such that $\frac{\pi D^2}{4R^2}$ is the solid angle subtended by the receiver,

T_o = transmittance of the optics (both receiver and transmitter),

T_W = transmittance of the intervening medium, i.e., two way attenuation loss in sea-water, and,

σ_T = target scattering cross sectional area, = $\rho A_T/\Omega_T$ (A_T is target area with A_T/R^2 being the solid angle subtended by the target, ρ, is the target reflectivity and Ω_T , the solid angle of the returned beam).

This equation may be used to calculate the maximum power required to detect a target at a particular range or to determine the maximum range of operation for a lidar of given transmitter power and receiver-detector sensitivity. The σ_T value for targets can vary substantially and in the simplest case, a flat, perfectly diffuse (Lambertian) target, reflecting at normal incidence, has a cross section of:

$$\sigma_T = \frac{\rho\ A_T}{\pi} \quad . \tag{A8.11}$$

Lambert's law states that the brightness (watts per mm-steradian) of an infinite diffuse scattering surface is constant as a function of look direct (a valid assumption for icebergs). This assumes that A_T is the target area illuminated and observed by the sampling system. If the target area is smaller than the transmitter beam size and the receiver field of view, it should be used for A_T. If the target area is larger than either the transmitter beam or the receiver field of view, then:

$$A_T = \frac{\pi}{4} R^2\ \alpha^2 \quad , \tag{A8.12}$$

where: $\alpha = \alpha_T$ (angle subtended by the target), if $\alpha_T < \alpha_r$, and,

$\alpha = \alpha_r$ (beam-width of the receiver, given by D/R), if $\alpha_T > \alpha_r$.

Thus, for a diffuse scatterer larger than the lidar beam and at normal incidence:

$$P_r = \frac{P_t\ T_W\ T_O\ \rho\ D^2}{4R^2} \quad . \tag{A8.13}$$

To determine a practical maximum range, the following parameters are assumed as typical:

Average pulse power = 0.5 J,

Pulse length = 10 x 10^{-9}s (providing a range resolution of 1.5 m),

T_0 = 0.25,

T_w = 1 dB/m (as per Section A8.2),

ρ = 0.7, and,

D = 5 cm and 0.65 cm.

Thus, P_t = 0.5 x 10^8 w, (average power divided by pulse length),

and the values of P_r at various ranges for the two sizes of receiver optics are shown in Table A-11. A number of photo-conductive or photodiode detectors are available which are sensitive to the wavelength band of interest. Spectral reference curves of some of the common detectors used in the visible and near-infrared wave lengths are shown in Figure A-19. Laser envelope detectors can, for short-pulse modulation and low background noise, operate as quantum-limited devices. Quantum-limited detection occurs when the minimum receiver signal, P_r, is determined by:

$$P_r = \frac{\rho_n h \gamma}{\eta T} \qquad \text{(A8.14)}$$

where: ρ_n = required minimum number of signal photoelectrons,

h = Plank's constant = 6.626 x 10^{-3} J s,

γ = optical frequency, c/λ,

η = quantum efficiency of the detector, and,

T = observation time.

The signal current, i_s, is related to the received power, P_r, by:

$$i_s = \frac{P_r \eta e}{h\gamma} \quad , \qquad \text{(A8.15)}$$

where, e is the electron charge.

The usual figure of merit for detection is given by D^*, which is expressed in cm $Hz^{1/}$ W^{-1} raised periods

TABLE A-11

Power Received at various target ranges
for two different receiver optics sizes (D)

Target range (m)	Power received (W) for D = 5 cm	Power received (W) for D = 0.65 cm
5	37×10^{-3}	22.2×10^{-1}
10	9.25×10^{-4}	5.55×10^{-2}
20	2.3×10^{-5}	1.38×10^{-3}
30	0.6×10^{-6}	0.36×10^{-4}
40	$.15 \times 10^{-7}$	0.9×10^{-6}
50	$.0375 \times 10^{-8}$	2.25×10^{-8}
60	0.94×10^{-11}	5.64×10^{-10}
70	0.235×10^{-12}	1.41×10^{-11}
80	0.06×10^{-13}	0.36×10^{-12}
90	1.5×10^{-15}	0.9×10^{-13}
100	0.375×10^{-16}	2.25×10^{-15}

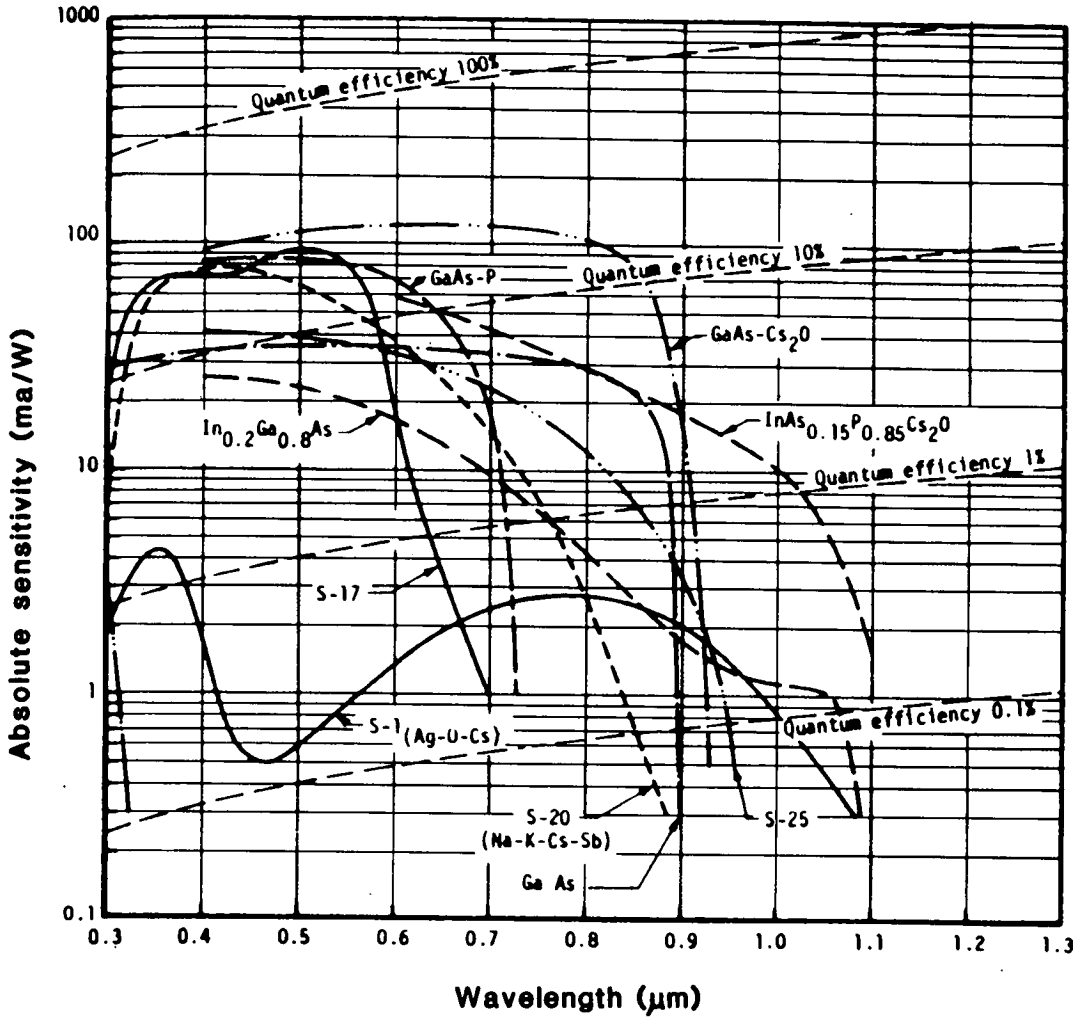

Fig. A-19. Spectral response of some of the more common detectors used in the visible and near infrared wavelengths (Baker and Scott 1975).

$cm \cdot Hz^{1/2} \cdot W^{-1}$, that is, normalized to the detector area and the bandwidth. The typical sensitivity of a detector-preamplifier combination is 2×10^{-12} W $Hz^{-1/2}$. If a 50-MHz band-width is assumed then:

$$P_r > (2 \times 10^{12} \text{ W/Hz}) (5 \times 10^7 \text{ Hz}) = 1.4 \times 10^{-8} \text{ W.} \quad \text{(A8.16)}$$

Thus, P_r should be greater than or equal to 1.4×10^{-8}W for target detection. These minimum detection levels correspond to ranges of 40-50 m depending on the size of the receiver optics as per Table A-11. These two optic sizes provide beam-widths of α_t or α_r, equal to approximately 0.1 and 1 mrad, respectively, which at a range of 45 m correspond to target areas of 0.45 cm and 4.5 cm. If the required solid angle coverage is Ω_T, the time necessary to cover or scan the sector with a pulse repetition frequency of f_r is:

$$t = \frac{\Omega_T}{\alpha_t^2 \, f_r} \quad , \quad \text{(A8.17)}$$

if one pulse per angular resolution cell is assumed. Assuming the coverage needed is over a solid angle of steradians (corresponding to a target size of 45 m x 45 m) and the f_r is equal to 5,000 pulses per second, then the time required for scanning is 200 and 2,000 seconds for the large and small beam-widths, respectively. The 2,000 seconds is a significantly long time, requiring scene and sensor stability for useful data acquisition. The equivalent number of samples for the two beam-widths are $10^6$and 10^7.

A number of lasers are available which provide radiation at the required wavelenghts corresponding to low attenuation. Two of particular interest are Nd: glass and X2Nd:YAG. Both are optically pumped solid state crystal pulse lasers providing radiation at 0.53 μm. Typical energy outputs are 2 J with a pulse width of 30 ns and pulse repetition frequencies usually less than 30 per second. The Nd:YAG laser has pulse widths of 5 to 100 ms and pulse repetition frequencies of 1 to 10,000 per second. The energy per pulse is usually around 0.1 to 1000 mJ. The most popular detectors for operation at 0.53 μm are the S-20 (see Figure A-19) with a quantum efficiency of around 10%. Rise times or response times approach 0.1 ns.

In summary, lidars operating at a wavelength of 0.53 μm appear capable of imaging the underwater portion of an iceberg. However, the operating ranges are limited to

about 40-50 m. These sensors offer very small beam-widths and, thus, may take a long time to scan a target. Accordingly, the following requirements exist to make lidars usable in the intended application:

- large beamwidths, perhaps up to 50 mrad;

- high pulse repetition frequencies (greater than 5,000 per second) and fast beam-scanning to reduce target scan time;

- sensor stabilization; and,

- continuous knowledge of sensor attitude and the ability to change this attitude.

A8.4.2 ACTIVE - LLLTV

This section is concerned with a sensor that uses a laser or some other artificial source of light to illuminate a target. However, unlike a radar, the low-light-level television (LLLTV) is considered as a detector and a receiver. The main advantages offered by such a system are the relatively wide fields-of-view, but small resolutions, and the ease of video image generation, display, and recording. Such an active imaging system has been considered before (e.g., Julian and Bricks 1976). The back-scatter from the intervening medium (sea-water), just like in any other active system, is not a problem as a result of the pulsing of the laser and the gating of the LLLTV, so that it detects a return signal only from a limited range around the target of interest.

A LLLTV system uses an imaging tube with or without image intensifiers. The image cameras or TV tubes perform scanning operations by means of a framed electron beam, thereby providing very high scan rates, high resolutions, and wide fields of view without moving components. Image intensifiers are not electro-optical camera tubes, and do not yield electrical output signals; they are essentially light amplifiers. The LLLTV systems in common use today are the silicon vidicon and its derivatives -- the SIT (silicon intensified target) tube, and, the ISIT (intensified silicon intensified target) tube, and, the fibre optically coupled single diode, double diode, or microchannel image intensifier systems (Baker and Scott 1975), which are based on the plumbicon or vidicon tube.

The camera tube is the most important part of a LLLTV system. A schematic representation of a SIT tube is shown

in Figure A-20. The responses of typical camera tubes as a function of face plate (photo cathode) illumination are compared in Figure A-21. The addition of an image intensifier provides a light gain in excess of 60 (some intensifiers have scans of 200 and 1,000). Thus, an ISIT tube may be operated down to around 10^{-7} lux, the photo-electron or quantum noise limit, at which level large integration times are required to build up a reasonable picture. The good response of the S20 or the S25 (see Figure A-19) photo cathode to the blue green part of the spectrum (0.48 to 0.55 μm wavelength) makes it ideal for underwater applications.

The LLLTV camera tubes can be remotely scanned horizontally (pan) and vertically (tilt) and their focal lengths can be changed along with any other adjustments. The selection of a camera and lens system is determined by the requirements for sensitivity, range, and resolution. The range of operation is determined primarily by the lens, and a basic lens system is illustrated in Figure A-22. The relationship between the angular field of view (α, in degrees) of the LLLTV camera, the focal length (f) of the optics, and the dimensions (X_c) of the photocathode is:

$$f = \frac{X_c}{2 \tan \alpha/2} \quad . \qquad \text{(A8.18)}$$

Many camera tubes specify the photocathode in terms of the diameter of the camera tube, typically around 40 mm. With a tube of diameter, D, using a standard 4:3 aspect ratio (horizontal to vertical lines) for scanning, the effective width of the photo cathode is equal to 0.8 D and the height is equal to 0.6 D. The number of scan lines comprising an image on the photocathode is given by:

$$n = \frac{X_T \; f \; N}{X_c \; R} \quad , \qquad \text{(A8.19)}$$

where: X_T = height (or depth)of the target (m),

f = focal length of the lens as calculated in the preceding equation (mm),

N = total number of scan lines oriented perpendicular to the height (or depth) dimension of the target (usually about 500 in number),

X_c = height of the photocathode (mm) containing the N scan lines, and,

R = distance to the target (m).

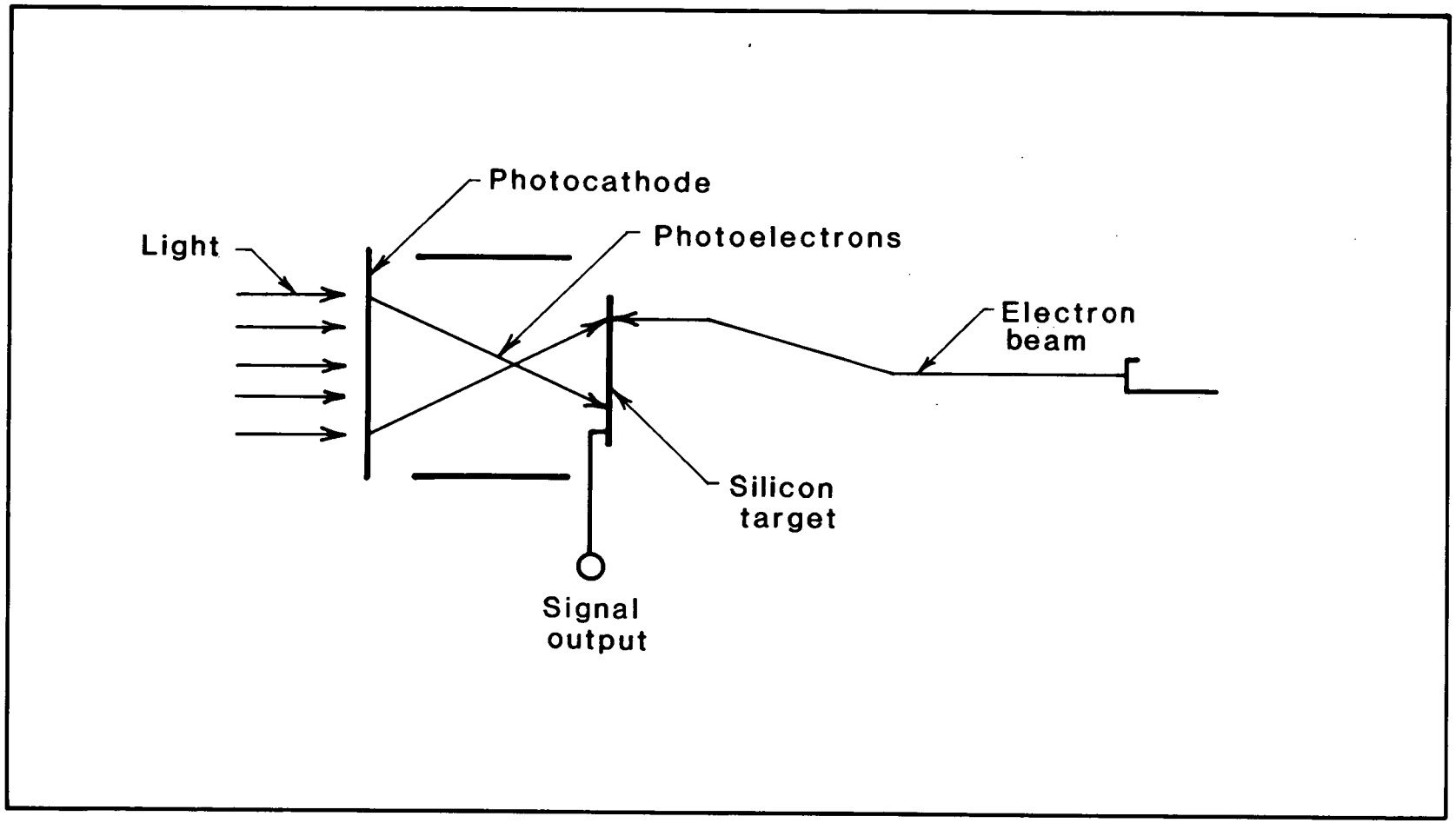

Fig. A-20. Schematic representation of SIT tube.

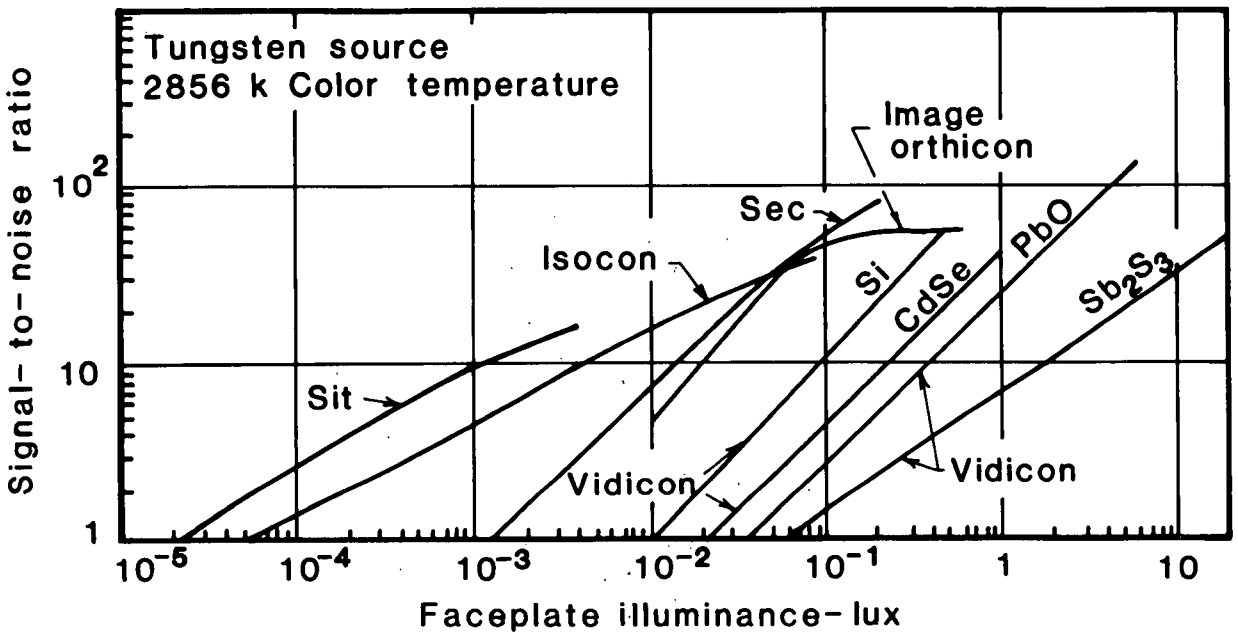

Fig. A-21. Signal-to-noise ratio characteristics of typical camera tubes.

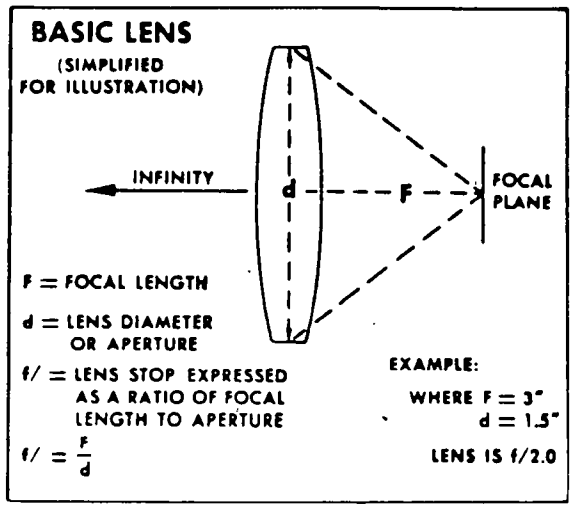

Fig. A-22. Illustration of a basic lens.

Standard low-cost zoom lenses are available in focal lengths from 15 to 350 mm, the most common having ranges of 15 to 150 mm and 16 to 160 mm. Thus, fields of view (α) of 9° to 90° are typically achievable with a photocathode diameter of 40 mm. The fields-of-view (expressed as width x height) for various focal lengths at varying distances from the camera are given in Figure A-23. Thus, a 25 mm focal length lens has a field of view of 25 m x 18.75 m at 50 m.

A typical resolution achievable with a camera tube such as SIT is around 15 line pairs (lp) per mm whereas the total scan lines typically vary from 250 to 500. Thus, the spatial resolution achievable is significantly better than a metre. For the example considered above (25-mm focal length, field of view of 25 m x 18.75 m) it is 20 cm or better.

The response time of typical photocathode imaging tubes is better than 1 ns. Thus, the use of 20-30 ns pulse lengths for a laser, as considered in Section A8.4.1 with a lidar, is equally applicable here. If the LLLTV on-time is made equal to the pulse length (τ), then the radius of the foot-print covered during one pulse length at range, R, is given approximately by $\sqrt{c\tau R}$, with an associated viewing angle of $\sqrt{c\tau/R}$. At a range of 50 m and for a pulse length of 30 ns, the diameter and angle of the illuminated field-of-view are approximately 42 m and 49° respectively; values comparable with the LLLTV field of view. For larger periods of time, an annulus is illuminated. Thus, the output beam of the laser needs to be expanded from a characteristic divergence of about 5 mrad to more than 50° by appropriate optics. Moreover, uniform intensity needs to be maintained over such a large field of view.

LLLTV systems typically have large dynamic ranges (better than 60 dB). The full image at the photocathode can be readout and displayed at the conventional rate of 30 frames per second. At least one pulse per frame needs to be transmitted. It may be possible to provide some integration by providing more than one pulse per frame, and each pulse gated to the same range. This appears possible as the return time for a 100 m range is less than 1 μs, whereas the time for reading just one TV line is typically 63.5 μs. Thus, there is no significant loss of information (1.5 % of one line). It will also be possible to provide image integration by gating successive frames to the same range.

The sampling in range has to be provided by gating each frame to a different return time. It also seems

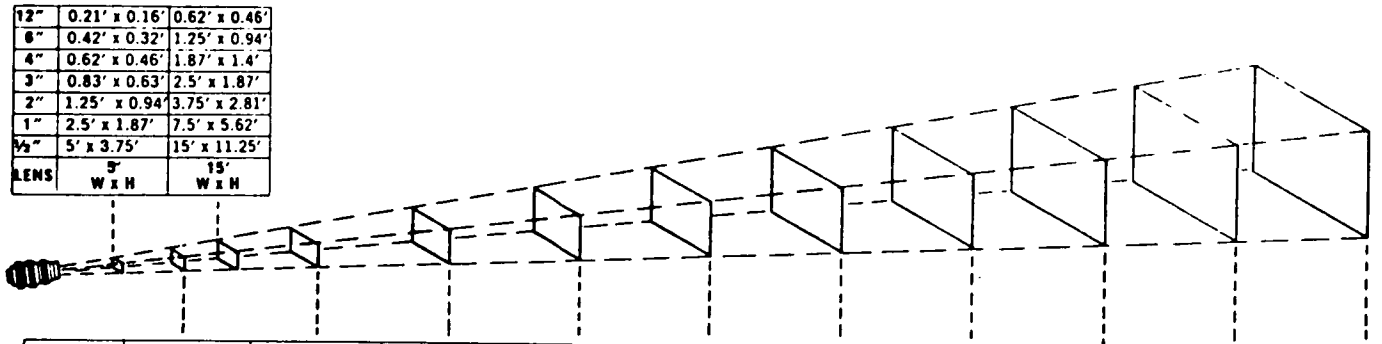

LENS	5' W x H	15' W x H
12"	0.21' x 0.16'	0.62' x 0.46'
6"	0.42' x 0.32'	1.25' x 0.94'
4"	0.62' x 0.46'	1.87' x 1.4'
3"	0.83' x 0.63'	2.5' x 1.87'
2"	1.25' x 0.94'	3.75' x 2.81'
1"	2.5' x 1.87'	7.5' x 5.62'
½"	5' x 3.75'	15' x 11.25'

LENS	10' W x H*	20' W x H	30' W x H	40' W x H	50' W x H	60' W x H	70' W x H	80' W x H	90' W x H	100' W x H
½"	10' x 7.5'	20' x 15'	30' x 22.5'	40' x 30'	50' x 37.5'	60' x 45'	70' x 52.5'	80' x 60'	90' x 67.5'	100' x 75'
1"	5' x 3.75'	10' x 7.5'	15' x 11.25'	20' x 15'	25' x 18.75'	30' x 22.5'	35' x 26.25'	40' x 30'	45' x 33.75'	50' x 37.5'
2"	2.5' x 1.87'	5' x 3.75'	7.5' x 5.62'	10' x 7.5'	12.5' x 9.37'	15' x 11.25'	17.5' x 13.12'	20' x 15'	22.5' x 16.87'	25' x 18.7'
3"	1.67' x 1.25'	3.33' x 2.5'	5' x 3.75'	6.67' x 5'	8.33' x 6.25'	10' x 7.5'	11.67' x 8.75'	13.33' x 10'	15' x 11.25'	16.7' x 12.5'
4"	1.25' x 0.94'	2.5' x 1.88'	3.75' x 2.81'	5' x 3.75'	6.25' x 4.69'	7.5' x 5.63'	8.75' x 6.56'	10' x 7.5'	11.25' x 8.44'	12.5' x 9.4'
6"	0.83' x 0.63'	1.67' x 1.25'	2.5' x 1.88'	3.33' x 2.5'	4.17' x 3.13'	5' x 3.75'	5.83' x 4.38'	6.67' x 5'	7.5' x 5.63'	8.3' x 6.3'
12"	0.42' x 0.32'	0.83' x 0.62'	1.25' x 0.94'	1.66 x 1.21'	2.08' x 1.56'	2.5' x 1.87'	2.92' x 2.29'	3.33' x 2.5'	3.75' x 2.81'	4.2' x 3.2'

NOTES: *WIDTH OF FIELD (W) $= \frac{\text{LENS TO SUBJECT DISTANCE (D)}}{\text{2 X LENS FOCAL LENGTH (inches)}}$

HEIGHT OF FIELD (H) = 0.75 X W

*WIDTH, HEIGHT AND DISTANCE MUST BE MEASURED IN THE SAME UNITS i.e. INCHES, FEET, METERS, etc. (FOCAL LENGTH IS MEASURED IN INCHES)

Fig. A-23. Typical field of view at various distances and lens focal lengths.

possible to increase the on-time of the LLLTV for each transmit pulse to more than one pulse length (several times the pulse duration up to the inter-pulse period). In such a case, an appropriate range resolution equivalent to half a pulse length can still be maintained by subtracting successive frames obtained by gating to the returned energy to an incremental delay equal to the pulse length. Typical depths of field (distance to an object within which its image remains in focus) for various focal lengths and lens stop or aperture settings are shown in Table A-12. Accordingly, a suitable three-dimensional image can be generated by appropriate data processing.

The operating ranges of an active LLLTV can be obtained by following the same procedure as followed by the lidar systems in the preceding section. However, this does not seem to be necessay, as the sensitivity of the LLLTV and the detector used in the lidar example are about the same (both are quantum noise limited). Thus, for the same pulse power it should be possible to obtain similar ranges, i.e., up to about 50 m on the average.

In summary, it appears possible to use an active-LLLTV (a laser-based LLLTV) and obtain operational ranges averaging around 50 m or better with fields of view in excess of 50 degrees. The typical achievable resolutions are of the order of 0.5 m in the azimuth direction and better than 4.5 m in range. The requirements for using such a system are the following:

- An appropriate projection or optics system to expand the divergence of the laser output beam to fields of view greater than 50° to as much as 90°; and,

- maintenance of uniformity of illumination and high average power within such a large field of view.

In any optical sensor system it will be necessary to account for the variations in the refractive index, especially as a function of depth (which accounts for light ray refraction or bending in accordance with Snell's law), to generate proper target geometry. The observation time of the active systems (typically varying from several nanoseconds up to perhaps a millisecond) largely ensures scene stability. Targets larger than the system field of view can be imaged by electronic or mechanical scanning and by merging overlapping scenes. The larger field-of-view achievable with an LLLTV system is of great benefit in finding a target and tracking it.

TABLE A-12

Typical depth of field at various object distances and lens focal lengths

Object distance (ft)	Focal length (ft)		
	1/2" Lens		
	f/1.5	f/5.6	f/16
5	4 to 7	2 to 60	1.2 to inf.
10	6 to 35	2.7 to inf.	1.5 to inf.
20	8.5 to inf.	3 to inf.	1.7 to inf.
40	11 to inf.	3.5 to inf.	1.8 to inf.
	1" Lens		
	f/1.5	f/5.6	f/16
5	4.6 to 5.5	3.8 to 7.4	2.6 to inf.
10	8.5 to 12.2	6 to 29.5	3.4 to inf.
25	17.3 to 45.3	9.4 to inf.	4.3 to inf.
50	26.3 to 490	11.5 to inf.	4.7 to inf.
	2" Lens		
	f/2.5	f/5.6	f/16
5	4.8 to 5.2	4.4 to 5.4	4.1 to 6.5
10	9.3 to 10.8	8.6 to 12	6.8 to 18.9
25	2.1 to 30.8	17.6 to 42.9	11.4 to inf.
50	36.3 t0 80.1	27.2 to 307	14.7 to inf.
	3" Lens		
	f/4	f/8	f/16
10	9.5 to 10.6	9.1 to 11.2	8.3 to 12.6
20	18.1 to 22.3	16.5 to 25.3	14.1 to 34.5
50	39.6 to 67.9	33 to 105	24.3 to inf.
inf.	188 to inf.	93.8 to inf.	46.9 to inf.
	4" Lens		
	f/4.5	f/8	f/16
20	18.7 to 21.4	17.9 to 22.7	16.1 to 26.3
30	27.2 to 33.4	25.4 to 36.6	22.1 to 46.9
50	42.8 to 60'	38.5 to 71.2	31.3 to 124
inf.	296 to inf.	166.7 to inf.	83.3 to inf.
	6" Lens		
	f/4.5	f/8	f/16
20	19.4 to 20.6	19 to 21.1	18.1 to 22.4
50	46.5 to 54	44.1 to f7.7	39.5 to 68.2
100	87 to 118	78.9 to 136	65.2 to 214
inf.	677 to inf.	375 to inf.	187.5 to inf.

APPENDIX 9

SPECIFICATIONS AND PARAMETERS

APPENDIX 9

SPECIFICATIONS AND PARAMETERS

TABLE A-13

Specification for Mesotech Model 971 Colour Sonar
(as provided by OSPS)

Operating Frequency	100 kHz	330 kHz	675 kHz
Transducer Beam Pattern			
Conical	2.2°	2.1°	1.7°
Fan (Horiz./Vert.)	2.2°/40°	2.1°/30°	1.7°/30°
Sounding Cone @ 100 m	3.8 m	3.7 m	3.0 m
Nominal Range Coverage	300-500 m	120-200 m	60-100 m
Pulse Length (usec)	250	200	100
Scanning/Sounding Rate	200/400/800 soundings per 180		
Scales	5 - 500 m	5 - 200 m	5 100m
Weight in Water	10 lbs.	3 lbs.	2 lbs.
Range Accuracy		0.10 m	
Timing/Range Resolution		0.02 m	
Acoustic Power Output		103 dB	
Data Format	OSPS provides a wide choice of data recording, processing capabilities and visual presentations		
Recording Capability	Digital (profiling) RGB Video (imaging)		
Readout/Display	Colour CRT Display modes: sector, polar, perspective, sidescan, linear and test mode		
Max Working Depth	1000 m Standard 3000 m Available		
Deployment	Stationary/towed/pipe/cable /sea chests/over-the-side/ R.O.V. etc.		

TABLE A-14

Technical Parameters for TIMS-1

Target Geometry	
Maximum radial range (delay time)	400 m (533 ms)
Minimum radial range (delay time)	150 m (200 ms)
System	
Beam-widths	1.5°
Number of beams	22 (± 16.5)
Scan rate	1 beam (1.5°)/9 ms
Profiling rate	2 profiles/s
Electrical	
Operating frequency	100 kHz
Length of probing pulse (resolution)	2 ms (1.5 m)
Wavelength	1.5 cm
Mechanical	
Transducer length (with shading)	68 cm
Maximum controllable tilt	16.5°
Thickness of the projector dome	16 cm
Scanning velocity (16.5 sector	167°/s

TABLE A-15

Specification for Inertial Reference System
(as provided by the manufacturer)

VERTICAL REFERENCE (pitch and roll)
Pitch ---------- 85 Degrees
Roll ---------- 360 Degrees
Accuracy ---------- 0.1 Degree reference to True Vertical

AZIMUTH REFERENCE (yaw)
Yaw ---------- 360 Degrees
Accuracy ---------- 0.1 Degree
Yaw Drift ---------- Less than 0.1 Degree/Min.
Yaw caging system locks gyro pick off in zero position.
Spin axis of yaw gyro erects to horizontal for continuous operation, non-tumbling.

PITCH, ROLL AND TAW RATE OUTPUTS
Rate Range ---------- 40 Degrees/Second (Min. Detectable Rate 0.01 /Sec.)
Output ---------- 5.0 VDC
Accuracy ---------- 0.5% at Null, 1.0% at Full Rate
Damping ---------- 0.7 Nominal
Natural Frequency ---------- More than 23 Hz

VERTICAL FORE-AFT AND LATERAL
ACCELERATION OUTPUTS
Acceleration Range ---------- 5G
Output ---------- 5.0 VDC
Accuracy ------ Null 0.1% of Full Range to 0.2% at Full Scale
Natural Frequency ---------- More than 130 Hz
Damping (Electrical) ---------- 0.4 to 0.7

ENVIRONMENTAL CONDITIONS
Note: Rate and acceleration outputs for nominal 100K load
Temperature ---------- 30 F to 165 F
Vibration ---------- 2G from 20 to 33 Hz; 0.036 D.A. from 33 to 52 Hz; 5G from 52 to 500Hz.
(ref. MIL-STD-810B Curve 514-IM)
Shock ---------- 50G, 11 1 Millisecond
Case Seal ------- Pressure Tight, Altitude Zero to 30,000 Ft.
Weight ---------- 35 Lbs.

TABLE A-16

Summary of Technical Parameters for TIMS-2

Geometry	
Maximum radial depth of the profiled iceberg	100 m
Maximum angular iceberg size as seen by sensor	60°
Scanning System	
Beam	4° x 1.5°
Number of beams	15 (60°)
Scan rate	15 beams per one probing pulse
Electrical	
Operating frequency	100 kHz
Length of probing pulse (resolution)	2 ms (1.5 m)
Signal Acquisition	
Number of multiplexed channels	41
Total band	40 kHz
Sampling Rate	120 kHz
Mehanical	
Projector length	60 cm
Hydrophone Array length	31 cm

REFERENCES

Alberts, W.M. 1965. Underwater acoustics handbook II. Pennsylvania State University Press.

Allen, J.H. 1971. Cruise report - CSS Dawson, June 2-12, 1971. Memorial University of Newfoundland.

Allen, J.H. 1972. Iceberg study - Saglek, Labrador, Cruise report - CSS Dawson, Aug. 7-26, 1972. Memorial University of Newfoundland.

Allen, J.H. 1973. Cruise report - CSS Dawson, June 1-11, 1973. Memorial University of Newfoundland.

AMETEK/Straza. 1981. Transducer catalog. Bulletin Number A/SE-7101.

Angelbeck, A.W. 1966. Application of a laser scanning and imaging system to underwater viewing. Proceedings of Photo-Optics Seminar, Santa Barbara, California. Society of Photo-Optical Instrumentation Engineers (SPIE), P.O. Box 10, Bellingham, Washington, October.

Baker, L.R. and R.M. Scott II. 1975. Electo-optical remote sensors with related optical sensors. Chapter 7 In: Manual of Remote Sensing, R.G. Reeves (editor-in-chief), American Society of Photogrammetry, Falls Church, VA. pp 325-366.

Bazeley, D.P. (ed.). 1982. Impulse radar applications. C-CORE News, Vol 7: No. 2, June.

Benedict, C.P. 1971. A description of Project ICE (iceberg Cross-Section Echo), Proceeding of the Canadian Seminar on Icebergs, Canadian Department of National Defence, pp. 115-123.

Benedict, C.P. 1972, Project ICE (Iceberg Cross-Section Echo). Memorial University of Newfoundland.

Berktay, H.O. 1967. Some proposals for underwater transmitting applications of non-linear acoustics. Journal of Sound and Vibration, 6: 244-254.

Bjorno, L.V. 1977. Excitation of selected modes in shallow water propogation. Proceedings of Ultrasonics International 1977, JPC Science and Technology Press Ltd., Guildford, England.

Bjorno, L.V., J. Folsberg, and L. Pedersen. 1979. Experimental studies of parametric arrays in a shallow water test basin. Journal de Physique, October.

Bohman, C., J. Harshman, R. Kurth, G. Ott, H. Sloate, and R. Steel. 1975. High rate, parametric sonar underwater telemetry experiments. Sperry Research Center Report No. SCRCSCR-75-6, Sudbery, MA.

Bradshaw, A.L. and K.E. Schliecher. 1980. Electrical conductivity of sea water. IEEE Journal of Oceanic Engineering. OE-5: 50-62.

Breslau, L.R., J.E. James, and M.D. Trammel. 1970. The underwater shape of a grounded ice island off Prudhoe Bay. Proceedings of the 1970 Offshore Technology Conference, American Institute of Mining, Metallurgy and Petroleum Engineering, pp. 753-766.

Brooks, L.B. and F.F. Sabins. 1979: Discussion of "Airborne radar sounding of Arctic Icebergs" by J.R. Rossiter, B.B. Narod and G.K.C. Clarke. Proceedings of the 5th International Conference on Port and Ocean Engineering Under Arctic Conditions (POAC 79), Trondheim, appended to paper reviewed, Vol. 3, pp 357-358.

Brooks, L.D. 1979: Another hypothesis about iceberg draft proceedings of the 5th International Conference on Port and Ocean Engineering Under Arctic Conditions,(POAC 79), University of Trondheim - Norwegian Institute of Technology, Vol. 1, pp. 241-252.

Burdic, W.S. 1984. Underwater acoustic system analysis. Prentice-Hall, Inc.

Carlin, B. 1960. Ultrasonics. McGraw-Hill, New York.

Christian D., D. Diamond, J. Lever, et al. 1984. Observations from an iceberg in Freshwater Bay, St. John's. C-CORE. Publication No. 84-6, 13 p.

Clarke G.K.C. 1984. Letter to Byron Dawe, dated February 23, 1984. Department of Geophysics and Astronomy, University of British Columbia.

Clay, C.S. and H. Medwin. 1977. Acoustic oceanography: principles and applications. John Wiley and Sons.

Culbertson, C.R. 1979. The parametric receiving array in an inhomogeneous medium. Proceedings of Conference, Underwater Applications of Non-Linear Acoustics.

Danish Hydraulic Institute. 1979. Vol. 4, Icebergs. In: Environmental conditons offshore west Greenland. Horsholm, Danish Hydraulic Institute, 130 p.

Deily, F.H. 1979. Aerial reconnaissance and subsea profiling of sea ice in the bering sea. Proceedings of the 5th International conference on Port and Ocean Engineering under Arctic Conditions, University of Trondheim - Norwegian Institute of Technology, pp. 207-219.

Denbigh, P.N. 1975. A stereospcopic system for three-dimensional imagins. Ultrasonic International 1975 Conference Proceedings 24-26 March, London. pp. 80-83.

Duntley, S.Q. 1963. Light in the sea. Journal Optical Society of America, Vol. 53, No. 2, February.

El-Tahan, M. and H.W. El-Tahan. 1982. Estimation of iceberg draft. Oceans '82 Conference Record, Washington D.C. pp. 689-695.

Ewing, G.C. (edition). 1965. Oceanography from space. Woods Hole Oceanographic Institution, Woods Hole, MA. WHO Ref. No. 65-10.

Flemming, B.W., M. Klien and P.N. Denbigh. 1982. Recent developments in side scan sonar techniques. ABC Press (Pty) Ltd.

Francois, R.E. 1973. The unmanned arctic research submersible system. Marine Technology Society Journal, January - February, pp: 46-48.

Good, R.R., K.G. Anderson and H. H. Lanziner. 1984. Ice/berm interaction study using rotary sidescan sonar and acoustic profiling systems. 16th Annual Offshore Technology Conference, Houston, Texas, May 7-9. pp. 95-111.

Goodman, R.H., E. Outcalt and B.B. Narod. 1977. Radar techniques in the measurement of floating ice thickness. Proceedings of the fourth Canadian Symposium on Remote Sensing, Quebec City, May 1977, pp. 459-468.

Hale, G.M. and M.R. Querry. 1973. Optical constants of in the 200 mm to 200 um wavelength region. Applied Optics 12: 555-563.

Horton, C.W. 1974. The penetration of highly directional acoustic beams in a sedimentary bottom. Applied Research Laboratory, University of Texas, Austin Report ARL-TR-74-28, 16 July.

Hotzel, I.S. and J.D. Miller. 1983. Icebergs: their physical dimensions and the presentation and application of measured data. Annals of Glaciology 4: 116-123.

ICE Engineering Ltd. 1983. Iceberg survey, Strait of Belle Isle, Newfoundland. Report submitted to Bedford Institute of Oceanography by ICE Engineering Ltd.

Juliano, J.F. and B.G. Bricks. 1976. Active gated TV system using a lead vapor laser illuminator and low-light level TV. Digest of Technical Papers, Conference on Laser and Electro-Optical Systems, Society of Photo-Optical Instrumentation Engineers, P.O. Box 10, Bellingham, Washington.

Kan, T.S., C.S. Clay and J.M. Berkson. 1974. Sonar mapping of the underside of pack ice. Journal of Geophysical Research, January pp. 483-488.

Keil, T. and A. Immarco. 1968. Recent underwater range-gated measurements. Proceedings of SPIE Underwater Photo-Optical Instrumentation Applications Seminar, San Diego, California, February.

Kinsler, L.E. and A.R. Frey. 1962. Fundamentals of acoustic. John Wiley and Sons, Inc., New York.

Konrad, W.L. 1979. Applications of the parametric acoustic source. Proceedings of the Underwater Applications of Non-linear Acoustic conference, p. 1.1, University of Bath, U.K. 10-11 September.

Kovacs, A. 1977 a. Iceberg thickness profiling. Proceedings of the Fourth International Conference on Port and Ocean Engineering Under Arctic Condiitions, St. John's, 26-30 September, 1977. pp: 556-567.

Kovacs, A., 1977b. Iceberg thickness profiling and crack detection. Proceedings of the first Internatinal Conference and Workshop on Iceberg Utilization, Ames, 2-6 October 1977. pp 131-145.

Kovacs, A. 1979. Review of airborne radar sounding of Artic icebergs by J.R. Rossiter, B.B. Narod and G.K.C. Clarke. Proceedings of the Fifth International Conference on Port and Ocean Engineering Under Arctic Conditions (POAC 79) Trondheim, appended to paper reviewed, 13-18 August 1979. Vol 3, P. 356.

Kristensen, M. and V.A. Squire, and S.C. Moore. 1982. Tabular icebergs in ocean waves. Mature 192: 669-671.

Kritz, J. 1977. Parametric array doppler sonar. Institute of Electronics and Electrical Engineering, Journal of Ocean Engineering, OE-2: 190-200.

Langford, C.J. 1984. Acoustic navigation systems and applications. Maritime Technical Services Limited, Calgary, Alberta. 56 pp.

Leshack, L.A. 1983. Artic ocean ice deformation chart using sonar data recorded from nuclear submarines. Proceedings of the 7th International Conference on Port and Ocean Engineering under Arctic Conditions, University of Helsinki. pp. 148-157.

Lyon, W.K. 1961. Ocean and sea ice research in the Arctic ocean via submarine. Transactions of the New York Academy of Sciences, Division of Oceanography and Meterology, New York Academy of Sciences. pp. 662-674.

Lyon, W.K. 1967. Undersea profiles of sea ice observed by submarine. Proceedings of the conference on the Physics of Snow and Ice, Sapporo, Japan, Institute of Low Temperature Science, Hokkaiddo University. pp. 707-711.

Mesotech. 1983. Operator's manual. Mesotech Model 971 Colour Imaging Sonar. 98 p.

Mittleman, J.R. and R.T. Malloy. 1971. Stereo side-scan sonar imagery. 7th Annual Conference of Marine Technology Society pp. 395-417.

Monzingo, R.A. 1980. Introduction to adaptive arrays. John Wiley and Sons, Inc., New York.

Muir T.G. 1979. Some simple propagation models for linear and parametric sources in shallow water. Applied research laboratoriess, University of Texas at Austin, Texas 78712, USA.

Muir, T.G. and J.R. Clynch. 1976. Propogation of parametric waves in shallow water. Proceedings of Institute of Acoustics, Underwater Acoustics Group Meeting, AUWE, England.

Muir T.G., R.L. White and R.J. Clunch. 1974. Experimental model studies of nonlinear effects in normal mode propagation. In: Sound Propagation in Shallow water. O.F. Hastrup and O.V. Olesen (Editors) SACLANT ASW Center Conference Proceedings, No. 14, November.

Munsey, C.J. 1968. An electro-optical underwater search and visibility enhancement technique. Proceedings of SPIE (Society of Photo-Optical Instrumentation Engineers) Underwater Photo-optical Instrumentation Applications Seminar, San Diego, California, February.

Murray, J.E. 1969. The drift deterioration and distribution of icebergs in the North Atlantic Ocean. Ice Seminar, Canadian Institute of Mining and Metallurgy, Special Publication 10: pp. 3-18.

Napoleoni, J.G. and M. Jozan. 1980. Arctic exploration: the Labrador case - production schemes and iceberg studies. Journal of the Society for Underwater Technology, Vol 6, No. 3, pp. 17-23.

NORDCO. 1980. Iceberg draft measurement Labrador Sea, 1979. Report submitted to Total Eastern by NORDCO Limited, February.

OCEANO. 1983. Oceans outlook, Vol. 2 No. 3, Summer.

Pousi, T. and M. Luukkala. 1975. A narrow beam sonar to measure the submarine profile of an ice ridge. Helsinki/Stockholm, Winter Navigation Research Board, Research Report, November.

Quazi, A.H., D.M. Viccione, M.R. Lackoff and R.R. Kurth. 1977. "Results of high data rate underwater acoustic communications experiments". In 9th International congress on Acoustics, Madrid, Spain, July 04-90.

Remotec Applications, Inc. 1982. An assessment of impulse radar as a iceberg draft measurement tool. Contract report prepared for the centre for Cold Ocean Resources Engineering. 82-8, 47 pp.

Robe, R.Q. 1976 Height to draft ratios of icebergs. Proceedings of the 3rd International Conference on Port and Ocean Engineering under Arctic Conditions, Institute of Marine Sciences University of Alaska, pp. 407-415.

Rossiter, J. R. and K.A. Gustajtis. 1978. Iceberg sounding by impulse radar. Nature, 271: 48-50.

Rossiter, J.R. and A. Gustajtis. 1979. Determination of iceberg underwater shape with impulse radar. Desalination 29: 99-107.

Rossiter, J.R., B.B. Narod, and G.K.C. Clarke. 1979. Airborne radar sounding of arctic icebergs. Proceedings of the Fifth International Conference on Port and Ocean Engineering Under Arctic Conditions (POAC 79), Trondheim, August 13-18, Vol., pp. 289-305.

Salbield, A.P. 1976. Acoustic methods of underwater navigation. Southwest Regional Melting, Taunton, Somerset, Southwest Regional Meeting, Taunton, Somerset.

Skolnik, M.I. (editor-in-chief). 1970. Radar handbook. McGraw-Hill Book Company, Toronto. 1536 pp

Slater, P.M. 1975. Photographic systems for remote sensing. Chapter 6 In: Manual of remote sensing, R.G. Reeves (Editor-in-chief), American Society of Photogrammetry, Falls Church, VA. pp 51-74.

Spetcht, M.R., D. Needler and N.L. Fritz. 1973. New Color film for water-photography penetration. Photogrammetric Engineering, 39: 35 p.

Suits, G.H. 1975. The nautre of electomagnetic radiation. Chapter 3 In: Manual of Remote Sensing, R.G. Reeves (Editor-in-chief), American Society of Photogrammetry, Falls Church, V.A.

Suklov, B.P. 1977. Measurement of iceberg draaft. Proceedings of the First International Conference and Workshop on Iceberg Utilization A.A. Husseiny (Editor) Ames Iowa, USA. pp: 265-275.

Swift, D.W. and G.V. Thompson. 1972. Seeing in the dark. The Radio and Electronic Engineer. pp: 403-408.

Swithinbank, C.W.M. 1972. Arctic pack ice from bellow. Sea Ice - Proceedings of an International Conference, Reykjavik, Iceland, 10-13 May 1971, National research council of Iceland. pp. 246-254.

Swithinbank, C. 1977. Remote sensing of iceberg thickness. Proceedings of the First International conference and Workshop of Iceberg Utilization, Ames, 2-6 October 1977. pp: 100-107.

Tolstoy, I. and C.S. Clay. 1966. Ocean acoustics. McGraw-Hill, New York.

Tucker, D.G. 1965. The exploitation of non-linearity in underwater acoustics. Journal of sound vibration: 429-434.

Tucker, D.G. and B.K. Gazey. 1966. Applied underwater acoustics. Pergamon Press.

Urick, R.J. 1975. A british submarine expedition to the North Pole. Polar Record 18: 487-491.

Wadhams, P., 1977. A British submarine expedition to the North Pole. Polar Reocrd 18: 487-491.

Wadhams, P. and M. Kristensen. 1983. The response of Antarctic icebergs to ocean waves. Journal of Geophysical Reserach, 88: 6053-6065.

Watson, R.D. et al. 1974. Prediction of the Fraunhofer line detectivity of luminescent materials. Proceedings of the Ninth Symposium on Remote Sensing of Environment, Environmental Reserach Institute of Michigan, Ann Arbor, Michigan, April. P. 1969.

Wolfe, W.L. and G.J. Zissis (Editors. 1978. The infrared handbook. Prepared by the Infrared Information and analysis (IRIA) centre, Environmental Research Institute of Michigan, Ann Arbor, Michigan, for the Office of naval Research, Department of the Navy, Washington, D.C.

Zielinski, A. 1980. A towed sonar system for iceberg profiling (TIP). Memorandum dated 21 April 1980.